

# **THESIS**

## **The function of Activin receptor type IIB signaling in adult skeletal muscle**

Inaugural-Dissertation  
to obtain the academic degree  
Doctor rerum naturalium (Dr. rer. nat.)

### **Submitted to**

The Department of Biology, Chemistry and Pharmacy

Freie Universität, Berlin

And

Ecole doctorale ED515 «Complexité du vivant »

Université Pierre et Marie Curie, Paris

by

**KARIMA RELIZANI**

from Algiers

**2014**

The research work presented in this thesis has been carried out from September 2010 till June 2014 in the laboratories:

« Biothérapies des maladies du système neuromusculaire » UMR-UPMC-AIM-UM76, Inserm U974, CNRS UMR 7215, Université Pierre et Marie Curie, Paris, France.

« Biothérapies des maladies neuromusculaires » UFR des sciences de la santé Simone Veil, Université Saint-Quentin en Yvelines, France.

« AG Schuelke, Center and Department of Neuropediatrics, Charité Universitätsmedizin, Berlin, Germany.

Referees:

Dr. Delphine Duprez –UPMC representative and chair of the thesis committee

Dr. Anne Bonnieu- External examiner

Prof. Dr. Hadi Al-hasani – External examiner

Dr. Daniel Horbelt- Postdoctoral research fellow from FU

Supervisor: Dr. Helge Amthor- Thesis supervisor, UPMC

Supervisor: Prof. Dr. Petra Knaus –FU representative

Guest: Prof. Markus Schuelke, Charité

Date of Defense: 07 July 2014

## **Abstract**

Myostatin, a growth factor of the TGF- $\beta$  family that signals through the activin receptor-IIB (ActRIIB), has been identified as an important negative regulator of skeletal muscle growth. However, its effect on muscle energy metabolism and energy dependent muscle function remains largely unexplored. I here investigated the consequence of impaired ActRIIB signaling for muscle metabolism in two experimental models, i) the constitutive myostatin knockout mice and ii) following pharmacological administration of soluble ActRIIB in adult mice. Our results demonstrate that myostatin knockout mice develop a strong fatigability, a decrease in mitochondrial respiration and a molecular signature towards a glycolytic metabolism. As these findings may be explained by the congenital shift towards fast glycolytic muscle fibers in these mice, I investigated the effect of inhibition of ActRIIB signaling in adult mice. I provide evidence, notably for the *mdx* mouse, model for Duchenne muscular dystrophy, that ActRIIB blockade, despite an unchanged fiber type distribution, leads to extreme exercise intolerance. This was associated with pathologically increased serum lactate levels and myopathic features. In-depth biochemical and molecular analysis demonstrates that blockade of ActRIIB signaling down-regulates the ATP channel porin, reduces muscle capillarization and leads to a consecutive deficiency in oxidative phosphorylation. I also show that ActRIIB regulates key determinants of muscle metabolism, such as Ppar $\beta$ , Pgc1 $\alpha$ , and Pdk4, thereby optimizing different components of muscle energy metabolism. Taken together, my results demonstrate that ActRIIB blockade provokes a metabolic myopathy, especially in the context of dystrophic muscle, in which an underlying metabolic stress already exists. In conclusion, I cannot recommend the use of ActRIIB signaling blockade as a therapeutic strategy for muscle diseases.

## **Zusammenfassung**

Myostatin, ein Signalmolekül der TGF- $\beta$ -Familie, vermittelt seine Wirkung über den Aktivin-Rezeptor-IIB (ActRIIB) und ist ein extrem starker Hemmer des Skelettmuskelwachstums. Andere Wirkungen des Myostatin, insbesondere die ihm zugeschriebene Regulierung des Muskelenergiestoffwechsels und der energieabhängigen Muskelfunktion, sind noch weithin unerforscht. Ich habe in meiner Arbeit die Folgen einer gestörten ActRIIB-Signalübertragung für den Muskelstoffwechsel anhand zweier Experimentalmodelle untersucht: i) in einem konstitutiven Myostatin-knockout-Mausmodell (*Mstn*<sup>-/-</sup>) und ii) mittels einer pharmakologischen ActRIIB-Blockade in adulten Mäusen durch Behandlung mit löslichem ActRIIB-Rezeptor. Unsere Ergebnisse zeigen, dass die *Mstn*<sup>-/-</sup>-Mäuse unter körperlicher Belastung schnell ermüden. Diese vermehrte muskuläre Ermüdbarkeit geht mit einer verminderten mitochondrialen Atmung und einer molekularen Veränderung zugunsten des glykolytischen Stoffwechsels einher. Diese Veränderungen könnten einer angeborenen Muskelfaserverteilungsstörung zugunsten glykolytischer Fasern zugeschrieben werden, die bei der *Mstn*<sup>-/-</sup>-Maus typischerweise auftritt. Ich habe deshalb die Auswirkung einer ActRIIB-Blockade in der adulten Maus untersucht und konnte zunächst zeigen, dass es dabei zu keiner Faserverteilungsstörung kommt. Eine ActRIIB-Blockade führt insbesondere im *mdx*-Mausmodell der Muskeldystrophie Duchenne zu einer extremen Belastungsintoleranz. Dies geht einher mit einer pathologischen Serumlaktaterhöhung und zunehmenden Zeichen einer Muskelerkrankung. Ich konnte mittels biochemischer und molekularbiologischer Analysen zeigen, dass eine Inhibierung der ActRIIB-Wirkung sowohl zu einer verminderten Bildung des ATP-Kanalproteins Porin führt, als auch zu einer verminderten Anzahl von Muskelkapillaren und zu einem sich daraus ergebenden Defizit der oxidativen Phosphorylierung. Ich habe weiterhin herausgefunden, dass der ActRIIB-Signalweg wichtige Kontrollgene des Muskelstoffwechsels reguliert, wie z.B. Ppar $\beta$ , Pgc1 $\alpha$  und Pdk4, wodurch im gesunden Muskel der oxidative Energiestoffwechsel optimiert wird. Zusammenfassend zeige ich in meiner Arbeit, dass die ActRIIB-Blockade eine metabolische Muskelerkrankung hervorruft. Diese tritt besonders bei einer vorgeschädigten dystrophen Skelettmuskulatur auf, da bei dieser Erkrankungsgruppe schon vor Behandlung eine metabolische Schädigung besteht. Aufgrund meiner Ergebnisse kann ich die Anwendung einer ActRIIB-Blockade als Therapiestrategie für Muskelerkrankungen nicht empfehlen.

Key words: myostatin, ActRIIB, knockout, myopathy, metabolism, Duchenne muscular dystrophy.

## Acknowledgements

Firstly I would like to thank the members of my thesis committee to give me the great honor to evaluate my research work.

*Dr. Delphine Duprez* to have accepted to chair the thesis committee.

*Prof. Hadi Al-hasani* and *Dr. Anne Bonnieu* to have taken the delicate task to examine my work.

*Prof. Petra Knaus* and *Dr. Daniel Horbelt* to have accepted to represent the Freie Universität. And of course, not forgetting my supervisors, *Prof. Helge Amthor* and *Prof. Markus Schülke*, who gave me the chance to realize a dream: **to do research**.

My adventure started when I met *Helge*, who trusted me, who gave me the opportunity to join his small team and the chance to work in a highly motivated environment. *Helge*, this is why I would say Thank-You. I will also say Thank-You for your support and trust that maintained throughout my research, for your presence and your availability in the most important moments, as well as your kindness and generosity. I would of course like to thank *Dr. Christophe Hourdé* and *Dr. Etienne Mouisel* for their help and advice when I started in the team, for their contribution in teaching me. Not forgetting the other PhD students of our team: *Dr. Elija Schirwis* and the future *Dr. Amalia Stantzou* to whom I say a big Thank-You for all the good time we spent together in and outside of the lab, for your patience, your generosity, your support and listening.

I would also like to take this opportunity to thank *Dr. Luis Garcia* who has opened the doors of his laboratory and has given me free access to all equipment, Thank-You *Luis* also for your valuable advice and your generosity. Many thanks go to the whole team: *Rachid, Valerie, Graziella, Aurélie G, Cyriac, Guillaume, Pierre Olivier and Aurélie A*. When we first met, we were still at the 105 (boulevard de l'hôpital), where we spent a great time. Three years later we find ourselves in Saint-Quentin, but the adventure continues. For *Gabriella* and *Jakub* our new PhD students, your thesis adventure begins, then you will see that the happy ending is sooner than you expect. Without forgetting the old team of the 105, I especially thank *Christel* for her availability and her patience and wish her all the best. *Stephanie, France, Susanne, Maëva, Carole, Simin and the Barkats team*, I would to say Thank-You to all of you.

Having started my PhD in the laboratory in Paris, now I'm flying to Berlin to join the team of Markus. Thank-You to my co-supervisor **Markus**, who directed and supervised me throughout my research, for his support and kindness, Thank-You **Markus** for your presence and availability. When I went to Berlin I was afraid, then you welcomed me in your group and I immediately felt home. It was really great to work with you. **Barbara, Can, Susanne, Mina, Anna, Jana, Friederike**: a great team we spent together, especially during our special international dinners. I want to thank from the deepest of my heart **Susanne** for her invaluable help and support for my project and for her friendship and trust, I wish you the best because you really deserve it. A special Thank to you **Can**. I am glad to have met you and to have had a great time sharing. I really got lucky that our paths crossed but as you know I do not believe in luck. Thank-You for this pure friendship

I am profoundly grateful to **Susanne Wissler**, for all her kindness and her help along all these years with all the administrative and bureaucratic issues.

A specialy, I would like to say Thank-You to all MyoGrad students, for your friendship and all the great time we spent together. Especially: **Despoina, Petra, William, Adeline, Esma, Anna and Séverine**.

A big Thank-You to all my friends who support me beyond the borders, who supported me all these years and who continue to believe in me and always encouraged me to go further. **Dina, Radia, Zineb, Rym, Imane, Fayrouz, Amar, Tayeb, Sofiane Yacine, Chahine, Sofiane and Fouad**.

A huge Thank-You to my family, my parents and my sisters: **Nabila, Wassila and Doria**, and to my mother especially, who made sure that I could achieve my dreams and who encouraged me to continue my studies, who has always believed in me and supported me in my efforts even if it sometimes seemed impossible.

Finally, thanks to all those who have contributed from far or near to the accomplishment of this work. All of you a **BIG THANK YOU!!!**



# Table of Contents

Acknowledgements .....	4
LIST OF ABBREVIATIONS .....	11
INTRODUCTION .....	13
1. CHAPTER: THE SKELETAL MUSCLE .....	14
1.1 General introduction .....	14
1.2 Structure of muscle tissue .....	14
1.3 Muscle fibers and properties .....	15
1.3.1 Contractile properties .....	16
1.3.2 Metabolic properties .....	18
1.4 Glucose and lipid metabolism of skeletal muscle .....	19
1.4.1 The anaerobic metabolic pathway in muscle .....	20
1.4.2 The aerobic metabolic pathway in muscle .....	20
1.4.3 The PPAR signaling and metabolism .....	23
1.4.4 Targets of the PPARs .....	25
1.5 Regulation of muscle mass .....	25
1.5.1 Muscle atrophy .....	25
1.5.2 Muscle hypertrophy .....	28
1.6 Muscle regeneration .....	29
1.7 Response of skeletal muscle to repetitive muscle damage .....	30
2. CHAPTER: DUCHENNE MUSCULAR DYSTROPHY .....	31
2.1 History and disease description .....	31
2.2 The <i>DMD</i> gene .....	32
2.3 Mutations of the <i>DMD</i> gene .....	33
2.4 Dystrophin and the Dystrophin Associated Protein Complex .....	33
2.5 Dystrophin isoforms .....	34
2.6 The Dystrophin Associated Protein Complex .....	36
2.7 Animal models for DMD .....	38
2.7.1 The mdx mouse .....	38
2.7.2 The GRMD dog .....	38
2.7.3 The HFMD cat .....	39
2.8 Revertant fibers .....	39
2.9 Treatment strategies for DMD .....	40
2.9.1 Gene therapy .....	40

2.9.2	The exon skipping.....	42
2.9.3	Cell therapies.....	43
2.9.4	The pharmacological approach .....	43
3.	CHAPTER: MYOSTATIN .....	46
3.1	Myostatin gene and protein structure .....	46
3.2	The myostatin knockout mouse model.....	48
3.3	Myostatin expression .....	49
3.4	The myostatin signaling pathway.....	50
3.5	Regulation of myostatin activity.....	51
3.5.1	Molecules binding myostatin .....	52
3.6	The function of myostatin .....	54
3.6.1	Myoblast cell proliferation .....	54
3.6.2	Myoblast cell differentiation .....	55
3.6.3	Muscle cell regeneration.....	55
3.6.4	The role of myostatin in adipogenesis .....	56
3.6.5	Contractile phenotype.....	57
3.6.6	Muscle metabolism .....	57
3.7	Therapeutic strategies based on myostatin blockade .....	58
3.7.1	The different approaches to induce myostatin blockade .....	58
3.7.2	Myostatin blockade as a therapy against DMD.....	61
	AIMS OF THE THESIS.....	65
	RESULTS.....	68
1.	Part 1: Role of myostatin in the regulation of muscle energetic metabolism in mouse models..	69
1.1	Effect of the ActRIIB blockade in wildtype and mdx mice.....	69
1.2	Effect of the absence of myostatin in the <i>Mstn</i> <sup>-/-</sup> mouse model .....	116
2.	Part 2: The role of the myostatin blockade in combination with gene therapy muscular dystrophy.....	141
	GENERAL DISCUSSION .....	155
1.	Myostatin and muscle force.....	158
2.	Myostatin and endurance capacity.....	160
3.	Myostatin and muscle metabolism .....	162
4.	Myostatin and mitochondria.....	164
5.	Myostatin and vascularization .....	166
6.	Myostatin and heart muscle .....	167
7.	Myostatin blockade as a therapeutic strategy.....	168

## LIST OF FIGURES AND TABLES

Figure 1: The skeletal muscle structure.....	15
Figure 2: The skeletal muscle sarcomere. ....	16
Figure 3: The interaction of myosin and actin during the contraction of a muscle fiber. ....	17
Figure 4: Cellular process of the metabolism. ....	20
Figure 5: The glycolytic pathway.....	21
Figure 6: The mitochondrial $\beta$ -oxidation. ....	21
Figure 7: The Krebs cycle. ....	22
Figure 8: The oxidative phosphorylation. ....	23
Figure 9: PPAR $\delta$ activation.....	24
Figure 10: Different signaling pathways involved in the regulation of hypertrophy and atrophy of muscle.....	27
Figure 11: Mode of rising from the ground.....	31
Figure 12: Microscopic images of cross-sections of human skeletal muscle.....	32
Figure 13: schematic representation of the reading frame hypothesis. ....	33
Figure 14: Schematic of the structure of dystrophin. ....	34
Figure 15: The different dystrophin isoforms. ....	36
Figure 16: DAPC complex (Dystrophin associated protein complex). ....	37
Figure 17: Myostatin mouse model. ....	46
Figure 18: Genomic tructure of the myostatin gene. ....	46
Figure 19 : Structure of the myostatin protein.....	47
Figure 20: Activation of the myostatin protein. ....	48
Figure 21: The myostatin signaling pathway. ....	51
Figure 22: Role of myostatin in the regulation of proliferation and differentiation of myoblasts. ....	54
Figure 23: Role of myostatin in the regulation of muscle growth.....	56
Figure 24: Muscle force production after overload treatment.....	156
Table 1: Characteristics of muscle fiber types .....	18
Table 2: Proteins with an influence on myostatin action.....	51



## **LIST OF ABBREVIATIONS**

**2'OMePS:** 2'-O-methyl phosphorothiorate  
**4E-BP1:** 4E-Binding Protein 1  
**5'UTR:** 5' Untranslated region  
**AAV:** Adeno-Associated Virus  
**Acetyl-CoA:** Acetyl Co Enzyme A  
**ACS:** AcylCoA Synthetase  
**ActRIIB:** Activin Receptor IIB  
**Acyl-CoA:** Acyl-Co Enzyme A  
**AIDS:** Acquired ImmunoDeficiency Syndrome  
**ALK:** Activin Like Kinase  
**AO:** Antisense Oligonucleotide  
**ATP:** Adenosine Tri-Phosphate  
**Ay:** Agouti lethal yellow  
**BMD:** Becker Muscular Dystrophy  
**BMP:** Bone Morphogenetic Protein  
**CDK2:** Cyclin Dependent Kinase 2  
**CK:** Creatine Kinase  
**CKI:** Cyclin dependent Kinase Inhibitor  
**CYTc:** Cytochrome c  
**DAPC:** Dystrophin Associated Protein Complex  
**DMD:** Duchenne Muscular Dystrophy  
**dnActRIIB:** dominant negative Activin Receptor IIB  
**eIF2B:** eukaryotic Initiation Factor 2B  
**FA:** Fatty Acids  
**FADH:** Flavine Adenine Dinucleotide  
**FLRG:** Follistatin Related Gene  
**FoxO:** Forkhead box O  
**FST:** Follistatin  
**GASP1:** Growth and Differentiation Factor Associated Serum Protein 1  
**GDF:** Growth and Differentiation Factor  
**GRMD:** Golden Retriever Muscular Dystrophy  
**GSK3 $\beta$ :** Glycogen Synthase Kinase 3 $\beta$   
**HFMD:** Hypertrophic Feline Muscular Dystrophy  
**HGF:** Hepatocyte Growth Factor  
**HIV:** Human Immunodeficiency Virus  
**hSGT:** human Small Glutamine-rich Tetratricopeptide  
**ICDH:** Isocitrate Dehydrogenase

**IGF:** Insulin like Growth Factor  
**IL-6:** Interleukine 6  
**JNK:** Jun NH2-terminal Kinase  
**kDa:** kilo Daltons  
**LAP:** Latency Associated Peptide  
**LDH:** Lactate Dehydrogenase  
**MAFbx:** Muscle Atrophy F-box  
**MAPK:** Mitogen-Activated Protein Kinase  
**Mdx:** X-linked muscular dystrophy  
**MRF:** Myogenic Regulatory transcription Factor  
**mRNA:** messenger RNA  
**MSTN:** Myostatin  
**mTOR:** mammalian Target of Rapamycin  
**MuRF1:** Muscle Ring Finger protein 1  
**MyHC:** Myosin Heavy Chain  
**Myf5:** Myogenic Factor 5  
**MyoD:** Myogenic Differentiation  
**NADH:** Nicotinamide Adenine Dinucleotide  
**NFκB:** Nuclear Factor kappa-B  
**OXPHOS:** Oxidative Phosphorylation  
**Pax 7:** Paired Box Protein 7  
**PCR:** Polymerase Chain Reaction  
**PDH:** Pyruvate Dehydrogenase  
**PDK:** Pyruvate Dehydrogenase Kinase  
**PGC1α:** Peroxisome Proliferator Activated Receptors γ Co-activator-α  
**PPARs:** Peroxisome Proliferator Activated Receptors  
**PPMOs:** Phosphorodiamidate Peptide Morpholino Oligomers  
**rAAV:** recombinant Adeno-Associated Virus  
**RNAi:** RNA interference  
**ROS:** Reactive Oxygen Species  
**RXR:** Retinoid X Receptor  
**S6K:** S6 Kinase  
**SC:** Satellite Cell  
**SDH:** Succinate Dehydrogenase  
**TCap:** Titin Cap  
**TGFβ:** Transforming Growth Factor-β  
**TNF:** Tumor Necrosis Factor  
**VDAC:** Voltage Dependent Anion Channel

# INTRODUCTION

# 1. CHAPTER: THE SKELETAL MUSCLE

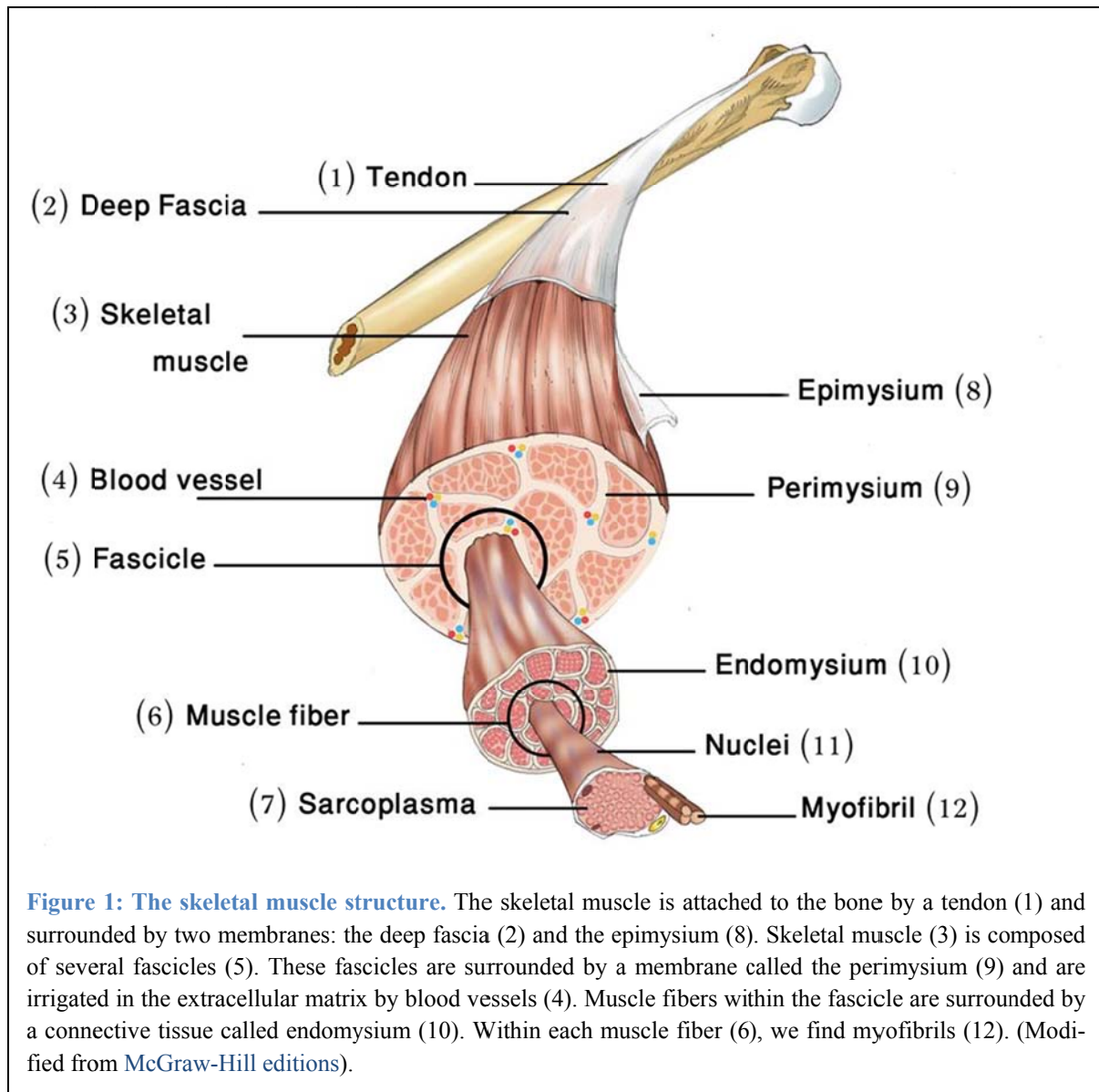
## 1.1 General introduction

Muscles are contractile tissues classified into three categories: cardiac, smooth and skeletal muscles. Cardiac and smooth muscles are “involuntary” muscles (their action being not under voluntary control) that allow the contraction of internal organs such as heart, stomach, intestine, bronchi, blood vessels or uterus. Their actions enable vital functions such as blood circulation and digestion. Skeletal muscle activity can be voluntary and allows movement of the organism itself such as for locomotion and interaction with the environment. The single exception is the diaphragm, which controls breathing and is under both autonomic and direct motor control. Cardiac and skeletal muscles have a characteristic “striated” appearance due to the organization of their myofilaments, whereas the smooth muscle cells do not have a striated appearance.

The voluntary contraction of the striated skeletal muscle is an essential property for its function, including maintenance of posture, generation of heat from muscle activity, and enabling movement *via* force transduction on bones through tendons. It also serves as the body’s major protein reservoir and as a key player of metabolism. It contributes significantly to the health of the individual by maintaining protein homeostasis. The alteration of this function leads to loss of muscle mass, which is also called muscle atrophy or sarcopenia. This can occur during aging and in a number of diseases such as cancer, HIV infection and neuromuscular disorders.

## 1.2 Structure of muscle tissue

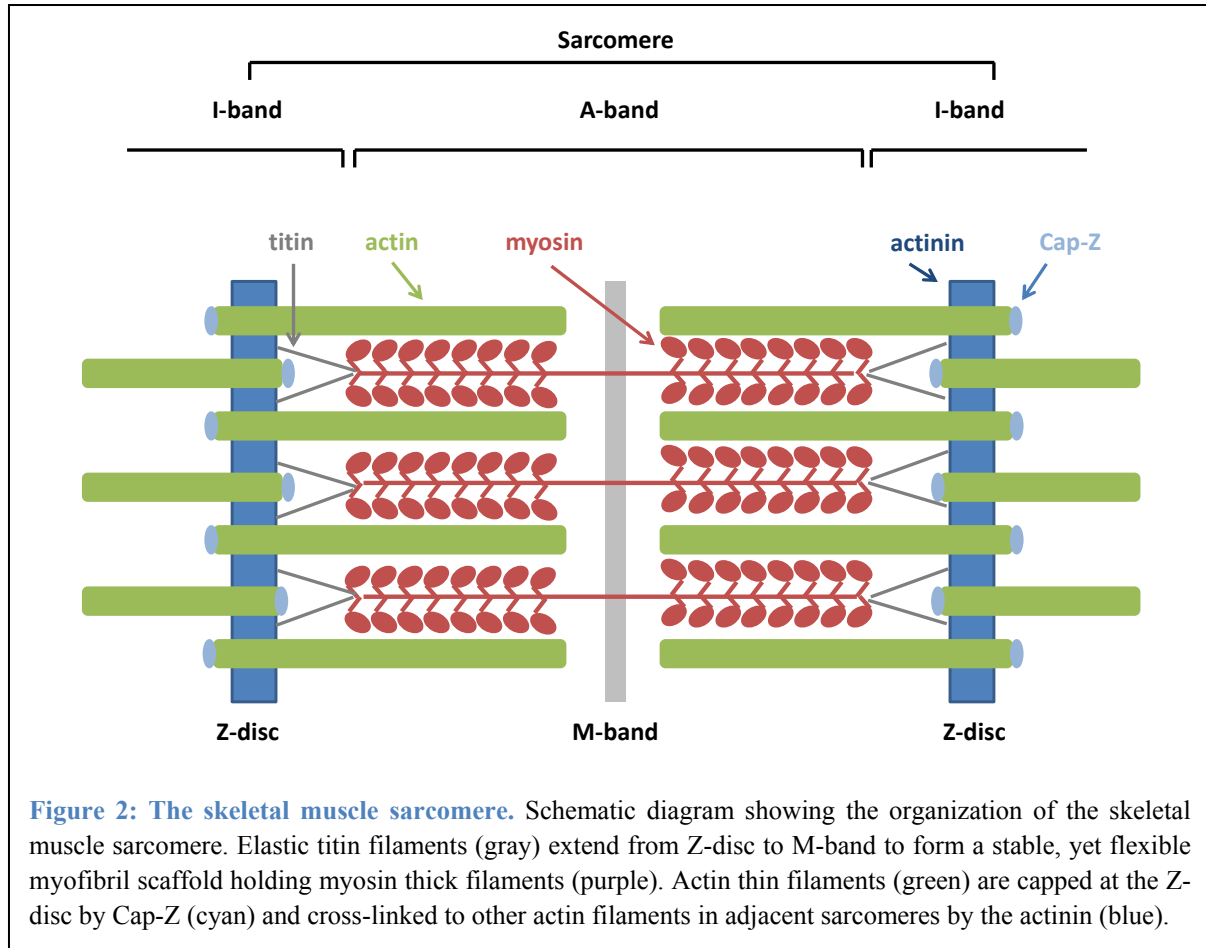
Skeletal muscle is composed of cylindrical muscle cells (also called muscle fibers) as well as connective tissue cells, adipocytes, nerve and endothelial/vascular cells. The muscle fibers which are responsible for the contraction are grouped in a fascicle surrounded by an envelope of connective tissue that is called perimysium. Each fiber is itself surrounded by an envelope called endomysium. The whole muscular tissue is covered by a layer of external connective tissue which is called epimysium. Within a fascicle, the connective tissue of the endomysium surrounds the individual fibers of skeletal muscle and interconnects the adjacent muscle fibers (Figure 1).



### 1.3 Muscle fibers and properties

Skeletal muscle is composed of multinucleated, elongated contractile cells called myofibers or muscle fibers. Muscle fibers have a diameter between 10 and 100  $\mu\text{m}$ , and a length, which can reach 30 cm (Wheater and Burkitt 1987). Each myofiber contains bundles of protein filaments called myofibrils that extend the entire length of the cell. A myofibril is composed of a chain of sarcomeres, which is the functional unit of contraction (Figure 2). A sarcomere contains the myosin, which forms the thick filament, and the actin, which forms the thin filament. Thin and thick filaments slide past each other during muscle contraction and each sarcomere shortens to 70% of its uncontracted, resting length (Darnell, Lodish et al. 1990). Each muscle fiber is surrounded by a plasma membrane and an outer basement membrane (basal lamina). Dur-

ing development, multinucleated muscle fibers are formed by the fusion and differentiation of mononucleated cells. Satellite cells are localized between the plasma membrane and the basal lamina of the muscle fiber and are believed to represent a muscle stem cell population capable of cell division for muscle growth and repair ((Campion 1984); (Blau, Dhawan et al. 1993); (Cornelison and Wold 1997)).



### 1.3.1 Contractile properties

The molecular basis of a muscle contraction can be described by the “sliding filament” theory. Two types of filaments are involved in this process, the thick filaments (myosin) and the thin filaments (actin). In the presence of ATP and calcium, actin filaments slide along myosin filaments thus allowing the shortening of the muscle necessary for a complete muscle contraction. The detailed process is depicted in (Figure 3).

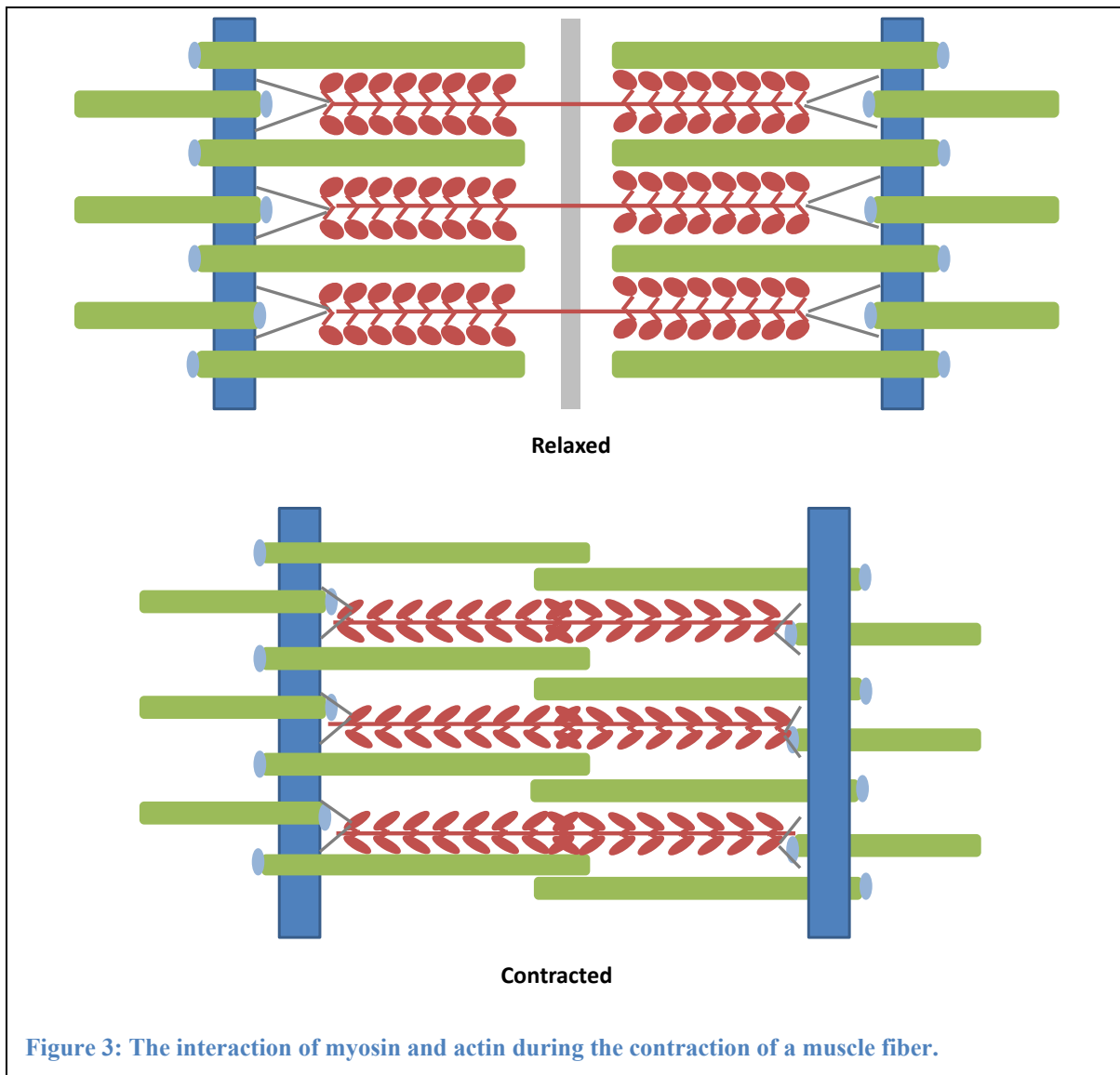


**Figure 3: The interaction of myosin and actin during the contraction of a muscle fiber.**

The speed at which a muscle fiber contracts depends on its metabolic and contractile properties. There are two types of muscle fibers, the type I and type II fibers. Muscle fibers type I have a metabolism that is based primarily on the aerobic respiration. Their contractions are slow but fatigue resistant and therefore able to support long-term moderate activity. They are mostly found in the postural muscles. Muscle fibers types II are divided in mouse into IIA, IIB and IIX. Like the fiber type I, muscle fiber types IIA contain many mitochondria and myoglobin. However, they are less resistant to long fatiguing activity as compared to type I fibers. Muscle fiber types IIB cause rapid, short and powerful contractions. They operate under anaerobic conditions and are needed during short intense exercise.

The contractile properties of muscle fibers and thus their classification are based on the measurement of the ATPase activity of myosin (Brooke and Kaiser 1970) or on the separation of myosin heavy chain isoforms by electrophoresis ((Schiaffino, Gorza et al. 1989); (Gorza 1990); (Duris, Renand et al. 1999)). The type I fibers (slow) and type IIA, IIX and IIB (fast) express MyHC isoforms I, IIa, IIx and IIb, respectively (Table 1). In addition to these adult myosin isoforms, other isoforms have been identified in the foetus: embryonic, fetal and alpha-cardiac MyHC ((Weydert, Barton et al. 1987); (Picard, Gagniere et al. 1995); (Gagniere, Picard et al. 1999)).

## 1.3.2 Metabolic properties

The muscle fibers can also be distinguished according to their metabolic type (oxidative *versus* glycolytic). There are two major types of fibers: oxidative fibers (type I fibers) and glycolytic fibers (type II fibers) (Table 1).

**Table 1: Characteristics of muscle fiber types**

Fiber Types		Myosin heavy chain Isoforms	Contraction speed	Metabolism	ATPase activity
Slow	I	I	Slow	Oxydatif	Low
	IIA	IIa	Fast	Oxydo-glycolytic	High
Fast	IIX	IIx		Oxydo-glycolytic	
	IIB	IIb		Glycolytic	

The measurement of enzyme activities is often used to determine the metabolic type of muscle fibers; for example, the activities of the isocitrate dehydrogenase (ICDH) or the succinate dehydrogenase (SDH), two mitochondrial enzymes of the Krebs cycle, are used to characterize the aerobic oxidative metabolism of the muscle fiber. The measurement of the lactate dehydrogenase (LDH), an enzyme that catalyzes the conversion of pyruvate to lactate during anaerobic glycolysis, is used to characterize the anaerobic glycolytic metabolism ((Robelin, Picard et al. 1993); (Gagniere, Picard et al. 1999)). The oxidative capacity of the muscle fibers has an inverse relationship with the diameter of the muscle fiber (Cassens and Cooper 1971).

### 1.4 Glucose and lipid metabolism of skeletal muscle

Mitochondria are specialized organelles and function as the energy center for the cell, which makes them essential for the survival of eukaryotic cells. They show significant differences between the heart muscle and skeletal muscle, both in their oxidative capacity ((Ogata and Yamasaki 1985); (Ventura-Clapier, Kuznetsov et al. 1998)) and the nature of their preferred substrates (Bahi, Koulmann et al. 2004).

Each mitochondrion consists of four major compartments that differ in composition, activity and function: [1] An **outer membrane** that is permeable to molecules with a molecular weight of less than 6 kDa, separates the mitochondria from the cytoplasm. [2] An **inner membrane** delimits the [3] **intermembrane space** from the [4] **mitochondrial matrix**, which contains various enzyme complexes of different metabolic pathways such as the Krebs cycle, the respiratory chain and the beta-oxidation of fatty acids.

#### *The outer mitochondrial membrane*

It contains multiple copies of a transport protein called porin, which forms together with the adenine nucleotide transporter (ANT) a large aqueous channel through the lipid bilayer. This membrane is permeable to molecules of up to 10,000 daltons, including small proteins and short chain fatty acids. Porin is also called the ‘Voltage-dependent anion channel’ (VDAC). It is the main channel for metabolites that regulate the mitochondrial respiration. In addition, several enzymes of various metabolic pathways may be associated with the outer membrane through interaction with porin. As examples, the hexokinase, the glycerolkinase, and the acyl-CoA synthetase (ACS) regulate mitochondrial function *via* interaction with the VDAC (Brdiczka, Kaldis et al. 1994).

#### *The inner mitochondrial membrane*

With reduced and selective permeability, the inner membrane constitutes a barrier for maintaining a concentration gradient of ions and metabolites between the intermembrane space and the mitochondrial matrix. Because of its low permeability, the inner membrane has many transport systems for ion exchange and metabolites. The transport of the substrates is carried out by more or less complex systems.

### 1.4.1 The anaerobic metabolic pathway in muscle

Under conditions of reduced oxidative capacity (insufficient amount of mitochondria or lack of oxygen), glycogen/glucose is converted into pyruvate by anaerobic glycolysis (Figure 4). The pyruvate is then converted into lactate in the cytosol in the presence of the enzyme lactate dehydrogenase (LDH). This process also leads to the reoxidation of the coenzyme  $\text{NADH}_2$  to  $2\text{H}^+$  and  $\text{NAD}^+$ . The energy balance of anaerobic glycolysis is relatively poor, because it leads to the net production of only two ATP molecules per molecule glucose.

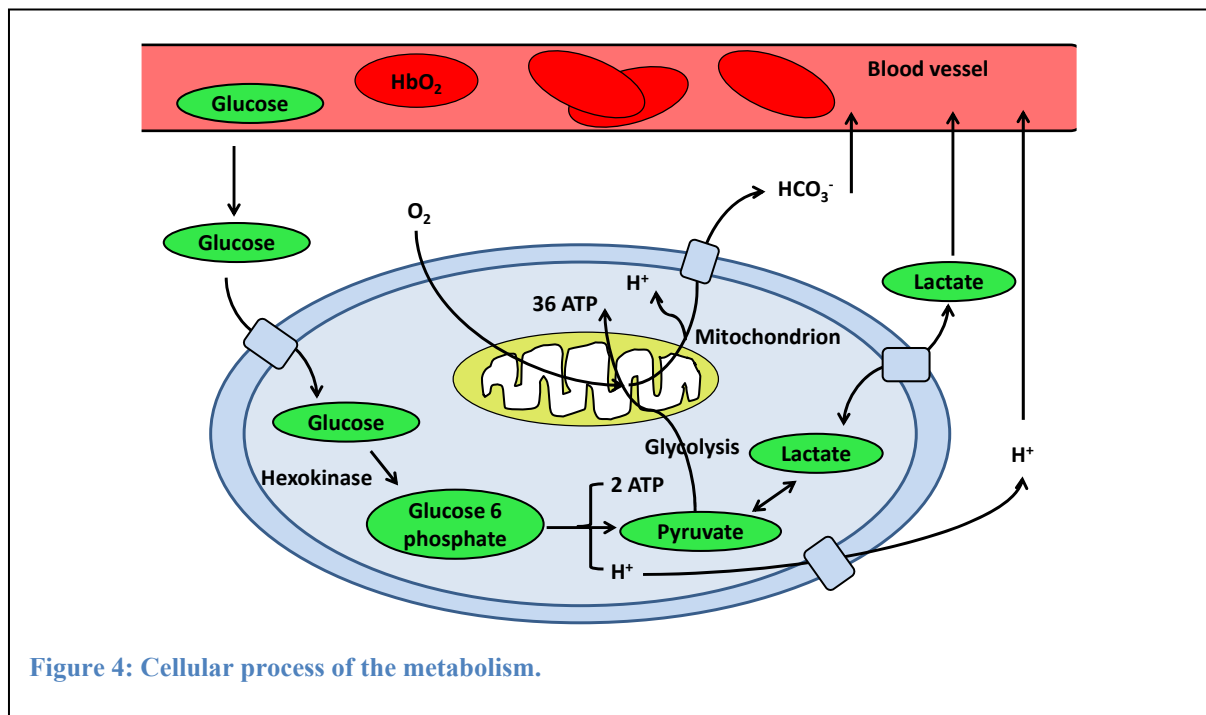


Figure 4: Cellular process of the metabolism.

### 1.4.2 The aerobic metabolic pathway in muscle

Energy for normal mobility and during prolonged physical exercise is provided by the aerobic pathway, whereas the anaerobic pathway is being used only during high intensity exercise with short duration. The aerobic pathway requires the supply of substrate and oxygen. The muscle will then oxidize the available substrates through different successive pathways:

#### *The aerobic glycolysis*

Glycolysis is the oxidation of glucose to pyruvate. It produces two molecules of ATP and two molecules of  $\text{NADH}_2$ . The pyruvate that is produced in the cytosol then enters into the mitochondria by active transport. Thereafter, pyruvate is further metabolized to acetyl-Coenzyme A (acetyl-CoA) by oxidative decarboxylation under the action of three enzymes, which form the pyruvate dehydrogenase complex (PDH) (Figure 5).

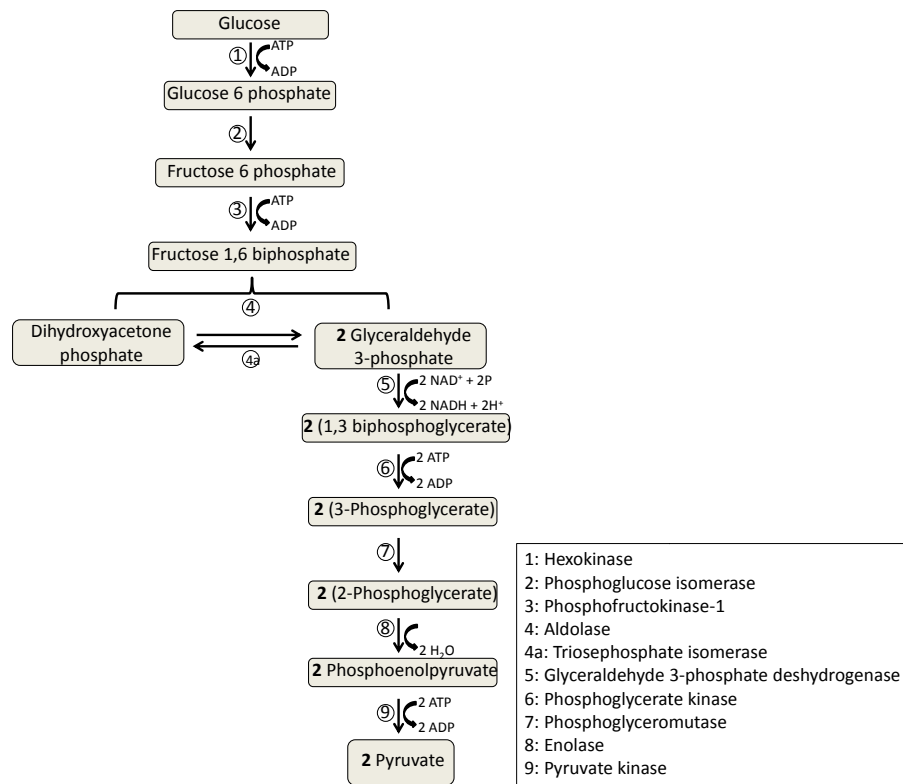


**Figure 5: The glycolytic pathway:** In the case of insufficient oxygen, the cell produces energy by fermentation (glycolysis) to operate the system. This is much less effective than the oxidative catabolism way, and the substrates are only partially degraded. In the presence of oxygen, mitochondria oxidize organic substrates producing energy directly used by the cells and releasing CO<sub>2</sub>.

## The mitochondrial $\beta$ -oxidation

Once the acyl-CoA from fatty acids (FA) are transported into the mitochondria through the carnitine shuttle, a series of transformations gradually and repeatedly removes two carbon atoms at each turn of the cycle. This repeated processing is called  **$\beta$ -oxidation** and produces one molecule of FADH<sub>2</sub>, of NADH<sub>2</sub> and of acetyl-CoA at each cycle of acyl-CoA degradation (Figure 6).

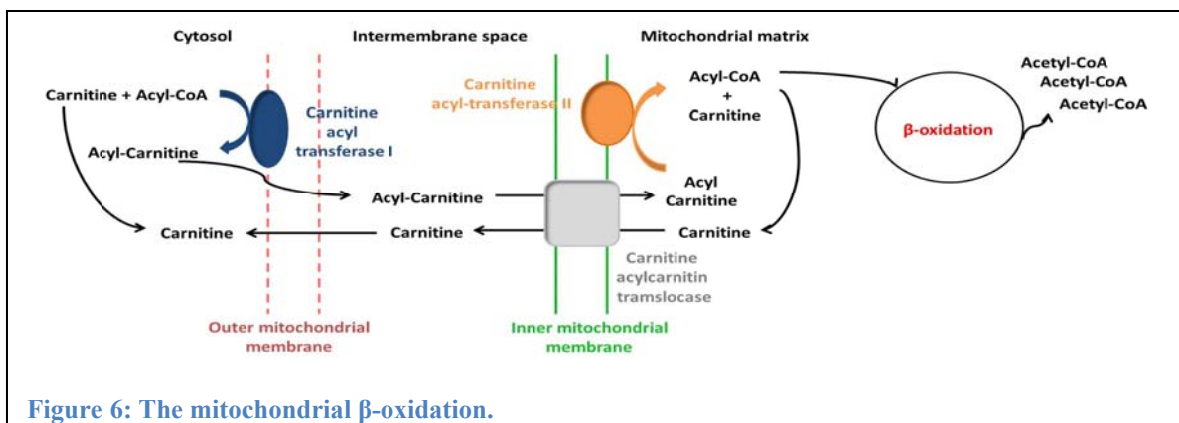


**Figure 6: The mitochondrial  $\beta$ -oxidation.**

## The Krebs cycle

The Krebs cycle consists of a series of biochemical reactions, whose purpose is to produce the reduced equivalents ( $\text{NADH}_2$  and  $\text{FADH}_2$ ) to be used in the production of ATP by the respiratory chain. This reaction chain forms a cycle since the last metabolite, the oxaloacetate, is also involved in the first reaction. It is the final common pathway of all acetyl-CoA molecules, whether resulting from glycolysis or the  $\beta$ -oxidation (Figure 7).

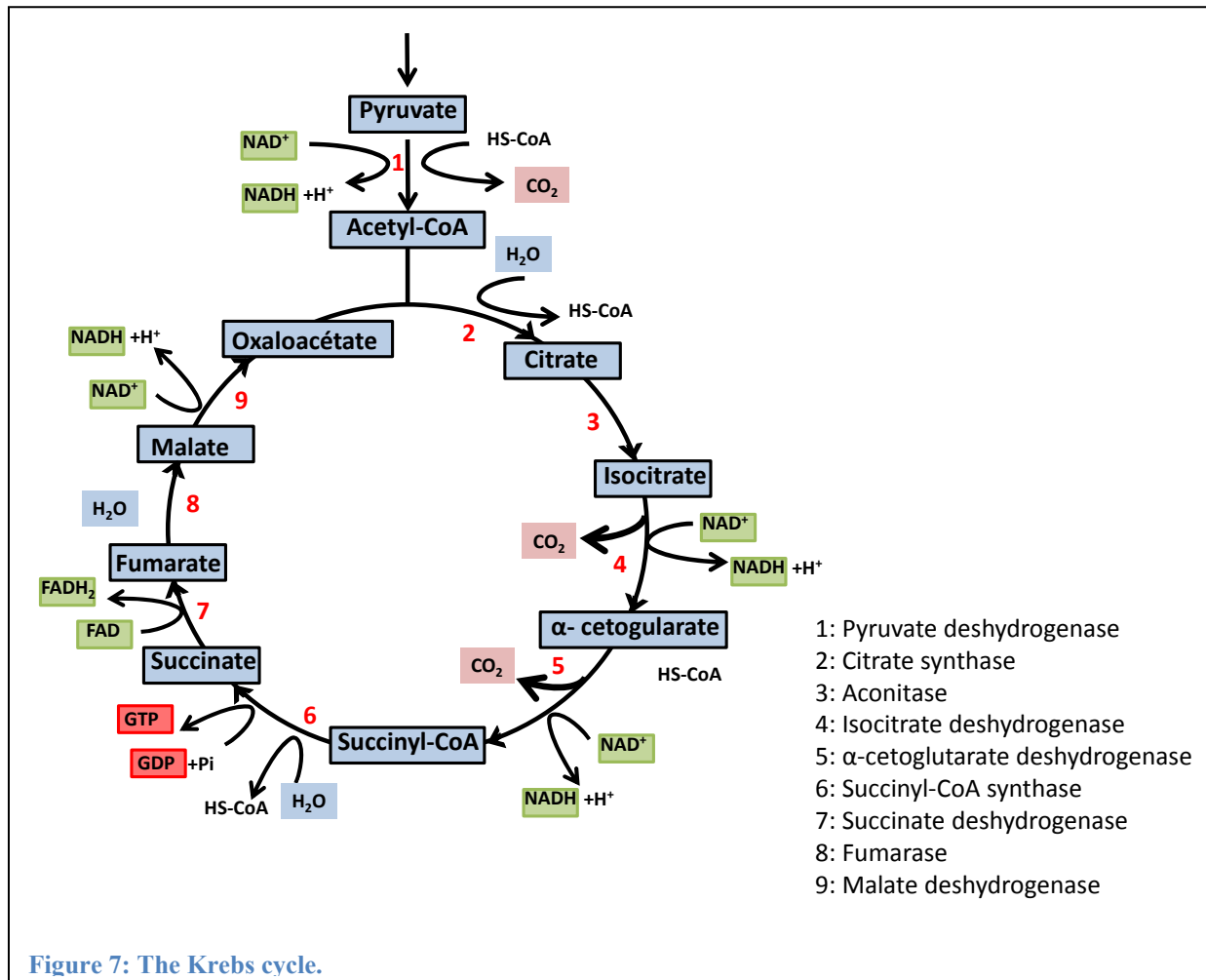


Figure 7: The Krebs cycle.

## The oxidative phosphorylation

The term oxidative phosphorylation (OXPHOS) is employed to describe the coupling between the oxidation of the reduced equivalents and phosphorylation of ADP. This process involves five complexes with multiple subunits, which are located at the inner membrane and form the respiratory chain. Oxidation of  $\text{NADH}_2$  at Complex I (NADH:ubiquinone reductase) and of succinate/ $\text{FADH}_2$  at Complex II (succinate:ubiquinone reductase) releases the electrons, which are transported along the electron transport chain first onto ubiquinone (Q), then to

Complex III and from there to cytochrome C (CYTC). Complex IV (Cytochrom C oxidase) then transfers the electrons onto molecular oxygen:

Complex I  $\Rightarrow$  Q  $\Rightarrow$  Complex III  $\Rightarrow$  CYTC  $\Rightarrow$  Complex IV  $\Rightarrow$  O<sub>2</sub> and

Complex II  $\Rightarrow$  Q  $\Rightarrow$  III  $\Rightarrow$  CYTC  $\Rightarrow$  Complex IV  $\Rightarrow$  O<sub>2</sub>

The electron transfer is achieved through a series of oxidation-reduction reactions with various constituents of the complex, which is coupled to the translocation of H<sup>+</sup> from the matrix into the innermembrane space (only through complexex I, III, and IV) The final electron acceptor is oxygen, which is reduced to water by complex IV.

The electrochemical gradient of H<sup>+</sup> generates a potential difference on both sides of the inner membrane ( $\Delta\Psi = -220\text{mV}$ ) and constitutes a source of electrochemical energy for the synthesis of ATP powered by ATP synthase or complex V (Figure 8).

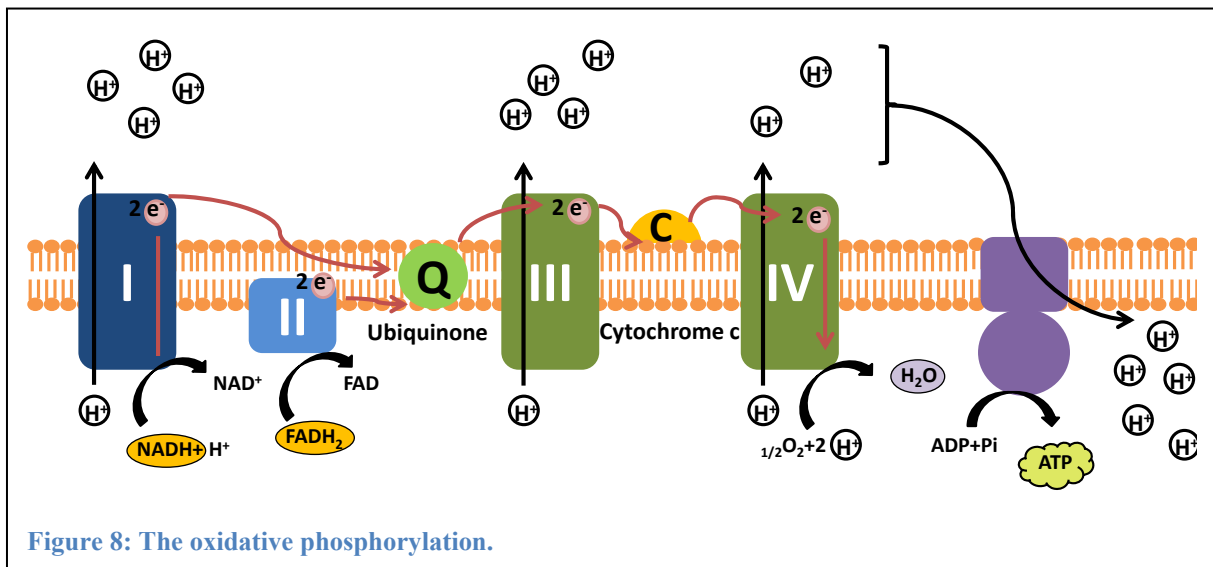


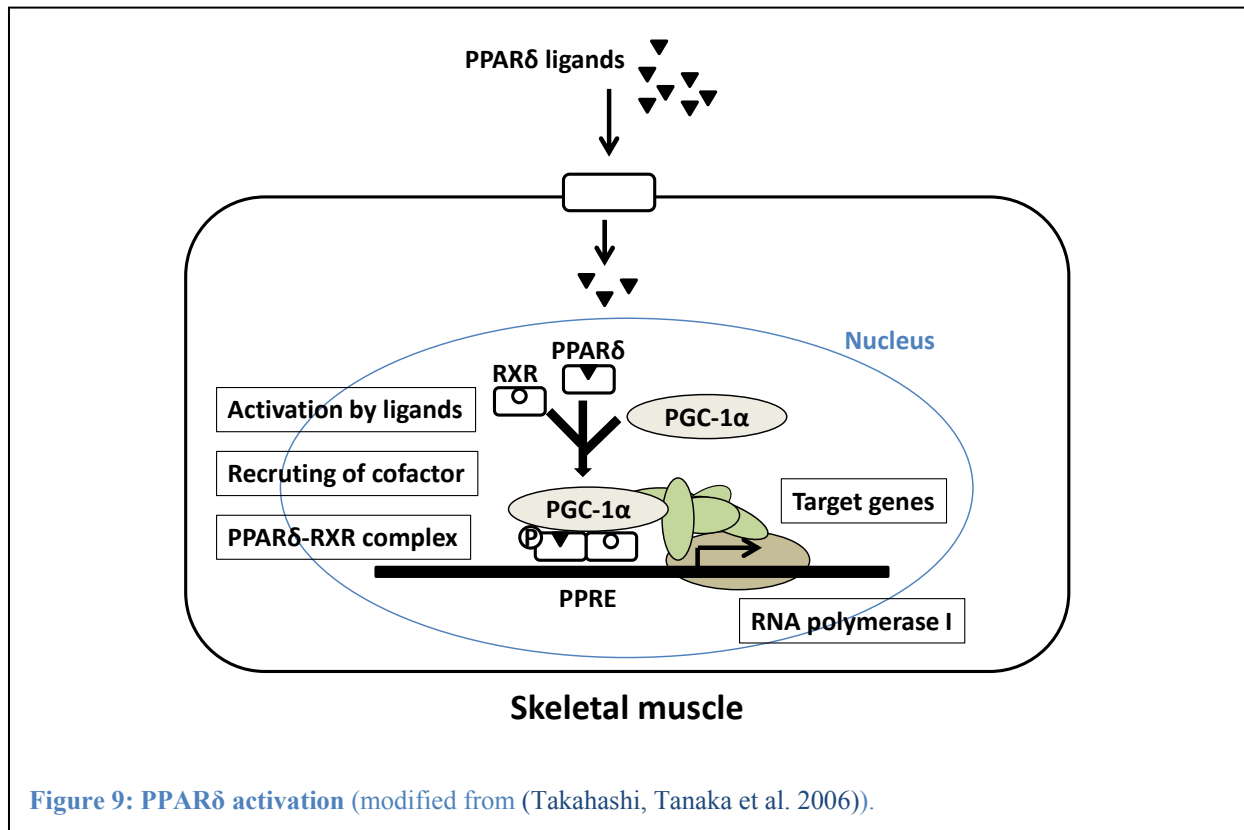
Figure 8: The oxidative phosphorylation.

### 1.4.3 The PPAR signaling and metabolism

PPARs (peroxisome proliferator activated receptors) are transcription factors belonging to the nuclear receptor family. PPARs form heterodimers with retinoid X receptors (RXR), and through the assistance of co-activators such as PGC1α (peroxisome proliferator-activated receptor γ coactivator 1α), they regulate gene transcription (Figure 9). Three isoforms of PPAR exist in mammals, which differ in biological function and tissue distribution: PPARα, PPARγ and PPARδ (also called PPARβ).

The PPARα isoform is expressed in tissues with high metabolic flux, such as the heart and liver. The γ isoform is expressed in various tissues, such as the adipose tissue. PPARδ, how-

ever, is ubiquitously present in the body, with a significant level of expression in skeletal muscle. PGC1 $\alpha$  and PPAR $\delta$  have a synergistic action and interact physically with each other as shown by immuno-precipitation ((Wang, Lee et al. 2003); (Dressel, Allen et al. 2003)).



### *Metabolic phenotype and PPAR $\delta$*

It has been shown that PPAR $\delta$  plays an important role in the transport of fatty acids, their oxidation in muscle and in the control of glycemia (Takahashi, Tanaka et al. 2006).

#### *A) The conversion phenotype*

When PPAR $\delta$  is overexpressed in muscle, muscle fibers transform into a more oxidative phenotype ((Lunde, Ekmark et al. 2007); (Luquet, Lopez-Soriano et al. 2003)) with increased oxidative capacity of glycolytic muscle ((Luquet, Lopez-Soriano et al. 2003); (Wang, Zhang et al. 2004)).

#### *B) Resistance to the obesity*

Overexpression of a constitutive active form of PPAR $\delta$  resulted in mice resistant to obesity during a high fat diet program (Wang, Lee et al. 2003). In contrast, mice deficient in PPAR $\delta$  showed a decreased basal metabolism, decreased heat production, and glucose intolerance (Lee, Olson et al. 2006).

#### 1.4.4 Targets of the PPARs

The *PDK4* gene has been identified as a direct and specific target of PPAR $\delta$  (Degenhardt, Saramaki et al. 2007). In addition to this direct activation by PPAR $\delta$ , there exists also an indirect activation. It has recently been shown that FoxO1 is a specific target of PPAR $\delta$  (Nahle, Hsieh et al. 2008) and that FoxO1 in turn up-regulates the transcription of *PDK4* (Furuyama, Kitayama et al. 2003). The signaling pathway PPAR $\delta$   $\Rightarrow$  FoxO1  $\Rightarrow$  PDK4 may therefore create a positive feed-back loop and enhance the transcription of *PDK4*.

The kinase PDK4 phosphorylates the PDHc thereby decreasing its activity (Constantin-Teodosiu, Baker et al. 2009). Thus, activation of PPAR $\delta$  is able to inhibit PDH by activating the transcription of *PDK4*. However, the metabolic impact on the oxidation of pyruvate has so far not been investigated.

### 1.5 Regulation of muscle mass

The maintenance of muscle mass is dependent on different signaling pathways that control the balance between the processes leading to atrophy and hypertrophy. Atrophy is characterized by a decrease in fiber diameter and increased protein degradation. In contrast, hypertrophy is characterized by an increase in size of muscle fibers and an increase of protein synthesis.

#### 1.5.1 Muscle atrophy

Muscle atrophy or muscle loss can occur during pathophysiological conditions such as aging and cancer. It is characterized by a decrease in fiber diameter and number of cytoplasmic organelles such as nuclei and mitochondria. Muscle atrophy is characterized by a decrease in the number of myonuclei by apoptosis ((Allen, Roy et al. 1999); (Ferreira, Neuparth et al. 2008)). Such unbalance of the nucleocytoplasmic ratio impairs the balance between protein synthesis and proteolysis in favor of a decrease in protein synthesis. During muscle atrophy, the signaling pathways are deregulated towards proteolysis (Figure 10) with subsequent activation of the different enzyme systems necessary for this function, which are: the proteasome ubiquitin pathway-dependent ubiquitin-ligases MuRF1 (Muscle Ring Finger protein 1) and atrogin-1/MAFbx (Muscle Atrophy Fbox) ((Bodine, Latres et al. 2001); (Gomes, Lecker et al. 2001)).

#### *The FoxO pathway*

In skeletal muscle tissue, there are three isoforms of FoxO transcription factors (Forkhead box O), FoxO1, FoxO3 and FoxO4. This family of transcription factors plays a crucial role in protein degradation. Their function is inhibited by their phosphorylation *via* the Akt pathway.

Once phosphorylated, the FoxO proteins are excluded from the nucleus and cannot activate the expression of a number of target genes involved in muscle atrophy (also called atrogenes) such as atrogin-1/MAFbx and MuRF1.

Activation of FoxO proteins *via* their dephosphorylation occurs during muscle atrophy if the signaling pathways such as the PI3K/Akt (Phosphatidyl Inositol 3 Kinase) are deregulated (Stitt, Drujan et al. 2004). Overexpression of FoxO3 causes muscle atrophy (Sandri, Sandri et al. 2004). The role of FoxO3 is inhibited by the expression of PGC1 $\alpha$ , a member of the super-family of nuclear receptors acting as transcription factor of target genes (Sandri, Lin et al. 2006).

FoxO1 is also involved in the loss of muscle mass (Kamei, Miura et al. 2004). Transgenic mice overexpressing this factor have a body weight lower than that of control mice. FoxO1 is a negative regulator of the expression of genes encoding the structural proteins of type I fibers, such as the slow myosin isoform, the slow troponin isoform and the  $\alpha$ -tropomyosin, which leads to impaired skeletal muscle function (Kamei, Miura et al. 2004). In C<sub>2</sub>C<sub>12</sub> myoblasts, the activation of FoxO1 decreases the mTOR (mammalian Target Of Rapamycin) pathway, which is involved in the control of protein synthesis and increases the expression of 4EBP1 (eukaryotic initiation factor 4E binding protein 1). 4EBP1 is a negative regulator of initiation of translation and its upregulation thus leads to a decrease in protein synthesis (Southgate, Neill et al. 2007).

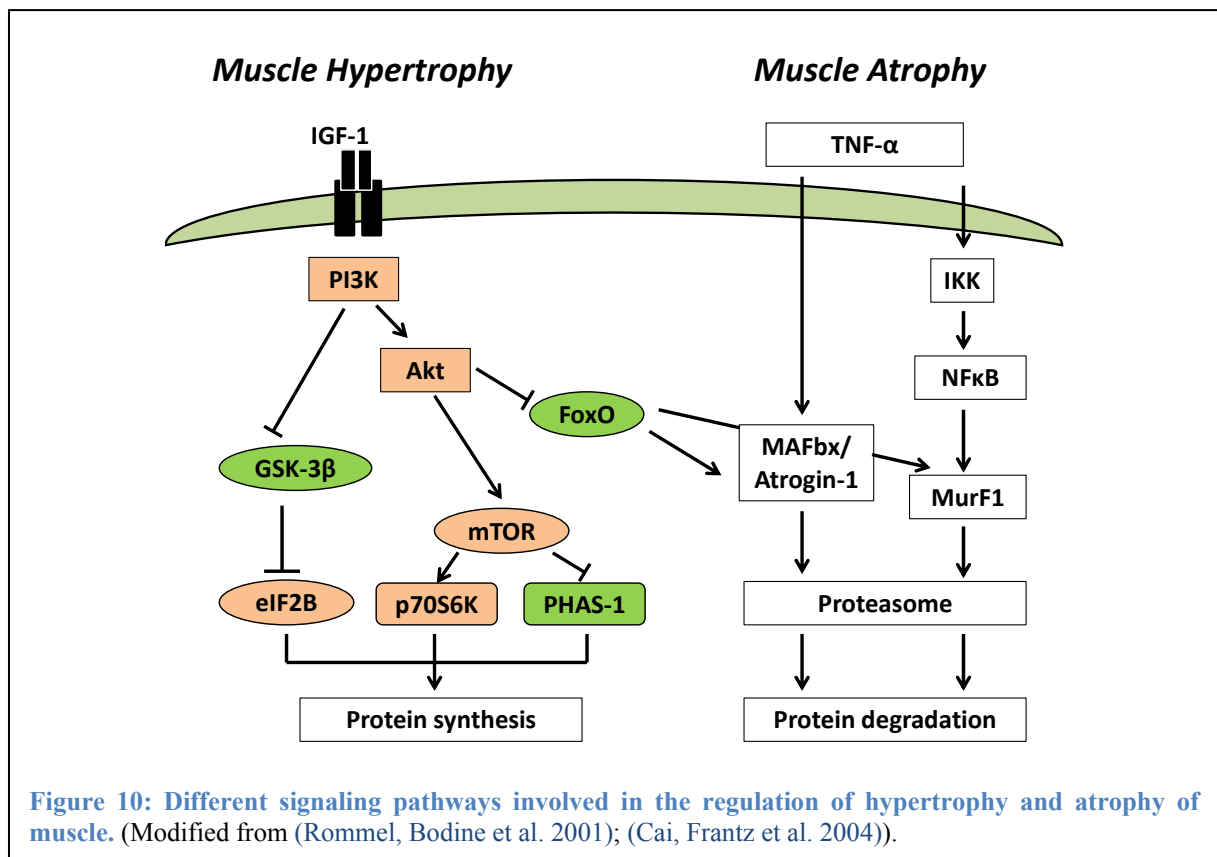
### *The NF $\kappa$ B pathway*

Activation of NF $\kappa$ B (nuclear factor kappa B) pathway is implicated in several pathophysiological conditions characterized by the loss of muscle mass. Indeed, the activation of NF $\kappa$ B in mice induces ubiquitin-dependent proteolysis and significant overexpression of the ligase MuRF1 but not atrogin-1/MAFbx (Figure 10) (Cai, Frantz et al. 2004). Consistent with these data, it was reported that NF $\kappa$ B knockout-mice are resistant to atrophy secondary to the expression inactivation of atrogenes like atrogin-1/MAFbx and MuRF1 (Hunter and Kandarian 2004).

### *The Myostatin/BMP pathway*

The growth factor myostatin (which will be detailed in chapter III) also contributes to muscle atrophy. Durieux and collaborators induced ectopic expression of the myostatin gene after electrotransfer into the *tibialis anterior* muscle of adult rats (Durieux, Amirouche et al. 2007). They reported that overexpression of myostatin causes a significant decrease in muscle mass,

fiber cross-sectional area and muscle protein content. No decrease in the number of fibers was found. The overexpression of myostatin has also caused a significant decrease in the expression of genes encoding muscle structural proteins (e.g. MyHCIIb, troponin I and desmin), as well as a decrease in the expression of MyoD and myogenin. Myostatin inhibits Akt phosphorylation and consequently induces an increase in active FoxO1. This activates the expression of related atrophy genes (McFarlane, Plummer et al. 2006). A recent study identified a critical role for the BMP pathway in adult muscle maintenance, growth and atrophy. The authors showed that inhibition of BMP signaling causes muscle atrophy, abolishes the hypertrophic phenotype of myostatin deficient mice and strongly exacerbates the effects of denervation (Sartori, Schirwis et al. 2013).



## The JNK and MAPK pathway

The studies performed on the *soleus* muscle of suspended rats have shown that the atrophy is associated with increased activity of P38 MAPK (Mitogen-Activated Protein Kinase) and JNK (Jun NH2-terminal kinase) (Childs, Spangenburg et al. 2003). JNK decreases protein synthesis *via* downregulation of the signal induced by insulin and a reduction of Akt activity.

This contributes to the development of insulin resistance during muscle atrophy (Hilder, Tou et al. 2003).

### *Oxidative stress*

Muscle atrophy may be associated with oxidative stress and the production of reactive oxygen species (ROS). It has been shown that NFκB signaling pathways (Li, Atkins et al. 1999) and FoxO (Furukawa-Hibi, Yoshida-Araki et al. 2002) can be activated by ROS. As a result, ROS and oxidative stress can initiate the activation of signaling pathways leading to muscle atrophy (Furukawa-Hibi, Yoshida-Araki et al. 2002).

### **1.5.2 Muscle hypertrophy**

Muscle hypertrophy is characterized by an increase in muscle mass resulting from an increase in the size (hypertrophy) and/or the number of fibers (hyperplasia). Several studies have shown the implication of satellite cells in muscle growth by promoting both protein synthesis and maintenance of the nuclear-cytoplasmic domain (ratio of cytoplasm/number of myonuclei) (Moss and Leblond 1971). Several signaling pathways are involved in the hypertrophic process and are responsible for the increase in protein synthesis and cell survival.

### *The IGF1-Akt signaling pathway*

The involvement of IGF1 in skeletal muscle hypertrophy has been shown by many studies. IGF1 leads to an increase of muscle mass by stimulating PI3K/Akt signaling pathway, an important pathway for protein synthesis (Rommel, Bodine et al. 2001). Its role has been confirmed in transgenic mice with overexpression of this factor in skeletal muscle, which causes muscle hypertrophy ((Coleman, DeMayo et al. 1995); (Musaro, McCullagh et al. 2001)). In addition, ectopic IGF1 expression in *gastrocnemius* and *soleus* muscles of adult mice also causes muscle hypertrophy (Alzghoul, Gerrard et al. 2004).

The molecular mechanisms responsible for muscle hypertrophy involve the PI3K/Akt pathway and its downstream targets (mTOR, S6K, eIF2B). Several studies have demonstrated the major role of Akt as a mediator of muscle hypertrophy ((Rommel, Bodine et al. 2001); (Lai, Gonzalez et al. 2004)). For example, the hypertrophy of muscle fibers can be induced through expression of a constitutively active form of Akt. The hypertrophy occurs *via* a marked increase in fiber size and the activation of the protein synthesis pathways (Lai, Gonzalez et al. 2004).

A recent study showed that transgenic mice overexpressing an active form of Akt1 have a muscle hypertrophy, which is due to the increase in the size specifically of muscle fibers type IIb and is accompanied by an increase in the strength of these mice (Izumiya, Hopkins et al. 2008). In contrast, mice with an inactivated Akt1 gene showed muscle growth retardation and muscle atrophy (Yang, Tschopp et al. 2004).

### *The mTOR/S6K pathway*

The mTOR pathway is one of the downstream targets of the PI3K/Akt signaling pathway. The role of mTOR in muscle growth has been demonstrated *in vivo* by the observation that administration of rapamycin, an mTOR inhibitor, blocks muscle hypertrophy (Pallafacchina, Calabria et al. 2002). The positive effect of mTOR on protein synthesis is mediated through the phosphorylation of the S6K protein (ribosomal protein S6 kinase) a protein involved in the regulation of mRNA translation into proteins (Ohanna, Sobering et al. 2005).

### *The GSK3 $\beta$ pathway*

Control of protein synthesis also requires the regulation of the activation of the protein GSK3 $\beta$  (glycogen synthase kinase 3  $\beta$ ), another downstream target of the PI3K/Akt pathway. GSK3 $\beta$  blocks activation of the eIF2B protein (eukaryotic initiation factor 2B), which is involved in protein synthesis. An *in vitro* study showed that inactivation of GSK3 $\beta$  induced significant hypertrophy of myotubes (Rommel, Bodine et al. 2001).

## 1.6 Muscle regeneration

Skeletal muscle is a stable tissue which under normal circumstances does not suffer much damage and requires little turnover from the nuclei. However, damage caused by mechanical or chemical trauma or disease causes a complete, fast and extensive regenerative response.

Muscle regeneration is characterized by two phases: a **degenerative phase** and a **regenerative phase**. The initial event in muscle degeneration is characterized by necrosis. This process is usually accompanied by an inflammatory reaction as evidenced by the infiltration of neutrophils and macrophages. After 48 hours, macrophages become the predominant cell type and act as phagocytes of cellular debris (Skuk, Caron et al. 2003).

Muscle degeneration is followed by the process of **muscle repair**, which is in some ways repeat steps of myogenesis. Satellite cells, the skeletal muscle stem cells, become activated and they leave their quiescent state, begin to proliferate and generate progenitors. At this stage, the expression of Pax7 decreases and favours the expression of Myf5 and MyoD. The

expansion of these cells provides enough cells to repair the damaged muscle. The expression of myogenin and Mrf4 initiates the differentiation and fusion of myoblasts with the broken fibers for their repair, or the fusion of multiple myoblasts to form newly regenerated fibers. Ultimately, regenerated muscle is morphologically and functionally identical as it was before its damage.

### **1.7 Response of skeletal muscle to repetitive muscle damage**

Muscle fiber integrity is strongly reduced in a number of neuromuscular disorders, notably in muscular dystrophies, leading to repetitive cycles of degeneration and regeneration. Muscle fibers in patients suffering from dystrophic muscle are very sensitive to mechanical stress or other events that can damage it, because it is much more fragile than normal muscle. Constant rounds of degeneration and regeneration require frequent and prolonged proliferation of satellite cells. If the satellite cells are exhausted, muscle cannot be repaired any more which leads to muscle wasting. Over time, the muscle fibers decrease in size and number, because they are not repaired and are gradually replaced by connective and adipose tissue ((Irintchev, Zweyer et al. 1997); (Luz, Marques et al. 2002)).

## 2. CHAPTER: DUCHENNE MUSCULAR DYSTROPHY

### 2.1 History and disease description

Duchenne muscular dystrophy (DMD) was described for the first time in 1852 by Edward Meryon. Then, the french physiologist Guillaume Benjamin Duchenne de Boulogne characterized the disease in more detail, which attributed his name to the disease. DMD is a recessive X-linked disorder, its incidence is about 1 in 3,500 in new born males around the world (Emery 1993). DMD is one of the more severe forms of muscular dystrophy and it is characterized by progressive muscle wasting and loss of strength. Around the age of 4 years a patient with DMD already suffers from an evident lack of strength. Due to the progressive nature of the muscle disease, there is a linear decline in muscle strength in the arms and the legs, making the children wheelchair dependent by the age of 7-12 years (Figure 11). In their teens many patients develop breathing difficulties that can result in fatal lung infections. DMD is characterized by a very high activity of creatine phosphokinase in the serum, which highlights the widespread damage of muscle tissue. Indeed, the muscle tissue of DMD patients shows evidence of multiple cycles of degeneration/regeneration. Over time, there is a replacement of muscle fibers by connective tissue (fibrosis) and fatty tissue that eventually fills the entire muscle. Patients usually die from respiratory or cardiac failure, or from pulmonary infections. Today, with well defined standards of care, notably the combination of non-invasive nocturnal ventilation, surgical vertebral arthrodesis and cardio-protective medication, life expectancy of patients has significantly improved up to 40 years. Although extremely rare, women can also be affected by DMD (Penn, Lisak et al. 1970). In the case of non-random X-inactivation most women are asymptomatic, but they have an increased risk to develop a cardiomyopathy.



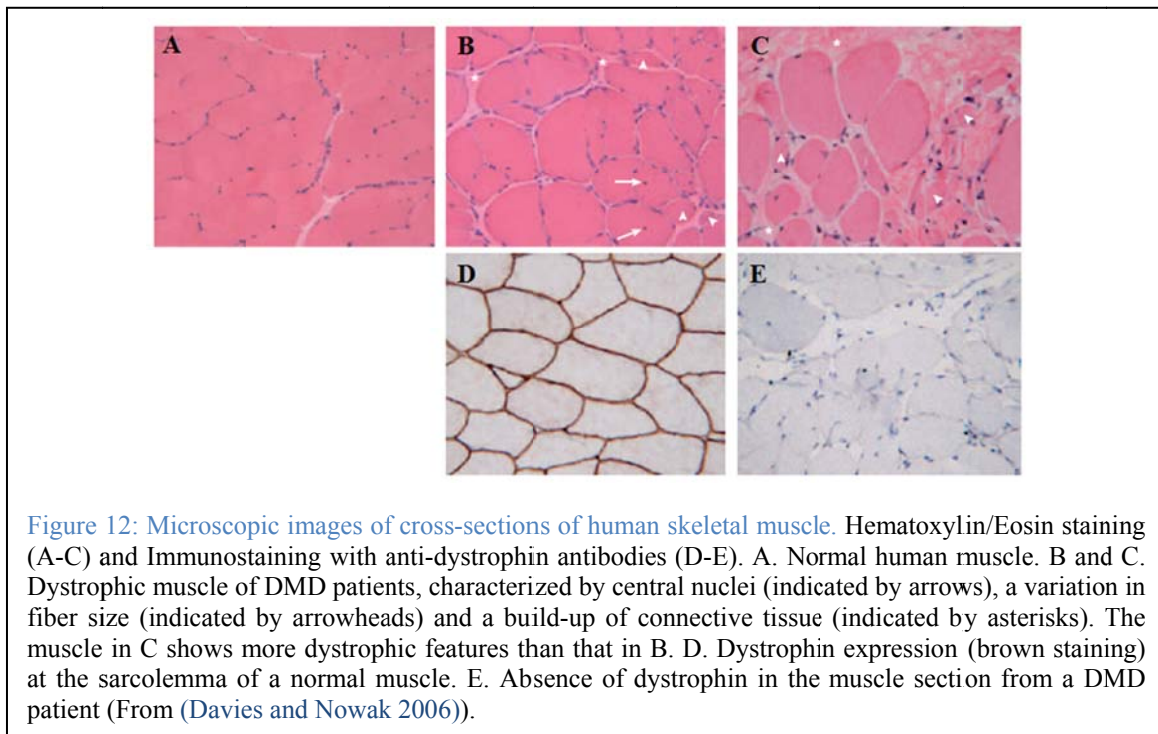
**Figure 11: Mode of rising from the ground (Gower's sign) of a boy suffering with Duchenne muscle dystrophy.** (from (Engel, Rodrigue et al. 1994)).

## 2.2 The *DMD* gene

The gene whose mutations is responsible for DMD was first located on the short arm of the X-chromosome in the Xp21 region, following the observation of a deletion in this region in DMD patients (Francke, Ochs et al. 1985), or of a translocation of this region (Jacobs, Hunt et al. 1981). The location of the DMD gene locus was then confirmed by the subtractive hybridization technique, and identification of the clone containing the *DMD* gene (Monaco, Bertelson et al. 1985). Gene fragments were first isolated (Monaco, Neve et al. 1986) before the cloning of the complete gene was achieved (Koenig, Hoffman et al. 1987).

Having a total size of 2.6 Mb, the *DMD* gene is the largest known human gene (Lander, Linton et al. 2001). It comprises 79 exons and very large introns (some exceed 100 kb). However, the size of the messenger RNA (mRNA) of the *DMD* gene is only 14 kb (Koenig, Hoffman et al. 1987).

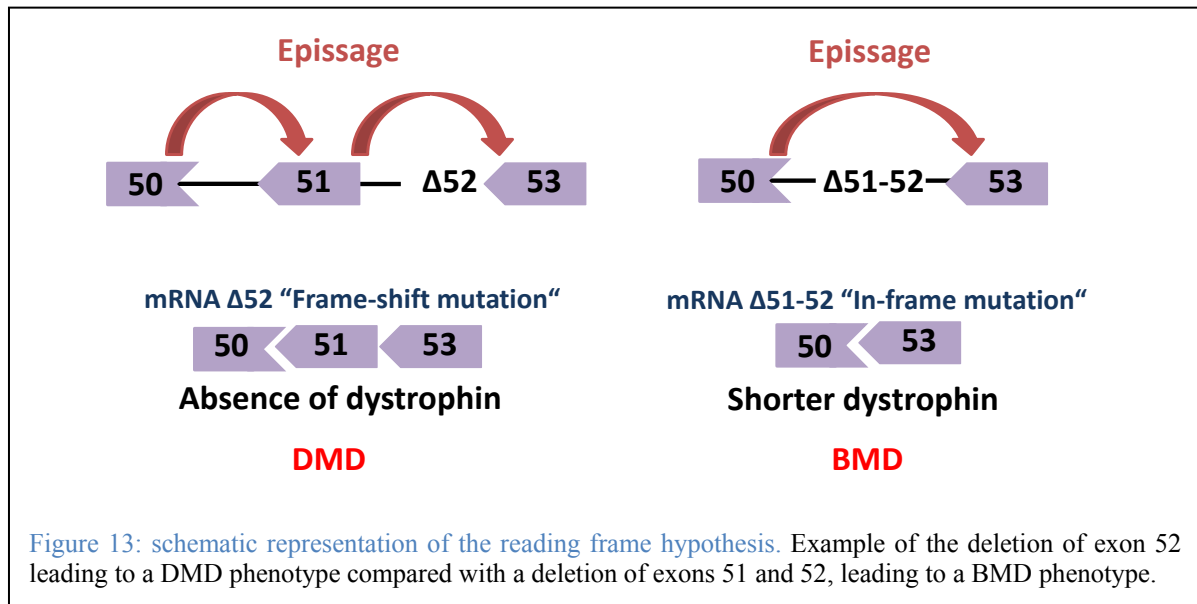
The protein encoded by the *DMD* gene was identified shortly after the cDNA cloning, and was called "dystrophin" (Hoffman, Monaco et al. 1987). Its expression is not detectable in DMD patients, neither by Western blot nor by microscopic analysis of cross sections of muscle biopsies, while it is detected and located at the sarcolemma on muscle biopsies from healthy subjects ((Bonilla, Samitt et al. 1988); (Watkins, Hoffman et al. 1988)) (Figure 12).



### 2.3 Mutations of the *DMD* gene

DMD is not the only disease caused by a mutation in the dystrophin gene. Becker muscular dystrophy (BMD) is characterized by less severe symptoms, slower disease progression and less severe muscle wasting than the DMD (Mostacciuolo, Lombardi et al. 1987). The cause for the difference between DMD and BMD is the conservation of the reading frame despite the mutation. This "reading frame hypothesis" has been verified in 96% of DMD patients and 93% of BMD patients (Tuffery-Giraud, Beroud et al. 2009).

Mutations that maintain the reading frame (in-frame mutations) generally result in a truncated but partly functional dystrophin and usually cause BMD. In DMD patients, however, mutations disrupt the reading frame (frame-shift mutations), which eventually lead to total absence of dystrophin (Koenig, Monaco et al. 1988) (Figure 13).



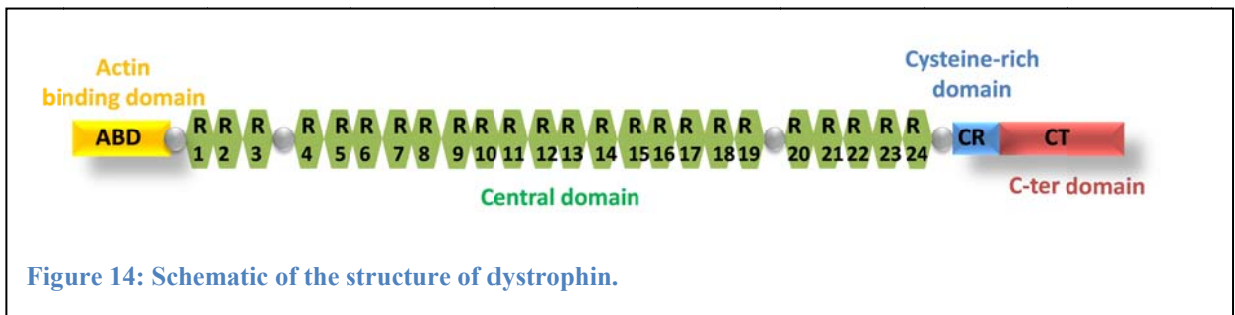
In DMD and BMD, 65% of the pathogenic changes are large partial deletions that usually affect multiple exons and 5% are partial duplications of one or more exons (Abbs and Bobrow 1992). The remaining 35% of the pathogenic changes are small duplications, deletions or point-mutations.

### 2.4 Dystrophin and the Dystrophin Associated Protein Complex

Dystrophin is a protein with a molecular weight of 427 kDa. It is located at the inner-membrane of the muscle cell, linked to a complex of many other proteins (Michele and Campbell 2003). The presence of dystrophin and its complex is important for the mechanical

stability of the cell membrane during muscle contraction and the muscle fibers' resistance to stretch. Dystrophin comprises four domains:

- The first 240 amino acids of the N-terminal portion of dystrophin form the **actin binding domain** (Hammonds 1987).
- The second part, the central domain consists of an  $\alpha$ -helix (**Rod domain**) of 24 tandem repeats that gives dystrophin a stick-like shape. This structure is similar to spectrin, another protein of the cytoskeleton (Koenig and Kunkel 1990).
- The third **cysteine-rich domain** binds to  $\beta$ -dystroglycan, the central part of the multimeric dystrophin complex. It is the  $\beta$ -dystroglycan, which forms the transmembrane bridge between the intracellular and extracellular proteins.
- The fourth part is the **C-terminal domain**, which binds to other members of the complex (Michele and Campbell 2003) (Figure 14).



These different regions allow dystrophin to bind to the proteins that form the DAPC complex (**D**ystrophin-**A**ssociated **P**rotein **C**omplex), and also to bind to the cytoskeleton, which is essential for maintaining the architecture and function of the muscle.

Dystrophin is found in all types of muscle tissue. The lack of dystrophin and its associated protein complex causes instability in the muscle fiber membrane. Thus, in DMD patients, physical stress caused by muscle contraction or stretching cause membrane ruptures (Zubrzycka-Gaarn, Bulman et al. 1988).

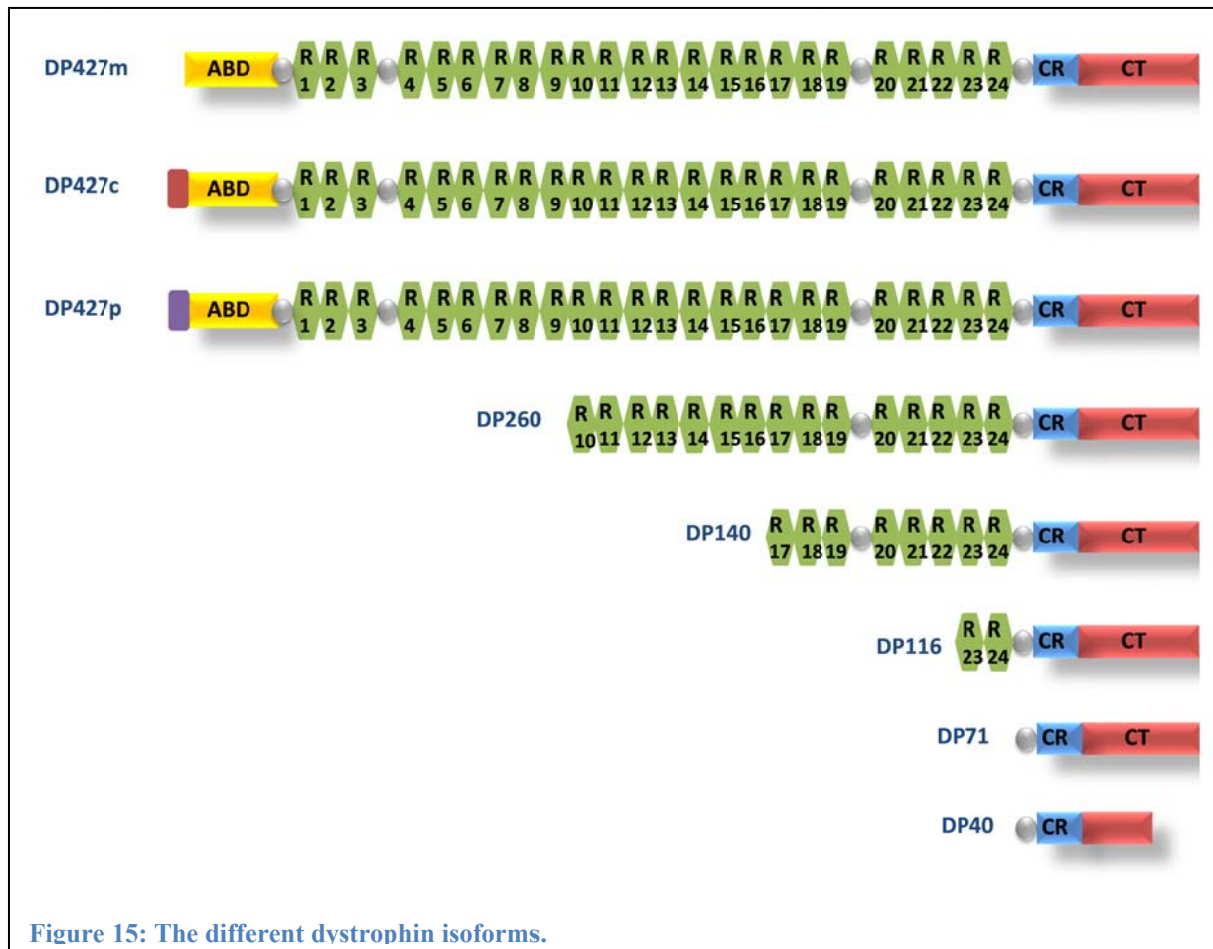
## 2.5 Dystrophin isoforms

Although dystrophin has initially been identified in skeletal muscle and in cardiomyocytes, there are at least seven promoters from which different isoforms are expressed. These isoforms can be divided into two classes: **full-length isoforms** of about 427 kDa, and **shorter isoforms**, which are expressed from internal promoters.

In addition to muscle dystrophin, also called Dp427m, two other full-length dystrophins are produced: Dp427c and Dp427p ((Boyce, Beggs et al. 1991); (Chelly, Hamard et al. 1990); (Gorecki, Monaco et al. 1992)). Both isoforms have their own first exon (Chelly, Hamard et al. 1990), which is spliced to exon 2 of the Dp427m transcript (Boyce, Beggs et al. 1991). The Dp427c isoform is mainly expressed in cortical neurons and in the hippocampus, while Dp427p is found in cerebellar Purkinje cells and also in skeletal muscle at a low level (Gorecki, Monaco et al. 1992). A fourth isoform of 427 kDa was detected at very low levels in lymphocytes (Nishio, Takeshima et al. 1994).

The shorter dystrophin isoforms are expressed from four internal promoters of the *DMD* gene and are named according to their molecular weight ((Byers, Lidov et al. 1993); (Hugnot, Gilgenkrantz et al. 1992); (Lidov, Selig et al. 1995)).

- The Dp260 isoform is preferentially expressed in the retina and is derived from a unique first exon located in intron 29, which is spliced to exon 30 of the Dp427m (D'Souza, Nguyen et al. 1995). Compared to the full-length 427 kDa isoform, Dp260 lacks the N-terminal domain, two hinge regions and nine spectrin-like repeats.
- The DP140 isoform is expressed in the central nervous system from a promoter located in intron 44 (Lidov, Selig et al. 1995). However, the methionine start codon for translation is located in exon 51, forming a very long 5' untranslated region (5'UTR) for this isoform. The DP140 has just the two hinge regions, five spectrin-like repeats, the cysteine-rich and the C-terminal domain.
- The DP116 isoform is specifically expressed in Schwann cells of the peripheral nervous system and in the embryonic brain. This isoform has a unique N-terminal domain encoded by an intron located in exon 55 and spliced to exon 56 of the Dp427m encoding the distal portion of the 21th repeat (Byers, Lidov et al. 1993).
- Isoforms Dp71 and DP40 are expressed ubiquitously in non-muscle tissue ((Hugnot, Gilgenkrantz et al. 1992); (Tinsley, Blake et al. 1993)). They both come from a single first exon present in intron 62, spliced to exon 63 ((Blake, Love et al. 1992); (Feener, Koenig et al. 1989)) and have a C- terminal alternative domain as compared to the other isoforms (Figure 15).

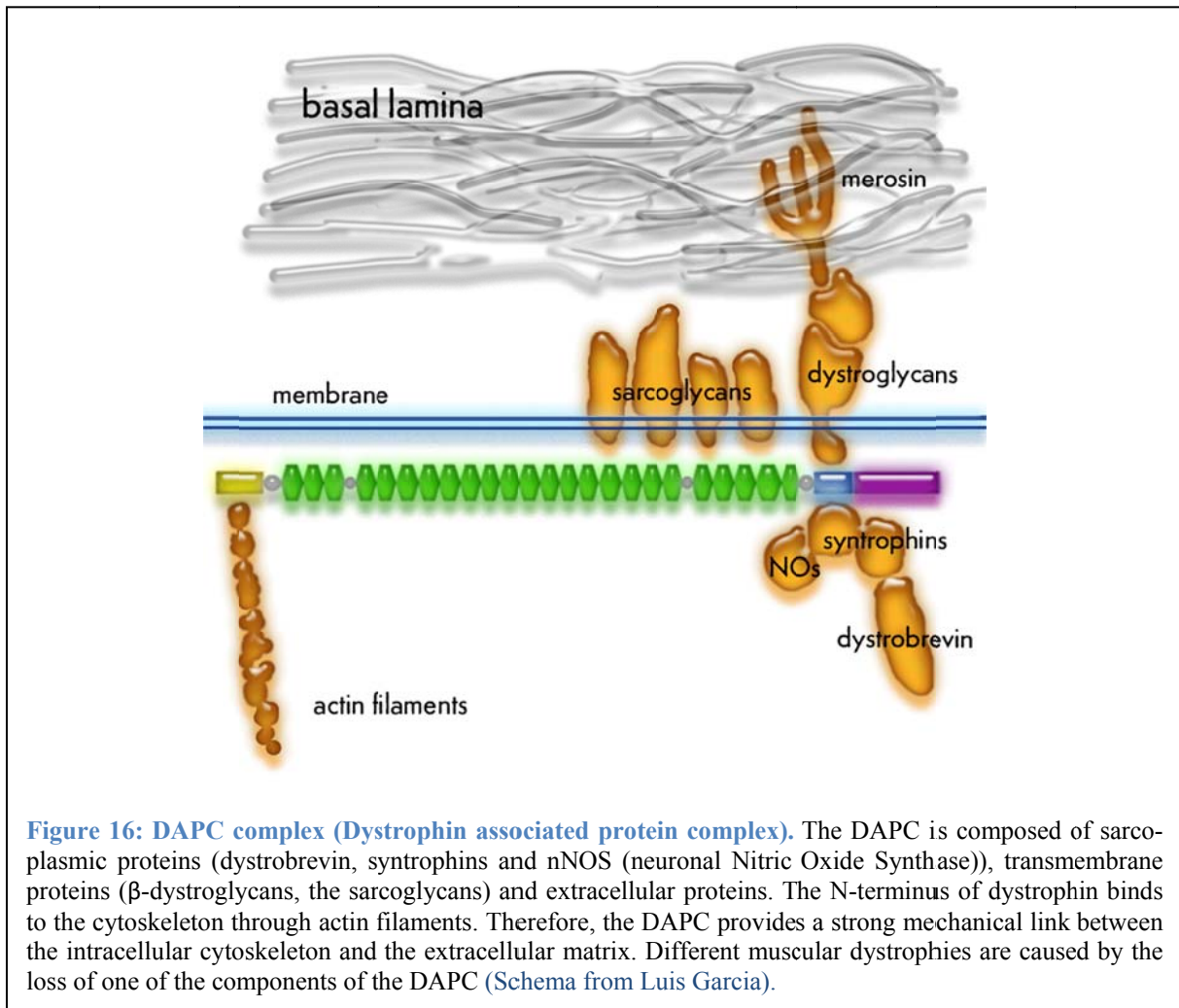


Dp427 is the only isoform with a binding domain for actin. The short isoforms can therefore just bind to the proteins of the DAPC, probably for stabilization (Blake, Weir et al. 2002). Moreover, they have other functions such as the Dp260 for the normal function of the retina (D'Souza, Nguyen et al. 1995) and the Dp71 a possible role for embryonic development (Howard, Dally et al. 1999). The nature of the symptoms present in DMD and BMD patients largely depends on the location of the mutation. For example, mutations that affect regions of the DMD gene involved in the expression of Dp427c, Dp427p, DP140, or DP116 can cause mental retardation ((Byers, Lidov et al. 1993); (Gorecki, Monaco et al. 1992)).

## 2.6 The Dystrophin Associated Protein Complex

At the level of the sarcolemma, dystrophin is part of a macromolecular protein structure called the "Dystrophin-Associated Protein Complex" (DAPC). This complex is essential for maintaining the structure of the muscle fiber. Dystrophin isoform Dp427m is bound to the intracellular cytoskeleton *via* its N-terminal domain, which is associated with the actin filaments while the C-terminal domain interacts with the proteins of DAPC and thereby transmit forces during muscle contraction (Lapidos, Kakkar et al. 2004). This multimeric complex is com-

posed of sarcoglycans  $\alpha$ ,  $\beta$ ,  $\gamma$  and  $\delta$ , sarcospan, dystroglycans  $\alpha$  and  $\beta$ , the dystrobrevins and syntrophins (Yoshida and Ozawa 1990). The actin filaments are bound to the N-terminal domain and to the spectrin like-repeats domain of dystrophin (Rybakova, Patel et al. 2000), while the  $\beta$ -dystroglycan, linked to the cysteine-rich domain, is associated non-covalently to the  $\alpha$ -dystroglycan to form the dystroglycan "subunit" of DAPC complex. To complete the link between the cytoskeleton and the extracellular matrix, the highly glycosylated  $\alpha$ -dystroglycan binds to laminin in the basal lamina (Ibraghimov-Beskrovnya, Ervasti et al. 1992). The dystrobrevins and syntrophins are both cytoplasmic proteins involved in cell signaling ((Bhat, Adams et al. 2013); (Davies and Nowak 2006)) and are linked to the C-terminal domain of dystrophin, whereas nNOS is localized at the sarcolemma and binds to the central domain of dystrophin (Lai, Thomas et al. 2009) (Figure 16).



Mutations in genes encoding the protein members of the DAPC have been associated with other forms of muscular dystrophies. For example, mutations in the sarcoglycans can lead to limb-girdle muscular dystrophy ((Tome, Evangelista et al. 1994); (Eymard, Romero et al. 1997); (Hack, Groh et al. 2000)).

### 2.7 Animal models for DMD

For DMD there are both natural and man-made animal models in which mutations in the dystrophin gene lead to muscle dystrophy with all its pathophysiological consequences. From the existing models I describe here the *mdx* mouse (**m**uscular **d**ystrophy, **X**-linked), which we used in our project, the GRMD dog (**G**olden **R**etriever **M**uscular **D**ystrophy), and the HFMD cat (**H**ypertrophic **F**eline **M**uscular **D**ystrophy).

#### 2.7.1 The *mdx* mouse

The *mdx* mouse was the first identified animal model for human DMD. This X-linked muscular dystrophy occurred spontaneously in the C57BL/10ScSn mouse line (Bulfield, Siller et al. 1984). A cytosine to thymine substitution in exon 23 results in a premature termination codon (Sicinski, Geng et al. 1989) and produces a nonfunctional truncated dystrophin, which is degraded (Hoffman, Monaco et al. 1987).

Similar to patients with DMD, *mdx* mice show an absence of the dystrophin protein and reduced dystrophin mRNA levels (Chamberlain, Gibbs et al. 1988). However, after an initial de- and regeneration cycle, clinical disease progression in the *mdx* mouse is much slower as in DMD patients if related to the respective life span (Bulfield, Siller et al. 1984).

During the first weeks of life, damaged fibers are replaced by new fibers. These are regenerated from satellite cells and are resistant to further degeneration. An exception to the comparably slow progression of the muscle pathology in the *mdx* mice is the rapid progressive degeneration of the diaphragm. Muscles from *mdx* mice have a significantly reduced specific strength as compared to normal mice (Lynch, Hinkle et al. 2001). Although *mdx* mice share not all pathological features with DMD patients, they are nevertheless a very attractive model for evaluating various therapeutic approaches.

#### 2.7.2 The GRMD dog

Several types of dystrophic dogs were described and the corresponding genetic cause determined ((Schatzberg, Olby et al. 1999); (Winand, Edwards et al. 1994)). The most studied and best characterized model to date is the Golden Retriever Muscular Dystrophy dog (GRMD). The mutation in the *Dmd* gene was found in the splice acceptor site of exon 7. This splice site

mutation leads to skipping of exon 7 in the mRNA, disrupts the open reading frame and leads to a stop codon in exon 8 (Sharp, Kornegay et al. 1992). Muscle weakness in these dogs becomes apparent around the age of 2 months and their lifespan is significantly reduced (Valentine, Cooper et al. 1990).

At the histological level, the histopathology is similar to that of DMD patients with a heterogeneity of fiber size, the presence of degenerated hypertrophied fibers, focal necrosis with macrophage infiltration as well as small regenerating fibers (Valentine, Cooper et al. 1988). The creatine kinase activities in serum are very high and with age the amount of connective tissue increases and also the percentage of central nuclei. There is a significant adipose metaplasia particularly in the temporal muscles, the diaphragm and biceps femoris. These characteristics make the GRMD dog a close model of the human disease.

### 2.7.3 The HFMD cat

The HFMD cat (Hypertrophic Muscular Dystrophy Felin) has a large deletion (200 kb) in the DMD promoter, which causes a deficiency of dystrophin in skeletal and cardiac muscles. These dystrophic cats were described as having Hypertrophic Feline Muscular Dystrophy (HFMD) due to predominantly hypertrophic phenotype they present. The disease is characterized by muscle degeneration and regeneration with accumulation of calcium deposits in the muscle fibers without development of fibrosis. However, dystrophic cats have not been widely used as DMD models due to the limited similarity of their phenotype with humans (Shelton and Engvall 2005).

## 2.8 Revertant fibers

In muscle biopsies of DMD patients and of animal models, often some clusters of fibers can be observed that express dystrophin ((Burrow, Coover et al. 1991); (Hoffman, Morgan et al. 1990)). In these so-called “revertant fibers”, the dystrophin is properly localized and probably functional since proteins of the DAPC can also be detected. These fibers are gathered in small groups and can range between 1 and 10% of muscle fibers in mice. The number of fibers increases with age in both DMD patients (Fanin, Danieli et al. 1995) and *mdx* mice (Lu, Morris et al. 2000).

The genesis of revertant fibers is unclear. However, mutation involves the restoration of the reading frame and the synthesis of a truncated dystrophin (Fanin, Danieli et al. 1995). Various hypotheses have been forwarded to explain this exon skipping: (i) The theory of “reversion by somatic suppression” (Winnard, Mendell et al. 1995) or (ii) the “alternative splicing” hypoth-

esis (Lu, Morris et al. 2000). The theory of somatic reversion ((Klein, Coover et al. 1992); (Winnard, Mendell et al. 1995)) involves the appearance of a second mutation correcting the effect of the first one. The hypothesis of alternative splicing seems also plausible (Wilton, Dye et al. 1997).

### 2.9 Treatment strategies for DMD

Until now, there is no effective therapy to stop the progression of the disease, although several promising experimental strategies are currently under investigation. These include gene therapy which aims to reintroduce a recombinant functional version of the dystrophin gene using adeno-associated vectors, lentiviral or adenoviral vectors, as well as the modification of pre-mRNA of dystrophin through splice modulation such as exon skipping. Several clinical trials in DMD patients have already been performed, with exon skipping being the most advanced therapeutic strategy. In parallel, cell therapies and pharmacological approaches such as the upregulation of utrophin or the inhibition of myostatin have also been studied.

All these strategies are facing major challenges imposed by the nature of the muscular dystrophy. Indeed, the skeletal muscle is the most abundant tissue in the body and is composed of large multinucleated fibers with nuclei that can no longer divide. Therefore, any strategy on cell or gene replacement must restore the expression of relevant genes in hundreds of millions of postmitotic nuclei, which are integrated in a highly structured cytoplasm and are surrounded by a thick basal lamina, but also have to deal with the immune responses to a “foreign” protein. Similarly, most pharmacological approaches would interact with the biochemical mechanisms of fiber degeneration that involve pathways such as calcium influx and activity of proteases. Inhibitors of these processes have often a systemic toxicity.

#### 2.9.1 Gene therapy

This approach makes use of the virus’ ability to enter a variety of cell types and express their genomes. The goal is to provide patients with an alternative functional copy of the *DMD* gene rather than repairing the locus in the genome of the patient. Most work in this field has tried to optimize the delivery methods for targeted expression and the long-term expression of dystrophin in the muscles of the whole body.

Three types of viral vectors have been used by researchers to study gene delivery to dystrophic muscle: **(i)** adenoviral vectors, **(ii)** adeno-associated, and **(iii)** lentiviral vectors. All three vectors have shown some success in transduction and stable expression in striated muscle, but only the Adeno-Associated Virus (AAV) has been used in clinical trials.

### *The Adeno-Associated Virus (AAV)*

The Adeno-Associated Virus (AAV) is a single-stranded DNA virus of 4.7 kb, which requires an association with an adenovirus or herpes virus for replication and assembly. There is a recombinant form (rAAV), which is not carrying viral genes and can be produced in high amounts in the absence of a "helper" virus. This rAAV is capable to infect both dividing and quiescent cells. The problem of the small size of the AAV genome has been corrected through production of dystrophin microgenes (mini and micro-dystrophin) by removing a large part of the "rod" domain and portions of the amino and carboxy terminal domain. The stable expression of genes following intramuscular injection of rAAV persists up to 2 years in mice and more than 7 years in dogs and rhesus monkeys ((Monahan, Samulski et al. 1998); (Herzog, Yang et al. 1999); (Rabinowitz and Samulski 1998)). Injections of a hybrid virus Ad/rAAV were also tried. In *mdx* mice it was possible to recover dystrophin in the majority of muscle fibers with this technique (Goncalves, van Nierop et al. 2005). The rAAV is of great interest for therapy development against muscular dystrophy thanks to its efficacy in reaching capillary networks and infect muscle tissue. This capability has been exploited to develop techniques for systemic delivery of genes in order to produce dystrophin in all skeletal muscles ((Wang, Zhu et al. 2005); (Koppanati, Li et al. 2009)). Unlike adenoviral vectors, AAV vectors appear to have low immunogenicity. A phase I trial for hemophilia B using rAAV2 reported no adverse effects in patients, who received intramuscular injections (Manno, Chew et al. 2003). However, further studies in dogs and humans suggested that these vectors have the potential to induce a cellular immune response that could strongly influence the nature of clinical applications ((Mingozzi, Meulenberg et al. 2009); (Mendell, Campbell et al. 2010); (Wang, Storb et al. 2010)).

### *The major problems of the rAAV gene delivery strategy*

The problems faced by this therapeutic approach comprise the **(i)** production of sufficient quantities of virus, **(ii)** the limited size of the AAV genome (the less immunogenic viral vector), **(iii)** the prevention of an immune response against the viral vector and the newly introduced dystrophin, which – due to its absence in the fetus – would be considered “foreign” by the body.

The problem of the large size (14 kb) of the dystrophin gene was quickly solved by the production of mini- and micro-dystrophins. Indeed, BMD patients may have only 46% of the full-length dystrophin and show only a moderate phenotype of the disease (England, Nicholson et al. 1990). Such gene deletions were the basis for the generation of a mini- and a

micro-dystrophin gene through removal of a large part in the rod domain to allow cloning into the AAV. Systemic administration of a mini-dystrophin with AAV9 has been very efficient in mice and dogs (Pichavant, Chapdelaine et al. 2010). However, a recent clinical trial using intramuscular injections of AAV2 in DMD patients did not restore good expression of dystrophin and induced a T-cell immune response to the epitopes of dystrophin (Mendell, Campbell et al. 2010).

### 2.9.2 The exon skipping

#### *The principle of exon skipping*

A large proportion of DMD cases are caused by a shift of the reading frame leading to the production of a nonfunctional truncated dystrophin. Furthermore, deletions which do not disrupt the reading frame allow the expression of a shorter but partially functional dystrophin as in BMD. Therefore, the DMD phenotype could be theoretically transformed into a BMD phenotype through restoration of the reading frame. In some cases such restoration would be possible *via* exclusion of an additional exon that follows the disruption of the reading frame using an antisense oligonucleotide (AO) during the splicing of the pre-mRNA.

Exon skipping is a promising approach that could benefit up to 83% of DMD patients with deletions (Aartsma-Rus, Fokkema et al. 2009). Antisense oligonucleotides affect splicing by blocking the splice donor or acceptor sites by modifying the secondary structure of the mRNA. The efficiency of these techniques has been demonstrated in cell culture. It has also been tested in *mdx* mice (Alter, Lou et al. 2006) and showed an improvement of the phenotype. Skipping of exon 51 for example could be used for 13% of patients with DMD despite presence of different mutations.

#### *The major problems for the exon skipping strategy*

Several challenges stand between exon skipping drugs and their routine clinical use: **(i)** the restricted entrance to the cell, **(ii)** the relatively rapid elimination from the bloodstream, **(iii)** the variability in efficiency of exon skipping from one muscle to another, and **(iv)** their low efficiency in the heart. In addition, preclinical studies have shown that doses required for functional improvement are too high to make a lifelong treatment feasible that would be envisaged for the majority of patients. Because of this, much hope is placed on the development of PPMOs (Phosphorodiamidate Peptide Morpholino Oligomers), which are oligomers conjugated with peptides. PPMOs have a good potential to penetrate cells and to be easily internalized into muscle cells (Moulton and Moulton 2010) at lower doses ((Jearawiriyapaisarn,

Moulton et al. 2008); (Yin, Lu et al. 2008)) and are efficient in the heart ((Jearawiriyapaisarn, Moulton et al. 2010); (Wu, Moulton et al. 2008); (Wu, Lu et al. 2010)). However, cannot be as easily used in humans as they are highly allergenic.

### 2.9.3 Cell therapies

Cell therapies aim to introduce cells capable of differentiating into new muscle in diseased areas. These can either be myoblasts or stem cells that have the ability to differentiate into muscle cells. This strategy showed some degree of success with myoblast transplantation into the diseased tissue.

Myoblast transplantation involves their isolation from skeletal muscle of a healthy donor, their expansion in culture and administration to dystrophic tissue. The incorporation of myoblasts from the donor into myofibers of the patient leads to a functional gene complementation, which means the expression of both exogenous and host genes in the myofibers (Watt, Lambert et al. 1982). Following the promising results of transplantation into immunodepressed *mdx* mice ((Partridge, Morgan et al. 1989); (Vilquin, Asselin et al. 1994)), this therapy was tested in clinical trials. Unfortunately, these studies failed (Mendell, Kissel et al. 1995). The poor result was attributed to a combination of insufficient immunosuppression of the patients with an insufficient number of transplanted cells ((Gussoni, Pavlath et al. 1992); (Karpati, Ajdukovic et al. 1993); (Mendell, Kissel et al. 1995)). Current strategies are thus directed towards on the use of genetically modified donor myoblasts in order to reduce the patient's immune response ((Li, Kimura et al. 2005); (Kazuki, Hiratsuka et al. 2010)).

### 2.9.4 The pharmacological approach

#### *Pharmacological overexpression of utrophin*

Utrophin is a protein of about 395 kDa, encoded by a gene on chromosome 6 in humans. The primary structure of utrophin is very similar to dystrophin (80%), with an amino-terminal domain rich in cysteine and a carboxy-terminal domain displaying a significant similarity to dystrophin (Tinsley, Blake et al. 1992). Unlike dystrophin, which is expressed in the muscle and to a lesser extent in the brain, utrophin is ubiquitously expressed, mainly at the neuromuscular and myotendinous junctions ((Clerk, Morris et al. 1993); (Tome, Evangelista et al. 1994)). The utrophin is also expressed at the sarcolemma in muscle during development or regeneration ((Khurana, Watkins et al. 1991); (Tinsley, Blake et al. 1992)) and in skeletal muscle of *mdx* mice and DMD patients (Mizuno, Nonaka et al. 1993). Utrophin and dystrophin share a lot of binding partners, for example the actin of cytoskeleton or members of the

DAPC such as  $\alpha$ -dystrobrevin (Peters, Sadoulet-Puccio et al. 1998) and  $\beta$ -dystroglycan (Ishikawa-Sakurai, Yoshida et al. 2004), which bind to the carboxy-terminal domain of utrophin.

A promising pharmacological treatment for DMD seemed to increase the levels of utrophin expression in the muscle fibers of patients in order to compensate for the absence of dystrophin. Studies in the *mdx* mouse have shown that the elevated utrophin levels in dystrophic muscle fibers could restore the sarcolemmic expression of members of the DAPC complex and moderate the dystrophic phenotype (Tinsley, Potter et al. 1996).

Such drug therapies aimed on utrophin overexpression have many advantages as they should be effective for all DMD patients irrespective of their genetic defect and may be administered systemically because overexpression of utrophin in tissues other than muscle does not appear to cause adverse effects (Fisher, Tinsley et al. 2001).

### *Growth factors*

One of the characteristic of the DMD pathology remains the loss of muscle strength which is associated with loss of muscle mass. Some therapeutic approaches are therefore trying to compensate for this loss of muscle force acting on the activation of muscle progenitors or inhibiting negative regulators of muscle growth.

#### *A) Overexpression of IGF-1 (Insulin-like growth factor 1)*

IGF1 is a positive regulator of muscle growth, which acts on the activation and proliferation of muscle precursors. Overexpression of IGF1 prevents the loss of age-related muscle mass, causes hypertrophy and increased muscle strength. Studies in *mdx* mice showed an anatomical and biochemical improvement associated with restoration of muscle strength after administration of IGF1 (Barton, Morris et al. 2002).

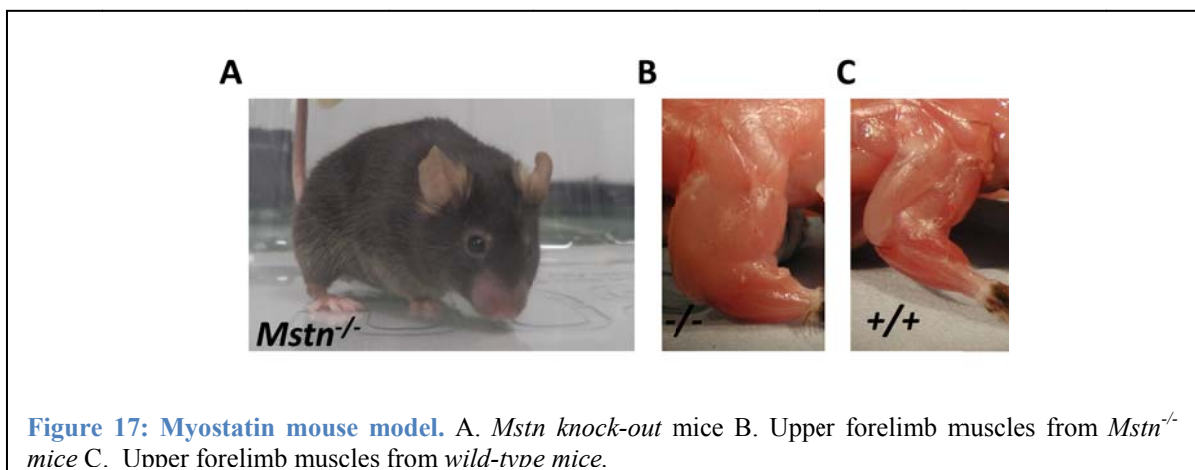
#### *B) Inhibition of myostatin*

Myostatin (also known as GDF8, **G**rowth and **D**ifferentiating **F**actor 8) was identified as a member of the superfamily of TGF- $\beta$  (**T**ransforming **G**rowth **F**actor  $\beta$ ) that negatively regulates muscle growth (McPherron, Lawler et al. 1997). Deletions in the myostatin gene are responsible for the impressive musculature found in Belgian Blue cattle (Grobet, Martin et al. 1997). A similar phenotype is detected in mice carrying deletions in the myostatin gene or expressing dominant negative transgenes ((Lee and McPherron 2001); (Zhu, Hadhazy et al. 2000)). Inhibition of endogenous myostatin synthesis can increase muscle mass and decrease fat mass (McPherron and Lee 2002). Studies have shown that blocking myostatin by antibod-

ies allowed an anatomical, physiological and biochemical improvement of dystrophic phenotype in *mdx* mice (Bogdanovich, Krag et al. 2002). Active mature myostatin can also be inhibited through the N-terminal part of its protein product consisting of approximately the first 300 amino acids (commonly called the "propeptide"), which is normally cleaved and has the ability to inactivate the mature protein by reassociation. The next chapter will introduce this molecule in more detail and describe the different strategies of inhibition that were used in our project.

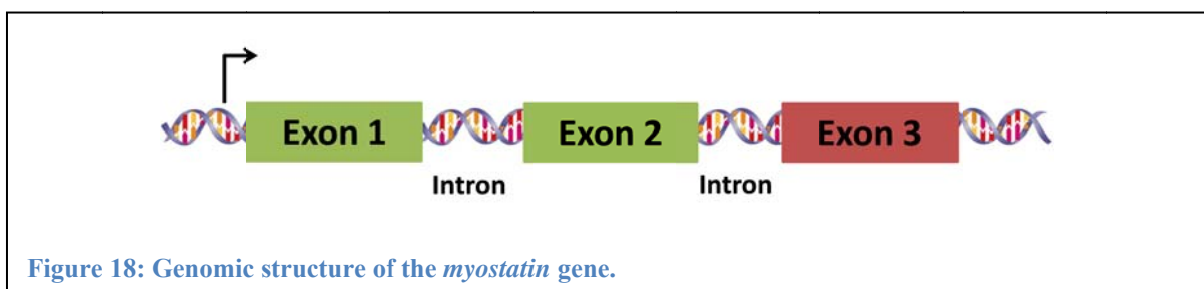
### 3. CHAPTER: MYOSTATIN

Myostatin, also called GDF8 (Growth and Differentiation Factor 8), is a secreted growth factor of the Transforming Growth Factor- $\beta$  (TGF $\beta$ ) superfamily that negatively regulates skeletal muscle mass (McPherron, Lawler et al. 1997). Like other members of the TGF- $\beta$  superfamily, myostatin is synthesized as a precursor protein with a signal sequence, an N-terminal propeptide domain, and a C-terminal active domain ((Sharma, Kambadur et al. 1999); (Hill, Davies et al. 2002)). Its inhibitory role in skeletal muscle growth was discovered by Lee *et al.* in 1997 when knockout of myostatin in mice resulted in a dramatic and widespread increase in skeletal muscle mass. Individual muscles of myostatin null mice weigh approximately twice as much as those of wildtype mice and this is the reasons of a combination of increased muscle fiber number (hyperplasia) and fiber size (hypertrophy) (McPherron, Lawler et al. 1997) (Figure 17).



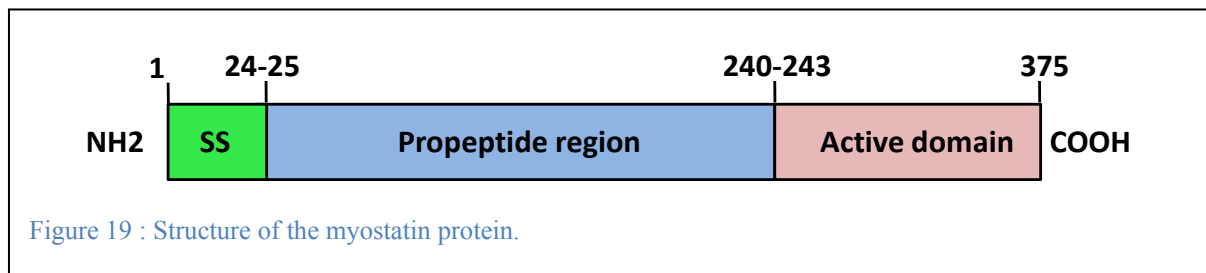
#### 3.1 Myostatin gene and protein structure

The myostatin gene is located on human chromosome 2q32.2 and on mouse chromosome 1. It comprises three exons and two introns and has a total length of 7.8 kb. Its mRNA contains 3.1 kb and encodes a protein of 375 amino acids (Gonzalez-Cadavid, Taylor et al. 1998) (Figure 18).

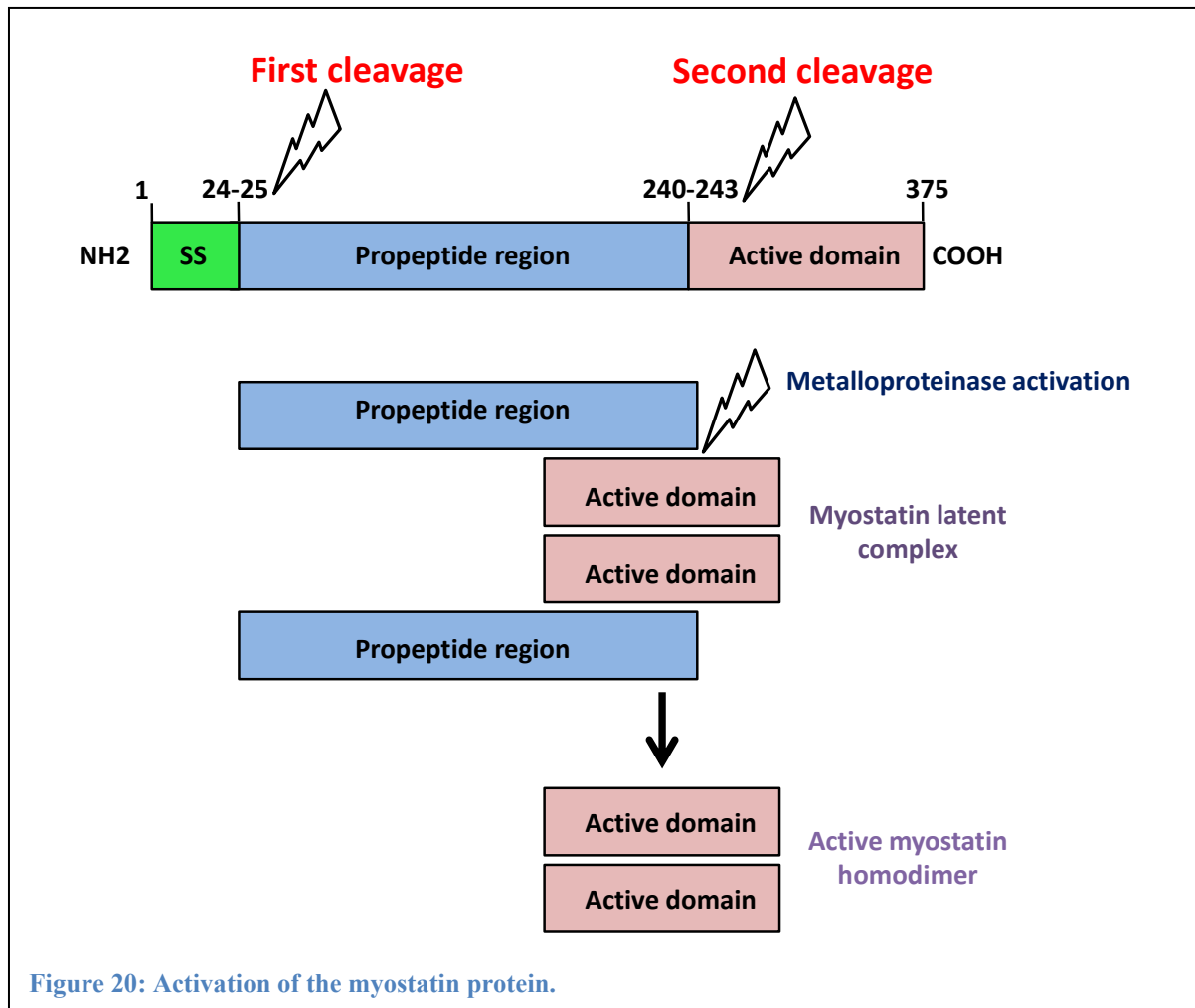


The myostatin amino acid sequence and function appears to be highly conserved across the species from mouse to humans. Mutations in the myostatin gene have been shown to result in a massive increase of muscle mass and size in various species ((McPherron and Lee 1997); (Grobet, Martin et al. 1997); (Kambadur, Sharma et al. 1997); (Schuelke, Wagner et al. 2004); (Clop, Marcq et al. 2006); (Mosher, Quignon et al. 2007) ; (Hill, Gu et al. 2010)).

The myostatin protein is synthesized as a precursor with a molecular weight of 52 kDa and undergoes two processes of proteolysis (McPherron, Lawler et al. 1997) (Figure 19).



The first cleavage removes the first 24 N-terminal amino acids corresponding to the signal sequence. The second cleavage occurs between amino acids 240 and 243 with the formation of a latent complex, which contains the propeptide and the myostatin homodimer linked to each other in a non-covalent fashion. The connection between the two units of the mature homodimer is provided by several disulfide bounds. The activation of the latent complex is achieved through the release of the active 26 kDa homodimer into the extracellular matrix after cleavage of the propeptide by the metalloproteinase BMP1/TLD at the aspartate residue at position 76 (Asp76) (Wolfman, McPherron et al. 2003) (Figure 20).



### 3.2 The myostatin knockout mouse model

The loss of myostatin function results in a strong increase in skeletal muscle mass. Individual muscles in adult *Mstn* knockout mice (*Mstn*<sup>-/-</sup>) weigh twice as much as those from *Mstn*<sup>+/+</sup> littermates. This muscle enlargement results from both myofibers hyperplasia and hypertrophy (McPherron, Lawler et al. 1997). The hypertrophic phenotype is due to an increase of the cytoplasmic volume without a change in the number of myonuclei. This hypertrophy results in an increase of the nuclear domain ((Qaisar, Renaud et al. 2012); (Wang and McPherron 2012); (Amthor, Otto et al. 2009)). In addition to increased muscle mass, *Mstn*<sup>-/-</sup> mice have increased insulin sensitivity and reduced adipose tissue mass (Savage and McPherron 2010).

The glycolytic fibers are fast-contracting fibers that fatigue rapidly, whereas oxidative fibers are slow-contracting fibers that are fatigue resistant. The *Mstn*<sup>-/-</sup> muscles show an increased number of the fast glycolytic type IIb fibers and a concomitant loss of oxidative type I and type IIa fibers. This phenomenon is associated with a mitochondrial depletion ((Amthor, Macharia et al. 2007); (McPherron, Lawler et al. 1997)) and reduced expression levels of the

peroxisome proliferator-activated receptor-gamma coactivator 1 $\alpha$  (PGC1 $\alpha$ ) (Lipina, Kendall et al. 2010).

Depending on the investigation, *Mstn*<sup>-/-</sup> mice demonstrate either an increase, no change or even a decrease in the force production ((Amthor, Macharia et al. 2007); (Mendias, Marcin et al. 2006); (Matsakas, Mouisel et al. 2010); (Whittemore, Song et al. 2003); (Schirwis, Agbulut et al. 2013)). The knockout of the *Mstn* gene causes increased fatigability during exercise protocols ((Matsakas, Mouisel et al. 2010); (Savage and McPherron 2010)). At the same time, Matsakas *et al.* demonstrated that endurance exercise training appears to significantly modify the skeletal muscle phenotype of *Mstn*<sup>-/-</sup> mice and improve their force generating capacity (Matsakas, Macharia et al. 2012). Interestingly, exercise not only improved force but also caused a reduction of muscle mass, decreased myofiber size and normalized the size of the myonuclear domain ((Savage and McPherron 2010); (Matsakas, Mouisel et al. 2010)).

In order to evaluate the postnatal effect of an abrogation of the myostatin function in mice, Grobet *et al.* generated a conditional *Mstn* knockout mouse model using gene targeting techniques. They demonstrated that the postnatal inactivation of the myostatin gene in striated muscle tissue caused a muscular hypertrophy phenotype (Grobet, Pirottin et al. 2003).

### 3.3 Myostatin expression

During development, myostatin expression is initiated in the myotome compartment of developing somites in mouse embryos and later becomes restricted to the cardiac and skeletal muscle in adults, but can also be detected to lesser extent in adipose tissue and the mammary gland ((McPherron, Lawler et al. 1997); (Sharma, Kambadur et al. 1999)). Myostatin expression is higher in fast glycolytic muscles than in slow oxidative muscles ((Carlson, Booth et al. 1999); (Wehling, Cai et al. 2000)). There is a positive correlation between the expression of myosin heavy chain type IIB (MyHCIIB) and myostatin mRNA abundance in skeletal muscle (Carlson, Booth et al. 1999) suggesting that fast-twitch muscles could be more sensitive to changes in myostatin expression.

*In vitro*, the myostatin gene is not, or only weakly expressed during the proliferative phase of myoblasts ((Mendler, Zador et al. 2000); (Rios, Carneiro et al. 2002); (Kocamis, Gahr et al. 2002); (Deveaux, Picard et al. 2003)). Its expression increases in the C<sub>2</sub>C<sub>12</sub> cells line when differentiation is induced and peaks three to four days after induction at the time of myoblast fusion ((Mendler, Zador et al. 2000); (Kocamis, Gahr et al. 2002)). In primary cultures of fetal myoblasts and satellite cells, the expression peak was observed at the beginning of the fusion

((Kocamis, Gahr et al. 2002); (Deveaux, Picard et al. 2003)) and mRNA-transcript abundance fell with differentiation.

### 3.4 The myostatin signaling pathway

The various elements of the myostatin signaling pathway were defined in 2003 by Rebbapragada *et al.* (Rebbapragada, Benchabane et al. 2003). The mature C-terminal dimer of myostatin binds with high affinity to ActRIIB (activin receptor IIB). It can also bind to ActRIIA, albeit to a lesser extent ((Lee and McPherron 2001); (Rebbapragada, Benchabane et al. 2003)). Following this binding, the intracellular signal cascade is initiated by recruitment of the type I receptor, which is either ALK4 (activin-like kinase-4) or ALK5. This formation allows phosphorylation of ALK4/5 which in turn leads to the phosphorylation and activation of Smad2 and Smad3. This activation allows then the interaction with the co-Smad and translocation of the complex into the nucleus to regulate the expression of myostatin target genes (Zhu, Topouzis et al. 2004). Another member of the Smad family, Smad 7, after stimulation by myostatin abrogates myostatin signalling through an inhibitory feedback loop ((Zhu, Topouzis et al. 2004); (Forbes, Jackman et al. 2006)). First, Smad 7 inhibits myostatin gene expression (Forbes, Jackman et al. 2006), second, inhibits Smad2/3 phosphorylation by ALK4/5 (Zhu, Topouzis et al. 2004) and third, interferes with the formation of the Smad2/3–Smad 4 complex resulting in the inhibition of myostatin signaling (Zhu, Topouzis et al. 2004) (Figure 21). Myostatin may compete with other molecules such as BMP7 for binding to the the ActRIIB receptor thus antagonizing them (Rebbapragada, Benchabane et al. 2003). Transgenic mice with a dominant negative form of the ActRIIB receptor that carries a mutation in its kinase domain, show a strong increase in muscle mass comparable to that observed in myostatin knockout mice (Lee and McPherron 2001). The increase in muscle mass in these mice is the result of hypertrophy and hyperplasia as already described in the myostatin knockout mice.

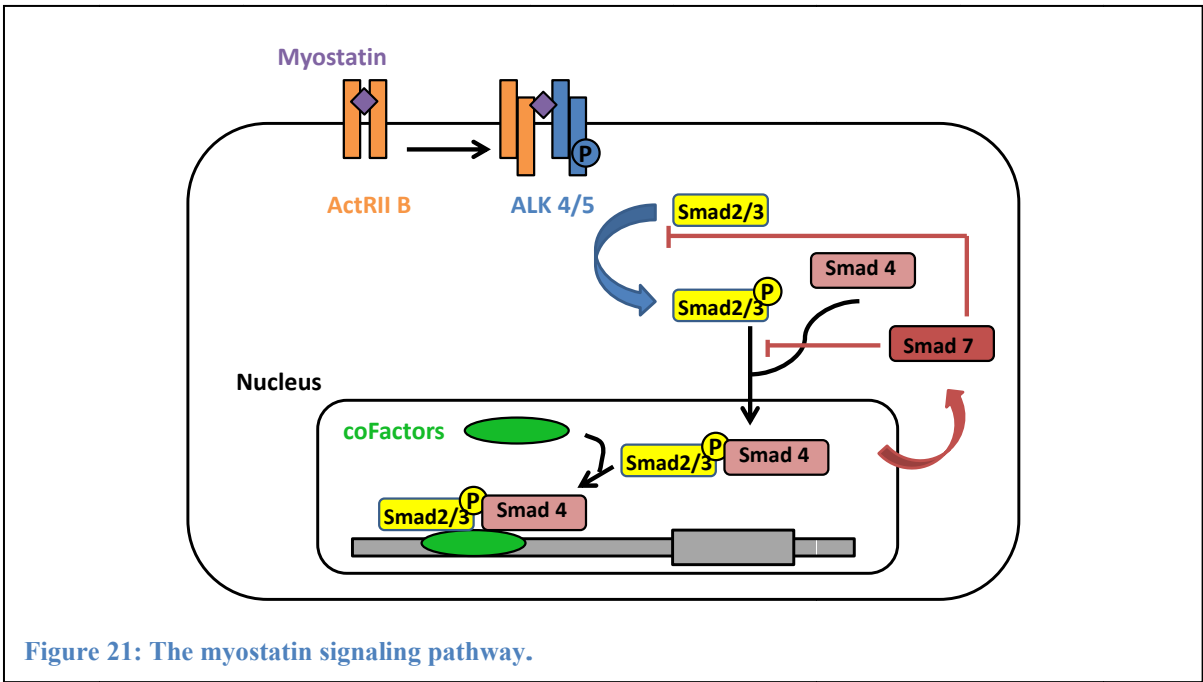


Figure 21: The myostatin signaling pathway.

3.5 Regulation of myostatin activity

Myostatin is synthesized and secreted by the myogenic cells and acts in an autocrine and paracrine manner. It is also found in blood, however, its biological activity is almost exclusively directed at the skeletal muscle. This suggests that circulating myostatin is inactive. Several proteins form latent complexes with myostatin thereby inactivating its function. Other molecules can prevent myostatin activation or secretion. Table 2 provides an overview of molecules interacting with myostatin.

Table 2: Proteins with an influence on myostatin action				
Myostatin binding proteins				
Localisation	Binding molecule	Myostatin form bound	Consequence of binding	References
Serum	Propeptide	Mature myostatin	Inhibits mstn receptor binding	[1]
	FLRG	Mature myostatin	Inhibits mstn receptor binding	[2]
	GASP1	Mature myostatin and propeptide	Inhibits mstn activation	[3]
Skeletal muscle	hSGT	N-terminal signal peptide	Inhibits mstn secretion and activation	[4]
	Titin cap	Mature mysotatin	Inhibits mstn latent complex formation and secretion	[5]
	Follistatin	Mature myostatin	Inhibits mstn receptor binding	[6]
	Decorin	Mature myostatin	Inhibits mstn receptor binding	[7]

[1] (Thies, Chen et al. 2001); [2] (Hill, Davies et al. 2002); [3] (Hill, Qiu et al. 2003); [4] (Wang, Zhang et al. 2003); [5] (Nicholas, Thomas et al. 2002); [6] (Amthor, Nicholas et al. 2004); [7] (Miura, Kishioka et al.

### 3.5.1 Molecules binding myostatin

#### *The myostatin propeptide*

Like several members of the TGF $\beta$  superfamily, myostatin is secreted in a latent form bound to its propeptide, also known as LAP "latency associated peptide". It is possible to release the active myostatin from its propeptide by acid treatment or heating (Zimmers, Davies et al. 2002). The cleavage of the propeptide by a member of the family of metalloproteases BMP1/tolloid "Bone Morphogenetic Protein 1" or by serine proteases such as plasmin and cathepsin D also allows the activation of myostatin (Wolfman, McPherron et al. 2003). If myostatin forms a latent complex with its propeptide, its binding to its receptor is not possible.

#### *FLRG*

Some of the latent circulating myostatin is associated to FLRG "Follistatin Related Gene". If TGF $\beta$  and activin signaling is activated, the phosphorylated Smads bind to the *FLRG* promoter resulting in an increased production of secreted FLRG (Bartholin, Maguer-Satta et al. 2002). As a negative feed-back loop, FLRG then forms a complex with myostatin and prevents its receptor binding.

#### *GASP-1*

GASP-1 "Growth and Differentiation Factor-Associated Serum Protein 1" is another protein that binds to mature myostatin and to the latent propeptide complex. It is highly expressed in skeletal muscle suggesting that it binds to myostatin during or shortly after its secretion. GASP-1 contains a follistatin domain and a protease inhibitor domain. Consequently, this protein regulates the activation of the latent complex although its release of the mature myostatin (Hill, Qiu et al. 2003).

These three proteins, propeptide, FLRG and GASP-1, have very different structures and all regulate the circulating myostatin. This highlights the importance of a strict and specific regulation of this growth factor. The propeptide, GASP-1 and FLRG form distinct complexes with myostatin and play different roles in the regulation of skeletal muscle mass (Hill, Qiu et al. 2003).

#### *hSGT*

Some studies show that hGST functions as a chaperone molecule involved in the folding and development of proteins (Schantl, Roza et al. 2003). hSGT plays a role in regulating myo-

statin secretion and activation *via* a direct interaction with its signal peptide in skeletal muscle cells (Wang, Zhang et al. 2003).

### *Titin-cap*

Titin-cap is a sarcomeric protein capable of binding mature myostatin to prevent the formation of the latent complex thereby inhibiting its secretion. This occurs without alteration of myostatin production or transformation (Nicholas, Thomas et al. 2002).

### *Follistatin*

Follistatin is known to be an antagonist of several members of the TGF $\beta$  family, including GDF11 (Growth and Differentiation Factor 11), which is highly similar to myostatin. The secretion of follistatin is highly related to myostatin. These two proteins interact directly and their interaction inhibits the effect of myostatin on muscle development (Amthor, Nicholas et al. 2004). As for myostatin, follistatin is also found in the serum. However, no complex with these two molecules have been identified in serum (Schneyer, Rzucidlo et al. 1994). An alternative splicing event generates two different isoforms of follistatin. The short form (FS-288) has a greater binding affinity to the surface of cells in the extracellular matrix than the long form (FS-315) ((Inouye, Guo et al. 1991); (Sugino, Kurosawa et al. 1993)). Indeed, follistatin contains a binding sequence for heparin allowing it to interact with proteoglycans on the cell surface. Hence, follistatin produced in the muscle is maintained in the extracellular matrix thus trapping and sequestering myostatin through complexation which then cannot circulate in the serum (Sugino, Kurosawa et al. 1993). It is impossible for the myostatin to bind its receptor if trapped in the extracellular matrix.

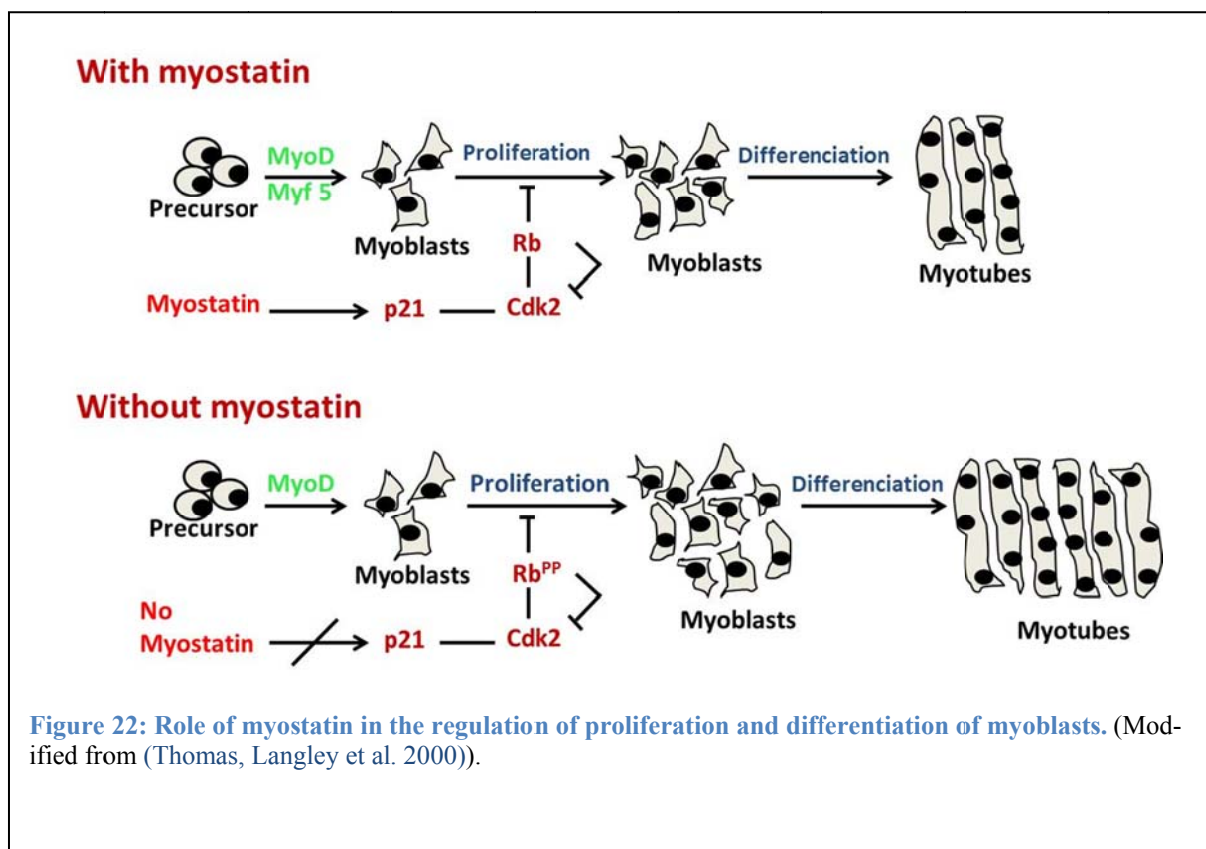
### *Decorin*

Decorin is a small proteoglycan rich on leucines which contains a protein core with attached chains of dermatan-sulfates. It is known to bind to members of the TGF $\beta$  superfamily and regulate their activities (Riquelme, Larrain et al. 2001). Decorin interacts with mature myostatin maintaining it in the extracellular matrix and keeping it away from its receptor on the cells surface (Miura, Kishioka et al. 2006).

### 3.6 The function of myostatin

#### 3.6.1 Myoblast cell proliferation

The mechanism by which myostatin controls the number of muscle fibers was described by Thomas *et al.* (Thomas, Langley *et al.* 2000). Myostatin inhibits the proliferation of C<sub>2</sub>C<sub>12</sub> myoblasts by preventing their cell cycle progression beyond the G1 phase. This inhibition is mediated by an increase of p21, an inhibitor of cyclin-dependent kinase (CKI), and a decrease in expression and activity of cdk2 (cyclin-dependent kinase 2) its binding partner cyclin-E. This is accompanied by an accumulation of Rb (**R**etinoblastoma) protein which is a major substrate of cdk2 and in its unphosphorylated state plays a role in the transcription of specific genes during the S-phase ((Thomas, Langley *et al.* 2000); (Langley, Thomas *et al.* 2004)). In the absence of functional myostatin, Rb protein is phosphorylated and causes myoblasts to proliferate ((Thomas, Langley *et al.* 2000); (Joulia, Bernardi *et al.* 2003)). This control of myoblast proliferation by myostatin is accompanied by a negative effect on both DNA and protein synthesis (Taylor, Bhasin *et al.* 2001). However, to which extent myostatin controls satellite cell proliferation is still unclear (Amthor, Otto *et al.* 2009) (Figure 22).

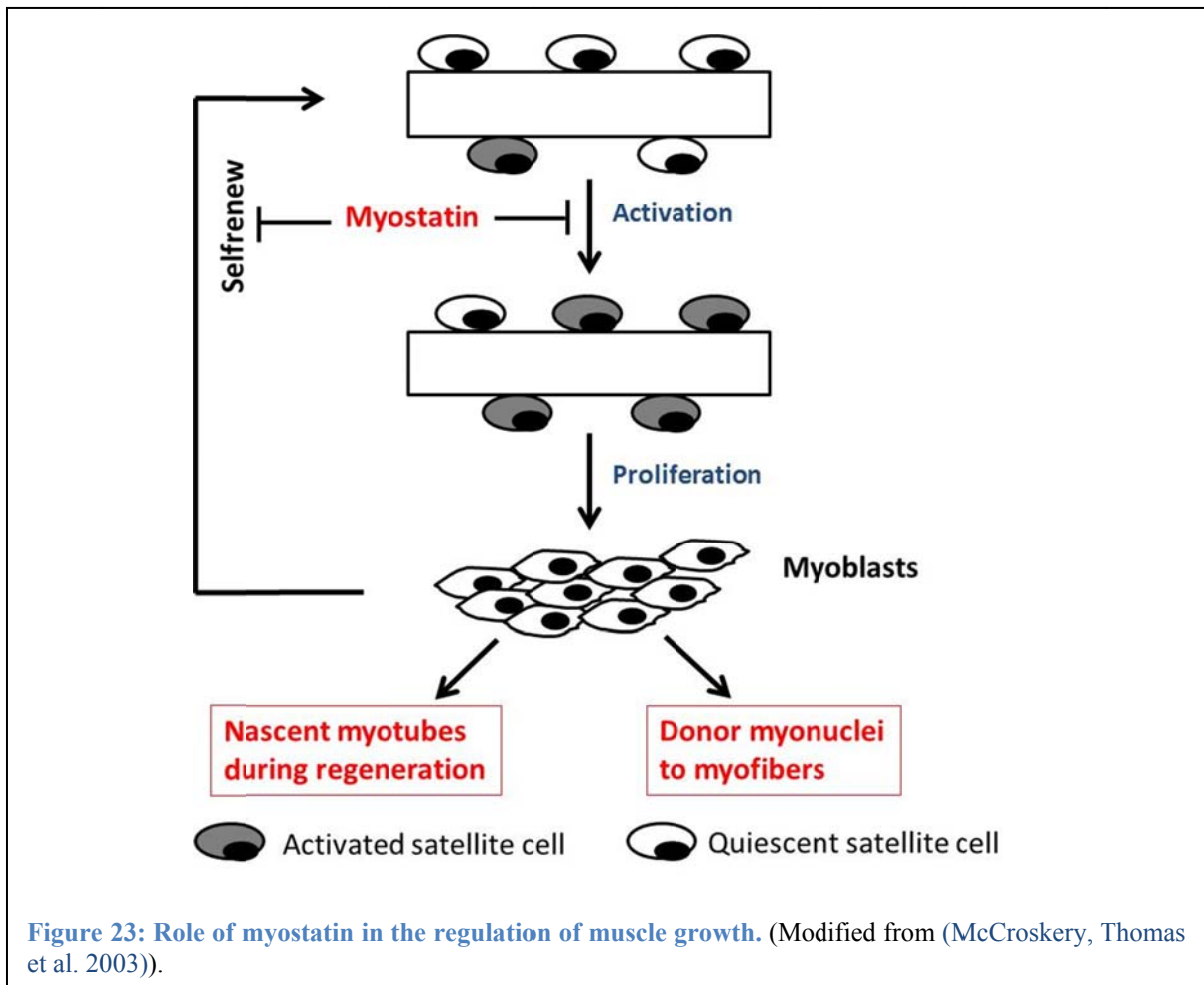


### 3.6.2 Myoblast cell differentiation

Myostatin also regulates myoblast differentiation through inhibition of the expression of myogenic transcription factors, such as Pax3, MyoD and Myf5, ((Rios, Carneiro et al. 2002); (Amthor, Huang et al. 2002)). In C<sub>2</sub>C<sub>12</sub> myoblasts, overexpression of myostatin reduces expression of genes encoding muscle structural proteins (MyHC IIb, Troponin I, desmin), and decreases the expression of myogenic transcription factors (MyoD, Myf5 and myogenin) ((Langley, Thomas et al. 2002); (Durieux, Amirouche et al. 2007)). It has been reported that overexpression or addition of myostatin to C<sub>2</sub>C<sub>12</sub> cells induces a decrease in MyoD and myogenin expression *via* activation of Erk1/2 ((Yang, Chen et al. 2006), (Huang, Chen et al. 2007)). The myogenic factors MyoD and Myf5 induce the activation of the *Mstn* promoter, which shows the existence of a negative feed-back loop between myogenic factors and myostatin (Salerno, Thomas et al. 2004).

### 3.6.3 Muscle cell regeneration

Some studies have shown that myostatin controls muscle fiber size by maintaining the satellite cells in a quiescent state and inhibiting protein synthesis (Thomas, Langley et al. 2000). These authors show that myostatin acts on the proliferation and differentiation of myoblasts during muscle growth, but also during regeneration. Recent data on the regeneration of skeletal muscle in *Mstn*<sup>-/-</sup> mice show the importance of myostatin in this process. In the absence of myostatin, there is an increase of activation and self-renewal of satellite cells ((McCroskery, Thomas et al. 2003); (Wagner, Liu et al. 2005)), an effect mediated by decreased expression of Pax7 (McFarlane, Hennebry et al. 2008) (Figure 23). However, other studies came to an opposite conclusion and show that there is no difference in the number of satellite cells or myonuclei in the absence of myostatin, and that the hypertrophy is the result of an increase of the cytoplasmic volume (Amthor, Otto et al. 2009). A recent study, suggested that myostatin inhibition induces first the increase of fibers size and then the activation of satellite cells (Wang and McPherron 2012).



### 3.6.4 The role of myostatin in adipogenesis

Myostatin is expressed at low levels in the adipose tissue. Its role in adipogenesis is suggested by the observation that loss of myostatin function in *Mstn*<sup>-/-</sup> mice also decreases body fat mass ((McPherron, Lawler et al. 1997); (Lin, Arnold et al. 2002); (McPherron and Lee 2002)) while the total weight of fat deposits is increased in transgenic mice overexpressing myostatin (Reisz-Porszasz, Bhasin et al. 2003). However, it remains to determine whether myostatin regulates adipogenesis directly. One possibility is that the effect of myostatin on adipose mass is the consequence of an alteration of skeletal muscle metabolism rather than a direct effect. This hypothesis is supported by Guo *et al.* (Guo, Jou et al. 2009) who show that inhibition of myostatin signaling *via* overexpression of dnActRIIB (dominant negative activin receptor type IIB) in adipose tissue does not induce any change in body composition. In contrast, inhibition of myostatin signaling in skeletal muscle resulted in a decrease of adipose mass (Guo, Jou et al. 2009). These results suggest the decrease in the adipose tissue in *Mstn*<sup>-/-</sup> mice to be due to an indirect effect of the impaired skeletal muscle.

### 3.6.5 Contractile phenotype

In addition to the regulation of muscle mass, myostatin also appears to regulate muscle fiber-type composition. In cattle lacking myostatin and in the myostatin null mice there is an increase in the percentage of fast type II fibers together with a decrease of slow type I fibers as compared to wildtype animals ((Girgenrath, Song et al. 2005); (Stavaux, Art et al. 1994)).

Thus the absence of myostatin leads overall to a faster and more glycolytic muscle phenotype. Hennebry *et al.* proposed that myostatin could regulate fiber type composition by regulating the expression of both myocyte enhancer factor 2 (MEF2) and MyoD during myogenesis (Hennebry, Berry et al. 2009). Indeed, in the muscles of *Mstn*<sup>-/-</sup> mice *Mef2*-expression is down-regulated. The transcription factor Mef2 is essential for the formation of slow type I fibers and for an increase of MyoD expression. However, the change towards muscle fiber type I is more likely a consequence of developmental processes since inhibition of myostatin in adult animals does not cause such a transformation (Girgenrath, Song et al. 2005).

### 3.6.6 Muscle metabolism

It is well known that genetic inactivation of the myostatin gene in mice not only induces muscle hypertrophy but also reduces body fat accumulation (McPherron and Lee 2002). A similar lean phenotype can also be observed in mice that overexpress a dominant negative Activin receptor type IIB (ActRIIB) transgene or following injection of the myostatin propeptide, which binds to and inhibits the function of myostatin ((Guo, Jou et al. 2009); (Zhao, Wall et al. 2005)). An increase in the percentage of glycolytic muscle fibers has been observed in *Mstn*<sup>-/-</sup> mice (Hennebry, Berry et al. 2009). It has been shown that the increase of glycolytic muscle fiber bulk could promote transcription of genes involved in fatty acid metabolism, improve hepatic fatty acid oxidation resulting in a decline of fat mass and an improved lipid metabolism (Izumiya, Hopkins et al. 2008). Consistent with the lean phenotype of *Mstn*<sup>-/-</sup> mice, muscle specific inhibition of myostatin leads to reduced fat mass and improved insulin sensitivity (Guo, Jou et al. 2009).

Inhibition of myostatin also leads to reduced adiposity and improved insulin sensitivity animal models for obesity. Lee *at al.* reported that crossing Agouti lethal yellow (Ay) mice (a mouse model for obesity) with *Mstn*<sup>-/-</sup> mice resulted in a reduction of adipose tissue, lower fasting blood glucose levels and elevated glucose tolerance if compared to the Ay mice alone (McPherron and Lee 2002).

Another study also demonstrated that enhanced muscle growth following myostatin inhibition has a positive effect on fat metabolism *via* an increase of adiponectin, PPAR $\alpha$  and PPAR $\gamma$  expression (Suzuki, Zhao et al. 2008).

### **3.7 Therapeutic strategies based on myostatin blockade**

There are several muscle diseases for which a myostatin inhibitor may provide a novel therapeutic approach. Sarcopenia or age related muscle atrophy, affects many elderly people and increases the risk of injury and impairs their quality of life. Increased muscle mass could restore muscle strength and prevent injuries. Cachexia is a form of muscle wasting that affects cancer patients or patients with severe cardiomyopathy. Increased muscle strength in cachectic patients may improve quality of life, improve response to cancer therapy, and increase life span. There are also a variety of muscular dystrophies, including Duchenne muscular dystrophy, for which increased skeletal muscle bulk may provide a therapeutic benefit.

Overexpression of myostatin in adult mice is responsible for the appearance of a cachexia with severe muscle atrophy (Zimmers, Davies et al. 2002). It also contributes to loss of muscle mass in patients affected with the HIV (Gonzalez-Cadavid, Taylor et al. 1998). In age-associated sarcopenia myostatin mRNA- and protein levels were found to be significantly increased ((Welle 2002), (Leger, Derave et al. 2008)). Such increase of myostatin signaling is accompanied by a decreased activity of pathways involved in muscle hypertrophy such as the IGF1/Akt pathway (Leger, Derave et al. 2008).

#### **3.7.1 The different approaches to induce myostatin blockade**

Many different strategies have been employed in order to inhibit either myostatin activity or expression such as **(i)** the use of antisense-oligonucleotides, **(ii)** the administration of the myostatin propeptide or **(iii)** of inhibitory-binding partners like follistatin, **(iv)** the administration of anti-myostatin blocking antibodies, **(v)** the use of RNA interference (RNAi) and **(vi)** the administration of a soluble ActRIIB receptor in order to inhibit the myostatin/ActRIIB pathway.

##### *Antisense oligonucleotides*

Different chemistries of antisense oligonucleotides were used: the 2'-O-methyl phosphorothioate (2'-OMePS) and the phosphorodiamidate morpholino oligomers (PMO). Both led to efficient exon skipping and knockdown of myostatin mRNA ((Kemaladewi, Hoogaars et al. 2011); (Kang, Malerba et al. 2011)). The administration of these antisense oligonucleotides increased muscle mass and myofiber size in wildtype mice.

Kemaladewi *et al.* demonstrated the possible combination of two antisense oligonucleotides to target two different genes, the *MSTN* as well as the *DMD* gene as a potential therapeutic strategy against DMD (Kemaladewi, Hoogaars *et al.* 2011).

### *Myostatin interfering RNA*

Short interfering RNAs (siRNAs) against myostatin have been administrated either locally into mouse skeletal muscle or intravenously. This caused a marked increase in muscle mass within a few weeks of application (Kinouchi, Ohsawa *et al.* 2008). These results suggest that myostatin silencing is a powerful therapeutic tool to increase muscle mass.

### *The myostatin propeptide*

Activation of myostatin requires the proteolytic cleavage of the propeptide by members of the BMP1/TLD family of metalloproteases (Wolfman, McPherron *et al.* 2003). Using a mutant form of the propeptide which is resistant to cleavage caused an increase of muscle mass after injection into adult mice, presumably by forming latent complexes that could not be activated by this group of proteinases ((Wolfman, McPherron *et al.* 2003); (Lee 2008)). Such an increase of muscle mass and force was also found after AAV-mediated overexpression of the mutant propeptide in rodent and canine animal models ((Bogdanovich, Krag *et al.* 2002); (Morine, Bish *et al.* 2010); (Bish, Sleeper *et al.* 2011)). The authors reported an improvement of the pathophysiology in the *mdx* mice following such treatment (Bogdanovich, Perkins *et al.* 2005).

### *Anti-myostatin antibodies*

Antibodies against myostatin were tested as another therapeutic strategy. These antibodies specifically bind and antagonize mature myostatin. Administration of anti-myostatin antibodies into wildtype and *mdx* mice led to an increase of muscle mass and function ((Bogdanovich, Krag *et al.* 2002); (Whittemore, Song *et al.* 2003)). The increase in muscle mass was also found after administration of anti-myostatin antibodies into mouse models of cancer cachexia, muscle disuse, sarcopenia, and DMD ((Murphy, Chee *et al.* 2011); (Murphy, Cobani *et al.* 2011); (Murphy, Koopman *et al.* 2010); (Murphy, Ryall *et al.* 2010)).

However, results in mouse models for limb-girdle muscular dystrophy and amyotrophic lateral sclerosis suggest that myostatin inhibition may be beneficial if instituted early or if the disease is still mild, but it may be ineffective in advanced disease stages ((Bogdanovich, McNally *et al.* 2008); (Parsons, Millay *et al.* 2006); (Holzbaur, Howland *et al.* 2006)).

### *Myostatin binding proteins*

In addition to the propeptide, other binding proteins are capable of regulating myostatin activity, including follistatin (FS), follistatin-related gene (FLRG) and growth and differentiation factor-associated serum protein (GASP) ((Hill, Davies et al. 2002); (Hill, Qiu et al. 2003); (Cash, Angerman et al. 2012)). Indeed, postnatal intramuscular injection of AAV encoding myostatin inhibitor-proteins resulted in long-term improvement of muscle size and strength in wildtype and *mdx* mice (Haidet, Rizo et al. 2008). The largest effect on muscle size and function was obtained by the follistatin construct (Haidet, Rizo et al. 2008), suggesting that follistatin is the most efficient inhibitor protein of myostatin in order to stimulate muscle growth. Overexpression of follistatin can further increase muscle growth even in mice that lack myostatin. This shows that further TGF $\beta$  related ligands may cooperate with myostatin in suppressing muscle growth (Lee 2007).

### *The soluble activin receptor type IIB (sActRIIB-Fc)*

A soluble form of the activin receptor type IIB was produced and used as a therapy to increase muscle mass. To stabilize the protein, the ActRIIB was fused to Fc-fragments, which allow systemic application in different species including human. This soluble receptor can sequester the free myostatin and others ligands and prevent their binding to the endogenous transmembrane receptors ((Lee, Reed et al. 2005); (Morrison, Lachey et al. 2009); (Sako, Grinberg et al. 2010); (Souza, Chen et al. 2008)). Many studies show the potential of sActRIIB-Fc to induce muscle growth and/or to prevent muscle loss in wildtype mice as well as in mouse models for different diseases. Treatment with sActRIIB-Fc improves muscle function in mouse models for DMD, amyotrophic lateral sclerosis and myotubular myopathy mouse by increasing muscle weight and strength ((Cadena, Tomkinson et al. 2010); (George Carlson, Bruemmer et al. 2011); (Morrison, Lachey et al. 2009); (Lawlor, Read et al. 2011)). In several animal models of cancer cachexia, blockade of the myostatin/ActRIIB pathway not only prevents further muscle wasting but also completely reverses prior skeletal muscle loss (Zhou, Wang et al. 2010). Regarding the promising potential of this molecule to inhibit the myostatin/ActRIIB pathway and to promote muscle growth and force generation, we decided to use this molecule in our project

### 3.7.2 Myostatin blockade as a therapy against DMD

#### *Myostatin blockade in the mdx mouse*

Many different studies were performed in order to evaluate the potential of interference with the myostatin signaling pathway as a therapeutic strategy against DMD ((Wagner, McPherron et al. 2002); (Bogdanovich, Krag et al. 2002)). Wagner *et al.* used *Mstn*<sup>-/-</sup>/*mdx* double knock-out mice and showed that the absence of myostatin stimulated muscle growth and force generation in *mdx* mice (Wagner, McPherron et al. 2002). At the histological level lack of myostatin increased fibers size and reduced fibrosis as well as fatty remodeling in the diaphragm muscle, suggesting an improvement of muscle regeneration.

Bogdanovich *et al.* also tested the ability of *in vivo* myostatin inhibition in order to ameliorate the dystrophic phenotype in the *mdx* mouse (Bogdanovich, Krag et al. 2002). Blockade of endogenous myostatin by monoclonal anti-myostatin antibodies for three months resulted in an increase in body weight, muscle mass, muscle size and absolute muscle strength in *mdx* mouse muscle. The authors further observed a significant drop of serum creatine kinase (CK) activities to almost normal values and interpreted this as a proof of improved muscle fiber degeneration. Murphy *et al.* found that young but not adult *mdx* mice responded to treatment with anti-myostatin antibodies (Murphy, Ryall et al. 2010).

Bogdanovich *et al.* also used the myostatin propeptide as an alternative therapeutic strategy. They found that treatment with recombinant propeptide increased muscle mass, improved muscle force and reduced CK activities and muscle fibrosis in *mdx* mice (Bogdanovich, Perkins et al. 2005). Qiao *et al.* used a modified myostatin propeptide which is resistant to cleavage, and induced a significant increase in skeletal muscle mass in normal as well as *mdx* mice (Qiao, Li et al. 2008). The treated *mdx* mice showed larger and more uniform myofibers, less fibrosis and lower serum CK activities. In addition, a grip force test and an *in vitro* tetanic contractile force test demonstrated improved muscle strength. A treadmill test, however, showed reduced endurance of the treated *mdx* mice as compared to their untreated counterparts.

Differently, Morine *et al.* used a recombinant AAV to overexpress a secretable dominant negative form of myostatin under a liver specific promoter. Systemic myostatin inhibition led to an increase of skeletal muscle mass and strength in both wildtype and *mdx* mice (Morine, Bish et al. 2010). The *soleus* muscle of *mdx* mice demonstrated the most profound improvement of force production and a shift towards faster myosin-heavy chain isoforms. Specific

force, however, decreased in *extensor digitorum longus* muscle and remained unchanged in the diaphragm.

Follistatin another therapeutic approach was also tested. Similar to the other approaches, overexpression of follistatin increased muscle mass, reversed muscle pathology and improved strength in the *mdx* mouse ((Haidet, Rizo et al. 2008); (Nakatani, Takehara et al. 2008)).

Different studies showed the beneficial effect of a soluble ActRIIB-Fc on the *mdx* muscle pathology. They demonstrated that myostatin/ActRIIB blockade pathway led to an increase in muscle mass with amelioration in muscle function ((Pistilli, Bogdanovich et al. 2011); (George Carlson, Bruemmer et al. 2011); (Morine, Bish et al. 2010)). Remarkably, Pistilli and collaborators showed that low-dose treatment of *mdx* mice with soluble ActRIIB-Fc improved specific force without effecting muscle mass (Pistilli, Bogdanovich et al. 2011).

Blockade of myostatin/ActRIIB signaling pathway, however, does not correct the molecular defect in DMD, which is the absence of dystrophin protein expression. For this, a double strategy combining the restoration of a quasi-dystrophin and the inhibition of myostatin pathway in *mdx* mice was proposed and studied by Dumonceaux and her collaborators. Interestingly, they found an improvement in both absolute and specific forces (Dumonceaux, Marie et al. 2010).

### *Myostatin blockade in the GRMD dog*

Before starting clinical trials in human patients, it is important to determine the potential of such a therapy in a more comparable disease model. Therefore, Bish *et al.* evaluated systemic myostatin inhibition in the golden retriever model of DMD (GRMD dog). In this study the authors injected a single dose of a self-complementary adeno-associated virus type 8 (AAV8) designed to express a secreted dominant-negative myostatin propeptide under a liver specific promoter. This strategy, as discussed above, had before been evaluated in the *mdx* mouse (Morine, Bish et al. 2010). The single injection was sufficient to induce an increase in muscle mass, a better preservation of muscle architecture and a reduction of serum creatine kinase (CK) activity and muscle fibrosis (Bish, Sleeper et al. 2011).

### *Clinical trials in men*

Wagner *et al.* reported in 2008 on the first clinical trial (phase I/II) on adult patients with different muscular dystrophies (BMD, fascioscapulohumeral dystrophy, and limb-girdle muscular dystrophy) using monoclonal anti-myostatin antibodies (MYO-29) for systemic myostatin blockade (Wagner, Fleckenstein et al. 2008). The study included 116 subjects and showed

good safety and tolerability. There was no significant improvement in muscle strength or muscle function in the treatment group, however, the trial was not powered for this.

Another phase II study was started in 2010 in DMD boys using a soluble form of the activin receptor type IIB coupled to an Fc-fragment (sActRIIB-Fc). The trial was labeled ACE-031 and registered under NCT01099761; NCT01239758 at <http://clinicaltrials.gov>. The study was designed to evaluate the potential of ACE-031 to provide disease-modifying effects on muscle quality that would translate into durable benefits on strength and function for boys with DMD. However, this trial had to be interrupted precociously based on some preliminary safety data. Some patients suffered from minor nosebleeds, gum bleeding, and/or small dilated blood vessels in the skin (see also <http://www.acceleronpharma.com/products/ace-031/>). Although the underlying mechanism for these side effects remains to be determined in detail, it is known that also Bmp9 and Bmp10 bind to the ActRIIB receptor, which are important regulators of angiogenesis ((Souza, Chen et al. 2008); (David, Mallet et al. 2008); (David, Mallet et al. 2007)). It is possible that myostatin is also implicated in the signaling of endothelial cells, since capillary density is strongly decreased in the absence of myostatin (Matsakas, Macharia et al. 2012).

Actually, a phase I clinical trial is ongoing for treatment of patients with BMD and sporadic inclusion body myositis (sIBM). This gene therapy trial is registered under NCT01519349 at <http://clinicaltrials.gov> and aims to evaluate the overexpression a human form of follistatin (FS-344) using a rAAV1.



# **AIMS OF THE THESIS**

## Aims of the thesis

Blockade of ActRIIB signaling is one of the promising therapeutic strategies because it rapidly stimulates skeletal muscle growth. Previous work of our laboratory investigated mainly the constitutive myostatin knockout mice and demonstrated a severe change of its contractile and oxidative properties. This led to the general hypothesis of my thesis that myostatin determines the oxidative metabolism of skeletal muscle. However, it should be pointed out that the constitutive *Mstn*<sup>-/-</sup> mice, despite being a very robust model for studying the role of ActRIIB signaling, have only limited value for predicting the effect of ActRIIB blockade at the postnatal stage because of their congenital fiber IIB predominance. We here investigated the abrogation of the myostatin/ActRIIB signaling pathway using a soluble form of the Activin receptor type IIB (sActRIIB-Fc) in adult *wild-type* and *mdx* mice. Prospective animal experimentation data will help in the development of therapies for neuromuscular disorders based on myostatin/ActRIIB blockade.

- **Aim 1**

**To investigate the role of myostatin signaling in the constitutive myostatin knock-out mouse *mstn*<sup>-/-</sup>.** In order to determine the role of myostatin on muscle energy metabolism and muscle function.

**Objectives:**

- to validate the effect of the absence of myostatin on muscle mass and function.
- to determine the effect of myostatin on the metabolic phenotype and endurance capacity.

- **Aim 2**

**To investigate the role of ActRIIB signaling in the regulation of muscle energy metabolism and energy muscle dependent function.** Based on our results from the constitutive *mstn*<sup>-/-</sup> mice we were interested to investigate the effect of postnatal ActRIIB inhibition in *wild-type* adult mice.

**Objectives:**

- to demonstrate the effect of ActRIIB inhibition on muscle mass and function.
- to determine the effect of ActRIIB inhibition on the metabolic muscle phenotype.

- **Aim 3**

**To investigate, how ActRIIB blockade affects the metabolism of skeletal muscle in a dystrophic context.** We seemed important to know how inhibition of ActRIIB signaling would affect the metabolic phenotype of skeletal muscle in a context of a dystrophic muscle, which is already damaged.

**Objectives:**

- to demonstrate the effect of ActRIIB inhibition on muscle mass and function.
- to determine the effect of ActRIIB inhibition on the metabolic phenotype of the dystrophic muscle.

- **Aim 4**

**To investigate the combine effect of treatment with sActRIIB-Fc and the restoration of the dystrophin protein on dystrophic muscle function.** It is important to determine if the myostatin inhibition confer an additional benefit to the correction of the deficient gene and the expression of the dystrophin protein in the context of Duchenne muscular dystrophy.

# RESULTS

## 1. Part 1: Role of myostatin in the regulation of muscle energetic metabolism in mouse models

### 1.1 Effect of the ActRIIB blockade in wildtype and mdx mice

**Project description:** The loss of muscle size and strength is one of the major problems in muscle diseases. Myostatin regulates skeletal muscle mass *via* its signaling through the activin receptor type IIB (ActRIIB). Previous work in our laboratory suggested that myostatin plays an important role for the oxidative metabolism in skeletal muscle by optimizing energy metabolism and energy dependent muscle function. However, it was unknown, how myostatin inhibition would influence the muscle function and metabolism if initiated postnatally, and especially in dystrophic muscle. We explored the hypothesis that myostatin/ActRIIB signaling is a key regulator of oxidative metabolism in the adult muscle.

**Experimental design:** *Mdx* and wildtype adult mice were treated for four months with sActRIIB-Fc, which is a powerful inhibitor of the ActRIIB signaling pathway.

**Aim 1:** To investigate the effect of ActRIIB signaling blockade on the function of normal and dystrophic skeletal muscle in the adult mouse.

**Work plan:** The effect of the treatment on muscle function was assessed by measuring muscle weight, muscle fiber distribution and muscle force. We also evaluated the exercise capacity of the mice and the level of the serum lactate before and after an exhaustive exercise.

**Aim 2:** To investigate the effect of a myostatin/ActRIIB signaling blockade on the capillarization of normal and dystrophic skeletal muscle in the adult mouse.

**Work plan:** In order to explain the considerable increase in fatigue after treatment with sActRIIB-Fc, we explored the extent of capillarization of the skeletal muscle in treated *mdx* and wildtype mice which would be a good indicator of the blood perfusion of the muscle.

**Aim 3:** To investigate the effect of the ActRIIB signaling blockade on muscle metabolism and mRNA levels of PPAR transcription factors of normal and dystrophic skeletal muscle in the adult mouse.

**Work plan:** The exercise intolerance and lactate acidosis following ActRIIB blockade suggested underlying changes in the mitochondrial muscle metabolism. To explain this phenom-

enon, we explored genes at the molecular level that are involved in muscle energy metabolism such as *Ppar $\beta$* , *Pgc1 $\alpha$*  (key transcription factors that promote oxidative metabolism in skeletal muscle), *Pdk4* (an inhibitor of the pyruvate dehydrogenase (Pdh) and regulatory switch of substrate utilization from glucose towards fatty acids) and *Cpt1b* (a mitochondrial protein involved in the transport of fatty acids).

**Aim 4:** To investigate the effect of ActRIIB signaling blockade on the mitochondrial enzyme activity of normal and dystrophic skeletal muscle in the adult mouse.

**Work plan:** We analyzed the activities of isolated respiratory chain complexes (COX, SDH) and key enzymes of  $\beta$ -oxidation (HADHA) and Krebs Cycle (Citrate Synthase).

**Aim 5:** To investigate the effect of ActRIIB signaling blockade on the porin expression of normal and dystrophic skeletal muscle in the adult mouse.

**Work plan:** We investigated the expression of the porin protein (VDAC), an ATP channel located in the outer mitochondrial membrane, by qPCR and by Western blot in the skeletal muscle from wildtype and *mdx* mice treated with sActRIIB-Fc.

## **Blockade of ActRIIB signaling triggers muscle fatigability and metabolic myopathy**

Karima Relizani<sup>1,2</sup>, Etienne Mouisel<sup>1,3</sup>, Benoit Giannesini<sup>4</sup>, Christophe Hourdé<sup>1</sup>, Ketan Patel<sup>5</sup>, Susanne Lützkendorf<sup>2</sup>, Kristina Jülich<sup>2</sup>, Alban Vignaud<sup>1</sup>, France Piétri-Rouxel<sup>1</sup>, Dominique Fortin<sup>6</sup>, Luis Garcia<sup>1</sup>, Stéphane Blot<sup>7</sup>, Olli Ritvos<sup>8</sup>, David Bendahan<sup>4</sup>, Arnaud Ferry<sup>1,9</sup>, Renée Ventura-Clapier<sup>6</sup>, Markus Schuelke<sup>2</sup> and Helge Amthor<sup>1,10,11</sup>

<sup>1</sup>Université Pierre et Marie Curie, Institut de Myologie, Unité mixte de recherche UPMC-AIM UM 76, INSERM U 974, CNRS UMR 7215, 75013 Paris, France; <sup>2</sup>Department of Neuropediatrics & NeuroCure Clinical Research Center, Charité Universitätsmedizin Berlin, 13353 Berlin, Germany; <sup>3</sup>Inserm UMR 1048, Université Paul Sabatier, Toulouse, France (present address); <sup>4</sup>Aix-Marseille Université, Centre National de la Recherche Scientifique (CNRS), Centre de Résonance Magnétique Biologique et Médicale UMR 7339, 13385, Marseille, France; <sup>5</sup>School of Biological Sciences, University of Reading, Reading, UK; <sup>6</sup>INSERM U 769, Université Paris-Sud, Châtenay-Malabry, France; <sup>7</sup>Unité de Neurologie, Ecole Nationale Vétérinaire d'Alfort, Université Paris Est, France; <sup>8</sup>Department of Bacteriology and Immunology, Haartman Institute, University of Helsinki, Helsinki, Finland; <sup>9</sup>Université Paris Descartes, 75006 Paris, France; <sup>10</sup>UFR des Sciences de la Santé, Université de Versailles Saint-Quentin-en-Yvelines, 78180 Montigny-le-Bretonneux, France; <sup>11</sup>Service Génétique Médicale, CHU Necker-Enfants Malades, Université Paris Descartes, France.

Correspondence should be addressed to:

Helge Amthor, MD, PhD

Laboratoire «Biothérapies des Maladies du Système Neuromusculaire»

UFR des Sciences de la Santé «Simone Veil»

Université de Versailles Saint-Quentin-en-Yvelines

2, avenue de la Source de la Bièvre

78180 Montigny-Le-Bretonneux, France

Email: [helge.amthor@uvsq.fr](mailto:helge.amthor@uvsq.fr)

or

Markus Schuelke, MD

NeuroCure Clinical Research Center and Department of Neuropediatrics

Charité Universitätsmedizin Berlin

Augustenburger Platz 1

D-13353 Berlin, Germany

Email: [markus.schuelke@charite.de](mailto:markus.schuelke@charite.de)

Short title: ActRIIB blockade triggers metabolic myopathy

### Abstract

Myostatin regulates skeletal muscle size *via* the activin receptor IIB (ActRIIB). However, its effect on muscle energy metabolism and energy dependent muscle function remains largely unexplored. This question needs to be solved urgently since various therapies for neuromuscular diseases based on blockade of ActRIIB signaling are being developed. Here we show in mice that four months of pharmacological abrogation of ActRIIB signaling by treatment with soluble ActRIIB-Fc triggers extreme muscle fatigability. This is associated with elevated serum lactate levels and a severe metabolic myopathy in the *mdx* mouse, an animal model of Duchenne muscular dystrophy. Blockade of ActRIIB signaling down-regulates Porin, a crucial ADP/ATP shuttle between cytosol and mitochondrial matrix leading to a consecutive deficiency of oxidative phosphorylation as measured by *in vivo* Phosphorus Magnetic Resonance Spectroscopy (<sup>31</sup>P-MRS). Further, ActRIIB blockade reduces muscle capillarization, which further compounds the metabolic stress. We show that ActRIIB regulates key determinants of muscle metabolism, such as Ppar $\beta$ , Pgc1 $\alpha$ , and Pdk4 thereby optimizing different components of muscle energy metabolism. In conclusion, ActRIIB signaling endows skeletal muscle with high oxidative capacity and low fatigability. The severe metabolic side effects following ActRIIB blockade caution against deploying this strategy, at least in isolation, for treatment of neuromuscular disorders.

**Key words:** ActRIIB, myostatin, metabolic myopathy, muscle fatigue, oxidative phosphorylation, beta-oxidation, Duchenne muscular dystrophy, *mdx* mouse.

## INTRODUCTION

Skeletal muscle has inbuilt control mechanisms to prevent overgrowth. This function is executed, at least in part, by secreted molecules including members of the transforming growth factor- $\beta$  (TGF- $\beta$ ) family, especially myostatin<sup>1</sup>. Myostatin signals *via* its transmembrane activin receptor IIB (ActRIIB) and suppression of this pathway stimulates muscle growth<sup>2-6</sup>. In the past few years, strategies have been developed to treat muscle dystrophies, muscle wasting and cachexia by blocking the myostatin/ActRIIB pathway with first of many clinical trials already being concluded (ClinicalTrials.gov NCT01099761, NCT01519349, NCT01423110, NCT01669174, NCT01601600, NCT01433263)<sup>7</sup>. However, it remains a matter of controversy whether the hypertrophic muscles that form as a result of blocking myostatin/ActRIIB signaling confer any functional benefit, because a number of groups have reported loss of specific force of larger muscles in myostatin knockout mice and a faster fatigability (*Mstn*<sup>-/-</sup>)<sup>8-11</sup>. In addition, myostatin knockout leads to a change of muscle contractile and metabolic characteristics towards a “glycolytic” phenotype<sup>9,12-15</sup>, commonly attributed to a change in muscle specification during development. In contrast to the constitutive myostatin deficiency of *Mstn*<sup>-/-</sup> mice, postnatal treatment with soluble activin IIB receptor (sActRIIB-Fc) in adult mice blocks myostatin/ActRIIB signaling and increases muscle force without altering the fiber type composition<sup>16,17</sup>. Similar results have been obtained in the *mdx* mouse model of Duchenne muscular dystrophy<sup>18,19</sup>. However, a recent transcriptome profiling demonstrated a down-regulation of genes involved in oxidative phosphorylation and mitochondrial function following treatment with sActRIIB-Fc<sup>20</sup>. Another study revealed a faster decline of muscle force following repetitive stimulation<sup>21</sup>. Whether those changes reflect solely a change towards a faster muscle phenotype or a relevant mitochondrial dysfunction is presently unknown. In the view of ongoing clinical trials we need to address the question of how myostatin blockade affects the metabolism of dystrophic muscle in *mdx* mice, which already has a preexisting deficit of mitochondrial function<sup>22-24</sup>. Here we explored the hypothesis that ActRIIB signaling is a key regulator of oxidative metabolism in the adult muscle. We thus set out to systematically investigate in adult wild-type and *mdx* mice, how postnatal blockade of ActRIIB signaling using sActRIIB-Fc might affect muscle energy metabolism and energy dependent muscle function. Our data conclusively show the importance of ActRIIB signaling as a pivotal link that acts to balance muscle size and strength against endurance capacity *via* optimization of energy metabolism.

## RESULTS

**ActRIIB blockade in adult wild-type mice increases fatigability.** Muscles of *Mstn*<sup>-/-</sup> mice, a model of constitutive inhibition of signaling *via* ActRIIB, exhibit a congenital fiber-type profile that is characterized by an increase in the number of fast “glycolytic” (MHCIIB) fibers and concomitant loss of “oxidative” (MHCI, MHCIIA) fibers, which entails changes in muscle function, exercise capacity and muscle metabolism<sup>8,12-15,25,26</sup>. To circumvent the effects of congenital fiber-type switching, we here inhibited ActRIIB signaling in adult wild-type mice with a soluble form of the activin receptor fused with the Fc-fragment of mouse IgG (sActRIIB-Fc). Four months of treatment promoted robust skeletal muscle growth together with a significant increase in total body weight, confirming previously published data (Fig. S1)<sup>3</sup>. Importantly, the increase in muscle mass was not accompanied by fiber-type conversion (Fig. S2). The absolute maximal force of *EDL* and *soleus* muscle increased in parallel with muscle size (Figs. 1a,c). Specific maximal force was conserved, implicating a proportional increase of force and muscle mass (Fig. 1b). However, sActRIIB-Fc treatment also increased muscle fatigue (Figs. 1c,d) and mice exhausted precociously during incremental speed running tests (Figs. 1e,g). Serum lactate, being already significantly increased at resting state, rose to pathological levels following incremental speed running (Figs. 1f,g). The concept of “Critical Speed” accurately reflects the capacity for aerobic exercise and is based on the proportional relationship between “covered distance” and “time to exhaustion” at different velocities<sup>27</sup>. During the four months treatment period, we found a steady decline in Critical Speed in the treatment and control group, however, the decline over time was by far larger in sActRIIB-Fc treated animals as compared to PBS-treated mice (Figs. 1h,i).

**Severe exercise intolerance in dystrophic *mdx* mice following treatment with sActRIIB-Fc.** In Duchenne muscular dystrophy and its *mdx* mouse model, oxidative metabolism is compromised due to membrane damage and the resulting intracellular calcium overload<sup>22-24</sup>. Having shown that ActRIIB blockade decreased aerobic exercise capacity in wild-type mice, we now investigated what effect administration of sActRIIB-Fc would have on the metabolic phenotype of *mdx* mice. This information would have important clinical implications for the strategies to use ActRIIB blockade for treatment of muscle dystrophies. Despite a massive increase in skeletal muscle mass after sActRIIB-Fc treatment (Fig. S1), absolute maximal force decreased in *soleus* muscle and most notably specific force in both *EDL* and *soleus* muscles (Figs. 2a,b), serving as functional evidence for increased myopathic changes of sActRIIB-treated dystrophic *mdx* muscle. Interestingly, sActRIIB-Fc treatment did not cause any greater force decline during repetitive stimulation (Figs. 2c,d). Electromyography excluded problems in neuromuscular transmission but revealed abnormal spontaneous potentials and the presence of complex repetitive discharges in both PBS and sActRIIB-Fc treatment groups of the *mdx* mice (Fig. S3). Such polyphasic potentials are characteristic of dystrophic *mdx* muscle<sup>28</sup>. As voluntary motor activity seemed reduced when observing sActRIIB-Fc treated *mdx* mice, we proceeded to analyze

their exercise behavior. Remarkably, at the end of the treatment period, sActRIIB-Fc treated *mdx* mice suffered from severe exercise intolerance associated with a pathological serum lactate increase (Figs. 2e-g, Video S1). It is important to note, that exercise capacity of *mdx* mice declined throughout the four months treatment period, however, to a far larger extent in sActRIIB-Fc treated *mdx* mice than in the PBS-treated control group (Figs. 2h,i).

**sActRIIB-Fc treatment affects muscle capillarization.** The ability of mitochondria to produce ATP critically depends on the oxygen supply *via* tissue blood perfusion, thus a combination of hypoperfusion plus exercise induced hypoxemia might explain the severe exercise intolerance. Treatment with sActRIIB-Fc caused a drop in capillary density especially in the oxidative *soleus* muscle from *mdx* mice with a subsequent increase in the capillary domain (Figs. 3a-d). The increase of the capillary domain was also found in glycolytic *EDL* muscles of *mdx* mice, albeit to a lesser degree (Fig. S4a-d). Treatment of mice as well as of C<sub>2</sub>C<sub>12</sub> myotubes with sActRIIB-Fc down-regulated expression of *Vegf-A* suggesting an indirect negative effect of myostatin blockade on capillary formation (Figs. 3e,f). Interestingly, *Vegf-A* expression in *mdx* mice was much lower than in wild-type mice, and treatment with sActRIIB-Fc did not decrease *Vegf-A* mRNA-abundance any further (Fig. 3e), suggesting the presence of additional mechanisms for regulating capillary density. In this regard the findings of Hayot *et al.* (2010) are of special interest, who reported an induction of myostatin expression in muscles of rats exposed to chronic hypoxia and in patients with chronic obstructive pulmonary disease (COPD). The authors interpreted these findings as a potential cause for the muscle wasting that is often seen in COPD-patients<sup>29</sup>. These findings, however, could also be interpreted as a compensatory up-regulation of myostatin to improve the metabolic functioning and to increase capillary density in a state of chronic hypoxia. It is of special interest that endothelial cells strongly express the mRNAs of transmembrane receptors (*ActRIIA/B* and *ALK4/5*) for myostatin or its homologs, whereas *myostatin* mRNA was only expressed at low levels (Fig. 3g). Treatment of endothelial cells (HUVEC cell line) with increasing dosages of recombinant myostatin *in vitro* increased the cell doubling time in culture, verifying a direct effect of myostatin or its homologs on endothelial cell proliferation (Fig. S4e), however, the exact ligands of muscle endothelial cell regulation *in vivo* remain to be determined.

**ActRIIB signaling regulates *Pgc1α* and *Ppar* transcription factors.** The exercise intolerance and lactic acidosis following ActRIIB blockade suggests underlying changes in muscle metabolism, a hypothesis supported by previous transcriptome profiling<sup>20</sup>. In agreement, we show that the copy numbers of *Pgc1α* and *Pparβ*, which are key transcription factors promoting oxidative metabolism in skeletal muscle, are down-regulated after treatment with sActRIIB-Fc (Figs. 4b,c) and following treatment of C<sub>2</sub>C<sub>12</sub> myotubes with sActRIIB-Fc (Fig. 4g). On the protein level, down-regulation of *Pgc1α* was more pronounced in the *mdx* muscle if referred to Desmin abundance (Fig. 4a). Such loss of oxidative properties was accompanied by a compensatory activity increase of Enolase, a key glycolytic enzyme

(Fig. 4d). Furthermore, mRNA levels of *Pdk4*, an inhibitor of pyruvate dehydrogenase (Pdh) and a regulatory switch of substrate utilization from glucose towards fatty acids<sup>30</sup>, was strongly decreased following sActRIIB-Fc treatment in *mdx* mice (Fig. 4e). We thus expected an inhibitory effect of sActRIIB-Fc treatment on  $\beta$ -oxidation and found a down-regulation of *Cpt1b* mRNA levels (Fig. 4f). Likewise, sActRIIB-Fc treatment of C<sub>2</sub>C<sub>12</sub> myotubes reduced expression of genes controlling oxidative metabolism and  $\beta$ -oxidation within 24 hours of treatment (Fig. 4g), implying a direct effect of myostatin signaling in the regulation of these genes.

We further focused our attention on the neuronal nitric oxide synthase (Nos1, nNos), because it is well known that the sarcolemmal presence of the Nos1 enzyme is strongly reduced in the absence of its binding partner dystrophin in patients with DMD and in *mdx* mice<sup>31,32</sup>. The resulting dysregulation of NO-synthesis entails a failure of contraction induced vasodilatation as well as changes in the cellular calcium homeostasis associated with exacerbated post-exercise fatigability, exercise-induced muscle edema and cell necrosis<sup>33-35</sup>. We thus wondered, whether sActRIIB-Fc treatment would influence sarcolemmal Nos1 expression, hence further compromising the pathophysiological effect of sActRIIB-Fc on vasculature and oxidative metabolism. As expected, we found a strong decrease of *Nos1* mRNA copy numbers in *mdx* muscles of both treatment groups in comparison to wild-type muscle (Fig. S11a), which was paralleled by a strong decrease of sarcolemmal expression of Nos1 protein in *mdx* muscle (Fig. S11b). Furthermore, treatment with sActRIIB-Fc diminished *Nos1* transcription in wild-type and *mdx* muscle (Fig. S11a). However, subsarcolemmal Nos1 protein content remained unchanged (Fig. S11b), and Western blot did not reveal any changes in Nos1 protein levels in wild-type mice (Fig. S11c), whereas Nos1 protein levels in *mdx* mice were below detection levels (data not shown). This suggests that sActRIIB-Fc treatment unlikely aggravates NO dysregulation of dystrophin deficient muscle, although further experiments are required to ascertain or to exclude a role of the ActRIIB-receptor on NO signaling.

**Reduced oxidative metabolism in *mdx* muscle following treatment with sActRIIB-Fc.** It should be noted that the mRNA and protein levels of key regulatory genes (Ppar $\beta$ , Pgc1 $\alpha$ ) important for oxidative metabolism (Figs. 4b-c) were significantly lower in *mdx* than in wild-type mice, supporting previous findings that oxidative muscle metabolism is depressed in dystrophic muscle to some extent<sup>22,36</sup>.

We therefore studied in real-time the response of the oxidative metabolism to a standardized bout of exercise in anesthetized *mdx* mice either treated with PBS (controls) or sActRIIB-Fc. Muscle function and energy metabolism were assessed strictly noninvasively in calf muscle with an innovative experimental setup using phosphorus (<sup>31</sup>P) nuclear magnetic resonance spectroscopy (MRS)<sup>37</sup>. An exercise bout of six minutes consisting of repeated maximal isometric contractions was induced *in vivo* by transcutaneous electro-stimulation. After induced repeated contractions fatigue levels (Fig.

5a), intracellular acidosis (Fig. 5b) as well as phosphocreatine (PCr) consumption (Fig. 5c) were similar in both groups. However, the time constant of post-exercise phosphocreatine re-synthesis ( $\tau$ PCr) was significantly prolonged in sActRIIB-Fc treated *mdx* mice (Figs. 5d,e). Given that PCr synthesis during the post-exercise recovery period relies exclusively on oxidative ATP synthesis,  $\tau$ PCr has largely been acknowledged as an important *in vivo* index of oxidative mitochondrial capacity. Hence the prolonged  $\tau$ PCr demonstrates that sActRIIB-Fc treatment reduces oxidative metabolism *in vivo*.

The MRS results pointed to an underlying functional deficit of the skeletal muscle respiratory chain complexes or  $\beta$ -oxidation in response to sActRIIB-Fc treatment. However, contrary to our hypothesis, we found (i) largely unaffected *ex vivo* activities of isolated key mitochondrial enzymes (Krebs cycle: citrate synthase [CS]; respiratory chain: cytochrome C oxidase [COX]; and  $\beta$ -oxidation: hydroxyacyl-CoA-dehydrogenase [HADHA]) and (ii) similar succinate dehydrogenase [SDH] and COX fiber profiles (Figs. S5-S7). In fact, COX and SDH enzyme activities even appeared somewhat increased in *EDL* muscles (Figs. S5c,d, S6a, S7a), likely reflecting a compensatory increase in response to decreased aerobic energy production. Furthermore, mitochondrial DNA (mtDNA) copy numbers remained largely unchanged following treatment with sActRIIB-Fc (Fig. S8a). The normal mtDNA copy numbers together with unaltered CS enzyme activities (Fig. S5a,b) let us conclude that ActRIIB blockade did not affect mitochondrial mass.

**Treatment with sActRIIB-Fc down-regulates Porin expression in wild-type and *mdx* muscle.** Given the abnormal post-exercise PCr re-synthesis ( $\tau$ PCr) along with normal respiratory chain activities, we wondered whether the ATP transport from the mitochondrial matrix into the cytosol of skeletal muscle cells might be affected, which might explain the diminished rate of aerobic energy production. Keeping with such hypothesis, decreased protein levels of Vdac3 had already been reported for *mdx* muscle, hinting towards a derangement of the ADP/ATP-shuttling system through the outer mitochondrial membrane *via* the Voltage Dependent Anion Channels (VDAC, syn. Porin<sup>38,39,40</sup>). In line with these findings, a proteomic survey of differentially expressed proteins from wild-type and *mdx* mouse hearts had discovered a substantial loss of Vdac1 protein<sup>41</sup>. Indeed, here we show that wild-type and to an even larger extent *mdx* muscles exhibited a considerable reduction of *Porin* mRNA-transcripts (Fig. S8a) and protein levels (Fig. S9) after sActRIIB-Fc treatment. This pushes the muscle even further into global mitochondrial dysfunction than dystrophin deficiency alone. Such secondary mitochondriopathy might explain the high lactic acidosis and rapid fatigability of sActRIIB-Fc treated *mdx* mice.

**Myopathic changes in *mdx* mice following treatment with sActRIIB-Fc.** We next investigated the consequences of sActRIIB-Fc treatment on the extent of muscle dystrophy in *mdx* mice. Muscles from both sActRIIB-Fc and PBS-treatment groups revealed typical dystrophic changes comprising muscle

fiber necrosis, regenerating fibers, fibers with central nuclei, inflammatory infiltrates, and increased fibrosis, which are difficult to quantify (Fig. S10a). Muscle degeneration is accompanied by a leak of cytoplasmic enzymes such as creatine kinase (CK). We measured serum CK levels, which were largely elevated in *mdx* mice from both treatment groups; however, we did not detect any significant differences since inter-individual variation was large (Fig. S10b). In *mdx* mice, muscle degeneration is followed by excessive regeneration with abundant splitting of regenerated fibers, which appear as small fiber profiles on transverse sections. Such excessive regeneration leads to an increase of muscle mass (see comparison between wild-type and *mdx* mice: Fig. S1). Following treatment with sActRIIB-Fc, muscles enlarged on average, if compared to PBS treatment, by  $\approx 1.6$  fold in *mdx* and by  $\approx 1.3$  fold in wild-type mice (Fig. S1). However, analysis of morphometric features of *EDL* muscles from sActRIIB-Fc treated *mdx* mice, revealed a further increase in the number of small fiber profiles if compared to PBS-treated *mdx* mice (Fig. S10c). This finding suggests that the excessive increase of muscle weight was triggered by abnormal regeneration and not by fiber hypertrophy. The *soleus* muscle of *mdx* mice, while not increasing its mass after sActRIIB-Fc treatment, exhibited an increased fiber size variation (Fig. S10d). In conclusion, the dystrophic phenotype of dystrophin deficient muscle persisted or even increased following treatment with sActRIIB-Fc.

## DISCUSSION

Myostatin/ActRIIB signaling exerts three major functions on skeletal muscle. (i) It acts to limit its size, (ii) promotes oxidative properties, and (iii) balances glucose *versus* fat utilization. The changes in muscle physiology in hypermuscular mice following treatment of adult mice with sActRIIB-Fc highlights the fact that myostatin/ActRIIB blockade confers little functional advantage over wild-type muscle due to its rapid fatigability. Improved muscle strength, however short lived, comes at the cost of increased fatigability and exercise intolerance, which is often seen in patients with mitochondrial disorders such as MELAS or MERRF syndrome<sup>42</sup>. Interestingly, muscle cramps are frequently observed in whippet dogs with homozygous *Mstn* mutations<sup>43</sup>. Moreover, “double muscle cattle”, several breeds of which have been identified to carry *Mstn* mutations<sup>44,45</sup>, are prone to exercise induced lactic acidosis and severe rhabdomyolysis<sup>46,47</sup>. In myostatin deficient animals, such exercise failure could be attributed to congenital fiber-type disproportion with a shift towards the expression of the fast IIB myosin heavy chain (MHC) isoform<sup>8,25,48</sup>, which is well known to be associated with loss of oxidative properties of skeletal muscle and increased fatigability<sup>9,13-15,48</sup>. In contrast to animals born with mutations in the *Mstn* gene, we show that blockade of ActRIIB signaling in adult wild-type mice beyond the period of muscle development does not have any impact on fiber-type composition, thus confirming previous reports<sup>17,49</sup>.

After sActRIIB-Fc treatment the mice exhibit clinical signs of early muscle fatigue, exercise intolerance, and lactic acidosis – characteristic signs for a depression of  $\beta$ -oxidation, a shift towards anaerobic glycolysis, and ATP-deficiency. Interestingly, whereas *ex vivo* mitochondrial respiratory chain enzyme activities and mtDNA copy numbers were within the normal range, *in vivo* <sup>31</sup>P-MRS clearly demonstrated a down-regulation of oxidative energy metabolism in sActRIIB-Fc treated *mdx* mice. We further demonstrate a significant loss of the Porin complex in sActRIIB-Fc treated mice, pointing towards an underlying defect of ATP-handling and ATP-transport as one causative mechanism for the metabolic phenotype. A second aggravating factor, which further compromised exercise tolerance, is the decrease of capillary density and the increase of the capillary domain. Previous reports attributed such reduced capillary density to the increase of muscle fiber size<sup>50,51</sup>. However, here we demonstrate a net numerical loss of capillaries per fiber following treatment with sActRIIB-Fc. This finding was most pronounced in *mdx* mice with a profound rarefaction of the capillary bed in dystrophic muscle. In dystrophinopathies diminished sarcolemmal Nos1 results in dysregulation of the capillary adaptive response to exercise leading to functional muscle ischemia<sup>33,52</sup>. Our protein analysis argues against a further aggravation of the capillary adaptive response by additional loss of Nos1 in sActRIIB-Fc treated animals, despite the fact that *Nos1* mRNA levels were clearly reduced. sActRIIB-Fc treatment of dystrophic *mdx* mice dramatically worsened the myopathic phenotype as shown by the large deficit in specific force. As lack of dystrophin *per se* alters mitochondrial function in DMD patients

and *mdx* mice<sup>22,23,36</sup>, the blockade of myostatin signaling initiates a vicious cycle resulting in severe secondary metabolic myopathy. We also found an increased fiber size variation after sActRIIB-Fc treatment of *mdx* mice pointing towards increased myopathic changes even at the tissue level.

In the past several investigators have used different strategies of interfering with the ActRIIB receptor mediated signaling pathway in order to treat *mdx* mice and GRMD dogs. This was done either through injection of sActRIIB-Fc<sup>19,53</sup>, AAV-mediated gene transfer<sup>18,54</sup> or antibodies directed against the ActRIIB receptor<sup>55</sup>. Overall the conclusions were optimistic about the usefulness of such strategy to treat dystrophinopathies. However, it should be noted that our results and conclusions differ from previously published work in various aspects. We think the reason for that mainly lies in the choice of endpoints to define success or failure of such a treatment. For DMD patients, clinically relevant and quantifiable improvements would comprise better performance in the six-minutes walk<sup>56</sup> and improvement of respiratory function. This implies the ability of the patient's body to maintain a certain workload for a prolonged time period and not just to be able to produce single bouts of maximum short-duration muscle activity as tested by tetanic muscle contractions<sup>18,19</sup> or by the whole body tension method<sup>53</sup>. In most studies the increase of muscle size was taken as an endpoint<sup>18,54,55</sup>, automatically assuming that big muscles are healthier muscles. This basic assumption is put into question by our results. None of the studies investigated endurance capacity, which evaluates the effect of a treatment on the physiology of the entire body over a longer time period and would thus be a relevant parameter that could translate into improvement of life quality in patients. Several studies, one using the identical sActRIIB-Fc compound<sup>19</sup>, reported a small, but significant decline of CK values after ActRIIB blockade<sup>18,19,54</sup>. We were unable to reproduce this finding, the reason for these differences remaining unresolved.

We show that myostatin controls the metabolic profile of skeletal muscle, and its blockade depresses the main molecular determinants of oxidative metabolism and  $\beta$ -oxidation. Interestingly, genetic inactivation of *Ppar $\beta$* , similar to myostatin/ActRIIB blockade, reduced oxidative properties of skeletal muscle<sup>58</sup>. This adds further evidence that myostatin controls the muscle oxidative phenotype *via* peroxisome proliferator-activated receptors (PPAR) and Pgc1 $\alpha$ , the downstream target of *Ppar $\beta$* , while the down-regulation of *Pdk4* indicates a shift away from  $\beta$ -oxidation towards glucose metabolism. These qPCR data are strongly corroborated by a recent transcriptome study following treatment with sActRIIB-Fc of wild-type mice<sup>20</sup>. However, we lack direct evidence to ascertain a shift towards higher glucose metabolism, although the down-regulation of *Pdk4* and up-regulation of Enolase can be counted as indirect indicators for such a change. The unfavorable combination of decreased vascularization and metabolic changes after ActRIIB blockade is likely to cause a rapid imbalance between increased cytosolic ATP hydrolysis and insufficient mitochondrial ATP synthesis during exhaustive exercise. The subsequent shift towards anaerobic glycolytic ATP synthesis explains the rapid fa-

tigability and the pathologically increased lactate production<sup>59</sup>. However, the metabolic adaption in response to myostatin may differ in diverse physiological and pathophysiological contexts, e.g. myostatin was reported to improve motor performance in aged mice<sup>60</sup>. Further work is required to elucidate the metabolic function of myostatin in different disease situations and during ageing.

In conclusion, our results suggest that myostatin/ActRIIB signaling optimizes oxidative metabolism of skeletal muscle leading to lower muscle fatigability and amelioration of endurance capacity. Such fundamental functions of myostatin should be taken into account in the development of therapies based on myostatin/ActRIIB blockade. However, it should be kept in mind that our experimental design does not allow to determine which effects can be ascribed to myostatin blockade alone and which to the inactivation of other TGF- $\beta$  family members such as bone morphogenetic proteins (BMP), growth and differentiation factors (GDF) and activins that may also be sequestered by the soluble ActRIIB. Further investigations are required to answer the question, such as whether emerging therapies based on PPAR agonists might be able to prevent such adverse effects of ActRIIB blockade on the oxidative metabolism and on exercise tolerance. Furthermore, dose regime studies could answer the question, whether short-term treatment or pulse treatment may circumvent secondary effects of myostatin/ActRIIB blockade on muscle metabolism.

## FIGURES

**Figure 1:** Treatment of adult wild-type mice with sActRIIB-Fc. All tests were done after a 4 months treatment of the wild-type mice with either sActRIIB-Fc or PBS (controls). (a) Absolute maximal force (n=10 for each condition), and (b) specific maximal force of *EDL* and *soleus* muscles (n=10 for each condition). (c) Force recordings during the fatigue protocol over 180 s, and (d) Fatigue resistance of *EDL* (n=9 for PBS treated mice and n=8 for sActRIIB-Fc treated mice) and *soleus* muscles (n=10 for PBS treated mice and n=9 for sActRIIB-Fc treated mice). (e) Running distances during incremental speed running until exhaustion (n=5 for each condition). (f) Serum lactate levels at rest and 5 min after incremental speed running until exhaustion (n=5 for each condition). (g) A plot depicting the relationship between travel distance until exhaustion during incremental speed running and serum lactate, which was measured 5 min after exhaustion, for individual mice (n=5 for each condition). (h) Critical Speed before and after 1, 2 and 4 months of treatment with sActRIIB-Fc in comparison to PBS-treated control mice (n=5 for each condition). (i) A plot depicts the proportional relationship between distance run (y-axis) and time to exhaustion (x-axis) at different velocities. The slope of the regression line indicates the Critical Speed. Values are shown as means  $\pm$  SEM. p-Values were calculated using the nonparametric U-Test.

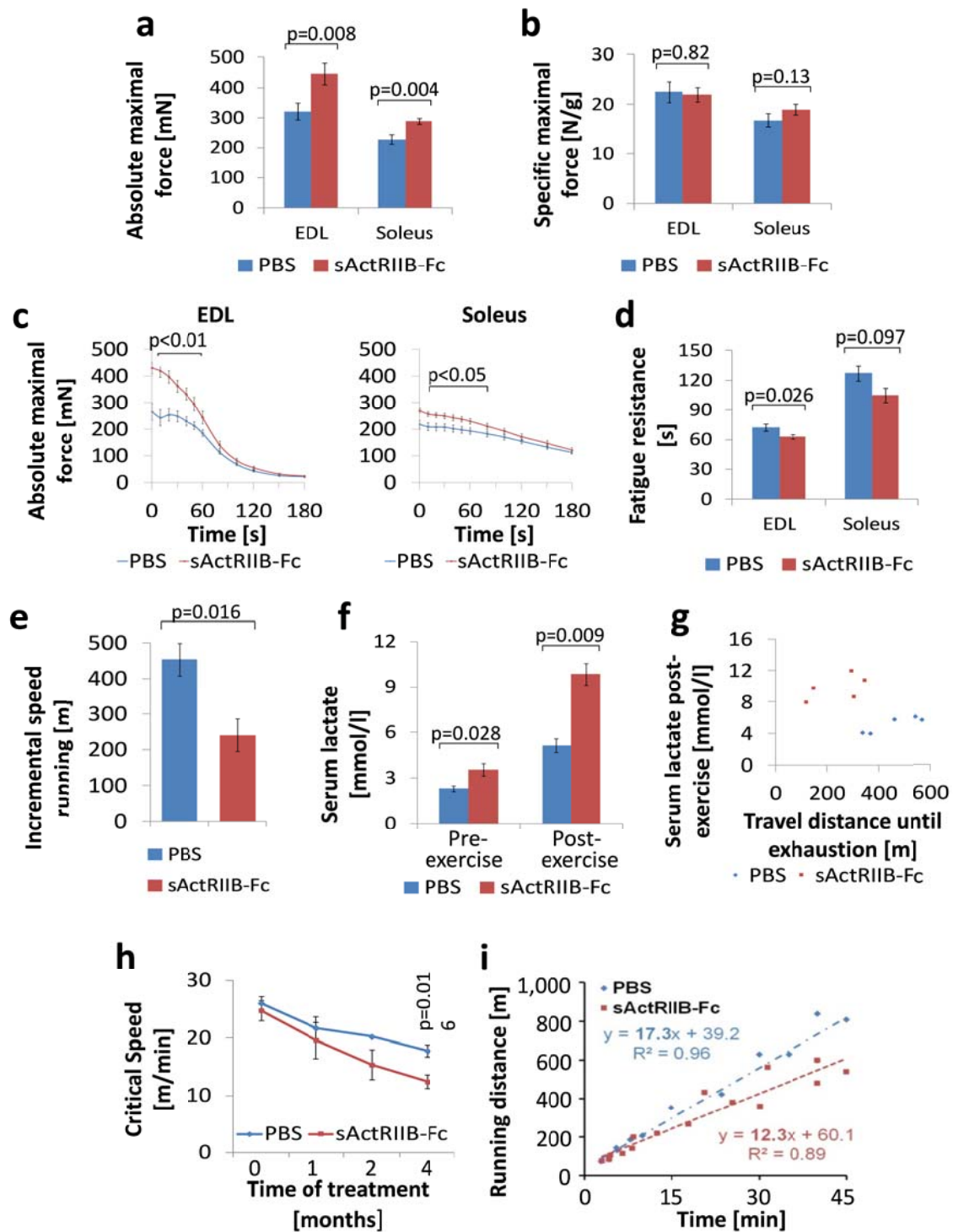


**Figure 2:** Treatment of adult *mdx* mice with sActRIIB-Fc. All tests were performed after a 4 months treatment of the *mdx* mice with either sActRIIB-Fc or PBS (controls). (a) Absolute maximal force (n=9 for each condition for *EDL* muscles and n=10 for each condition for *soleus* muscles), and (b) specific maximal force of *EDL* (n=9 for each condition) and *soleus* muscles (n=10 for each condition). (c) Force recordings during the fatigue protocol over 180 s of *EDL* and *soleus* muscles, and (d) fatigue resistance for *EDL* (n=8 for each condition) and *soleus* (n=10 for PBS treated mice and n=8 for sActRIIB-Fc treated mice). (e) Running distance during incremental speed running until exhaustion (n=5 for each condition). (f) Serum lactate levels at rest and 5 min after incremental speed running until exhaustion (n=5 for each condition). (g) A plot depicts the relationship between travel distance until exhaustion during incremental speed running and serum lactate, which was measured 5 min after exhaustion, for individual mice (n=5 for each condition). (h) Critical Speed before and after 1, 2 and 4 months of treatment with sActRIIB-Fc in comparison to PBS (n=5 for each condition). (i) A plot depicts the proportional relationship between distance run (y-axis) and time to exhaustion (x-axis) at different velocities. The slope of the regression line indicates the Critical Speed. Values are shown as means  $\pm$  SEM. p-Values were calculated using the nonparametric U-Test.

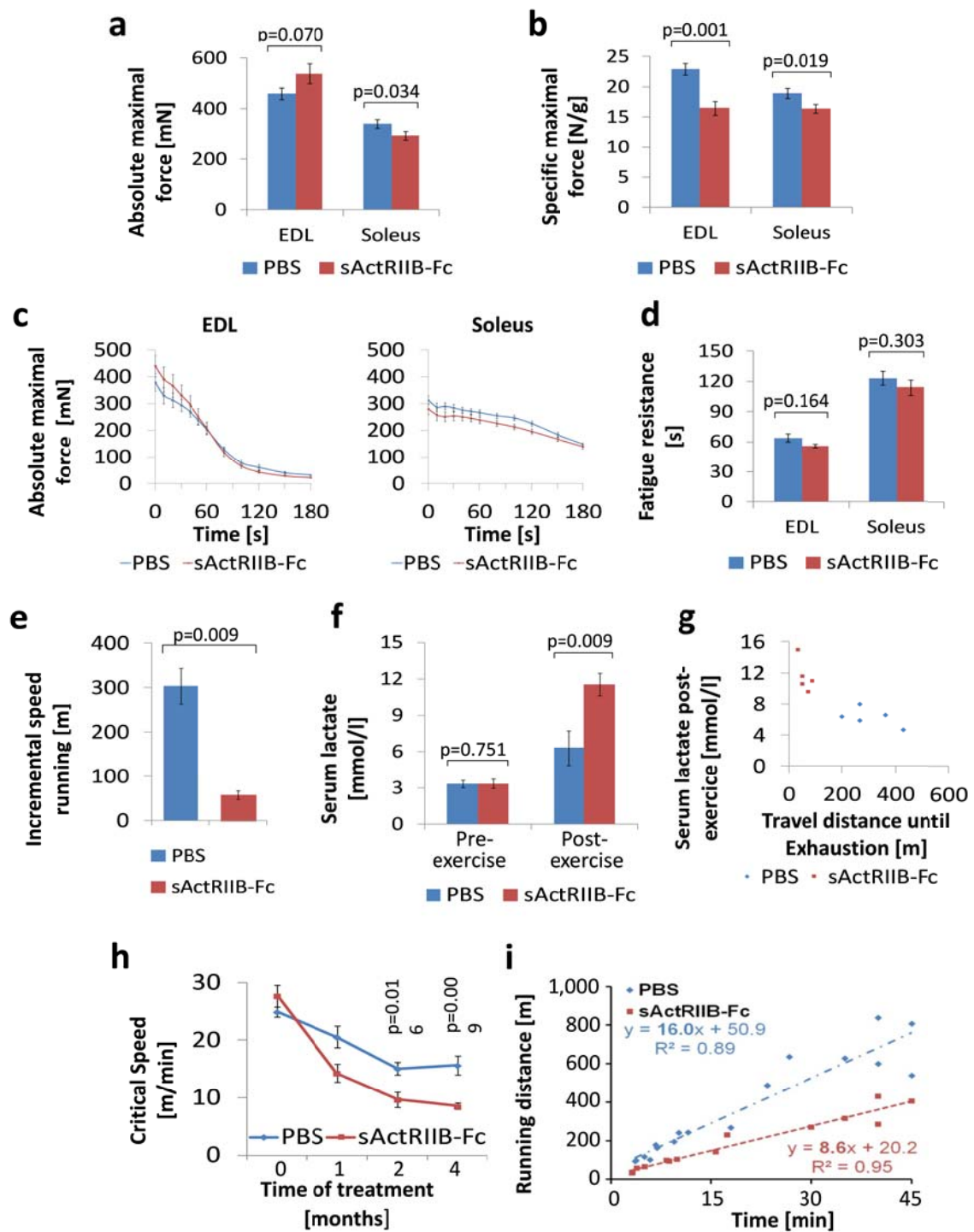


**Figure 3:** The effect of myostatin/ActRIIB signaling on vascularization. All investigations were done after a 4 months treatment of wild-type and *mdx* mice with either sActRIIB-Fc or PBS (controls). (a-d) Capillarization of wild-type *soleus* (n=430 fibers from PBS treated muscles (n=3) and n=300 fibers from sActRIIB-Fc treated muscles (n=3)) and *mdx soleus* muscle (n=605 fibers from PBS treated muscles (n=3) and n=836 fibers from sActRIIB-Fc treated muscles (n=4)). Histograms in (a) and (c) depict the distribution of capillaries per muscle fiber (in [%]), whereas diagrams in (b) and (d) depict the capillary domain, the fiber area per capillary (in [ $\mu\text{m}^2$ ]). Values are depicted as means  $\pm$  SEM. (e) *Vegf-A* relative mRNA-copy numbers as expressed per  $10^6 \times 18\text{S}$  rRNA copies in wild-type *TA* muscle (n=5 for each condition). (f) *Vegf-A* relative mRNA-copy numbers in  $\text{C}_2\text{C}_{12}$  myotubes following 24 h treatment with sActRIIB-Fc in comparison to control cultures (n=3 for each condition). (g) Relative mRNA-copy numbers of *MSTN* and myostatin receptors *ActRIIA/B* and *ALK4/5* in cultures of human umbilical vein endothelial cells (HUVEC) in comparison to muscle samples from a healthy control and a patient with Duchenne muscular dystrophy. Values are shown as means  $\pm$  SEM. p-Values were calculated using the nonparametric U-Test.

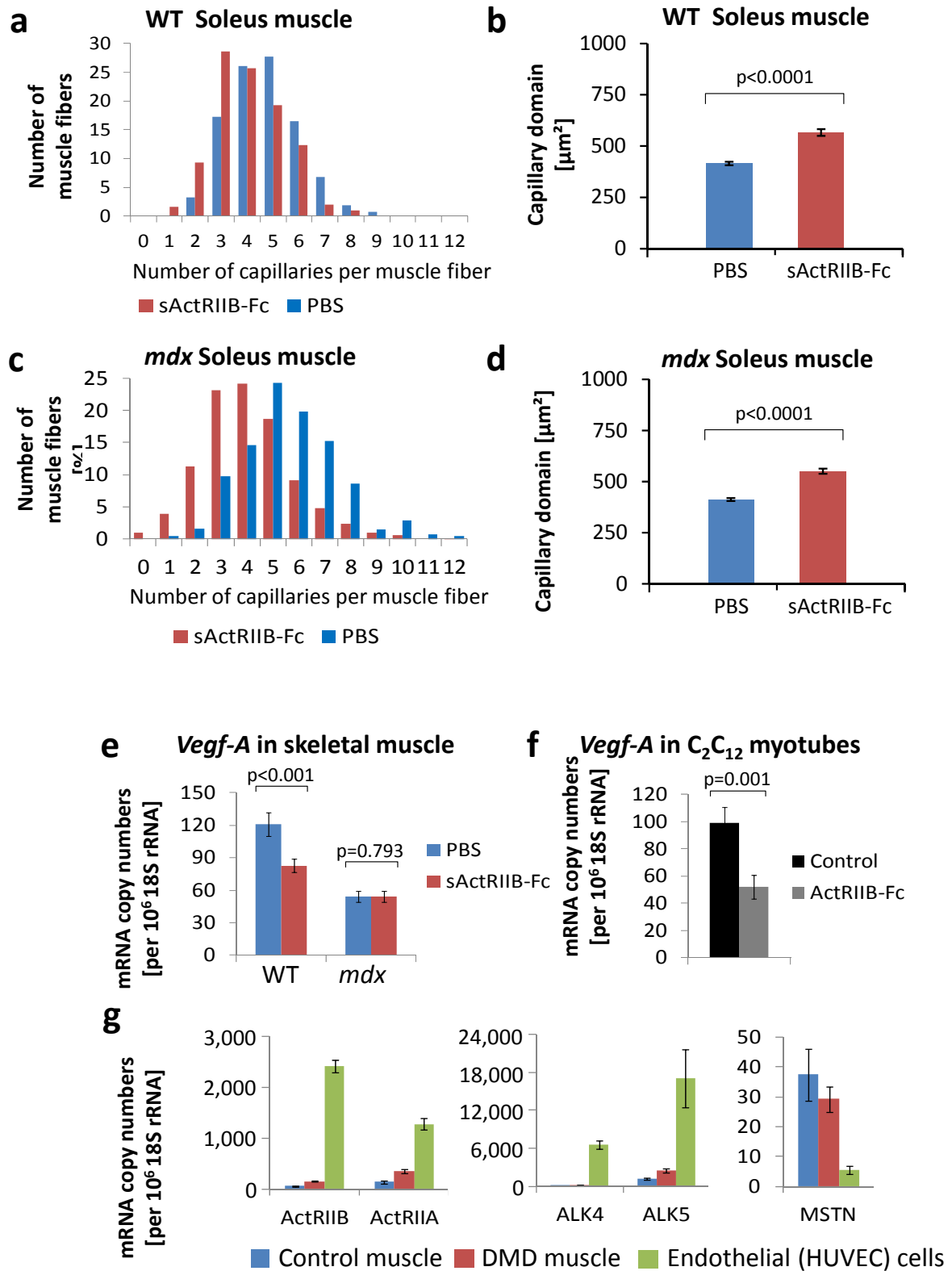


**Figure 4:** Effect of myostatin/ActRIIB signaling on muscle metabolic phenotype. All investigations were done after a 4 months treatment of wild-type (n=5 for each condition) and *mdx* mice (n=5 for each condition) with either sActRIIB-Fc or PBS (controls). (a) Western blots (left side) depict bands for Pgc1 $\alpha$  referenced to Desmin. The bar chart (right side) depicts the quotients of Pgc1 $\alpha$ /Desmin band densities. (b) *Pgc1 $\alpha$*  and (c) *Ppar $\beta$*  relative copy numbers in the *TA* muscle from wild-type and *mdx* mice as expressed per 10<sup>6</sup> x 18S rRNA copies. (d) Enolase enzymatic activity in *EDL* (n=5 for each condition) and *soleus* muscles (n=5 for each condition). (e-f) Relative mRNA-copy numbers of genes involved in the regulation of the oxidative metabolism in *TA* muscle from wild-type and *mdx* mice and (g) from C<sub>2</sub>C<sub>12</sub> myotubes following 24 h treatment with sActRIIB-Fc in comparison to control cultures (n=3 for each condition). Values are shown as means  $\pm$  SEM. p-Values were calculated using the non-parametric U-Test.

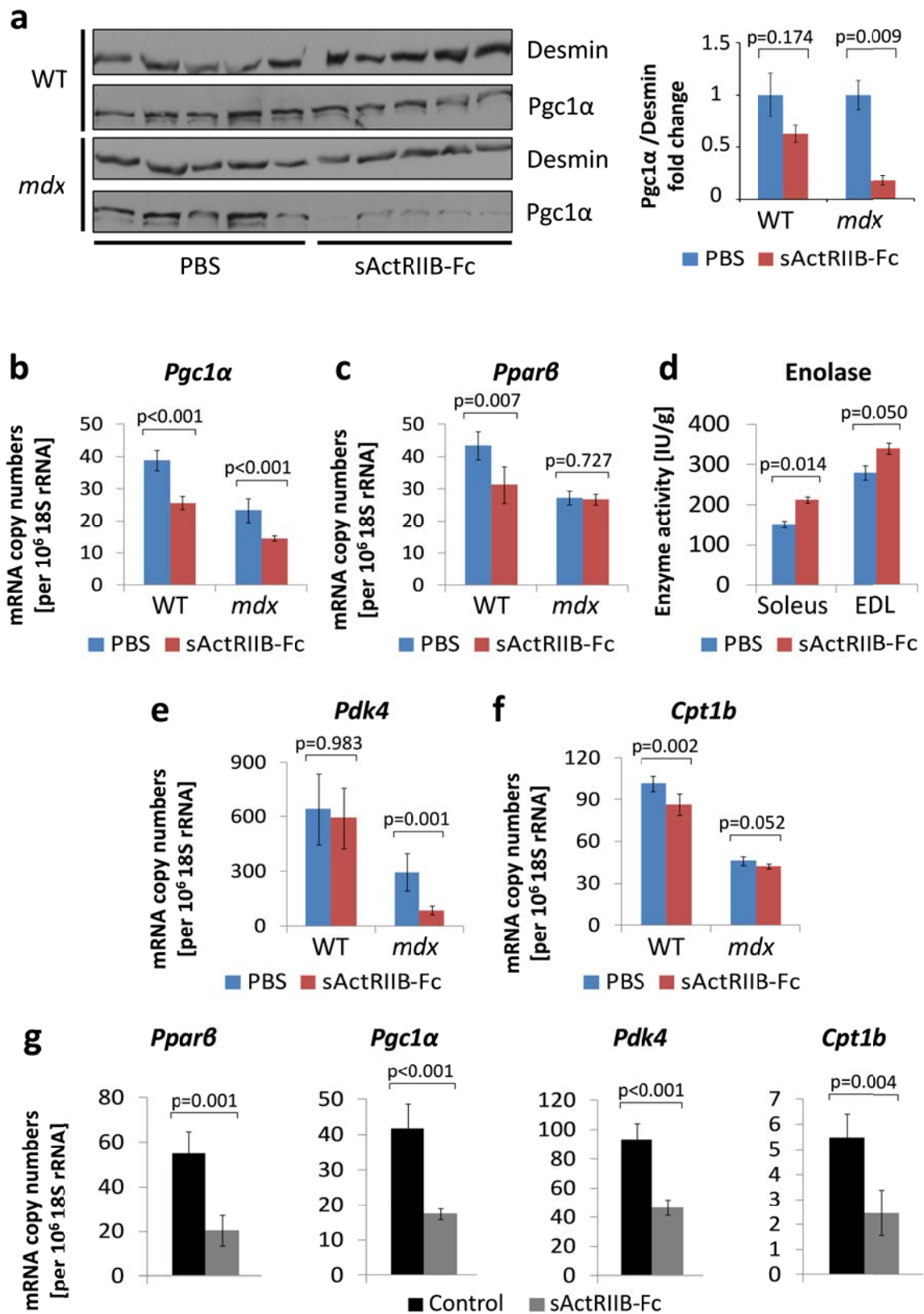
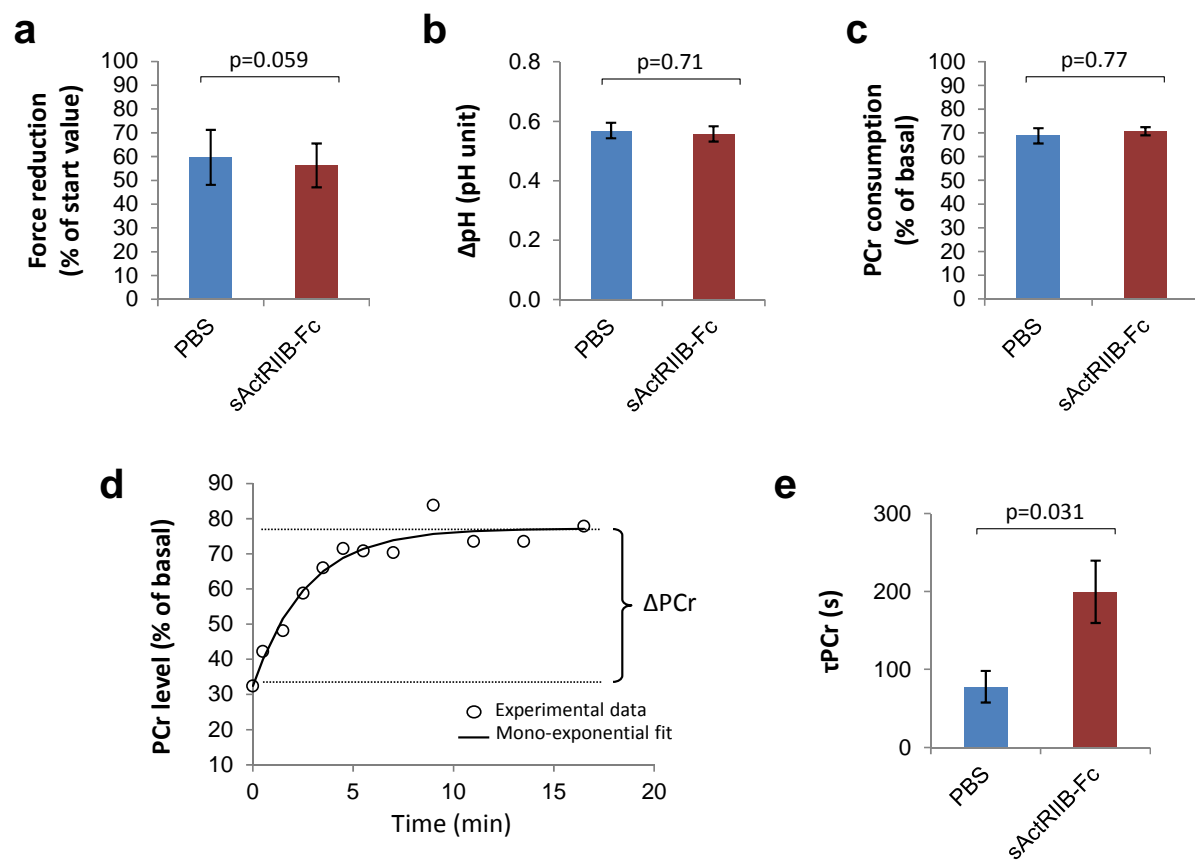


**Figure 5:** *In vivo* investigation of muscle function and oxidative metabolism in *mdx* calf muscles by non-invasive  $^{31}\text{P}$ -MRS. Investigations were done in *mdx* mice that were treated either with sActRIIB-Fc (n=5) or with PBS (controls; n=4). (a) The extent of force reduction was measured at the end of the 6 min period of electro-stimulation and is represented as percent of the starting value. (b) The drop of intracellular pH and (c) phosphocreatine (PCr) concentration was determined at the end of the 6 min *in vivo* electro-stimulation period. (d) For each animal, the post-stimulation time course of PCr was fitted to a mono-exponential function with a least mean-squared algorithm in order to calculate the PCr recovery time constant ( $\tau\text{PCr}$ ):  $\tau\text{PCr} = -t/\ln(\text{PCr}_t/\Delta\text{PCr})$ . During recovery from exercise, PCr is re-synthesized exclusively *via* oxidative ATP-synthesis. Thus the  $\tau\text{PCr}$  is considered a reliable *in vivo* index of mitochondrial oxidative capacity. (e)  $\tau\text{PCr}$  was significantly larger in sActRIIB-Fc treated *mdx* mice ( $200 \pm 39$  s *versus*  $78 \pm 20$  s in the control group), which is a strong *in vivo* indicator of an impaired oxidative mitochondrial metabolism in the sActRIIB-Fc treated *mdx* mice.



## MATERIALS AND METHODS

**Animals.** Male *mdx* mice (on a C57BL/10ScSn background) were bred in the animal facility of the Medical Faculty of Paris VI and kept according to institutional guidelines. Wild-type male C57BL/6J control mice were purchased from Charles River (France). Two-months-old wild-type and *mdx* mice were injected twice weekly subcutaneously with 10 mg/kg with the rodent form of the soluble activin receptor IIB (sActRIIB-Fc; Acceleron Pharma) for a total of four months before sacrifice. The methods of sActRIIB-Fc synthesis have previously been described<sup>61</sup>. All animal studies have been approved and were carried out under the laboratory and animal facility licenses A75-13-11 and A91-228-107.

**Evaluation of the critical speed.** Mice were subjected to three or four separate bouts of runs until exhaustion at various treadmill speeds (between 20 and 80 cm/s according to individual motor capacity, one run per day) according to previously published protocols<sup>27</sup>. Critical Speed, an index of the aerobic exercise capacity, was calculated from the slope (a) of the regression line, plotting the distance (y) against the time to exhaustion (x) from the different runs.

**Blood lactate assessment during exhaustive exercise.** Lactate concentrations were determined in blood samples collected from the tip of the tail using a *Lactate pro LT* device (Arkray Inc, Kyoto, Japan) at rest before exercise (0 min) and 5 min after treadmill running-induced exhaustion. Exhaustion was defined as the time point at which the mice were unable to run anymore and stayed on the grid despite repeated electric stimulation. The running test started at the lowest speed of 5 cm/s to allow a warm-up and then increased by 1 cm/s every 30 seconds until exhaustion. This protocol is illustrated by the Video S1 which demonstrates the running test of sActRIIB-Fc treated wild-type (left) and *mdx* mice (right) side by side. The starting speed of 5 cm/s was increased by 1 cm/s every minute until exhaustion of the *mdx* mouse at 19 cm/s after 14 minutes, while the wild-type mouse was still able to run at a speed of 40 cm/s.

**Electromyographic examination.** Electromyographic examination of the *triceps brachialis*, *tibialis*, *gastrocnemius* and *quadriceps femoris* muscles was performed in mice anesthetized with isoflurane. Standard non-invasive needle electromyography was conducted on a Viking Quest EMG apparatus (Viasys, Nicolet Biomedical, Madison, Wisconsin) using concentric bipolar needle electrodes. Inter-tational activity and pathological spontaneous activity were recorded.

**Measurement of contractile properties.** Absolute maximal isometric tetanic force (P0) was measured during tetanic contractions (frequency of 50-100 Hz, train of stimulation of 1,500 ms for *soleus* and 750 ms for *EDL*). Specific maximal isometric force (sP0) was given as the quotient between force and muscle weight. For analysis of fatigue resistance, muscles were stimulated at 75 Hz for 500 ms, every 2 seconds over 3 minutes. See details in the Online Supplementary Material.

**Western blot.** Protein was extracted from frozen *tibialis anterior* (TA) muscle of wild-type and *mdx* mice and processed as described<sup>62</sup>. Briefly, after homogenization of the muscle in RIPA buffer with a proteinase inhibitor cocktail (Complete®, Roche-Diagnostics) proteins were separated through denaturing SDS-PAGE with the Laemmli system and blotted onto nitrocellulose membranes by the semidry method (Biometra). The blots were probed with anti-Porin as primary antibody (VDAC 31HL, AB-2, Calbiochem), anti-PGC1 $\alpha$  (Santa-Cruz), anti-Nos1 (Abcam) and corresponding peroxidase-labeled secondary antibodies. The desmin and GAPDH bands were used as loading control for muscle. Bands were visualized by chemiluminescence. The protein bands were quantified by measuring their integrated density within a rectangle that covered the entire individual band and subtracting the integrated density of an empty rectangle of exactly the same size in the vicinity using the ImageJ software.

**Enzyme measurements.** Enolase, citrate synthase [CS], cytochrome C oxidase [COX] and hydroxyacyl-CoA-dehydrogenase [HADHA] activities were determined in extracts from frozen cryostat sections using a coupled enzyme assay<sup>63</sup> as detailed in the Online Supplementary Material.

**Histology and SDS-PAGE.** H&E, SDH and COX staining were performed using routine histological protocols. The following primary antibodies were used for immunohistochemistry: anti-CD31 (Pharmingen), anti-MHCIIA (SC-71, DSMZ), anti-MHCI (BAD5, DSMZ), anti-Nos1 (Abcam) and anti-Laminin (Dako) followed by secondary antibodies with various fluorophores (AlexaFluor®, Invitrogen). See details in the Online Supplementary Material.

Morphometric analysis of capillary number and capillary domains: Cryosections of 12  $\mu\text{m}$  of the EDL and *soleus* muscles of PBS- and sActRIIB-Fc treated animals were stained with anti-laminin to delineate the muscle fibers. Muscle capillaries were stained with anti-CD31. Fluorescent photographs were taken with a 20x objective on a Microscope (Zeiss, AxioImager Z1) and saved as TIFF files. These images were projected on a flatscreen coupled with a graphic tablet, which enabled the manual retracing of the muscle fiber outlines and the counting of capillaries that were found around it. For the EDL the fibers of the entire muscle cross section were analyzed and for the *soleus* muscle the fibers from 10 representative non-overlapping visual fields. For each muscle fiber we determined the cross sectional plane [ $\mu\text{m}^2$ ] and counted the number of bordering capillaries. The capillary domain [ $\mu\text{m}^2$ ] for each fiber was calculated by dividing its cross sectional plane by the number of bordering capillaries.

**Cell Culture.** C<sub>2</sub>C<sub>12</sub> cells were grown in DMEM (Gibco 41966-029) supplemented with 1% Pen/Strep and 20% FBS (Gibco 10500-064) to semiconfluency at 37°C and 5% CO<sub>2</sub> for 2 days. Thereafter the medium was replaced by DMEM + 10% horse serum (Gibco 26050-088) to induce fusion into multinucleated myotubes. sActRIIB-Fc was added to a final concentration of 200 ng/ml to the culture medium of the myotubes. After 24 h the myotubes were harvested by trypsinization, washed and pel-

leted for RNA extraction. Human umbilical vein endothelial cells (HUVEC) were grown to confluency, trypsinized and pelleted for RNA extraction. The doubling time of the cells was determined using the AlamarBlue reagents from Invitrogen (UK). Briefly, cells were plated at 20% confluency and allowed to settle for 12 h before introducing recombinant myostatin (R&D Systems). The cells were grown for 24 h before addition of 0.1 volume of AlamarBlue reagent and incubation at 37°C for 20 min before photometric analysis. The cells were then washed and cultured in fresh medium containing myostatin. Cell proliferation was monitored every 24 h for 4 days after initial introduction of myostatin. Cell number was determined by comparison of absorbance against a standard curve. All experiments were performed in triplicate.

**RT-qPCR.** Real-Time qPCR was performed according the SYBR Green® protocol (Applied Biosystems) on the Eco Real-Time PCR System (Illumina) with a HotStart Taq polymerase. For primer sequences see Online Supplementary Material. Fold changes were calculated according to the efficiency corrected  $-\Delta\Delta C_t$  method<sup>64</sup>. The use of normal and of DMD muscle from patients was covered by the approval of the ethical review board of the Charité (#216/2001). All patients or their legal guardians provided written informed consent according to the Declaration of Helsinki.

***In vivo MRS investigation of muscle function and oxidative metabolism.*** Mice were anesthetized with 4% isoflurane in 100% air at a flow of 3 l/min and were placed into a home-built cradle specifically designed for the strictly noninvasive MRS investigation of muscle function and energetics<sup>37</sup>. Throughout the experiment, anesthesia was maintained using a facemask continuously supplying 1.75% isoflurane in 33% O<sub>2</sub> (0.2 l/min) and 66% N<sub>2</sub>O (0.4 l/min). Animal body temperature was controlled by a rectal probe and maintained at physiological values by a feedback loop that regulated an electrical heating blanket. MR spectra were recorded in the 4.7 T horizontal magnet of a 47/30 Biospec Avance MR system (Bruker, Karlsruhe, Germany) equipped with a Bruker 120-mm BGA12SL (200 mT/m) gradient insert. Calf muscle were electro-stimulated transcutaneously to produce maximal repeated isometric contractions at a frequency of 1.7 Hz. Mechanical performance was measured using a foot pedal coupled to a force transducer. Concentrations of phosphorylated compounds and intracellular pH of the calf muscle were continuously measured with an elliptic (8 x 12 mm<sup>2</sup>) <sup>31</sup>P-MRS surface coil during 6 min of rest, 6 min of electro-stimulation and 16 min of recovery. MRS data were processed using a custom-written analysis program developed on the IDL software (Research System, Boulder, CO, USA). In order to determine the time constant of post-exercise phosphocreatine re-synthesis ( $\tau$ PCr, an *in vivo* index of oxidative mitochondrial capacity), the time course of phosphocreatine concentrations during the post-stimulation period was fitted to a mono-exponential function with a least mean-squared algorithm (Fig. 5d):  $\tau$ PCr =  $-t/\ln(PCr_t/\Delta PCr)$ , where  $\Delta$ PCr is the extent of PCr depletion measured at the start of recovery period.

**Statistical analysis.** Data were analyzed and significance levels calculated using the non-parametric Wilcoxon-Mann-Whitney U-Test, as stated in the legends and detailed in the Online Supplementary Material. Values are presented as means  $\pm$  SEM (Standard Error of the Mean). Significance levels were set at  $p < 0.05$ .

### ACKNOWLEDGMENTS

We would like to acknowledge Acceleron Pharma for the gift of sActRIIB-Fc. This work was supported by the Association Française contre les Myopathies towards H.A., A.F., A.V., L.A., L.G., and E.M., Association Monegasque contre les Myopathies and the Parents Project France towards H.A. and C.H., Aktion Benni & Co towards H.A., the Deutsche Forschungsgemeinschaft and the Université Franco-Allemand towards K.R., H.A. and M.S. (as part of the MyoGrad International Graduate School for Myology DRK 1631/1 and CDFA-06-11), and NeuroCure (Exc 257) to M.S. The authors do not declare any conflict of interest.

### AUTHORS' CONTRIBUTIONS

K.R., E.M., C.H., O.A., K.P., S.L., K.J., B.G., F.P.-R., L.A., A.V., D.F., S.B., A.F., M.S., H.A. performed the experiments; M.S. contributed patient material; O.R. contributed new reagents; K.R., E.M., D.F., S.B., B.G., D.B. A.F., R.V.C., M.S., H.A. analyzed the data; M.S. did the statistical analysis; K.R., E.M., B.G., D.B., M.S., H.A. wrote the manuscript, K.P. revised the article critically for important intellectual content. All authors read the final version of the manuscript and gave final approval of the manuscript to be published.

## Supplemental Online Information

### Supplemental methods

#### ***Measurement of contractile properties***

The contractile properties of *extensor digitorum longus* (*EDL*) and *soleus* muscles were studied *in vitro* according to previously published protocols <sup>1</sup>. Muscles were soaked in an oxygenated Tyrode solution (95% O<sub>2</sub> and 5% CO<sub>2</sub>) containing 58.5 mM NaCl, 24 mM NaHCO<sub>3</sub>, 5.4 mM KCl, 1.2 mM KH<sub>2</sub>PO<sub>4</sub>, 1.8 mM CaCl<sub>2</sub>, 1 mM MgSO<sub>4</sub>, and 10 mM glucose (pH7.4) and maintained at a temperature of 22°C. One muscle tendon was attached to a lever arm of a servomotor system (300B, Dual-Mode Lever, Aurora). After equilibration (30 min), field electrical stimulation was delivered through electrodes running parallel to the muscle. Pulses of 1 ms were generated by a high power stimulator (701B, Aurora). Absolute maximal isometric tetanic force (P<sub>0</sub>) was measured during tetanic contractions (frequency of 50-100 Hz, train of stimulation of 1, 500 ms for *soleus* and 750 ms for *EDL*). The muscle length was adjusted to an optimum (L<sub>0</sub>) that produced P<sub>0</sub>. Specific maximal isometric force (sP<sub>0</sub>) was calculated by dividing the force by the weight of the muscle. Fatigue resistance was then determined after a 5 min rest period. The muscles were stimulated at 75 Hz during 500 ms, every 2 s, for 3 min. The time taken for initial force to fall by 50% (*EDL*) or 30% (*soleus*) was then measured. All data were recorded and analyzed on a microcomputer, using the PowerLab system (4SP, AD Instruments) and software (Chart 4, ADInstruments).

#### ***Histology***

For CD31 expression, frozen unfixed 12 µm sections of *EDL* and *soleus* muscles were blocked 1 h in PBS plus 2% BSA and 2% SVF. Sections were then incubated overnight with primary antibodies: anti-CD31 (Pharmigen) and anti-laminin (Dako). After washes in PBS, sections were incubated 1 h at room temperature with secondary antibodies with various fluorophores (AlexaFluor®, Invitrogen). After washes in PBS, slides were mounted in Fluoromount-G (Southern Biotech).

For expression analysis of Myosin Heavy Chains (MHC) isoforms, primary antibodies were: anti-MHCI (hybridoma#BA-D5, Deutsche Sammlung von Mikroorganismen und Zellkulturen DSMZ) and anti-MHCIIa (hybridoma#SC-71, DSMZ). For MHC-immunohistochemistry, frozen unfixed 12 µm sections were blocked 1 h in PBS plus 2% BSA and 2% SVF. Sections were then incubated overnight with primary antibodies against laminin (Dako) and MHC I and MHCIIa isoforms. After washes in PBS, sections were incubated 1 h with secondary antibodies with various fluorophores (AlexaFluor®, Invitrogen). After washes in PBS, slides were finally mounted in Fluoromont-G (Southern Biotech). Morphometric analyses were made on whole sections of *EDL* and *soleus* muscles. Images were captured using a digital camera (Hamamatsu ORCA-AG) attached to a motorized fluorescence microscope (Zeiss Axi-

olmager Z1), and morphometric analyses were made using the MetaMorph v7.5 software (Molecular Devices).

For Nos1 expression, frozen unfixed 12 µm sections of EDL muscles were rehydrated in PBS, fixed with 4% PFA for 10 min, blocked in 4% BSA for 1 h. Sections were then incubated overnight at room temperature with primary antibodies: anti-Nos1 (Abcam). After washes in PBS, sections were incubated 1 h at room temperature with secondary antibodies with various fluorophores (AlexaFluor®, Invitrogen). After washes in PBS, slides were mounted in Fluoromount-G (Southern Biotech). Images were captured by confocal laser scanning microscope (Leica SPE DM2500).

## RT-qPCR

Total RNA was isolated from frozen muscle after pulverization in liquid nitrogen from C<sub>2</sub>C<sub>12</sub> cell pellets and from endothelial human cells with the Trizol® (Invitrogen) extraction protocol. Isolated RNA was quantified using the NanoDrop® ND-1000 spectrophotometer (Thermo Scientific) and cDNA was synthesized using the Thermoscript® RT PCR System (Invitrogen). After cDNA synthesis, Real Time PCR was performed by using the SYBR Green® PCR Master Mix Protocol (Applied Biosystems) in triplicate on the ECO Real-Time PCR System (Illumina) with a hotstart-Taq polymerase. A 10 min denaturation step at 94°C was followed by 40 cycles of denaturation at 94°C for 10 s and annealing/extension at 60°C for 30 s. Before sample analysis we had determined for each gene the PCR efficiencies with a standard dilution series (10<sup>0</sup>-10<sup>7</sup> copies/µl), which subsequently enabled us to calculate the copy numbers from the C<sub>t</sub> values<sup>2</sup>. mRNA levels were normalized to 18S rRNA. The sequences for the primers used are listed below:

Table of oligonucleotides used for RT-qPCR of mouse and human tissues

Gene	Primer sequence (5'–3')	Direction
<i>Oligonucleotide primers used for mice</i>		
<i>Pparβ</i>	AGCCACAACGCACCCTTT	forward
	CGGTAGAACACGTGCACACT	reverse
<i>Pgc1α</i>	GAAAGGGCCAAACAGAGAGA	forward
	GTAAATCACACGGCGCTCTT	reverse
<i>Vegf-A</i>	AAGCCAGCACATAGGAGAGATGA	forward
	TCTTTCTTTGGTCTGCATTCACA	reverse
<i>Cpt1b</i>	TCGCAGGAGAAAACACCATGT	forward
	AACAGTGCTTGGCGGATGTG	reverse
<i>Pdk4</i>	AGGTCGAGCTGTTCTCCCGCT	forward
	GCGGTCAGGCAGGATGTCAAT	reverse
<i>Nos1</i>	AAGGAGCAAGGAGGCCATAT	forward
	ATATGTTCTGAGGGTGACCCC	reverse
<i>Vdac1 (Porin)</i>	ACTGTGGAAGACCAGCTTGC	forward
	TGCTCCCTCTTGACCTGT	reverse
<i>MTCO2</i>	GCCGACTAAATCAAGCAACA	forward
	CAATGGGCATAAAGCTATGG	reverse

18S rRNA	CATTCGAACGTCTGCCCTATC	forward
	CTCCCTCTCCGGAATCGAAC	reverse
<i>Oligonucleotide primers used for humans</i>		
ACVR2B	AGCCGTCTATTGCCCA	forward
	CATGTACCGTCTCGTGCCTA	reverse
ACVR2A	AGGTTGTTGGCTGGATGAT	forward
	GCCCTCACAGCAACAAAAAT	reverse
ALK4	GTCTTGGTTCAGGGAAGCAG	forward
	GGACCCGTGCTCATGATAGT	reverse
ALK5	TTGCTCCAAACCACAGAGTG	forward
	TGAATTCCACCAATGGAACA	reverse
18S rRNA	CATTCGAACGTCTGCCCTATC	forward
	CTCCCTCTCCGGAATCGAAC	reverse

### **Measurement of enzyme activities**

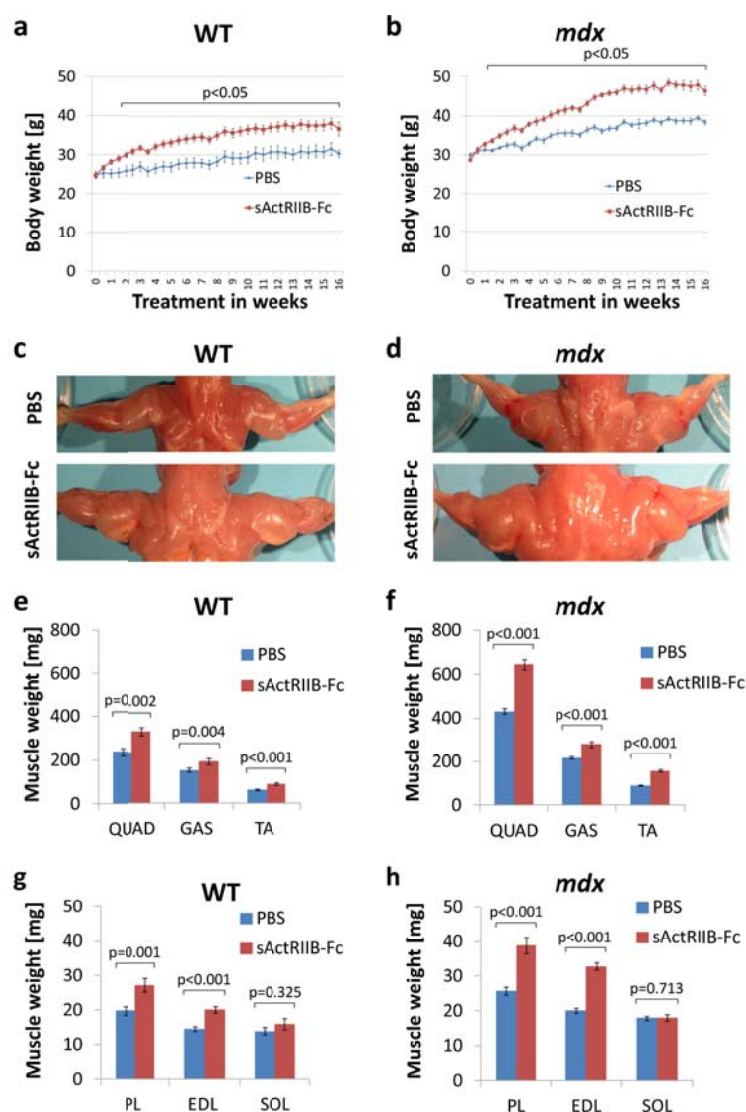
**[1] Enolase:** Enolase-catalyzed conversion of 2-phospho-d-glycerate to phosphoenolpyruvate at 25°C was monitored spectrophotometrically at 340 nm. Activity was expressed in international units (IU) per mg of protein.

**[2] Citrate synthase:** Citrate synthase-catalyzed conversion of oxaloacetate and acetyl-CoA to citrate at 30°C was monitored spectrophotometrically at 412 nm. Activity was expressed in international units (IU) per mg of protein.

**[3] Cytochrome C oxidase (COX):** Cytochrome C oxidase-catalyzed oxidation of cytochrome C at 30°C was monitored spectrophotometrically at 550 nm. Activity was expressed in international units (IU) per mg of protein.

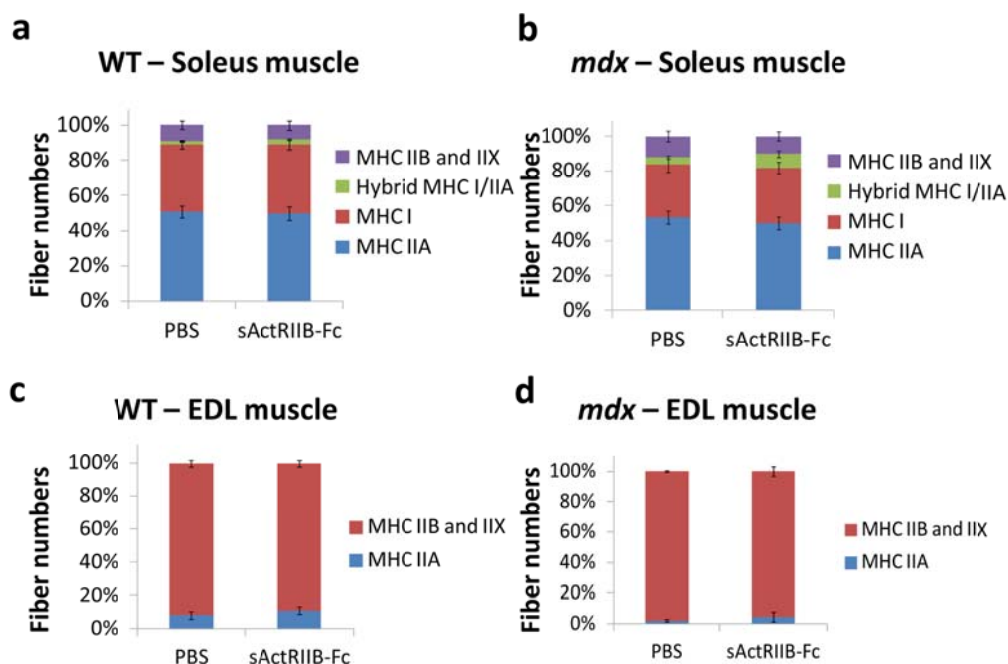
**[4] Hydroxyacyl CoA dehydrogenase (HADHA):** HADHA-catalyzed conversion of acetoacetyl-CoA to hydroxybutyryl-CoA at 30°C was monitored spectrophotometrically at 340 nm. Activity was expressed in international units (IU) per mg of protein.

## Supplemental Figures



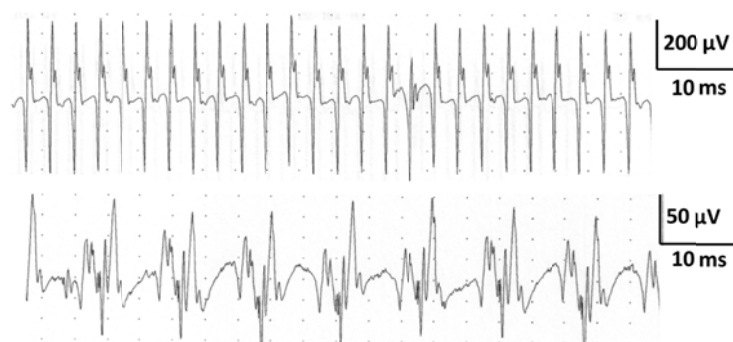
**Supplemental Figure 1.** Effect of sActRIIB-Fc on body weight and muscle weight in wild-type and *mdx* mice.

2-months-old wild-type mice (a,c,e,g) and *mdx* mice (b,d,f,h) were systemically treated for 4 months with sActRIIB-Fc or PBS (n=5 for each condition). (a,b) Effect of sActRIIB-Fc on body weight increase in comparison to PBS treated control mice. (c,d) Dorsal view on the upper shoulder girdle with fore limbs. (e-h) Effect of sActRIIB-Fc on muscle wet weight of *quadriceps* (QUAD), *gastrocnemius* (GAS), *tibialis anterior* (TA), *plantaris* (PL), *extensor digitorum longus* (EDL), and *soleus* (SOL) muscles (n=5 for each condition). Values are shown as means  $\pm$  SEM. p-Values were calculated using the nonparametric U-Test.



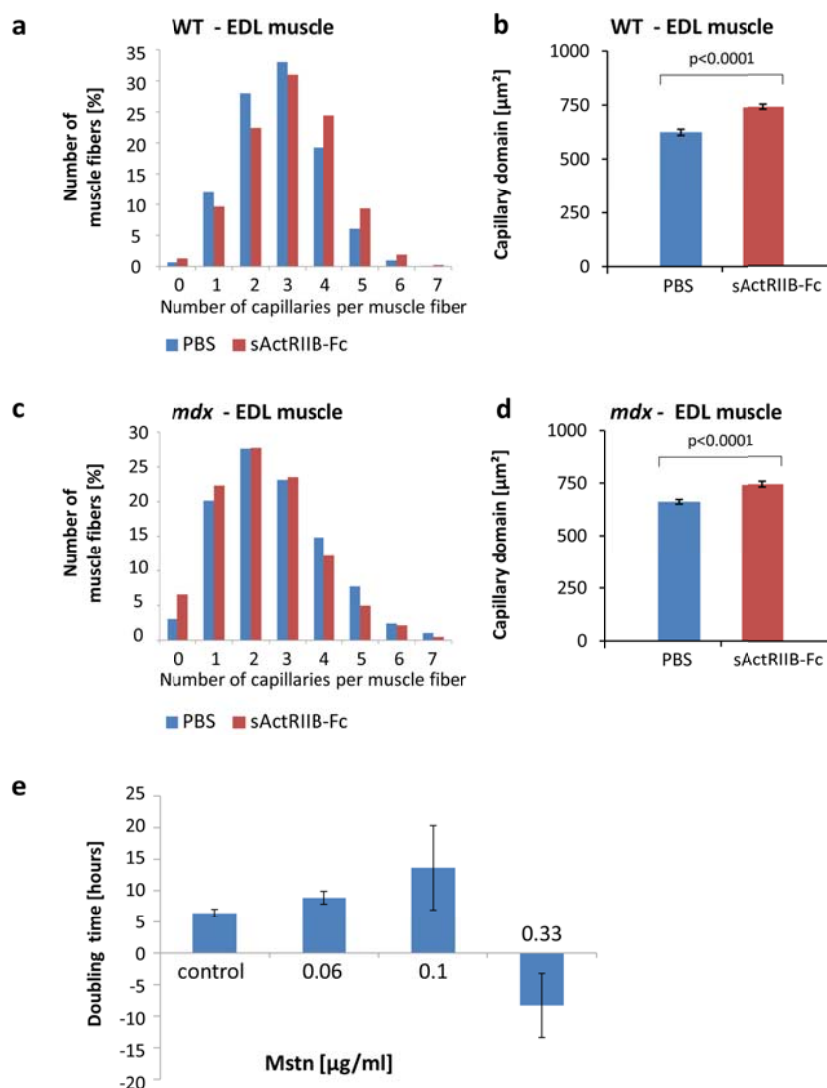
**Supplemental Figure 2. Effect of sActRIIB-Fc on fiber-type distribution of EDL and soleus muscles from wild-type and *mdx* mice.**

(a-d) Fiber-type distribution of *soleus* and *EDL* muscles from wild-type mice (a,c) and *mdx* mice (b,d) after 4 months treatment with sActRIIB-Fc compared to muscles from PBS treated control mice. (a,b) Fiber-type composition of the *soleus* muscle as shown by the relative fiber-type distribution from entire transverse sections following immunostaining with anti-MHC I and MHC IIA antibodies. Unstained fibers (non MHC I/IIA) were considered IIB or IIX. (c,d) Fiber-type composition of the *EDL* muscle as shown by the relative fiber-type distribution from entire transverse sections following immunostaining with anti-MHC I and MHC IIA antibodies. Unstained fibers (non MHC I/IIA) were considered IIB or IIX. MHC I positive fibers were only exceptionally seen and are therefore not depicted. Values are shown as means  $\pm$  SEM.



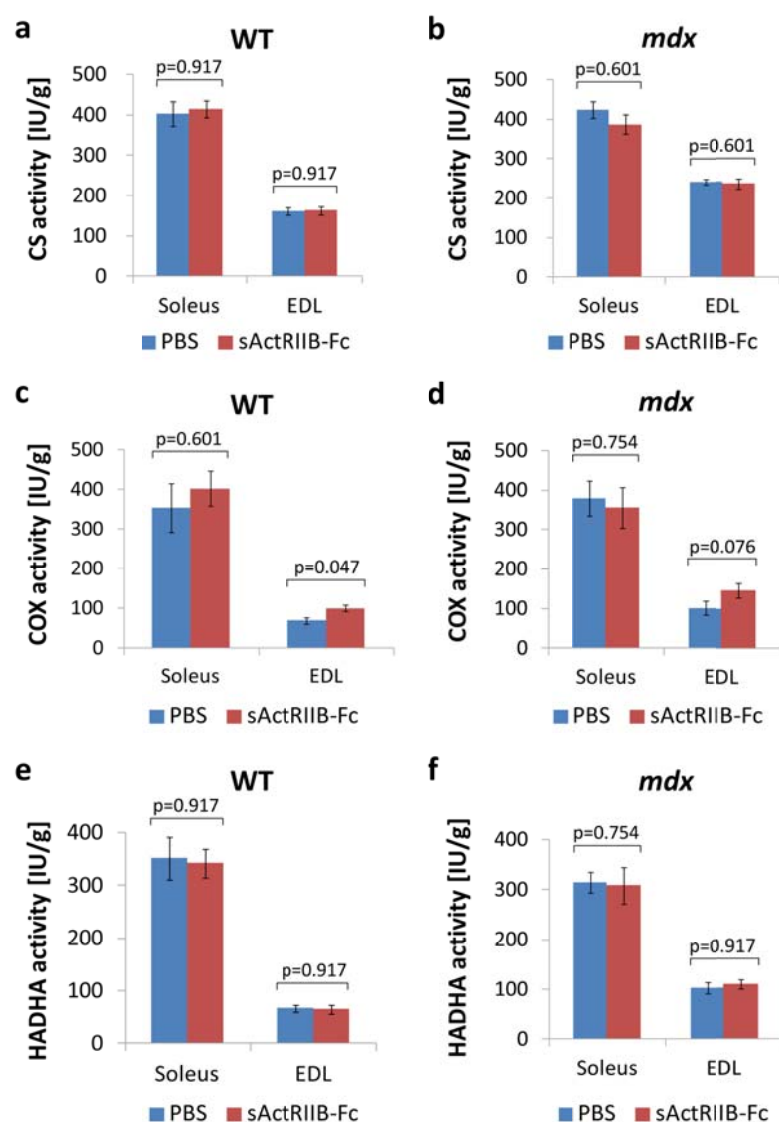
**Supplemental Figure 3. Effect of sActRIIB-Fc on EMG recordings of *mdx* mice.**

Examples of spontaneous potentials recorded under anesthesia in *triceps brachialis* muscle of *mdx* mice. The upper trace was recorded in a PBS treated mouse, the lower trace in a sActRIIB-Fc treated mouse. Both traces show complex repetitive discharges (sensitivity, 200  $\mu$ V/division upper trace, 50  $\mu$ V/division lower trace, sweep speed, 10 ms/division).



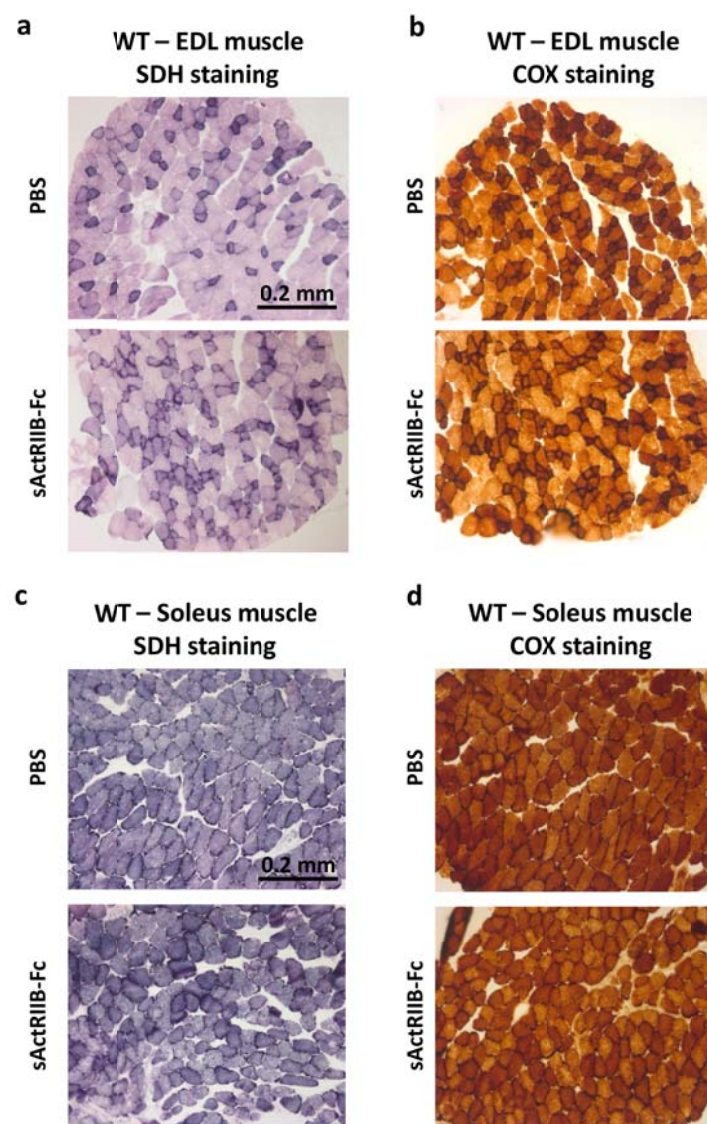
**Supplemental Figure 4. Effect of myostatin on capillaries and endothelial cell proliferation.**

(a-d) Investigations were done after a 4 months treatment of wild-type and *mdx* mice with either sActRIIB-Fc or PBS (controls). Plots in (a-d) depict capillarization of wild-type *EDL* ( $n=1625$  fibers from PBS treated muscles ( $n=3$ ) and  $n=2752$  fibers from sActRIIB-Fc treated muscles ( $n=4$ )) and *mdx EDL* muscle ( $n=2609$  fibers from PBS treated muscles ( $n=3$ ) and  $n=2137$  fibers from sActRIIB-Fc treated muscles ( $n=3$ )). Histograms in (a) and (c) depict the distribution of muscle fibers according to the number of capillaries per muscle fiber. Diagrams in (b) and (d) depict the capillary domain (average fiber area serviced per capillary [ $\mu\text{m}^2$ ]). Values are depicted as means  $\pm$  SEM. (e) Cultures of human umbilical vein endothelial cells (HUVEC) were treated for 24 h with recombinant myostatin at concentrations of 0.06, 0.10 and 0.33  $\mu\text{g/ml}$ . At low concentration (0.06  $\mu\text{g/ml}$ ), myostatin inhibited cell proliferation as the doubling time of cells in culture increased. Higher myostatin concentrations caused large variability of doubling time which was caused by cytotoxicity. All values are statistically significant relative to the control.



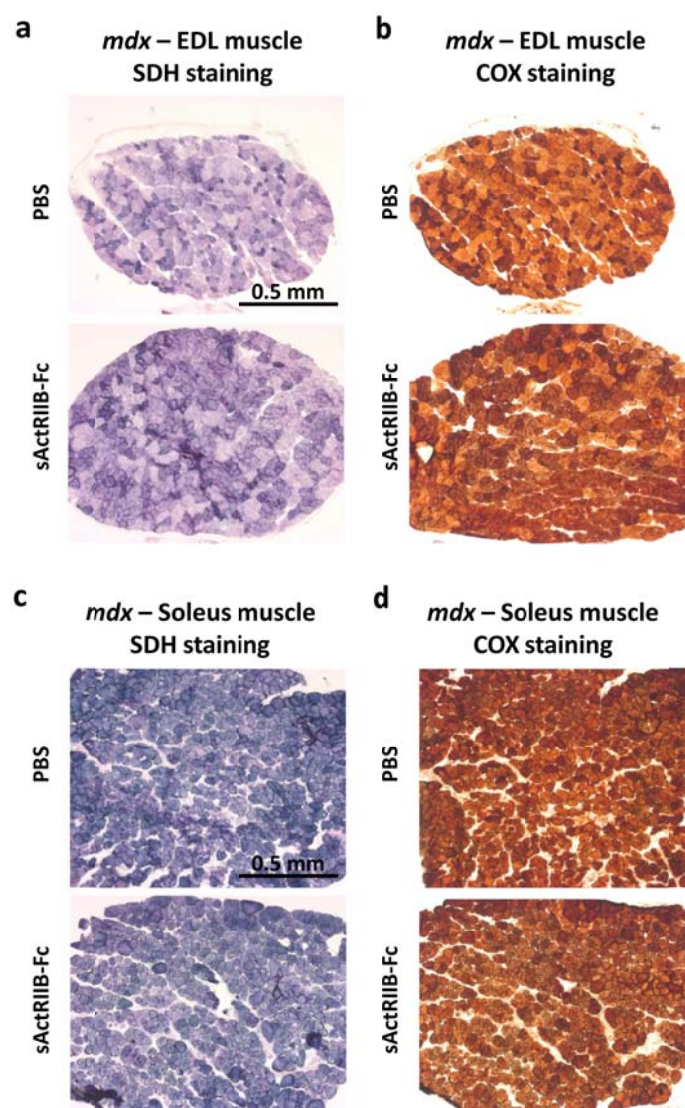
**Supplemental Figure 5. Effect of sActRIIB-Fc on enzymes activities of mitochondrial respiratory chain in *EDL* and *soleus* muscles from wild-type and *mdx* mice.**

(a-f) Wild-type and *mdx* mice were systemically treated with sActRIIB-Fc or PBS for 4 months and enzyme activities were measured in muscle homogenates from *EDL* (n=5 for each condition) and *soleus* muscles (n=5 for each condition) for (a,b) citrate synthase [CS], (c,d) cytochrome-C oxidase [COX] and (e,f) hydroxyacyl-CoA dehydrogenase [HADHA]. Values are shown as means  $\pm$  SEM. p-Values were calculated using the nonparametric U-Test.



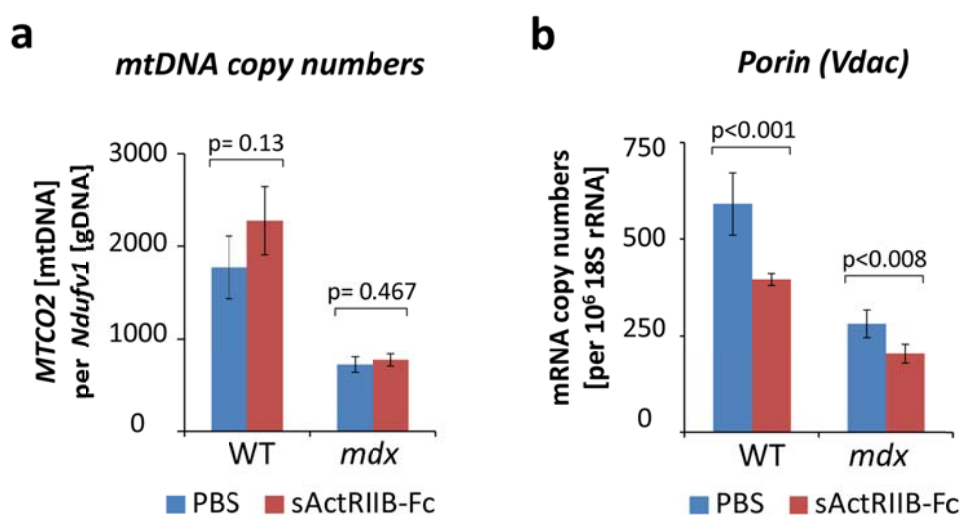
**Supplemental Figure 6.** Effect of sActRIIB-Fc on SDH and COX enzyme activity on muscle sections of *EDL* and *soleus* muscles from wild-type mice.

(a-d) Images of transverse sections of (a,b) *EDL* muscle and (c,d) *soleus* muscle from wild-type mice stained for (a,c) succinate dehydrogenase [SDH] activity and (b,d) cytochrome-C oxidase [COX] activity after 4 months treatment with sActRIIB-Fc in comparison to muscles from PBS treated control mice.



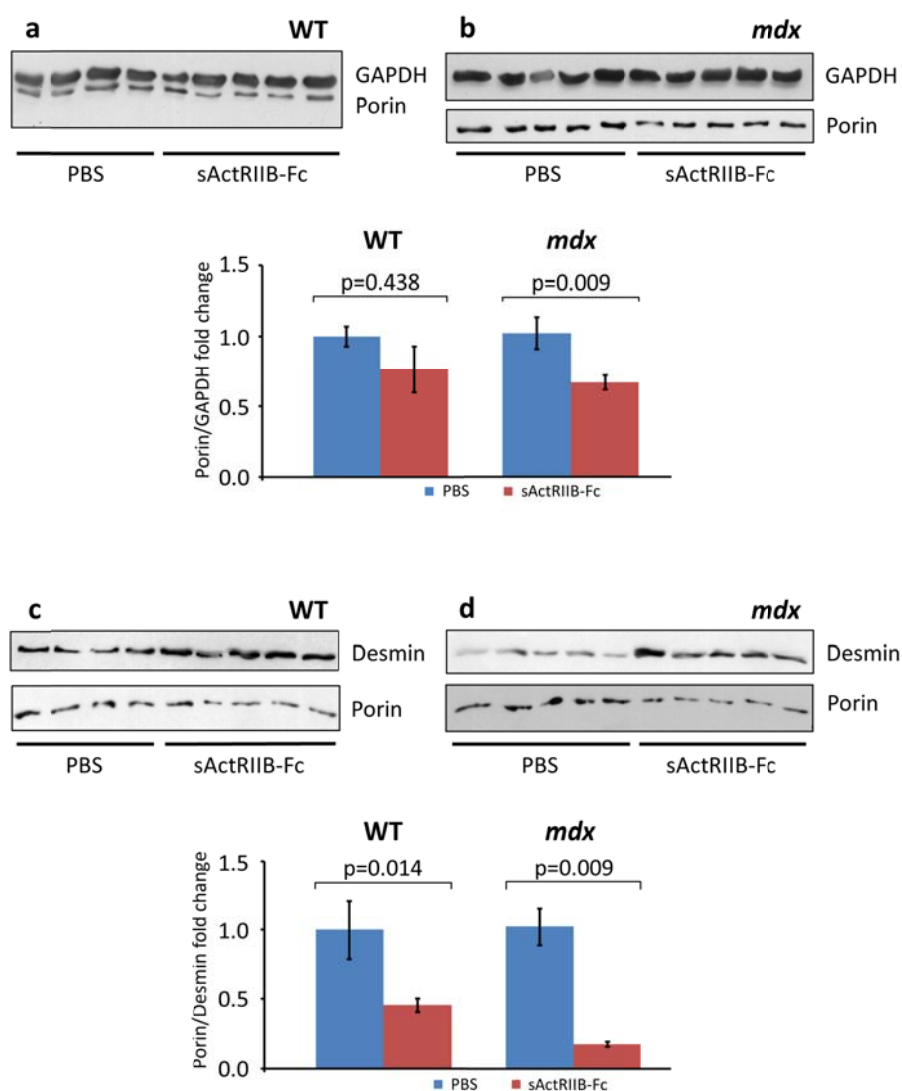
**Supplemental Figure 7: Effect of sActRIIB-Fc on SDH and COX enzyme activity on muscle sections of EDL and soleus muscles from *mdx* mice.**

(a-d) Images of transverse sections of (a,b) EDL muscle and (c,d) soleus muscle from *mdx* mice stained for (a,c) SDH activity and (b,d) COX activity after 4 months treatment with sActRIIB-Fc in comparison to muscles from PBS treated control mice.



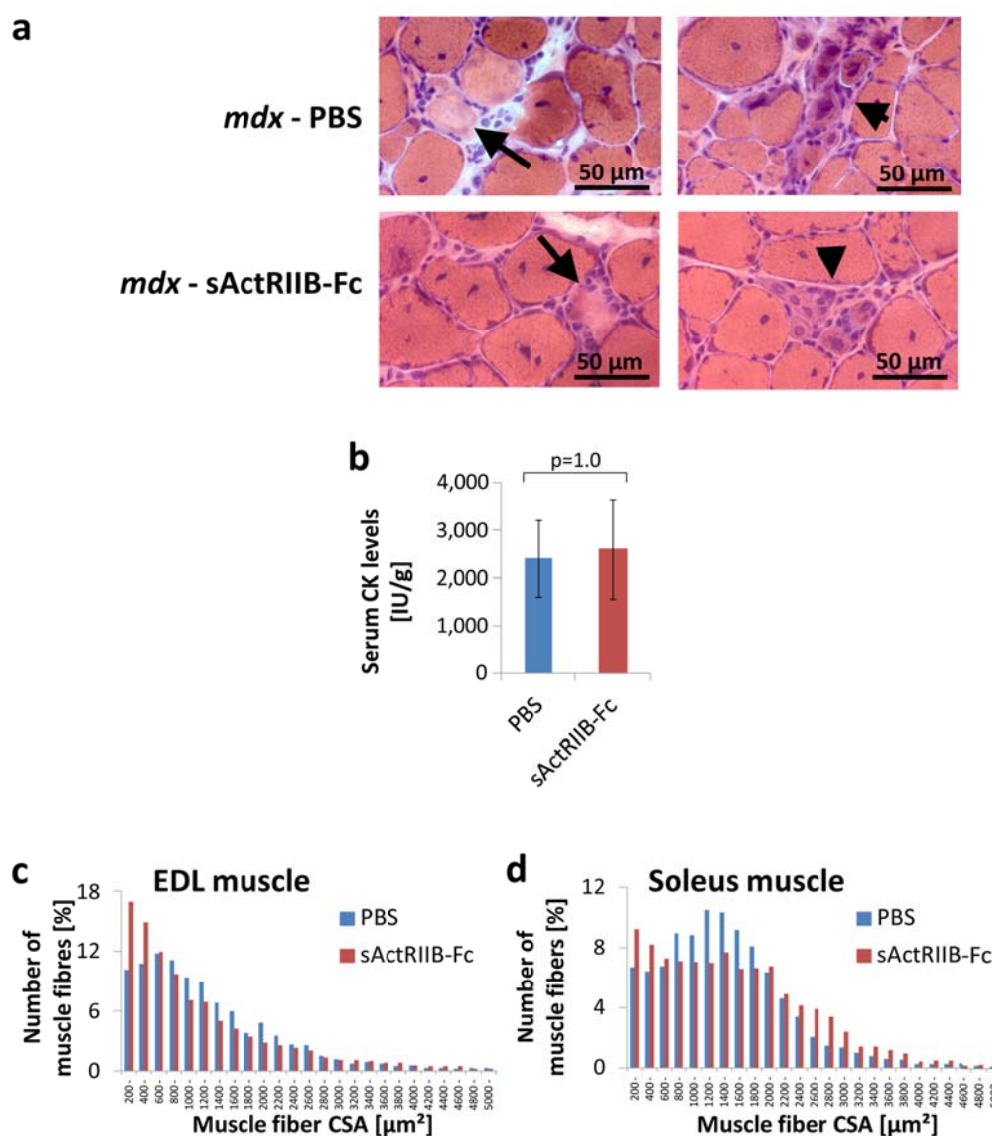
**Supplemental Figure 8.** Effect of sActRIIB-Fc on mitochondrial DNA copy number and transcription of the gene encoding the mitochondrial protein Porin in muscles from wild-type and *mdx* mice.

All investigations were done after a 4 months treatment of wild-type (n=5 for each condition) and *mdx* mice (n=5 for each condition) with either sActRIIB-Fc or PBS (controls). (a) mitochondrial DNA copy numbers expressed as the ratio between *MTCO2* [mtDNA] per *Ndufv1* [gDNA] copy numbers in the *TA* muscle from wild-type and *mdx* mice to quantify mtDNA/myonucleus ratio. (b) *Porin (Vdac1)* relative copy number in the *TA* muscle from wild-type and *mdx* mice as expressed per 10<sup>6</sup> x 18S rRNA copies. Values are shown as means  $\pm$  SEM. p-Values were calculated using the nonparametric U-Test.



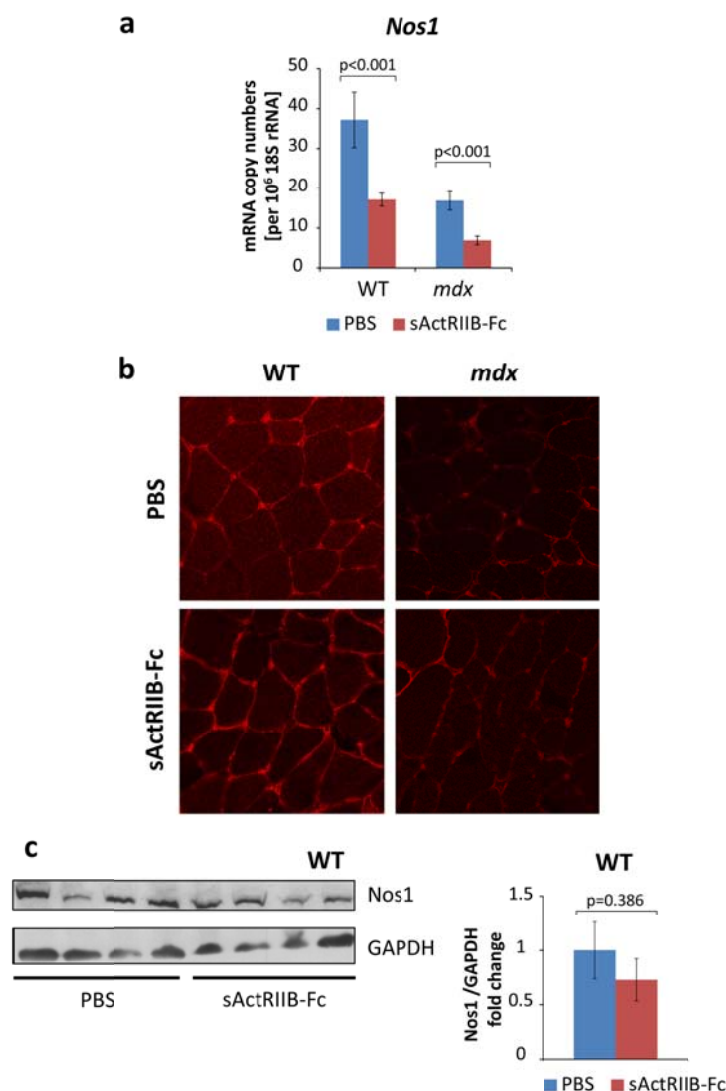
**Supplemental Figure 9. Effect of sActRIIB-Fc on the expression of the mitochondrial protein Porin in muscles from wild-type and *mdx* mice.**

The Western blots depict bands of Porin (Vdac1) referenced to GAPDH (a,b) and to Desmin (c,d) of TA muscles from wild-type (n=5 for each condition) (a,c) and *mdx* (n=5 for each condition) (b,d) mice after 4 months of treatment with sActRIIB-Fc in comparison to muscles from PBS treated control mice. The bar charts depict the quotients of Porin (Vdac1) band densities / GAPDH (Desmin) band densities with the average of the PBS-treated samples normalized to 1. Values are shown as means  $\pm$  SEM. p-Values were calculated using the nonparametric Man-Whitney-U-Test.



**Supplemental Figure 10. Effect of myostatin/ActRIIB signaling on muscle phenotype.**

(a,d) 2-months-old *mdx* mice were systemically treated for 4 months with sActRIIB-Fc (n=5 for each condition). (a) Cross section of the *soleus* muscle from *mdx* mice treated with sActRIIB-Fc, sectioned at mid belly level and stained with H&E (left image). Close-up showing muscle fibers with central nucleation, cellular infiltrates, endomysial fibrosis, and muscle fiber necrosis (arrow) (middle image) as well as regenerating muscle fibers (arrowhead) (right image). (b) Serum creatine kinase levels after 4 months of treatment with sActRIIB-Fc in comparison to PBS-treated *mdx* mice (n=5 for each condition). (c,d) The histogram depicts the cross sectional areas of muscle fibers from (c) *EDL* muscles and (d) *soleus* muscles after 4 months of treatment with sActRIIB-Fc in comparison to PBS-treated *mdx* mice. Values are shown as means  $\pm$  SEM. p-Values were calculated using the nonparametric U-Test. CSA, cross sectional area.



**Supplemental Figure 11. Effect of sActRIIB-Fc on the expression of Nos1 in muscles from wild-type and *mdx* mice.**

All investigations were done after a 4 months treatment of wild-type and *mdx* mice with either sActRIIB-Fc or PBS (controls). (a) *Nos1* relative copy number in the TA muscle from wild-type ( $n=5$  for each condition) and *mdx* mice ( $n=5$  for each condition) as expressed per  $10^6 \times 18S$  rRNA copies. Values are shown as means  $\pm$  SEM. p-Values were calculated using the nonparametric U-Test. (b) Representative images following immunohistochemistry against Nos1. (c) The Western blots depict bands of Nos1 referenced to GAPDH of TA muscles from wild-type mice ( $n=4$  for each condition). The bar charts depict the quotients of Nos1 band densities / GAPDH band densities with the average of the PBS-treated samples normalized to 1.

### Supplemental Videos



**Supplemental Video. Effect of sActRIIB-Fc on incremental speed running in *mdx* mice.**

The video demonstrates the effect of sActRIIB-Fc in *mdx* mice on aerobic exercise capacity during an incremental speed running test. *Right lane*: 6-months-old *mdx* mouse, which was treated for 4 months with sActRIIB-Fc (twice weekly subcutaneous injection of 10 mg/kg sActRIIB-Fc; mouse marked with a red spot). *Left lane*: 6-months-old *mdx* mouse, which was treated for 4 months with PBS (mouse marked with a blue spot). Mice were placed on the treadmill for one minute before starting the treadmill at a very low speed of 5 cm/s. Speed was subsequently increased by 1 cm/s each minute. The *mdx* sActRIIB-Fc treated mouse exhausted at a speed of 19 cm/s and was taken off the treadmill. The PBS treated *mdx* mice carried on running beyond 40 cm/s. The video is in \*.mov format and can best be viewed with the QuickTime® Viewer (free download from <http://www.apple.com/de/quicktime/download/>)

1. McPherron, AC, Lawler, AM and Lee, SJ (1997) Regulation of skeletal muscle mass in mice by a new TGF-beta superfamily member. *Nature* 387:83-90.
2. Lee, SJ and McPherron, AC (2001) Regulation of myostatin activity and muscle growth. *Proc Natl Acad Sci U S A* 98:9306-9311.
3. Lee, SJ, Reed, LA, Davies, MV, Girgenrath, S, Goad, ME, Tomkinson, KN *et al.* (2005) Regulation of muscle growth by multiple ligands signaling through activin type II receptors. *Proc Natl Acad Sci U S A* 102:18117-18122.
4. Rebbapragada, A, Benchabane, H, Wrana, JL, Celeste, AJ and Attisano, L (2003) Myostatin signals through a transforming growth factor beta-like signaling pathway to block adipogenesis. *Mol Cell Biol* 23:7230-7242.
5. Szlama, G, Kondas, K, Trexler, M and Patthy, L (2010) WFIKKN1 and WFIKKN2 bind growth factors TGFbeta1, BMP2 and BMP4 but do not inhibit their signalling activity. *FEBS J* 277:5040-5050.
6. Schuelke, M, Wagner, KR, Stolz, LE, Hubner, C, Riebel, T, Komen, W *et al.* (2004) Myostatin mutation associated with gross muscle hypertrophy in a child. *N Engl J Med* 350:2682-2688.
7. Wagner, KR, Fleckenstein, JL, Amato, AA, Barohn, RJ, Bushby, K, Escolar, DM *et al.* (2008) A phase I/II trial of MYO-029 in adult subjects with muscular dystrophy. *Ann Neurol* 63:561-571.
8. Amthor, H, Macharia, R, Navarrete, R, Schuelke, M, Brown, SC, Otto, A *et al.* (2007) Lack of myostatin results in excessive muscle growth but impaired force generation. *Proc Natl Acad Sci U S A* 104:1835-1840.
9. Matsakas, A, Mouisel, E, Amthor, H and Patel, K (2010) Myostatin knockout mice increase oxidative muscle phenotype as an adaptive response to exercise. *J Muscle Res Cell Motil* 31:111-125.
10. Mendias, CL, Marcin, JE, Calerdon, DR and Faulkner, JA (2006) Contractile properties of EDL and soleus muscles of myostatin-deficient mice. *J Appl Physiol* 101:898-905.
11. Qaisar, R, Renaud, G, Morine, K, Barton, ER, Sweeney, HL and Larsson, L (2012) Is functional hypertrophy and specific force coupled with the addition of myonuclei at the single muscle fiber level? *FASEB J* 26:1077-1085.
12. Baligand, C, Gilson, H, Menard, JC, Schakman, O, Wary, C, Thissen, JP *et al.* (2010) Functional assessment of skeletal muscle in intact mice lacking myostatin by concurrent NMR imaging and spectroscopy. *Gene Ther* 17:328-337.
13. Hennebry, A, Berry, C, Siriott, V, O'Callaghan, P, Chau, L, Watson, T *et al.* (2009) Myostatin regulates fiber-type composition of skeletal muscle by regulating MEF2 and MyoD gene expression. *Am J Physiol Cell Physiol* 296:C525-C534.
14. Ploquin, C, Chabi, B, Fouret, G, Vernus, B, Feillet-Coudray, C, Coudray, C *et al.* (2012) Lack of myostatin alters intermyofibrillar mitochondria activity, unbalances redox status, and impairs tolerance to chronic repetitive contractions in muscle. *Am J Physiol Endocrinol Metab* 302:E1000-E1008.
15. Savage, KJ and McPherron, AC (2010) Endurance exercise training in myostatin null mice. *Muscle Nerve* 42:355-362.

16. Akpan, I, Goncalves, MD, Dhir, R, Yin, X, Pistilli, EE, Bogdanovich, S *et al.* (2009) The effects of a soluble activin type IIB receptor on obesity and insulin sensitivity. *Int J Obes (Lond)* 33:1265-1273.
17. Cadena, SM, Tomkinson, KN, Monnell, TE, Spaits, MS, Kumar, R, Underwood, KW *et al.* (2010) Administration of a soluble activin type IIB receptor promotes skeletal muscle growth independent of fiber type. *J Appl Physiol* 109:635-642.
18. Morine, KJ, Bish, LT, Selsby, JT, Gazzara, JA, Pendrak, K, Sleeper, MM *et al.* (2010) Activin IIB receptor blockade attenuates dystrophic pathology in a mouse model of Duchenne muscular dystrophy. *Muscle Nerve* 42:722-730.
19. Pistilli, EE, Bogdanovich, S, Goncalves, MD, Ahima, RS, Lachey, J, Seehra, J *et al.* (2011) Targeting the activin type IIB receptor to improve muscle mass and function in the mdx mouse model of Duchenne muscular dystrophy. *Am J Pathol* 178:1287-1297.
20. Rahimov, F, King, OD, Warsing, LC, Powell, RE, Emerson, CP, Jr., Kunkel, LM *et al.* (2011) Gene expression profiling of skeletal muscles treated with a soluble activin type IIB receptor. *Physiol Genomics* 43:398-407.
21. Chiu, CS, Peekhaus, N, Weber, H, Adamski, S, Murray, EM, Zhang, HZ *et al.* (2013) Increased muscle force production and bone mineral density in ActRIIB-Fc-treated mature rodents. *J Gerontol A Biol Sci Med Sci* 2013 Mar 22. [Epub ahead of print].
22. Jongpiputvanich, S, Sueblinvong, T and Norapucsunton, T (2005) Mitochondrial respiratory chain dysfunction in various neuromuscular diseases. *J Clin Neurosci* 12:426-428.
23. Kuznetsov, AV, Winkler, K, Wiedemann, FR, von, BP, Dietzmann, K and Kunz, WS (1998) Impaired mitochondrial oxidative phosphorylation in skeletal muscle of the dystrophin-deficient mdx mouse. *Mol Cell Biochem* 183:87-96.
24. Millay, DP, Sargent, MA, Osinska, H, Baines, CP, Barton, ER, Vuagniaux, G *et al.* (2008) Genetic and pharmacologic inhibition of mitochondrial-dependent necrosis attenuates muscular dystrophy. *Nat Med* 14:442-447.
25. Girgenrath, S, Song, K and Whittemore, LA (2005) Loss of myostatin expression alters fiber-type distribution and expression of myosin heavy chain isoforms in slow- and fast-type skeletal muscle. *Muscle Nerve* 31:34-40.
26. Matsakas, A, Macharia, R, Otto, A, Elashry, MI, Mouisel, E, Romanello, V *et al.* (2012) Exercise training attenuates the hypermuscular phenotype and restores skeletal muscle function in the myostatin null mouse. *Exp Physiol* 97:125-140.
27. Billat, VL, Mouisel, E, Roblot, N and Melki, J (2005) Inter- and intrastrain variation in mouse critical running speed. *J Appl Physiol* 98:1258-1263.
28. Han, JJ, Carter, GT, Ra, JJ, Abresch, RT, Chamberlain, JS and Robinson, LR (2006) Electromyographic studies in mdx and wild-type C57 mice. *Muscle Nerve* 33:208-214.

29. Hayot, M, Rodriguez, J, Vernus, B, Carnac, G, Jean, E, Allen, D *et al.* (2011) Myostatin up-regulation is associated with the skeletal muscle response to hypoxic stimuli. *Mol Cell Endocrinol* 332:38-47.
30. Zhao, G, Jeoung, NH, Burgess, SC, Rosaaen-Stowe, KA, Inagaki, T, Latif, S *et al.* (2008) Overexpression of pyruvate dehydrogenase kinase 4 in heart perturbs metabolism and exacerbates calcineurin-induced cardiomyopathy. *Am J Physiol Heart Circ Physiol* 294:H936-H943.
31. Brenman, JE, Chao, DS, Xia, H, Aldape, K and Bredt, DS (1995) Nitric oxide synthase complexed with dystrophin and absent from skeletal muscle sarcolemma in Duchenne muscular dystrophy. *Cell* 82:743-752.
32. Chang, WJ, Iannaccone, ST, Lau, KS, Masters, BS, McCabe, TJ, McMillan, K *et al.* (1996) Neuronal nitric oxide synthase and dystrophin-deficient muscular dystrophy. *Proc Natl Acad Sci U S A* 93:9142-9147.
33. Thomas, GD, Sander, M, Lau, KS, Huang, PL, Stull, JT and Victor, RG (1998) Impaired metabolic modulation of alpha-adrenergic vasoconstriction in dystrophin-deficient skeletal muscle. *Proc Natl Acad Sci U S A* 95:15090-15095.
34. Heydemann, A and McNally, E (2009) NO more muscle fatigue. *J Clin Invest* 119:448-450.
35. Kobayashi, YM, Rader, EP, Crawford, RW, Iyengar, NK, Thedens, DR, Faulkner, JA *et al.* (2008) Sarcolemma-localized nNOS is required to maintain activity after mild exercise. *Nature* 456:511-515.
36. Percival, JM, Siegel, MP, Knowels, G and Marcinek, DJ (2013) Defects in mitochondrial localization and ATP synthesis in the mdx mouse model of Duchenne muscular dystrophy are not alleviated by PDE5 inhibition. *Hum Mol Genet* 22:153-167.
37. Giannesini, B, Vilmen, C, Le, FY, Dalmaso, C, Cozzone, PJ and Bendahan, D (2010) A strictly noninvasive MR setup dedicated to longitudinal studies of mechanical performance, bioenergetics, anatomy, and muscle recruitment in contracting mouse skeletal muscle. *Magn Reson Med* 64:262-270.
38. Guzun, R, Gonzalez-Granillo, M, Karu-Varikmaa, M, Grichine, A, Usson, Y, Kaambre, T *et al.* (2012) Regulation of respiration in muscle cells in vivo by VDAC through interaction with the cytoskeleton and MtCK within Mitochondrial Interactosome. *Biochim Biophys Acta* 1818:1545-1554.
39. Braun, U, Paju, K, Eimre, M, Seppet, E, Orlova, E, Kadaja, L *et al.* (2001) Lack of dystrophin is associated with altered integration of the mitochondria and ATPases in slow-twitch muscle cells of MDX mice. *Biochim Biophys Acta* 1505:258-270.
40. Massa, R, Marliera, LN, Martorana, A, Cicconi, S, Pierucci, D, Giacomini, P *et al.* (2000) Intracellular localization and isoform expression of the voltage-dependent anion channel (VDAC) in normal and dystrophic skeletal muscle. *J Muscle Res Cell Motil* 21:433-442.
41. Lewis, C, Jockusch, H and Ohlendieck, K (2010) Proteomic Profiling of the Dystrophin-Deficient MDX Heart Reveals Drastically Altered Levels of Key Metabolic and Contractile Proteins. *J Biomed Biotechnol* 2010:648501.

42. Janssen, AJ, Schuelke, M, Smeitink, JA, Trijbels, FJ, Sengers, RC, Lucke, B *et al.* (2008) Muscle 3243A-->G mutation load and capacity of the mitochondrial energy-generating system. *Ann Neurol* 63:473-481.
43. Mosher, DS, Quignon, P, Bustamante, CD, Sutter, NB, Mellersh, CS, Parker, HG *et al.* (2007) A mutation in the myostatin gene increases muscle mass and enhances racing performance in heterozygote dogs. *PLoS Genet* 3:e79.
44. Grobet, L, Martin, LJ, Poncelet, D, Pirottin, D, Brouwers, B, Riquet, J *et al.* (1997) A deletion in the bovine myostatin gene causes the double-muscling phenotype in cattle. *Nat Genet* 17:71-74.
45. McPherron, AC and Lee, SJ (1997) Double muscling in cattle due to mutations in the myostatin gene. *Proc Natl Acad Sci U S A* 94:12457-12461.
46. Holmes, JH, Robinson, DW and Ashmore, CR (1972) Blood lactic acid and behaviour in cattle with hereditary muscular hypertrophy. *J Anim Sci* 35:1011-1013.
47. Holmes, JH, Ashmore, CR and Robinson, DW (1973) Effects of stress on cattle with hereditary muscular hypertrophy. *J Anim Sci* 36:684-694.
48. Wegner, J, Albrecht, E, Fiedler, I, Teuscher, F, Papstein, HJ and Ender, K (2000) Growth- and breed-related changes of muscle fiber characteristics in cattle. *J Anim Sci* 78:1485-1496.
49. Welle, S, Bhatt, K, Pinkert, CA, Tawil, R and Thornton, CA (2007) Muscle growth after postdevelopmental myostatin gene knockout. *Am J Physiol Endocrinol Metab* 292:E985-E991.
50. Hulmi, JJ, Oliveira, BM, Silvennoinen, M, Hoogaars, WM, Ma, H, Pierre, P *et al.* (2013) Muscle protein synthesis, mTORC1/MAPK/Hippo signaling, and capillary density are altered by blocking of myostatin and activins. *Am J Physiol Endocrinol Metab* 304:E41-E50.
51. Personius, KE, Jayaram, A, Krull, D, Brown, R, Xu, T, Han, B *et al.* (2010) Grip force, EDL contractile properties, and voluntary wheel running after postdevelopmental myostatin depletion in mice. *J Appl Physiol* 109:886-894.
52. Sander, M, Chavoshan, B, Harris, SA, Iannaccone, ST, Stull, JT, Thomas, GD *et al.* (2000) Functional muscle ischemia in neuronal nitric oxide synthase-deficient skeletal muscle of children with Duchenne muscular dystrophy. *Proc Natl Acad Sci U S A* 97:13818-13823.
53. George, CC, Bruemmer, K, Sesti, J, Stefanski, C, Curtis, H, Ucran, J *et al.* (2011) Soluble activin receptor type IIB increases forward pulling tension in the mdx mouse. *Muscle Nerve* 43:694-699.
54. Bish, LT, Sleeper, MM, Forbes, SC, Wang, B, Reynolds, C, Singletary, GE *et al.* (2012) Long-term restoration of cardiac dystrophin expression in golden retriever muscular dystrophy following rAAV6-mediated exon skipping. *Mol Ther* 20:580-589.
55. Lach-Trifilieff, E, Minetti, GC, Sheppard, K, Ibebunjo, C, Feige, JN, Hartmann, S *et al.* (2014) An antibody blocking activin type II receptors induces strong skeletal muscle hypertrophy and protects from atrophy. *Mol Cell Biol* 34:606-618.

56. Goemans, N, Klingels, K, van den, HM, Boons, S, Verstraete, L, Peeters, C *et al.* (2013) Six-minute walk test: reference values and prediction equation in healthy boys aged 5 to 12 years. *PLoS One* 8:e84120.
57. Pistilli, EE, Bogdanovich, S, Garton, F, Yang, N, Gulbin, JP, Conner, JD *et al.* (2011) Loss of IL-15 receptor alpha alters the endurance, fatigability, and metabolic characteristics of mouse fast skeletal muscles. *J Clin Invest* 121:3120-3132.
58. Schuler, M, Ali, F, Chambon, C, Duteil, D, Bornert, JM, Tardivel, A *et al.* (2006) PGC1alpha expression is controlled in skeletal muscles by PPARbeta, whose ablation results in fiber-type switching, obesity, and type 2 diabetes. *Cell Metab* 4:407-414.
59. Robergs, RA, Ghiasvand, F and Parker, D (2004) Biochemistry of exercise-induced metabolic acidosis. *Am J Physiol Regul Integr Comp Physiol* 287:R502-R516.
60. Lebrasseur, NK, Schelhorn, TM, Bernardo, BL, Cosgrove, PG, Loria, PM and Brown, TA (2009) Myostatin inhibition enhances the effects of exercise on performance and metabolic outcomes in aged mice. *J Gerontol A Biol Sci Med Sci* 64:940-948.
61. Morrison, BM, Lachey, JL, Warsing, LC, Ting, BL, Pullen, AE, Underwood, KW *et al.* (2009) A soluble activin type IIB receptor improves function in a mouse model of amyotrophic lateral sclerosis. *Exp Neurol* 217:258-268.
62. Rajab, A, Straub, V, McCann, LJ, Seelow, D, Varon, R, Barresi, R *et al.* (2010) A new form of congenital generalized lipodystrophy (CGL4) with muscle rippling, cardiac arrhythmia and bone disease in patients with PTRF-CAVIN mutations. *PLoS Genetics*: in press.
63. Merkulova, T, Dehaupas, M, Nevers, MC, Creminon, C, Alameddine, H and Keller, A (2000) Differential modulation of alpha, beta and gamma enolase isoforms in regenerating mouse skeletal muscle. *Eur J Biochem* 267:3735-3743.
64. Pfaffl, MW (2001) A new mathematical model for relative quantification in real-time RT-PCR. *Nucleic Acids Res* 29:e45.

## 1.2 Effect of the absence of myostatin in the *Mstn*<sup>-/-</sup> mouse model

**Project description:** Myostatin is considered as a potent negative regulator of skeletal muscle mass. Mice lacking myostatin gene (*Mstn*<sup>-/-</sup>) exhibit a strong hypermuscular phenotype due to both myofiber hypertrophy and hyperplasia. The *Mstn*<sup>-/-</sup> muscle exhibits an increased number of fast glycolytic myofibers and a loss of oxidative fibers, which reflects a profound loss of oxidative metabolic properties of the muscle which are associated with mitochondrial depletion. Previous work suggested that such profound fiber type conversion in the absence of myostatin negatively alters muscle behavior during exercise, fatigability and mitochondrial function. We therefore investigated how myostatin regulates muscle energy metabolism and energy dependent muscle function in *Mstn*<sup>-/-</sup> mice and the role of myostatin in the regulation of the PPAR transcriptional activators in the energy metabolism of the skeletal muscle.

**Contribution to the project:** This project was principally conducted in the laboratory by a postdoctoral researcher Etienne Mouisel, and I worked with him on this project at the beginning of my thesis. For this study, I contributed experiments to decipher the role of myostatin in the regulation of PPAR transcription factors. I designed primers specific to each PPAR isoform and performed a quantitative PCR on the *Mstn*<sup>-/-</sup> and wildtype muscles. The results suggested that myostatin plays an important role to maintain the oxidative metabolism of the skeletal muscle *via* the PPAR signaling pathway. I also performed fiber type profiling and analyzed morphometric parameters of skeletal muscle from wildtype and *Mstn*<sup>-/-</sup> mice. I found an increase in the proportion of type IIb fibers, which was corroborated by the analysis of myosin heavy chain isoforms on SDS-PAGE thus confirming the conversion of the *Mstn*<sup>-/-</sup> muscles towards a more glycolytic phenotype.

## **Myostatin is a key mediator between energy metabolism and endurance capacity of skeletal muscle**

Etienne Mouisel<sup>1,2</sup>, **Karima Relizani**<sup>3,4</sup>, Laurence Mille-Hamard<sup>5</sup>, Raphaël Denis<sup>6</sup>, Christophe Hourdé<sup>1</sup>, Onnik Agbulut<sup>6</sup>, Ketan Patel<sup>7</sup>, Ludovic Arandel<sup>1</sup>, Susanne Lützkendorf<sup>3</sup>, Alban Vignaud<sup>8</sup>, Luis Garcia<sup>4,9</sup>, Arnaud Ferry<sup>1,10</sup>, Serge Luquet<sup>6,11</sup>, Véronique Billat<sup>5</sup>, Renée Ventura-Clapier<sup>12</sup>, Markus Schuelke<sup>3</sup> and Helge Amthor<sup>1,4,9§</sup>

<sup>1</sup>Sorbonne Universités, UPMC Univ Paris 06, Myology Center of Research and Inserm, UMRS974 and CNRS, FRE3617 and Institut de Myologie, F-75013, Paris, France.

<sup>2</sup>INSERM, UMR1048, Obesity Research Laboratory, Institute of Metabolic and Cardiovascular Diseases, 31432 Toulouse, France.

<sup>3</sup>Department of Neuropediatrics and NeuroCure Clinical Research Center, Charité Universitätsmedizin Berlin, 13353 Berlin, Germany.

<sup>4</sup>Laboratoire "End:icap", UFR des Sciences de la Santé, Université de Versailles Saint-Quentin-en-Yvelines, France.

<sup>5</sup>INSERM U 902, Université d'Evry-Val d'Essonne, Evry, France.

<sup>6</sup>Université Paris Diderot, Sorbonne Paris Cité, Unité de Biologie Fonctionnelle et Adaptative, CNRS EAC 4413, F-75205 Paris, France.

<sup>7</sup>School of Biological Sciences, University of Reading, Reading, UK.

<sup>8</sup>Généthon, 1 bis rue de l'Internationale, 91002 Evry, France.

<sup>9</sup>Laboratoire LIA-BAHN, Centre Scientifique Monaco, 98000 Monaco, MC.

<sup>10</sup>Université Paris Descartes, 75006 Paris, France.

<sup>11</sup>Centre National de la Recherche Scientifique-CNRS EAC 4413, F-75205 Paris, France.

<sup>12</sup>INSERM U 769, Université Paris-Sud, Châtenay-Malabry, France.

<sup>§</sup>Corresponding author: H. Amthor

Helge Amthor, MD, PhD

Laboratoire «End:icap»

UFR des Sciences de la Santé «Simone Veil»

Université de Versailles Saint-Quentin-en-Yvelines

2, avenue de la Source de la Bièvre

78180 Montigny-Le-Bretonneux, France

Email: [helge.amthor@uvsq.fr](mailto:helge.amthor@uvsq.fr)

### SUMMARY

Myostatin (Mstn) participates in the regulation of skeletal muscle size and emerges as a regulator of muscle metabolism. We here hypothesized that lack of myostatin profoundly depresses energy dependent muscle function. For this extent, we explored *Mstn*<sup>-/-</sup> mice as a model for constitutive absence of myostatin and AAV-mediated overexpression of myostatin propeptide as a model of myostatin blockade in adult wild-type mice. We show that muscles, which develop in constitutive lack of myostatin, although larger and stronger, fatigue extremely rapidly. Myostatin deficiency shifts muscle energy metabolism away from aerobic towards anaerobic mode as evidenced by decreased mitochondrial respiration and *PPARs* transcriptional regulator expression, increased enolase activity and exercise induced lactic acidosis. In consequence, constitutively reduced myostatin signaling diminishes exercise capacity, while the hypermuscular state of *Mstn*<sup>-/-</sup> mice increases oxygen consumption and energy cost of running. We wondered whether these results are the mere consequence of the congenital fiber type switch towards a glycolytic phenotype of constitutive *Mstn*<sup>-/-</sup> mice. We therefore over-expressed myostatin propeptide in adult mice, which did not affect fiber type distribution. However, propeptide mediated myostatin blockade also caused larger muscle fatigability and decreased exercise capacity as well as decreased *PPAR-β/δ* and *PGC1-α* expression. In conclusion, our results suggest that myostatin endows skeletal muscle with high oxidative capacity and low fatigability, thus optimizing the delicate balance between muscle mass and force, energy metabolism and endurance capacity.

### KEYWORDS

myostatin, exercise capacity, muscle fatigue, PPAR.

## INTRODUCTION

Skeletal muscle has inbuilt control mechanisms to prevent overgrowth, which are executed at least in part by secreted molecules of the transforming growth factor- $\beta$  (TGF- $\beta$ ) family, the most important being myostatin (Mstn). Suppression of myostatin signaling stimulates muscle growth, however, the functional benefits arising from myostatin deficiency remain under debate, because the larger muscles of myostatin knockout mice lose specific force (4, 28, 34, 40). On the other hand, a heterozygous *Mstn*-mutation in racing dogs (whippets) increases performance in short distance races (37), which could be explained by a fiber type conversion from oxidative to glycolytic phenotype. Previous work suggested that such profound fiber type conversion in the absence of myostatin negatively alters muscle exercise behavior, fatigability and muscle mitochondrial function (6, 15, 18, 29, 39, 42). However, a direct effect of myostatin on muscle metabolism has not yet firmly established despite increasing evidence for an important impact of TGF- $\beta$ /Smad signaling pathway on energy homeostasis (9, 13, 32, 47). Moreover, the question remains open, whether previously observed metabolic and functional changes are the mere consequence of congenital fiber type conversion following constitutive lack of myostatin or whether myostatin regulates muscle metabolism in a direct fashion. We here hypothesised that myostatin regulates energy dependent muscle function and that this can be independent of the muscle fiber type phenotype. We first characterised in detail the muscle contractile, metabolic and functional phenotype of constitutive *Mstn*<sup>-/-</sup> mice and demonstrate a profound deficit for aerobic exercise. We then compared this phenotype to the effect of myostatin blockade in adult muscle and likewise found an increased fatigability and reduced capacity for aerobic exercise following overexpression of myostatin propeptide despite an unchanged fiber type composition. These data and the role of myostatin in the regulation of *PPAR* transcriptional activators comprehensively illustrate the importance of myostatin as a pivotal link that acts to balance muscle size and strength against endurance achieved by an optimization of energy metabolism.

## RESULTS

**Decreased endurance exercise capacity and voluntary motor activity in myostatin deficiency**

An index for endurance exercise capacity is the maximal oxygen uptake per body weight ( $\text{VO}_2\text{max}$  [ml  $\text{O}_2$ /min/kg]), which was determined at incremental treadmill speeds in metabolic cages. Initially, the oxygen uptake is proportional to the running speed but levels off at a plateau, the so-called  $\text{VO}_2\text{max}$ , beyond which no further increase is possible. Nevertheless, running velocity can still increase beyond the speed at  $\text{VO}_2\text{max}$  to reach the maximal velocity ( $v\text{Peak}$  [m/min]) before exhaustion of the animals.  $\text{VO}_2\text{max}$  of  $Mstn^{-/-}$  mice was reduced by 10% ( $p=0.004$ ; Figure 1A) and a similar tendency was shown for  $v\text{Peak}$  in comparison with  $Mstn^{+/+}$  mice ( $p=0.13$ ; Figure 1B), while  $Mstn^{+/-}$  mice had an intermediate phenotype. Hence, such decreased oxygen consumption *in vivo* parallels the decreased OXPHOS rates *in vitro*. However, absolute  $\text{VO}_2\text{max}$  [ml/min] of  $Mstn^{-/-}$  mice was increased by 14% ( $p=0.004$ ; Figure 1C) owing to a respectively 20% and 24% increase of total and lean body mass ( $p<0.01$ ; data not shown). In consequence, the energy cost of running (Running Economy at 13 m/min) was increased by 15% in  $Mstn^{-/-}$  as compared to  $Mstn^{+/+}$  mice ( $p=0.01$ ; Figure 1D).

“Critical Speed” accurately reflects the capacity for aerobic exercise and is based on the proportional relationship between distance run and time to exhaustion at different velocities (8).  $Mstn^{-/-}$  mice became exhausted more rapidly, resulting in a 30% lower Critical Speed as compared with  $Mstn^{+/+}$  mice ( $15.9\pm1.2$  vs  $22.9\pm1.2$  m.min<sup>-1</sup>,  $p<0.001$ ; Figure 1E). These findings provide further evidence that the double muscle phenotype we observed in  $Mstn^{-/-}$  mice ( $16.4\pm0.3$  vs  $8.4\pm0.2$  mg for *soleus* muscle, as compared to  $Mstn^{+/+}$  mice,  $p<0.001$ ; similar observations were made for others hindlimb muscles) cannot compensate for inefficient energy metabolism to maintain endurance capacity. The “Respiratory Exchange Ratio” (RER),  $\text{CO}_{2\text{eliminated}}/\text{O}_{2\text{consumed}}$ , indicates the type of fuel being metabolized to supply the body with energy. Resting and maximal RER were slightly increased in  $Mstn^{+/-}$  mice and even further increased in  $Mstn^{-/-}$  mice as compared with wildtype animals (Figure 1F). This implicates a preference for glycolysis over fatty acid oxidation, which is considered to be disadvantageous for endurance exercise (46).

In order to evaluate the impact of a decreased endurance capacity on voluntary locomotion, total night-time activity was measured and revealed no significant difference between  $Mstn^{-/-}$  and  $Mstn^{+/+}$  mice, although we observed a trend towards lower total motor activity in myostatin deficiency ( $1,792\pm279$  counts /12 hours and  $2,333\pm255$  counts /12 hours respectively,  $p=0.16$ ). However, upon a metabolic challenge consisting of food deprivation,  $Mstn^{-/-}$  mice failed to increase their motor activity as compared to the marked increase seen in  $Mstn^{+/+}$  mice (Figure 1G), which further demonstrates that myostatin deficiency impairs motor activity.

### Profound fatigability of myostatin deficient skeletal muscle

In order to assess the respective part of skeletal muscle fatigability on the decreased endurance capacity observed in myostatin deficient mice, we next determined how muscle force was maintained upon repetitive stimulation. *Soleus* muscle from *Mstn*<sup>-/-</sup> mice fatigued far more rapidly following repetitive stimulation ( $t_{[30\% P_0]} = 72$  s) as compared to *Mstn*<sup>+/+</sup> *soleus* ( $t_{[30\% P_0]} = 100$  s;  $p < 0.001$ ), while heterozygous *Mstn*<sup>+/-</sup> muscle had an intermediate phenotype (Figure 2A). Remarkably, myostatin deficient muscle, despite being about twice as strong at the beginning of the experiment ( $389 \pm 11$  vs  $233 \pm 5$  mN for *soleus* absolute maximal tetanic force  $P_0$ , as compared to *Mstn*<sup>+/+</sup> mice,  $p < 0.001$ ), fatigued so rapidly that absolute maximal force dropped to *Mstn*<sup>+/+</sup> levels after 3 min of repetitive tetanic stimulation (Figure 2B). This rapid force decline caused the specific force of *Mstn*<sup>-/-</sup> muscles to decrease from 91% at the start to 59% at the end of the fatigue protocol in comparison to *Mstn*<sup>+/+</sup> muscles ( $p = 0.04$  and  $p < 0.001$  respectively; Figure 2C). Interestingly, similar results were found for the fast glycolytic *extensor digitorum longus* (EDL, -21% concerning the fatigue index in *Mstn*<sup>-/-</sup> vs *Mstn*<sup>+/+</sup>) muscle as well as for the entire posterior lower leg compartment (fatigue index was decreased by 48% in *Mstn*<sup>-/-</sup> vs *Mstn*<sup>+/+</sup>), for which measurements were performed *in situ* to maintain blood perfusion during the stimulation protocol (data not shown).

### Increased glycolysis and decreased mitochondrial respiration rates in myostatin deficiency

To investigate whether increased muscle fatigability in the absence of myostatin resulted from increased anaerobic glucose metabolism-induced muscle acidosis, we determined serum lactate levels after exhaustive treadmill exercise. In *Mstn*<sup>-/-</sup> mice, serum lactate was already elevated at resting state and increased disproportionately to  $12.1 \pm 1.1$  mmol/l at 5 min post exercise as compared to  $5.1 \pm 0.4$  mmol/l in controls ( $p < 0.001$ ; Figure 2D). The elevated serum lactate in myostatin deficient mice concurred with an increased enzymatic activity of enolase (Figure 2E), a key component of glycolysis. To determine whether lactate accumulation resulted from defective oxidative phosphorylation (OXPHOS), we investigated mitochondrial respiration rates *in situ* for OXPHOS complexes I, II and IV. *Mstn*<sup>+/+</sup> muscles revealed higher respiration rates for the predominantly oxidative *soleus* muscle as compared with the predominantly glycolytic EDL muscle (Figure 2G). Remarkably, the absence of myostatin decreased OXPHOS rates of the *soleus* muscle to the level of *Mstn*<sup>+/+</sup> EDL muscles, and *Mstn*<sup>-/-</sup> EDL further lost OXPHOS activity of up to 42% (Figure 2G). It is unlikely that such OXPHOS reduction was merely due to mitochondrial depletion, because complex I (Cxi) activity remained unaltered. The CxII/Cxi and CxIV/Cxi ratios decreased in myostatin deficient muscle, which might be an indicator for qualitative changes in the assembly of the cytochrome c oxidase (complex IV) and of the entirely nuclear encoded succinate dehydrogenase (complex II), (Figure 2F). In fact, the biochemical profile of mitochondria from *Mstn*<sup>-/-</sup> *soleus* muscle resembled that of *Mstn*<sup>+/+</sup> EDL mitochondria and

suggested a shift of mitochondrial qualities from the "slow oxidative" to the "fast glycolytic" type. This shift in metabolic activity was accompanied by a profound conversion of the contractile phenotype of *Mstn*<sup>-/-</sup> *soleus* muscle away from slow/oxidative myosin heavy chain type 1 (MHC-1) towards fast/glycolytic MHC-2x/MHC-2b (Figures 3A-C). In line with these observations are the findings that the  $K_m(\text{ADP})$  in resting *soleus* muscle was much higher than that for EDL muscle (Figure 2H).  $K_m(\text{ADP})$  was decreased by addition of creatine, in both EDL and *soleus* muscle demonstrating the coupling between mitochondrial creatine kinase and the adenine nucleotide translocase. Absence of myostatin lowered the  $K_m(\text{ADP})$  of the *soleus* muscle towards the level of the fast glycolytic EDL muscle, and the  $K_m(\text{ADP})$  of *Mstn*<sup>-/-</sup> EDL decreased even further (Figure 2H).

### **Decreased expression of PPAR transcription factors in myostatin deficient muscle**

We next aimed to gain molecular insight explaining the metabolic dysregulation observed in myostatin deficiency. We hypothesized that myostatin might act in a signaling cascade upstream of PPAR transcriptional regulators since inactivation of myostatin and inactivation of *PPAR $\delta$ / $\delta$*  (43) had both resulted in a similar loss of oxidative phenotype. In wildtype mice, as expected, *PPAR $\delta$ / $\delta$* , *PPAR $\alpha$*  and *PPAR $\gamma$*  mRNA expression levels were 2-3 times higher in the predominantly oxidative *soleus* muscle than in the predominantly glycolytic EDL muscle. As predicted, transcription of *PPARs* in the *soleus* muscle of *Mstn*<sup>-/-</sup> mice (Figure 3D) fell to about the level seen in *Mstn*<sup>+/+</sup> EDL muscle (Figure 3E), while in EDL muscle of *Mstn*<sup>-/-</sup> mice, levels of *PPARs* fell below the already low values found in *Mstn*<sup>+/+</sup> EDL, although this was statistically significant only for *PPAR $\alpha$*  (Figure 3E). Together, these results suggest that myostatin may promote high oxidative metabolism in skeletal muscle *via* PPAR signaling.

### **Myostatin blockade by AAV-propeptide in adult mice increases fatigability.**

To determine the role of myostatin on energy dependent muscle function during adulthood, we over-expressed myostatin propeptide using AAV as expression vectors. Injection of AAV2/8-propeptide into the femoral artery led to robust transgene expression (Figure 4A) and slight increase of the lower leg muscle weights (Figure 4B). Importantly, *soleus* muscle fatigued more rapidly after propeptide treatment (Figure 4D), despite only minimal changes of absolute maximal and specific force at the start of the fatigue protocol (Figure 4D) and an unaltered fiber-type composition (Figure 4C). Interestingly, expression of *PPAR- $\delta$ / $\delta$*  and *PCG1- $\alpha$*  transcripts were reduced (Figure 4E), suggesting changes in the regulation of oxidative metabolism independent of muscle fiber type composition. Moreover, myostatin propeptide treatment diminished exercise capacity 6 months following systemic intravenous treatment with myostatin AAV2/8-propeptide (Figures 4F and 4G). Hence we were able to show that myostatin blockade in adult wild-type mice caused a similar deficit in aerobic muscle properties as shown for *Mstn*<sup>-/-</sup> mice and that these effects were independent of muscle fiber type constitution.

## DISCUSSION

Myostatin exerts a dual function on skeletal muscle as it limits its size and promotes oxidative properties. We here show that myostatin acts to economize muscle energy expenditure, because smaller muscle requires less oxygen during exercise. The higher OXPHOS activity and lower respiratory exchange ratio point towards increased fatty acid consumption as a preferred fuel in the presence of myostatin and suggests higher energy efficiency as compared with the energetically less efficient glycolysis in states of myostatin deficiency. The emerging property of myostatin to save fuel combined with a simultaneous increase in running endurance and maximal running velocity might explain the high conservation of myostatin during evolution and the rare occurrence of myostatin mutations. The comparison of muscle physiology between hypermuscular myostatin knockout and wildtype mice sheds light on the fact that myostatin deficient muscle confers little functional advantage over wildtype muscle due to its rapid fatigability. We have demonstrated that the fatigability and diminished capacity for forced and voluntary motor activities seen in *Mstn*<sup>-/-</sup> described by us and others (18, 29, 39, 42) goes in parallel with a reduction of muscle OXPHOS activities. Interestingly, recent *in vivo* investigations using <sup>31</sup>P MRS supports our findings as the relative contribution of oxidative ATP production to total ATP turnover was reduced following repeated isometric contractions of *Mstn*<sup>-/-</sup> muscles, whereas ATP cost of contraction was increased (15). Thus, muscle strength due to myostatin deficiency comes at the cost of exercise intolerance, which is often seen in patients with mitochondrial disorders such as MELAS or MERRF syndrome (24). Interestingly, muscle cramps are frequently observed in whippet dogs with homozygous *Mstn* mutations (37). Moreover, “double muscle cattle”, several breeds of which have been identified to carry *Mstn* mutations (17, 30), are prone to exercise induced lactic acidosis and severe rhabdomyolysis (20, 21).

However, a number of questions result from our work. We ask, whether the observed decrease in oxidative metabolism and energy dependent muscle function is an indirect effect and a consequence of the profound congenital fiber type changes that is typically found in constitutive absence of myostatin. We therefore blocked myostatin in adult wildtype mice using myostatin propeptide, which did not affect fiber type composition, and this is in agreement with previous studies following blockade of myostatin or its activin IIB receptor (ActRIIB) signaling (3, 11, 12, 36). Importantly, treatment with soluble ActRIIB-Fc to block myostatin and homologues signaling factors caused a molecular signature away from oxidative metabolism (41). Supporting the hypothesis that myostatin regulates oxidative metabolism independently of muscle fiber composition, we here found that treatment with myostatin propeptide caused muscle fatigability and decreased aerobic exercise capacity.

We show that myostatin deficiency impacts on expression of *PPARα/β/γ* transcription factors, which control metabolic properties but not muscle mass (43, 45). This indicates that myostatin may control

the muscle oxidative phenotype notably *via* PPAR activity. Indeed, downstream targets of PPAR- $\beta$  such as *PGC1- $\alpha$*  and *Cox4* were down-regulated in *Mstn*<sup>-/-</sup> mice (26). Furthermore, knockout of PPAR- $\beta$ , similar to *Mstn*<sup>-/-</sup> mice, reduced oxidative properties of skeletal muscle (43). Importantly, we here show, that myostatin blockade in adult mice following overexpression of myostatin propeptide also reduced expression of PPAR- $\beta$  and *PGC1- $\alpha$* , supporting the hypothesis that myostatin directly regulates oxidative metabolism. However, the exact molecular mechanism remains to be elucidated as yet little is known about direct molecular targets of myostatin signaling.

Interestingly, distinct but complementary effects on the metabolic profile of obese insulin-resistant mice occur when PPAR- $\beta$  and myostatin are activated and inhibited, respectively (7). Moreover, work on myostatin-mediated effects through AMPK (23, 44, 48) raise a number of questions concerning mediators and signaling pathways implicated on muscular metabolic effects of myostatin. It would be of interest to substantiate these findings by an analysis of muscle microRNA network as this was recently shown to control metabolism *via* action on nuclear receptors such as PPARs (14).

A further question concerns the problem whether muscle hypertrophy following lack of myostatin entails changes in oxidative muscle metabolism. In fact, we previously have shown that long-term exercise improved contractile and metabolic features of *Mstn*<sup>-/-</sup> mice, however, these improvements came at the expense of muscle hypertrophy as muscles lost in size (28). These results suggest that the regulation of muscle size and metabolic phenotype by myostatin is linked, however, it remains to be determined whether the regulation of both processes can be dissociated from each other.

Can we generalize the conclusion of our work that lack or blockade of myostatin always negatively affects aerobic muscle function? It is important to note that previous work demonstrated a beneficial effect of myostatin blockade during ageing (38). It is quite likely that protection from muscle atrophy, often caused by pathologically up-regulated myostatin, such as during sarcopenia, cardiac and tumor cachexia, and the resulting protection from functional and metabolic decline that mediates myostatin blockade by far outweighs the negative effect of such blockade on muscle metabolism (19, 27, 49). Similarly, myostatin blockade improved running performance in obese and insulin resistant (*ob/ob*) mice (7), again, benefits on insulin signaling and glucose metabolism in these mice may largely outweigh potential negative effects on muscle oxidative metabolism, especially if combined with a PPAR- $\beta$  agonist. It should be noted that treatment of adult mice under high fat diet with soluble ActRIIB did not alter fat mass and glucose metabolism (33), whereas treatment of obese and insulin resistant mice (*ob/ob*) with anti-myostatin antibodies improved glucose homeostasis and glucose tolerance (7). In fact, the metabolic changes following myostatin blockade could be beneficial for patients with insulin resistance, and recently it was shown that AAV-propeptide overexpression mediated higher glucose uptake in skeletal muscle, which is likely mediated by an up-regulation of

membrane glucose transporters (12). Thus, further work is required to define under which circumstances myostatin blockade could exert beneficial effects to combat insulin resistance and overweight.

In conclusion, our results suggest that myostatin optimizes oxidative metabolism of skeletal muscle thereby decreasing muscle fatigability and ameliorating endurance exercise properties. These fundamental functions of myostatin should be taken into account when developing therapies based on myostatin blockade. Further investigations are required to answer the question whether emerging therapies based on PPAR agonists might be able to prevent adverse effects of myostatin blockade on the oxidative metabolism and exercise tolerance.

## FIGURES

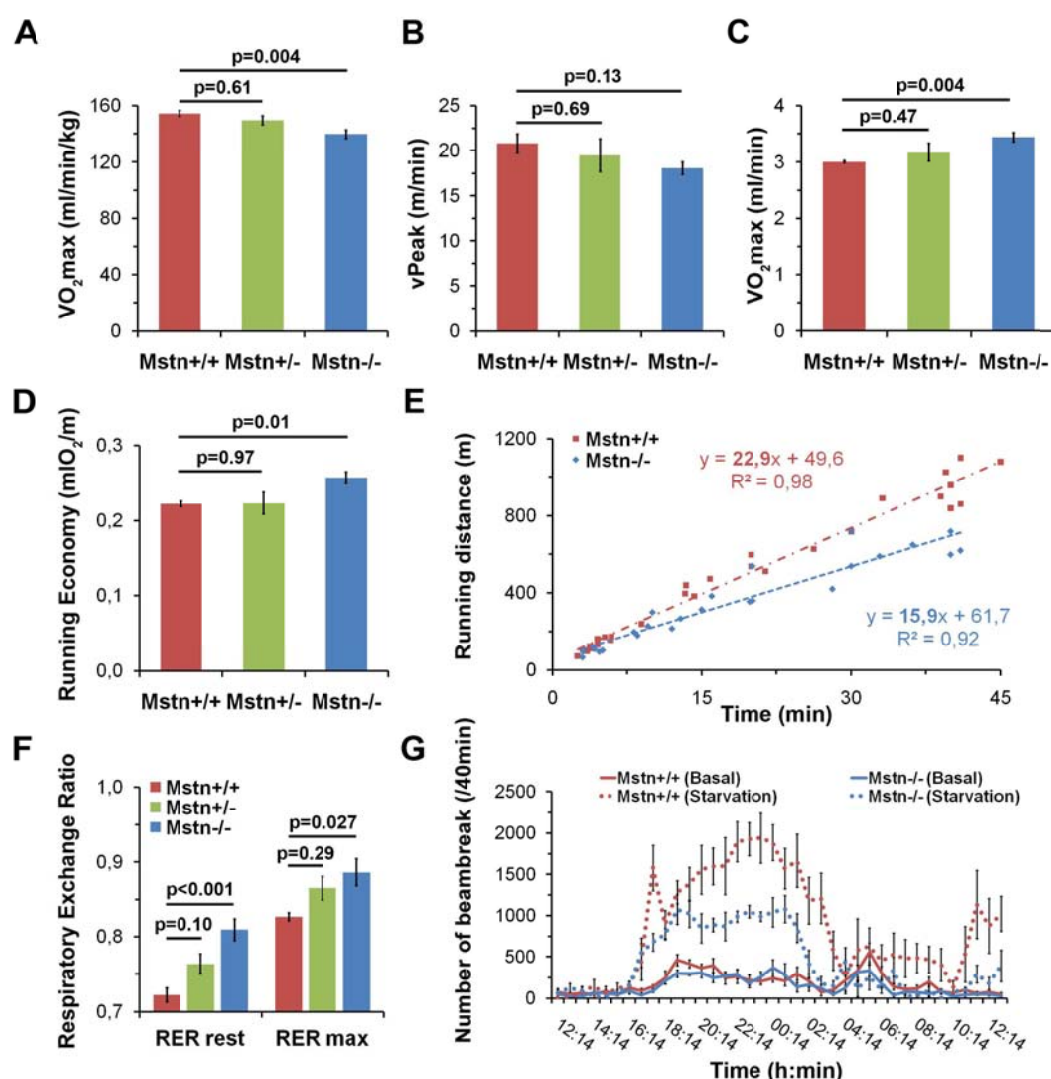


**Figure 1:** Global motor activity and energy expenditure of adult *Mstn*<sup>-/-</sup>, *Mstn*<sup>+/-</sup>, and *Mstn*<sup>+/+</sup> mice. (A) Maximal oxygen uptake ( $VO_{2max}$ ) normalized to body weight. (B) Peak running velocity reached after sequential increase of treadmill speed ( $v_{Peak}$ ). (C) Whole body absolute maximal oxygen consumption. (D) Energetic cost of running measured as oxygen consumption per distance run at 13 m/min running speed. (E) The plot depicts the proportional relationship between distance run (y-axis) and time to exhaustion (x-axis) at different velocities. The regression lines together with regression equations indicate the critical speed. (F) Respiratory Exchange Ratio (RER) at rest and at  $v_{Peak}$ . (G) Effects of 24 h food restriction (dashed line) or free feeding (plain line) on total activity (beambreaks/40 min). Values are shown as means $\pm$ SEM. Number (n) of mice examined: n=6 *Mstn*<sup>-/-</sup>; n>8 *Mstn*<sup>+/-</sup> and *Mstn*<sup>+/+</sup>.

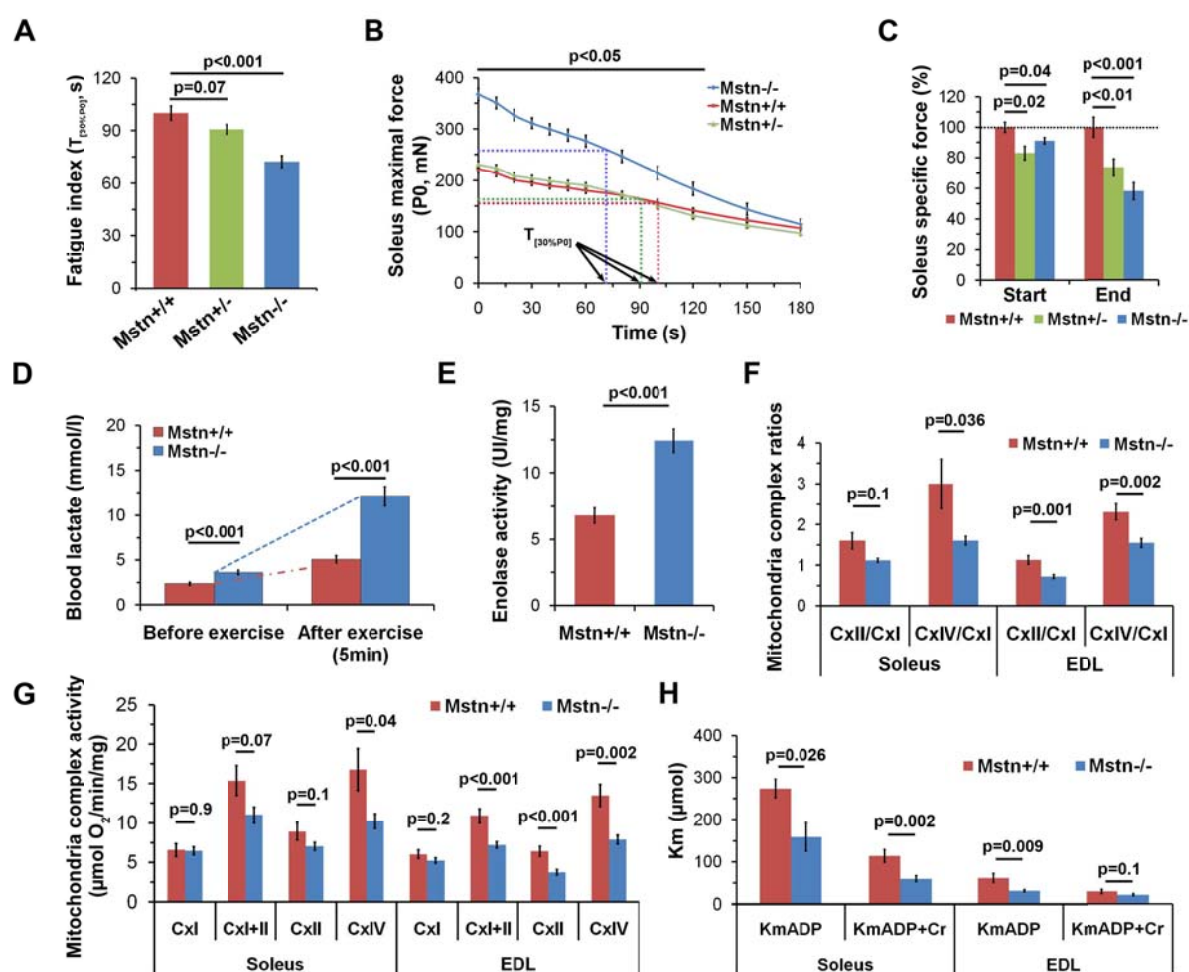


**Figure 2:** Effect of myostatin deficiency on muscle force and metabolic properties. (A-C) Studies of muscle fatigue and force in the *soleus* muscles from 4-months-old female *Mstn*<sup>+/+</sup>, *Mstn*<sup>+/-</sup> and *Mstn*<sup>-/-</sup> mice. (A) Fatigue index of the *soleus* muscles given as the time [s] during which the force had declined by 30% ( $T_{[30\%P0]}$ ). (B) Force recordings during the fatigue protocol over 180 s. (C) Specific force at the beginning and at the end of the fatigue protocol. (D-H) Metabolic measurements before and after exercise. (D) Serum lactate levels at rest and 5 min after exhaustive running exercise. (E) Enolase enzymatic activity of the *soleus* muscle. (F) Ratios of respiration rates of mitochondrial complexes of *soleus* and EDL muscles. (G) Mitochondrial respiration rates for complex I, II and IV of *soleus* and EDL muscles. (H) Km for ADP and ADP+creatine of *soleus* and EDL muscles. Values are shown as means $\pm$ SEM. Number (n) of muscles analysed:  $n \geq 6$  for each genotype.

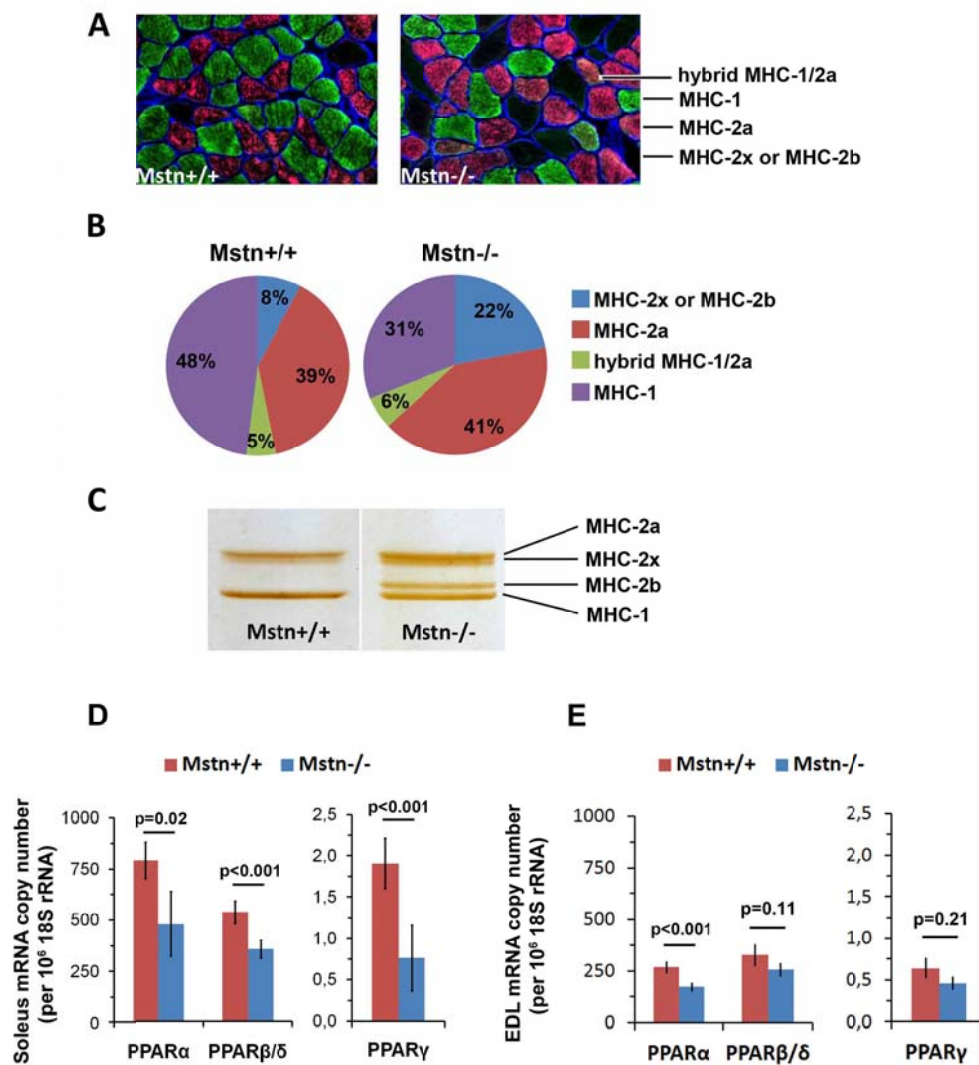


**Figure 3:** Effect of myostatin deficiency on myofiber type composition (A-C) and expression of *PPAR* transcription factors (D-E). (A) Images of fiber type composition of *soleus* muscle from *Mstn*<sup>-/-</sup> mice and *Mstn*<sup>+/+</sup> mice. Immunohistochemistry was performed to depict MHC-1 fibers (green), MHC-2a fibers (purple), MHC-1/2a hybrid fibers (orange), non-stained MHC2x or MHC2b fibers (black) and Laminin (blue). (B) Relative fiber type distribution from entire transverse sections of *soleus* muscle following immunostaining described above. (C) SDS-page electrophoresis of MHC isoforms shows an additional band of MHC-2b expression in *Mstn*<sup>-/-</sup> mice. (D-E) *PPAR* $\alpha$ ,  $\beta/\delta$  and  $\gamma$  mRNA relative copy number in the *soleus* muscle (D) and *EDL* muscle (E) from *Mstn*<sup>+/+</sup> mice and *Mstn*<sup>-/-</sup> mice expressed per 10<sup>6</sup> 18S rRNA copies. Values are shown as means  $\pm$  SEM. Number (n) of muscles analysed: n $\geq$ 5 for each genotype.

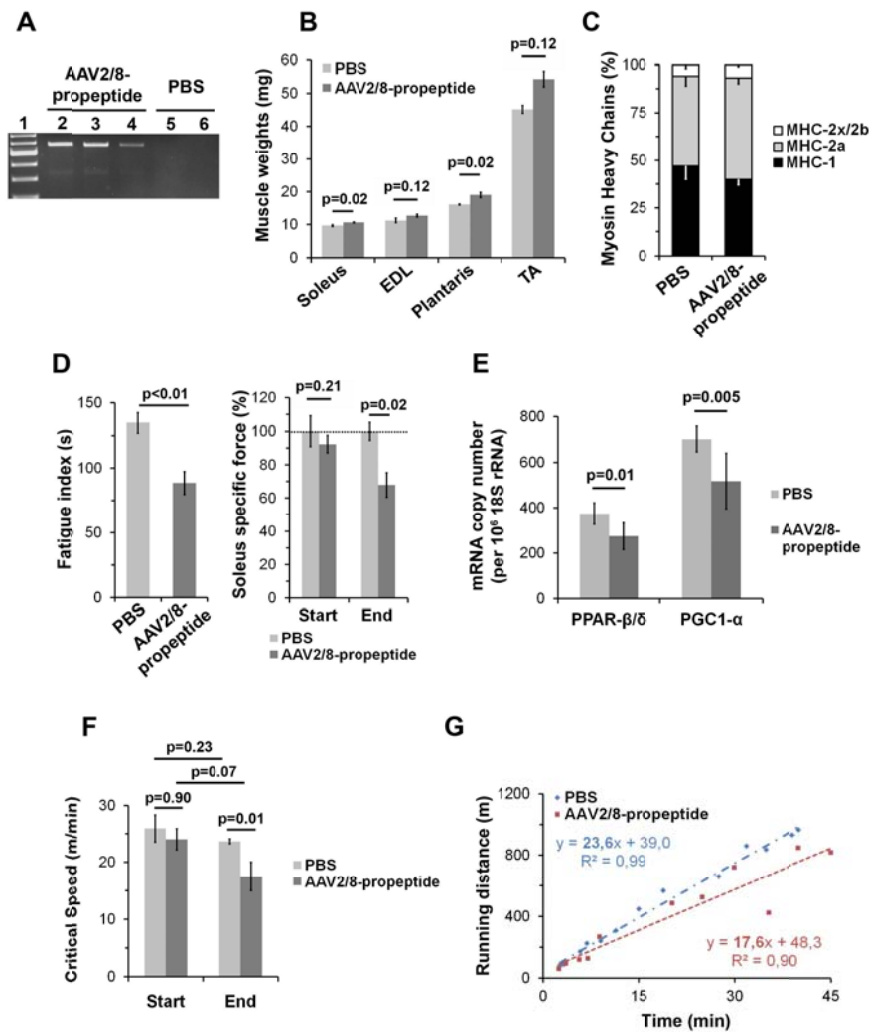


**Figure 4:** Muscular and systemic effects of AAV-propeptide-mediated adult myostatin blockade. (A-E) Functional, morphometric and metabolic analysis of the hindlimb muscles one month after injection of AAV2/8-myostatin-propeptide or PBS into femoral arteries of 2-months-old C57BL/6J mice. (A) RT-PCR depicting exogenous myostatin-propeptide expression only after AAV2/8 transfection (lane 1: molecular weight marker; lanes 2-6: individual muscles). (B) Wet weights for *soleus*, *extensor digitorum longus* (EDL), *plantaris* and *tibialis anterior* (TA) muscles. (C) *Soleus* relative myofiber type distribution. (D) Fatigue index (left) and specific tetanic force (right) of the *soleus* muscle at the beginning and at the end of the fatigue protocol. (E) *PPAR- $\beta/\delta$*  and *PGC1- $\alpha$*  mRNA relative copy number in the TA muscle. (F-G) Exercise capacity of C57BL/6J mice treated systemically (i.v) with AAV2/8-myostatin-propeptide or PBS. (F) Effect of AAV2/8-myostatin-propeptide on critical speed before and 6 months after systemic application. (G) The plot depicts the proportional relationship between distance run (y-axis) and time to exhaustion (x-axis) at different velocities. The slope of the regression line indicates the Critical Speed. Values are shown as means  $\pm$  SEM. Number (n) of muscles or mice examined: n=4-6.

## Methods

### Animals

*Mstn*<sup>+/+</sup>, *Mstn*<sup>+/-</sup> and *Mstn*<sup>-/-</sup> mice, on a C57BL/6J background (31), were bred using a heterozygous mating system in the animal facility of CERFE (Evry, France) and kept according to institutional guidelines. Investigations on mice (from 2 to 6 months old) were carried out under the laboratory and animal facility licenses A75-13-11 and A91-228-107. Partly, C57BL/6J control mice (*Mstn*<sup>+/+</sup>) were purchased from Charles River (France). Body mass composition (lean tissue mass, fat mass, free water and total water content) was analyzed using an Echo Medical systems' EchoMRI (Whole Body Composition Analyzers, EchoMRI, Houston, USA).

### Evaluation of exercise performance

#### **[A] Evaluation of the Critical Speed**

The Critical Speed (CSp) defines the proportional relationship between distance run and time to exhaustion at different velocities. Mice were exercised on a 10.6 x 30-cm double-lane treadmill (LE 8709, Bioseb, Chaville, France) as published (8). The protocol consisted of four runs at various speeds (between 20 and 80 cm.s<sup>-1</sup> according to individual motor capacity, one run per day) leading to exhaustion between 3 and 45 min. CSp is based on the hyperbolic relationship between speed and time to fatigue during separate bouts of exhaustive runs performed at different speeds. Therefore, CSp was calculated from the slope (a) of the regression line, plotting the distance (y) versus the time to exhaustion (x) from the four runs, according to the equation  $y = ax + b$  (b being the anaerobic distance capacity).

#### **[B] Blood lactate assessment during exhaustive exercise**

Lactate concentration was determined in blood samples (5 µl) collected from the tip of the tail using a Lactate pro LT device (Arkray Inc, Kyoto, Japan) at the time points 0 and 5 min after treadmill running-induced exhaustion. Exhaustion was defined as the time point at which mice could not run anymore and stayed on the grid despite repeated electric shocks. The running test started at the lowest speed of 5 cm.s<sup>-1</sup> to allow a warm-up and was increased by 1 cm.s<sup>-1</sup> every 30 seconds until exhaustion.

#### **[C] Measurement of maximal oxygen consumption**

An index of endurance exercise capacity is the maximal oxygen uptake per body weight (VO<sub>2</sub>max). Initially, oxygen uptake is proportional to the running speed, and this relationship peaks at a plateau, the so-called VO<sub>2</sub>max. Oxygen consumption was measured by means of a rapid-flow, open-circuit indirect calorimeter fitted with a one-lane motorised treadmill (Columbus Instrument, Columbus,

OH) as published (25). The single-lane test treadmill was placed in a metabolic chamber. Ambient air was flushed through the chamber at a rate of  $0.66 \text{ l} \cdot \text{min}^{-1}$ , and gas samples were extracted to measure oxygen content (Oxymax, Columbus instrument, Columbus, OH). Gas samples were dried, measured every 15 s and oxygen consumption ( $\text{VO}_2$ ) was calculated using Oxymax software. The gas analyzers were calibrated with standardized gas mixtures before every test session (Air Products, Paris, France), as recommended by the manufacturer. The test described below provided a measure of  $\text{VO}_{2\text{max}}$ , defined as the highest oxygen consumption attained during the testing protocol. The velocity attained by the mouse at this  $\text{VO}_{2\text{max}}$  was then considered as the  $\text{vVO}_{2\text{max}}$ . The maximal velocity ( $\text{vPeak}$ ) was measured at the end of the test.

### **[D] Incremental test load**

Mice were treadmill exercised on with adjustable belt speed ( $0\text{--}99.9 \text{ m} \cdot \text{min}^{-1}$ ) and electric shock bars ( $0\text{--}2 \text{ mA}$ ) at the rear of the belt to provide a stimulus encouraging each mouse to run. Over a one week period, the mice were familiarised with the treadmill through the completion of four 10 min running sessions from  $0$  to  $9 \text{ m} \cdot \text{min}^{-1}$ . The mice subsequently performed an incremental exercise test, without slope. The exercise intensity was increased by  $3 \text{ m} \cdot \text{min}^{-1}$  (starting from  $10 \text{ m} \cdot \text{min}^{-1}$ ) every 3 min, and the exercise continued until exhaustion.

### **Measurement of voluntary locomotion**

Total voluntary locomotor activities were determined in individual cages with bedding, food and water (Labmaster, TSE Systems GmbH). Animals were acclimated in individual cages for 48 hours before experimental measurements. Each cage was embedded in a frame with an infrared light beam-based activity monitoring system, allowing measurement of total locomotion. Data collection was recorded every 40 minutes during the whole experiments and expressed by number of beam break. Mice had access to food and water *ad libitum* except for the 12 hours fasting in order to stimulate motor activity of mice.

### **Measurement of contractile properties**

The contractile properties of *extensor digitorum longus* (EDL) and soleus muscles were studied *in vitro* according to previously published protocols (2). Muscles were soaked in an oxygenated Tyrode solution (95%  $\text{O}_2$  and 5%  $\text{CO}_2$ ) containing 58.5 mM NaCl, 24 mM  $\text{NaHCO}_3$ , 5.4 mM KCl, 1.2 mM  $\text{KH}_2\text{PO}_4$ , 1.8 mM  $\text{CaCl}_2$ , 1 mM  $\text{MgSO}_4$  and 10 mM glucose (pH7.4) and maintained at a temperature of  $22^\circ\text{C}$ . One muscle tendon was attached to a lever arm of a servomotor system (300B, Dual-Mode Lever, Aurora). After equilibration (30 min), field electrical stimulation was delivered through electrodes running parallel to the muscle. Pulses of 1 ms were generated by a high power stimulator (701B, Aurora). Absolute maximal isometric tetanic force ( $P_0$ ) was measured during tetanic contractions (frequency of 50–100 Hz, train of stimulation of 1,500 ms for *soleus* and 750 ms for *EDL*). The

muscle length was adjusted to an optimum ( $L_0$ ) that produced  $P_0$ . Specific maximal isometric force ( $sP_0$ ) was calculated by dividing the force by the estimated cross-sectional area (CSA) of the muscle. Assuming muscles have a cylindrical shape and a density of  $1.06 \text{ mg}\cdot\text{mm}^{-3}$ , the CSA corresponds to the volume of the muscle divided by its fiber length ( $L_f$ ). The  $L_f$  to  $L_0$  ratio of 0.70 (soleus) or 0.45 (EDL) was used to calculate  $L_f$ . Maximal power ( $P_{\text{max}}$ ) was determined from force-velocity data that were obtained by eliciting contractions (train of 1,000 ms, 150 Hz) at 3-5 different afterloads (10-40%  $P_0$ ). Specific  $P_{\text{max}}$  ( $sP_{\text{max}}$ ) was calculated by dividing  $P_{\text{max}}$  by muscle weight. Fatigue resistance was then determined after a 5 min rest period. The muscles were stimulated at 75 Hz during 500 ms, every two second, for 3 min. The time taken for initial force to fall by 50% (EDL) or 30% (*soleus*) was then measured. All data were recorded and analyzed on a microcomputer, using the PowerLab system (4SP, AD Instruments) and software (Chart 4, ADInstruments).

The isometric contractile properties of *gastrocnemius* (+ *soleus*) were studied *in situ* as previously described (22). Mice were anesthetized (pentobarbital sodium, 50 mg/kg). Supplemental doses were given as required to maintain deep anesthesia throughout the experiments. The foot was fixed with clamp and the knee was immobilized using stainless steel pins. The distal tendon of the *plantaris* muscle was cut. The Achilles tendon was attached to an isometric force transducer (Harvard). Great care was taken to ensure that the blood and nerve supply remained intact during surgery. The sciatic nerves were severed proximally and stimulated distally by a bipolar silver electrode using supra-maximal square wave pulses of 0.1 ms duration. All isometric measurements were made at an initial muscle length of  $L_0$ . Force productions in response to tetanic stimulations ( $P_0$ ) were successively recorded (pulse frequency from 50 to 150 Hz, train duration of 500 ms), at least 1 min was allowed between each contractions. The muscle mass ( $m$ ) was measured to calculate  $sP_0$ . Fatigue resistance was then determined after a 5 min rest period. The muscle was stimulated during 500 ms at 100 Hz, every 2 s, for 3 min. The duration corresponding to a force decreased by 50% was noted. After contractile measurements, the animals were killed with an overdose of pentobarbitone. Muscles were then weighed, frozen in liquid nitrogen or in isopentane pre-cooled in liquid nitrogen and stored at  $-80^\circ\text{C}$  until histology or biochemical analyses.

### **Mitochondrial respiration and cytosolic enzyme measurements**

#### **[A] Measurement of OXPHOS activity**

The mitochondrial respiration was studied *in situ* in saponin-skinned fibers. Briefly, fibers were separated under a binocular microscope in *solution S* at  $4^\circ\text{C}$  (see below) and permeabilized in *solution S* with  $50 \mu\text{g}/\text{ml}$  of saponin for 30 min. After being placed 10 min in *solution R* (see below) to wash out adenine nucleotides and creatine phosphate, skinned separated fibers were transferred in a 3 ml water-jacketed oxygraphic cell (Strathkelvin Instruments, Glasgow, UK) equipped with a Clark elec-

trode, as previously described (5), under continuous stirring. *Solutions R* and *S* contained the following: 2.77 mM CaK<sub>2</sub>EGTA, 7.23 mM K<sub>2</sub>EGTA (100 nM free Ca<sup>2+</sup>), 1 mM free Mg<sup>2+</sup>, 20 mM taurine, 0.5 mM DTT, 50 mM potassium-methane sulfonate (160 mM ionic strength), and 20 mM imidazole (pH 7.1). *Solution S* also contained 5.7 mM Na<sub>2</sub>ATP, 15 mM creatine-phosphate, while *solution R* contained 5 mM glutamate, 2 mM malate, 3 mM phosphate, and 2 mg/ml FA free bovine serum. After the experiments, fibers were harvested and dried, and respiration rates were expressed as micromoles of O<sub>2</sub> per minute per gram dry weight. *Solution R<sup>-</sup>* was similar to *solution R* without substrates and was used to determine maximal VO<sub>2</sub> rates for different substrates.

### **[B] Measurement of the maximal muscular oxidative capacities**

After the determination of basal respiration rate  $V_0$ , the maximal fiber respiration rate was measured at 22°C in the presence of saturating concentration of ADP (2 mM), as phosphate acceptor and glutamate-malate as mitochondrial substrates ( $V_{GM}$ ). The acceptor control ratio was  $V_{GM}/V_0$  and represented the degree of coupling between oxidation and phosphorylation.

### **[C] Measurement of the respiratory chain complexes**

When  $V_{GM}$  was recorded, electron flow goes through complexes I, II, III, and IV. Then 4 min after this  $V_{GM}$  measurement, the complex I was blocked with amytal (2 mM), and then complex II was stimulated with succinate (25 mM). In these conditions, mitochondrial respiration was effected by complexes II, III, and IV ( $V_S$ ). After that, *N,N,N',N'*-tetramethyl-*p*-phenylenediamine dihydrochloride (TMPD, 0.5 mM) and ascorbate (0.5 mM) were added as an artificial electron donor to cytochrome-*c*. In these conditions, cytochrome-*c* oxidase (complex IV) was studied as an isolated step of respiratory chain ( $V_{TMPD}$ ). The ratios  $V_S/V_{GM}$  and  $V_{TMPD}/V_{GM}$  allow exploration of complexes I, II, and IV.

### **[D] Measurement of cytosolic enzyme**

Enolase activity was determined in extracts from frozen cryostat sections using a coupled enzyme assay (35).

### **Immunostaining and SDS-Page**

For MHC-immunohistochemistry, primary antibodies were: MHC-1 (hybridoma#BA-D5, Deutsche Sammlung von Mikroorganismen und Zellkulturen DSMZ), MHC-2a (hybridoma#SC-71, DSMZ), MHC-2x (hybridoma#6H1, Developmental Studies Hybridoma Bank) and MHC-2b (hybridoma#BF-F3, DSMZ). Briefly, frozen unfixed 10 µm sections were blocked 1 h in PBS plus 1% BSA, 1% sheep serum, 0.01% Triton X-100 and 0.001% sodium azide. Sections were then incubated overnight with primary antibodies against laminin (Dako) and MHC isoforms. After washes in PBS, sections were incubated 1 h with secondary antibodies. Slides were finally mounted in Fluoromont (Southern Biotech). Morphometric analyses were made on whole *soleus* muscles. Images were captured using a digital cam-

era (Hamamatsu ORCA-AG) attached to a motorized fluorescence microscope (Zeiss AxioImager.Z1), and morphometric analyses were made using the software MetaMorph 7.5 (Molecular Devices).

For MHC gel electrophoresis, the muscles were extracted on ice for 60 minutes in 4 volumes of extracting buffer (pH 6.5) as previously described (10). Following centrifugation, the supernatants were diluted 1:1 (v/v) with glycerol and stored at -20 °C. MHC isoforms (MHC-1, MHC-2a, MHC-2x, MHC-2b) were separated on 8% polyacrylamide gels which were made in the Bio-Rad mini-Protean II Dual slab cell system as described previously (1). The gels were run for 31 hours at 72 V (constant voltage) at 4°C. Following migration, the gels were silver stained. The positions of the different MHC bands were confirmed by Western blotting using antibodies directed against different MHC isoforms. The gels were scanned using a video acquisition system.

### **Production and injection of AAV-propeptide mediated adult myostatin blockade**

The myostatin propeptide construct, prepared by PCR amplification of C57Bl6 cDNA, using the primers 5'-CCG CTC GAG ATG ATG CAA AAA CTG CAA ATG-3' and 5'-CCG GGA TCC CTA TTA GTC TCT CCG GGA CCT CTT-3', was introduced into an AAV-2-based vector between the 2 inverted terminal repeats and under the control of the cytomegaly virus promoter using the *XhoI* and *BamHI* sites. The AAV myostatin propeptide was produced in human embryonic kidney 293 cells by the triple-transfection method using the calcium phosphate precipitation technique with both the pAAV2 propeptide plasmid, the pXX6 plasmid coding for the adenoviral sequences essential for AAV production, and the pRepCAP plasmid coding for AAV8 capsid. The virus was then purified by 2 cycles of cesium chloride gradient centrifugation and concentrated by dialysis. The final viral preparations were kept in PBS solution at -80°C. The particle titer (number of viral genomes) was determined by a quantitative PCR.

Detailed procedure for intra-arterial injection was previously described (16). Briefly, anesthetized 2 month old C57BL/6J wild-type male mice underwent femoral artery and vein isolation of right hindlimb. After clamping the femoral vein and two collaterals, a catheter was introduced in the femoral artery and the AAV preparation ( $2.5 \times 10^{12}$  vg per injection) was injected in a volume of 1 ml per 20g of body weight at a rate of  $100 \mu\text{l.s}^{-1}$ . Then, left hind limb was processed in the same manner and injected with a same volume of PBS. For systemic delivery,  $1 \times 10^{13}$  vg of AAV2/8-myostatin propeptide was injected into the retro-orbital sinus or with PBS for controls.

## RT-qPCR

Total RNA was extracted from frozen muscle after pulverization in liquid nitrogen and from cultured C<sub>2</sub>C<sub>12</sub> cell pellets with the TRIzol® (Invitrogen) extraction protocol. 2.25 µg total RNA were reversely transcribed using the Thermoscript RT PCR System (Invitrogen) with random hexamers in 60 µl reaction volume of which we used 4 µl for each subsequent qPCR-reaction and 2 µl of a 1:10 dilution for the 18S reference gene. We used the following oligonucleotide primers for qPCR: *18S rRNA* (reference gene): (F) 5'-CAT TCG AAC GTC TGC CCT ATC-3', (R) 5'-CTC CCT CTC CGG AAT CGA AC-3'; *Ppar-α*: (F) 5'-GGG CAA GAG AAT CCA CGA AG-3', (R) 5'-CGT CTT CTC GGC CAT ACA CA-3'; *Ppar-β/δ*: (F) 5'-AGC CAC AAC GCA CCC TTT-3', (R) 5'-CGG TAG AAC ACG TGC ACA CT-3'; *Ppar-γ*: (F) 5'-CGA GTC TGT GGG GAT AAA GC-3', (R) 5'-GGA TCC GGC AGT TAA GAT CA-3'; *PGC1-α*: (F) 5'-GAA AGG GCC AAA CAG AGA GA-3', (R) 5'-GTA AAT CAC ACG GCG CTC TT-3'. The qPCR for each sample was run with the SYBR Green® protocol (Applied Biosystems) in triplicate on an ABI PRISM 7700 sequence detection system (Applied Biosystems) with a hotstart Taq polymerase. A 10 min denaturation step at 94°C was followed by 45 cycles of denaturation at 94°C for 10 s and annealing/extension at 60°C for 30 s. Before sample analysis we had determined for each gene the PCR efficiencies with a standard dilution series (10<sup>0</sup>-10<sup>7</sup> copies/µl), which subsequently enabled us to calculate the copy numbers from the C<sub>t</sub> values, using the  $\Delta\Delta C_t$  method.

## Statistical analysis

Data were analysed using either one-way ANOVA, followed by Tukey post-hoc test, or paired/unpaired Student's t tests. Values are presented as means ± SEM. The significance level was set at p<0.05.

### ACKNOWLEDGEMENTS

We would like to acknowledge Stéphanie Rimbaud for helping with the mitochondrial respiration protocol and the Functional & Physiological Exploration Platform (FPE, Université Paris Diderot, Sorbonne, Paris Cité, BFA, EAC 4413 CNRS, F-75205 Paris, France).

### GRANTS

This work was supported by the Association Française contre les Myopathies towards HA, AF, AV, LG, and EM, Association Monegasque contre les Myopathies and the Parents Project France towards HA and CH, Aktion Benni & Co towards HA, the Deutsche Forschungsgemeinschaft and the Université Franco-Allemand towards KR, HA and MS (as part of the MyoGrad International Graduate School for Myology DRK 1631/1 and CDFA-06-11), and NeuroCure Exc 257 to MS.

### DISCLOSURE

No conflicts of interest, financial or otherwise, are declared by the authors.

### AUTHORS' CONTRIBUTIONS

EM, KR, LMH, RD, CH, OA, LA, SL, AV, AF and HA carried out the experiments. VB assisted in the measurement of maximal oxygen uptake during exercise. SL assisted in the voluntary locomotor activity experiments. RVC assisted in the mitochondrial respiration experiments. EM, MS and HA carried out all the analyses and the figures. HA designed the study and drafted the manuscript with the help of EM, KP, LG and MS. All authors read and approved the final manuscript.

## LITERATURE

1. **Agbulut O, Noirez P, Beaumont F, and Butler-Browne G.** Myosin heavy chain isoforms in postnatal muscle development of mice. *Biol Cell* 95: 399-406, 2003.
2. **Agbulut O, Vignaud A, Hourde C, Mouisel E, Fougerousse F, Butler-Browne GS, and Ferry A.** Slow myosin heavy chain expression in the absence of muscle activity. *Am J Physiol Cell Physiol* 296: C205-214, 2009.
3. **Akpan I, Goncalves MD, Dhir R, Yin X, Pistilli EE, Bogdanovich S, Khurana TS, Ucran J, Lachey J, and Ahima RS.** The effects of a soluble activin type IIB receptor on obesity and insulin sensitivity. *Int J Obes* 33: 1265-1273, 2009.
4. **Amthor H, Macharia R, Navarrete R, Schuelke M, Brown SC, Otto A, Voit T, Muntoni F, Vrbova G, Partridge T, Zammit P, Bunker L, and Patel K.** Lack of myostatin results in excessive muscle growth but impaired force generation. *Proc Natl Acad Sci U S A* 104: 1835-1840, 2007.
5. **Athea Y, Viollet B, Mateo P, Rousseau D, Novotova M, Garnier A, Vaulont S, Wilding JR, Grynberg A, Veksler V, Hoerter J, and Ventura-Clapier R.** AMP-activated protein kinase  $\alpha 2$  deficiency affects cardiac cardiolipin homeostasis and mitochondrial function. *Diabetes* 56: 786-794, 2007.
6. **Baligand C, Gilson H, Menard JC, Schakman O, Wary C, Thissen JP, and Carlier PG.** Functional assessment of skeletal muscle in intact mice lacking myostatin by concurrent NMR imaging and spectroscopy. *Gene Ther* 17: 328-337, 2010.
7. **Bernardo BL, Wachtmann TS, Cosgrove PG, Kuhn M, Opsahl AC, Judkins KM, Freeman TB, Hadcock JR, and LeBrasseur NK.** Postnatal PPAR $\delta$  activation and myostatin inhibition exert distinct yet complimentary effects on the metabolic profile of obese insulin-resistant mice. *PLoS One* 5: e11307, 2010.
8. **Billat VL, Mouisel E, Roblot N, and Melki J.** Inter- and intrastrain variation in mouse critical running speed. *J Appl Physiol* 98: 1258-1263, 2005.
9. **Brown ML, Bonomi L, Ungerleider N, Zina J, Kimura F, Mukherjee A, Sidis Y, and Schneyer A.** Follistatin and follistatin like-3 differentially regulate adiposity and glucose homeostasis. *Obesity* 19: 1940-1949, 2011.
10. **Butler-Browne GS, and Whalen RG.** Myosin isozyme transitions occurring during the postnatal development of the rat soleus muscle. *Dev Biol* 102: 324-334, 1984.
11. **Cadena SM, Tomkinson KN, Monnell TE, Spaits MS, Kumar R, Underwood KW, Pearsall RS, and Lachey JL.** Administration of a soluble activin type IIB receptor promotes skeletal muscle growth independent of fiber type. *J Appl Physiol* 109: 635-642, 2010.
12. **Cleasby ME, Jarmin S, Eilers W, Elashry M, Andersen DK, Dickson G, and Foster K.** Local Overexpression of the Myostatin Propeptide Increases Glucose Transporter Expression and Enhances Skeletal Muscle Glucose Disposal. *Am J Physiol Endocrinol Metab*, 2014.

13. **Fournier B, Murray B, Gutzwiller S, Marcaletti S, Marcellin D, Bergling S, Brachat S, Persohn E, Pierrel E, Bombard F, Hatakeyama S, Trendelenburg AU, Morvan F, Richardson B, Glass DJ, Lach-Trifilieff E, and Feige JN.** Blockade of the activin receptor IIb activates functional brown adipogenesis and thermogenesis by inducing mitochondrial oxidative metabolism. *Mol Cell Biol* 32: 2871-2879, 2012.
14. **Gan Z, Rumsey J, Hazen BC, Lai L, Leone TC, Vega RB, Xie H, Conley KE, Auwerx J, Smith SR, Olson EN, Kralli A, and Kelly DP.** Nuclear receptor/microRNA circuitry links muscle fiber type to energy metabolism. *J Clin Invest* 123: 2564-2575, 2013.
15. **Giannesini B, Vilmen C, Amthor H, Bernard M, and Bendahan D.** Lack of myostatin impairs mechanical performance and ATP cost of contraction in exercising mouse gastrocnemius muscle in vivo. *Am J Physiol Endocrinol Metab* 305: E33-40, 2013.
16. **Gonin P, Arandel A, Van Wittenberghe L, Marais T, Perez N, and Danos O.** Femoral intra-arterial injection: a tool to deliver and assess recombinant AAV constructs in rodents whole hind limb. *J Gene Med* 7: 782-791, 2005.
17. **Grobet L, Martin LJ, Poncelet D, Pirottin D, Brouwers B, Riquet J, Schoeberlein A, Dunner S, Menissier F, Massabanda J, Fries R, Hanset R, and Georges M.** A deletion in the bovine myostatin gene causes the double-musled phenotype in cattle. *Nat Genet* 17: 71-74, 1997.
18. **Hennebry A, Berry C, Siriott V, O'Callaghan P, Chau L, Watson T, Sharma M, and Kambadur R.** Myostatin regulates fiber-type composition of skeletal muscle by regulating MEF2 and MyoD gene expression. *Am J Physiol Cell Physiol* 296: C525-534, 2009.
19. **Heineke J, Auger-Messier M, Xu J, Sargent M, York A, Welle S, and Molkentin JD.** Genetic deletion of myostatin from the heart prevents skeletal muscle atrophy in heart failure. *Circulation* 121: 419-425, 2010.
20. **Holmes JH, Ashmore CR, and Robinson DW.** Effects of stress on cattle with hereditary muscular hypertrophy. *J Anim Sci* 36: 684-694, 1973.
21. **Holmes JH, Robinson DW, and Ashmore CR.** Blood lactic acid and behaviour in cattle with hereditary muscular hypertrophy. *J Anim Sci* 35: 1011-1013, 1972.
22. **Hourde C, Vignaud A, Beurdy I, Martelly I, Keller A, and Ferry A.** Sustained peripheral arterial insufficiency durably impairs normal and regenerating skeletal muscle function. *J Physiol Sci* 56: 361-367, 2006.
23. **Hulmi JJ, Oliveira BM, Silvennoinen M, Hoogaars WM, Ma H, Pierre P, Pasternack A, Kainulainen H, and Ritvos O.** Muscle protein synthesis, mTORC1/MAPK/Hippo signaling, and capillary density are altered by blocking of myostatin and activins. *Am J Physiol Endocrinol Metab* 304: E41-50, 2013.
24. **Janssen AJ, Schuelke M, Smeitink JA, Trijbels FJ, Sengers RC, Lucke B, Wintjes LT, Morava E, van Engelen BG, Smits BW, Hol FA, Siers MH, Ter Laak H, van der Knaap MS, Van Spronsen FJ, Rodenburg RJ, and van den Heuvel LP.** Muscle 3243A-->G mutation load and capacity of the mitochondrial energy-generating system. *Ann Neurol* 63: 473-481, 2008.

25. **Kemi OJ, Loennechen JP, Wisloff U, and Ellingsen O.** Intensity-controlled treadmill running in mice: cardiac and skeletal muscle hypertrophy. *J Appl Physiol* 93: 1301-1309, 2002.
26. **Lipina C, Kendall H, McPherron AC, Taylor PM, and Hundal HS.** Mechanisms involved in the enhancement of mammalian target of rapamycin signalling and hypertrophy in skeletal muscle of myostatin-deficient mice. *FEBS Lett* 584: 2403-2408, 2010.
27. **Macdonald EM, Andres-Mateos E, Mejias R, Simmers JL, Mi R, Park JS, Ying S, Hoke A, Lee SJ, and Cohn RD.** Denervation atrophy is independent from Akt and mTOR activation and is not rescued by myostatin inhibition. *Dis Model Mech* 2014.
28. **Matsakas A, Macharia R, Otto A, Elashry MI, Mouisel E, Romanello V, Sartori R, Amthor H, Sandri M, Narkar V, and Patel K.** Exercise training attenuates the hypermuscular phenotype and restores skeletal muscle function in the myostatin null mouse. *Exp Physiol* 97: 125-140, 2012.
29. **Matsakas A, Mouisel E, Amthor H, and Patel K.** Myostatin knockout mice increase oxidative muscle phenotype as an adaptive response to exercise. *J Muscle Res Cell Motil* 31: 111-125, 2010.
30. **McPherron AC, and Lee SJ.** Double muscling in cattle due to mutations in the myostatin gene. *Proc Natl Acad Sci U S A* 94: 12457-12461, 1997.
31. **McPherron AC, Lawler AM, and Lee SJ.** Regulation of skeletal muscle mass in mice by a new TGF-beta superfamily member. *Nature* 387: 83-90, 1997.
32. **McPherron AC.** Metabolic functions of myostatin and GDF11. *Immunol Endocr Metab Agents Med Chem* 10: 217-231, 2010.
33. **McPherron AC, Guo T, Wang Q, and Portas J.** Soluble activin receptor type IIB treatment does not cause fat loss in mice with diet-induced obesity. *Diabetes Obes Metab* 14: 279-282, 2012.
34. **Mendias CL, Marcin JE, Calerdon DR, and Faulkner JA.** Contractile properties of EDL and soleus muscles of myostatin-deficient mice. *J Appl Physiol* 101: 898-905, 2006.
35. **Merkulova T, Dehaupas M, Nevers MC, Creminon C, Alameddine H, and Keller A.** Differential modulation of alpha, beta and gamma enolase isoforms in regenerating mouse skeletal muscle. *Eur J Biochem* 267: 3735-3743, 2000.
36. **Morine KJ, Bish LT, Selsby JT, Gazzara JA, Pendrak K, Sleeper MM, Barton ER, Lee SJ, and Sweeney HL.** Activin IIB receptor blockade attenuates dystrophic pathology in a mouse model of Duchenne muscular dystrophy. *Muscle Nerve* 42: 722-730, 2010.
37. **Mosher DS, Quignon P, Bustamante CD, Sutter NB, Mellersh CS, Parker HG, and Ostrander EA.** A mutation in the myostatin gene increases muscle mass and enhances racing performance in heterozygote dogs. *PLoS Genet* 3: e79, 2007.
38. **Murphy KT, Koopman R, Naim T, Léger B, Trieu J, Ibebunjo C, and Lynch GS.** Antibody-directed myostatin inhibition in 21-mo-old mice reveals novel roles for myostatin signaling in skeletal muscle structure and function. *FASEB J* 24: 4433-4442, 2010.
39. **Ploquin C, Chabi B, Fouret G, Vernus B, Feillet-Coudray C, Coudray C, Bonniieu A, and Ramonatxo C.** Lack of myostatin alters intermyofibrillar mitochondria activity, unbalances redox

status, and impairs tolerance to chronic repetitive contractions in muscle. *Am J Physiol Endocrinol Metab* 302: E1000-1008, 2012.

40. **Qaisar R, Renaud G, Morine K, Barton ER, Sweeney HL, and Larsson L.** Is functional hypertrophy and specific force coupled with the addition of myonuclei at the single muscle fiber level? *Faseb J* 26: 1077-1085, 2012.

41. **Rahimov F, King OD, Warsing LC, Powell RE, Emerson CP Jr, Kunkel LM, and Wagner KR.** Gene expression profiling of skeletal muscles treated with a soluble activin type IIB receptor. *Physiol Genomics* 43: 398-407, 2011.

42. **Savage KJ, and McPherron AC.** Endurance exercise training in myostatin null mice. *Muscle Nerve* 42: 355-362, 2010.

43. **Schuler M, Ali F, Chambon C, Duteil D, Bornert JM, Tardivel A, Desvergne B, Wahli W, Chambon P, and Metzger D.** PGC1alpha expression is controlled in skeletal muscles by PPARbeta, whose ablation results in fiber-type switching, obesity, and type 2 diabetes. *Cell Metab* 4: 407-414, 2006.

44. **Shan T, Liang X, Bi P, and Kuang S.** Myostatin knockout drives browning of white adipose tissue through activating the AMPK-PGC1 $\alpha$ -Fndc5 pathway in muscle. *FASEB J* 27: 1981-1989, 2013.

45. **Wagner KD, and Wagner N.** Peroxisome proliferator-activated receptor beta/delta (PPARbeta/delta) acts as regulator of metabolism linked to multiple cellular functions. *Pharmacol Ther* 125: 423-435, 2010.

46. **Weber JM.** Metabolic fuels: regulating fluxes to select mix. *J Exp Biol* 214: 286-294, 2011.

47. **Yadav H, Quijano C, Kamaraju AK, Gavrilova O, Malek R, Chen W, Zervas P, Zhigang D, Wright EC, Stuelten C, Sun P, Lonning S, Skarulis M, Sumner AE, Finkel T, and Rane SG.** Protection from obesity and diabetes by blockade of TGF- $\beta$ /Smad3 signaling. *Cell Metab* 14: 67-79, 2011.

48. **Zhang C, McFarlane C, Lokireddy S, Bonala S, Ge X, Masuda S, Gluckman PD, Sharma M, and Kambadur R.** Myostatin-deficient mice exhibit reduced insulin resistance through activating the AMP-activated protein kinase signalling pathway. *Diabetologia* 54: 1491-1501, 2011.

49. **Zhou X, Wang JL, Lu J, Song Y, Kwak KS, Jiao Q, Rosenfeld R, Chen Q, Boone T, Simonet WS, Lacey DL, Goldberg AL, and Han HQ.** Reversal of cancer cachexia and muscle wasting by ActRIIB antagonism leads to prolonged survival. *Cell* 142: 531-543, 2010.

## 2. Part 2: The role of the myostatin blockade in combination with gene therapy muscular dystrophy.

**Project description:** Duchenne muscular dystrophy is a severe neuromuscular disease characterized by progressive degeneration of the skeletal muscle. One of the most promising therapeutic strategies based on, RNA splice-modulation (so-called exon skipping) of the *DMD* premessenger RNA. The adeno-associated virus AAV-U7 mediates exon skipping and restores the dystrophin protein in *mdx* mice. The soluble activin receptor type IIB linked to the Fc fragment (sActRIIB-Fc) is used to inhibit the myostatin/ActRIIB signaling pathway in order to promote the skeletal muscle growth and function. We hypothesized that the combined treatment with the AAV-U7 and the sActRIIB-Fc may synergistically improve the dystrophic phenotype in the *mdx* mouse. We therefore investigated the effect of each treatment alone and in combination on muscle strength and function.

**Contribution to the project:** This project was performed in collaboration with the laboratory of Peter A.'t Hoen (Leiden University Medical Center in Netherlands). The study was mainly conducted by a post-doctoral researcher from each laboratory (Etienne Mouisel and Willem Hoogars). I contributed to this study and assisted during muscle forces measurements. I performed the immunostaining and the Western blot to verify the restoration of the dystrophin protein after the treatment with the AAV-U7. We found that the combination of the two strategies maintains the benefit of each treatment, but did not show any synergistic effects on the function of the *mdx* dystrophic skeletal muscle.



**Manuscript 3:** [Hum Gene Ther. 2012 Dec;23\(12\):1269-79. doi: 10.1089/hum.2012.056. Epub 2012 Sep 24.](#)

**Combined effect of AAV-U7-induced dystrophin exon skipping and soluble activin Type IIB receptor in mdx mice**



# **GENERAL DISCUSSION**





The inhibition of the myostatin/ActRIIB signaling pathway has many effects on a numbers of muscle properties, such as physiological, contractile or oxidative properties. During my thesis, I explored these effects in two mouse models, (i) the constitutive myostatin knockout mice and (ii) through inhibition of the ActRIIB signaling pathway by treatment of adult mice with the soluble activin receptor IIB.

My results, which I presented in the previous chapter, evoke a number of questions arise when regarding the multiple effects of myostatin on the regulation of muscle mass, function and metabolism.

## 1. Myostatin and muscle force

The constitutional absence of myostatin in the *Mstn*<sup>-/-</sup> mouse model produces an impressive hypermuscular phenotype. However, this excessive muscle growth is to variable extent associated with loss of specific force as reported by several publications ((Amthor, Macharia et al. 2007); (Mendias, Marcin et al. 2006)). Despite the fact that all these authors used exactly the same myostatin knockout mouse model from the same original source (Se-Jin Lee, Johns Hopkins University), force measurements differed considerably ranging from a diminished total and specific force as observed by Matsakas *et al.* (Matsakas, Macharia et al. 2012), to an increased absolute force with no or only little decreased specific force as observed by Schirwis *et al.* (Schirwis, Agbulut et al. 2013). The cause for these enormous differences in muscle force production as observed by these different authors remains unresolved.

### *What could cause such differences in the muscle force?*

One hypothesis addresses environmental factors, as the mice were bred in different animal houses. Mice may behave differently under one breeding condition or another, and the results of a study may also depend on the age of the animals and the timepoints of measurement. Notably, this concerns their voluntary motor behavior as this likely determines muscle physiological properties. However, this was not controlled in all these different studies. Interestingly, it has previously been shown that voluntary exercise capacity strongly varies between individual *Mstn*<sup>-/-</sup> mice (Matsakas, Mouisel et al. 2010), which further points to the fact that muscle mass increase not consistently improves motor performance in each individual mouse. The hypothesis that motor exercise influences muscle force was studied by Matsakas *et al.* (Matsakas, Macharia et al. 2012). They showed that the diminished force in *Mstn*<sup>-/-</sup> mice could be improved by endurance exercise. In this study, mice were subjected to a swimming exercise for 5 weeks, which improved their force production (Matsakas, Macharia et al.

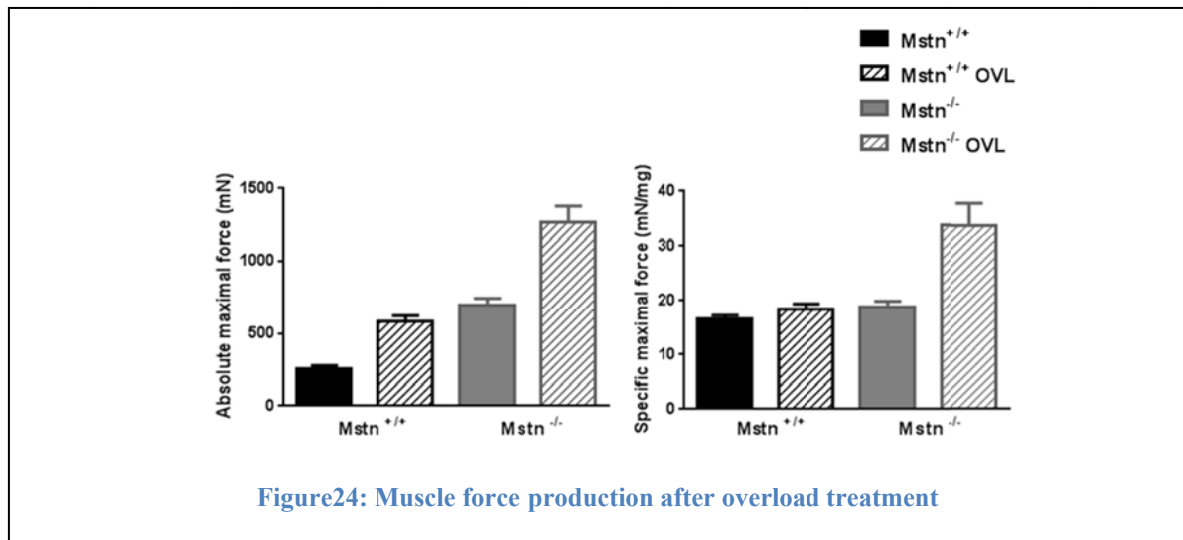
2012). However, the muscle became more oxidative and lost in weight and fiber size suggesting that myostatin deficiency could be antagonized by exercise (Matsakas, Macharia et al. 2012). This also demonstrates that the muscle mass and muscle metabolism are related with each other.

Regarding our knowledge on the role of myostatin on muscle function, we have to consider that our studies in rodents were performed using inbred laboratory mouse lines, notably on the C57BL6 background. I assume that voluntary motor activity is likely different between mice in captivity and in real wildtype mice, as is the free access to food. In fact, we have little information about what would be the consequence of hypermuscularity, leanness (loss of white body fat) and glycolytic phenotype in a real wildtype situation following loss of function of myostatin.

***Can an inbred mouse line really be considered being wildtype?***

My opinion is no, and this for the simple reason that mice have adapted to life in captivity for over 50 years, such as for the C57BL6 line. Such long-term inbreeding surely created a genetic adaptation to the captive environment. Indeed, a mutation in the *Tbc1d1* gene has been identified in the SJL mice line (lean Swiss Jim Lambert) that endows protection against obesity even with a calorie-rich diet because this mutation increases the use of lipids in the skeletal muscle (Chadt, Leicht et al. 2008). Thus, a mutation of the myostatin gene may be very disadvantageous in real wild life. This may be the reason that also in other species (cattle, sheep and dogs) spontaneous mutations are practically never found except in circumstances of selective breeding.

Having found that endurance exercise (swimming) ameliorated the force production of *Mstn*<sup>-/-</sup> mice, we here asked for the effect of other forms of exercise on the hypertrophic myostatin deficient muscle. In a yet unpublished work, we studied the effect of muscle overload, which is considered as a type of resistance training. Surprisingly, we found that the maximal force in *Mstn*<sup>-/-</sup> mice after overload was largely increased without further gain in muscle weight. This led to an enormous increase of the specific force (Figure 24). These results demonstrate the high plasticity inherent to skeletal muscle, which allows a rapid adaption in response to physiological stimuli.



There is still an ongoing debate about the cellular and molecular mechanisms that specify specific force, especially in the context of myostatin deficiency. I started to address this question and performed a transcriptome analysis following overload of *Mstn*<sup>-/-</sup> muscle. These results are not yet fully interpreted and verified, however, extracellular matrix adaption seems to play an overwhelming role in the regulation of muscle specific force. Other groups discussed a causative relation between nuclear domain and specific force production. It has been shown that the hypertrophic phenotype in the absence of myostatin resulted from an increase in the cytoplasmic volume without an increase in the number of myonuclei, thereby enlarging the nuclear domain ((Amthor, Otto et al. 2009); (Qaisar, Renaud et al. 2012); (Wang and McPherron 2012)). However, as we found (Figure 24) no difference in specific force between non-overloaded wildtype and *Mstn*<sup>-/-</sup> mice, we believe that other factors are responsible.

## 2. Myostatin and endurance capacity

We have demonstrated that larger muscles of *Mstn*<sup>-/-</sup> mice were associated with decreased endurance capacity.

### *Why are myostatin knockout mice more fatigable?*

In manuscript 2, *Mstn*<sup>-/-</sup> mice were analyzed in detail to determine their muscle function and metabolic phenotype. We found that maximal oxygen consumption (VO<sub>2max</sub>) was increased as compared to wildtype mice despite lower peak velocity. VO<sub>2max</sub>, if expressed per body weight, however, was reduced suggesting less oxygen consumption per unit of muscle tissue. On the other hand, oxygen consumption, the so-called “running economy”, was reduced, showing that larger muscles of *Mstn*<sup>-/-</sup> mice are energetically highly insufficient. In fact, the

absence of myostatin leads to an increased energy cost of muscle contraction (Giannesini, Vilmen et al. 2013).

In manuscript 1, we subjected wildtype and *mdx* mice to a treadmill exercise test and found that after treatment with sActRIIB-Fc, mice were no longer able to run the same distance as control mice. We observed a strong fatigability and pronounced exercise intolerance, notably in *mdx* mice. This suggests a relation between muscle mass and endurance capacity. Interestingly, cattle deficient in myostatin suffer from severe rhabdomyolysis and high lactate levels following exercise (Holmes, Ashmore et al. 1973).

***Does muscle hypertrophy decrease the ability for endurance exercise?***

It is common knowledge that the type of competitive sport is associated with different muscle mass phenotypes. Hence, long distance runners rather have a slim musculature as compared to the muscle hypertrophy of bodybuilders, weight lifters and sprinters. In fact, endurance exercise seems incompatible with muscle hypertrophy, such as our group has demonstrated for *Mstn*<sup>-/-</sup> mice that actually lost muscle mass after swim training (Matsakas, Macharia et al. 2012). Taken together our results suggest, that myostatin is a signaling molecule that optimizes skeletal muscle mass and force, energy metabolism and endurance capacity.

In the whippet dogs, it has been shown that myostatin deficiency improves racing performance. Mosher *et al.* observed that dogs heterozygous for the myostatin mutation are more muscular than wildtype dogs and are significantly faster during short distance racing competitions. One may assume that decreased myostatin levels in these dogs, similar as in mice or cattle, result in a conversion towards a more glycolytic phenotype that may be advantageous for short distance races. These results demonstrate for the first time that a mutation in the myostatin gene is linked to an increase of athletic performance (Mosher, Quignon et al. 2007). However, “bully” (=hypermuscular) homozygous *Mstn*<sup>-/-</sup> whippet dogs often suffer from muscle cramps. It should be noted here that muscle cramps could result from a metabolic dysfunction such as mitochondrial myopathy, however, this has never been analyzed in these animals. In 2004, Schuelke *et al.* described for the first time a human individual carrying a mutation in the myostatin gene. Interestingly, the mother of this little boy, who was heterozygous for this mutation, was a former high performance athlete (Schuelke, Wagner et al. 2004). Although, no other human case had been described so far, these findings may indicate, that reduced levels of myostatin may increase athletic short-term performance in humans.

### 3. Myostatin and muscle metabolism

#### *Does myostatin deficiency during development cause congenital changes of skeletal muscle metabolism?*

Studies of the *Mstn*<sup>-/-</sup> mouse model showed phenotype changes such as hypermuscularity (increase in size and number of fibers) (McPherron, Lawler et al. 1997) and a conversion of muscle fibers towards a more glycolytic phenotype ((Girgenrath, Song et al. 2005); (Hennebry, Berry et al. 2009)). This strongly suggests that the “metabolic signature” of the muscle has been prenatally defined during developmental stages because *Mstn*<sup>-/-</sup> animals are constitutive knockout mice. However, I am not aware of studies proving that gene or protein expression patterns changed towards a more glycolytic phenotype already at the prenatal or early postnatal stages. I would like to stress that muscle fibers first express developmental forms of myosin heavy chain (MHC), which is replaced in mice by adult forms only during early postnatal stages (Agbulut, Noirez et al. 2003). In this context it remains still unknown whether in *Mstn*<sup>-/-</sup> muscle precursors become determined towards a more glycolytic fate once they differentiate. Interestingly, blockade of the myostatin signaling pathway in adult mice by using either anti-myostatin antibodies, AAV-propeptide, or the soluble activin receptor type IIb, stimulated muscle growth **without** provoking changes in fiber type composition (Cadena, Tomkinson et al. 2010). These findings support the view that changes in the contractile muscle metabolic phenotype only occur following developmental abrogation of myostatin signaling as seen in constitutive *Mstn*<sup>-/-</sup> mice.

This over-simplification of the different roles of myostatin during prenatal and postnatal function eventually supported the rationale to develop therapeutic strategies based on myostatin blockade and their application to humans, because metabolic side effects were not expected. I consider these therapeutic trials, which were based solely on this assumption, as far too premature as insufficient preclinical work had been performed to clarify this point. I hypothesized that myostatin maintains its regulatory role on muscle metabolism through all developmental stages (including adulthood and muscle regeneration as in dystrophic *mdx* mice). This hypothesis forms the central rationale for my PhD-thesis and the herein presented results on the effect of myostatin/ActRIIB signaling in adult muscle.

Hence, metabolic features are not simply the consequence of developmental fiber type determination. I hypothesized that myostatin has a direct effect on muscle metabolism independently of its effects on muscle mass, contractile properties and fiber type composition.

A recent study on the gene expression profile of the skeletal muscle after a treatment with sActRIIB-Fc revealed changes in the expression of genes related to mitochondrial biogenesis and oxidative phosphorylation (Rahimov, King et al. 2011), which supports the above hypothesis. In fact, the gene expression profile in the sActRIIB-Fc treated mice was similar to that of *Mstn*<sup>-/-</sup> mice.

We first explored the PPAR signaling pathway, as PPAR transcription factors act as regulators of lipid metabolism and glucose homeostasis. In manuscript 1, I demonstrated that following treatment with sActRIIB-Fc, mRNA expression levels of *Pparδ* and other genes related to the PPAR signaling pathway were decreased, e.g. *Pgc1α* as a major factor of the regulation of mitochondrial biogenesis, and *Pdk4* as key protein in the regulation of glucose metabolism and fatty acids. This strongly suggests that the ActRIIB signaling pathway regulates the metabolism of skeletal muscle. However, these changes in gene regulation may appear secondary to other phenotype changes, considering that we treated mice for a period of 4 months. We hence turned our investigation to an *in vitro* system and treated C<sub>2</sub>C<sub>12</sub> cells with sActRIIB-Fc. Indeed, we again noted a decrease in the mRNA-expression of *Pparδ*, *Pgc1α*, *Cpt1b* and *Pdk4* already 24 hours following exposure to sActRIIB-Fc. This strongly indicates a direct effect of myostatin on the regulation of genes implicated in muscle metabolism.

***Can we conclude on the function of myostatin by performing solely loss of function experiments?***

Most studies to understand the role of myostatin used various strategies to inhibit myostatin signaling (anti-myostatin antibodies, AAV-propeptide, and sActRIIB-Fc). In my opinion, this is insufficient if we aim to determine the role of a given molecule, because alternative mechanisms or compensatory pathways may blunt or even distort the inhibitory effect. Therefore, it would be interesting to determine the effect of myostatin on skeletal muscle metabolism when overexpressing this molecule. Different strategies of myostatin overexpression could be considered, such as the use of ectopic AAV-mediated expression of myostatin or treatment with recombinant active myostatin. Studies of overexpression of myostatin have been conducted and showed a strong induction of muscle atrophy ((Zimmers, Davies et al. 2002); (Durieux, Amirouche et al. 2007)). We tried a similar experiment in our laboratory by engrafting myostatin expressing CHO cells into *Nude* mice. Unfortunately, the uncontrolled proliferation of CHO cells caused tumors to variable extent, and it was not possible to determine whether the cachexia was the result of overexpressing myostatin or ordinary tumor cachexia. Alternatively, I propose an experiment whereby to ectopically overexpress myostatin in the *Mstn*<sup>-/-</sup> mouse

as this would confirm whether the metabolic phenotype is fixed or whether the muscle metabolism could be reverted towards a more oxidative phenotype.

#### 4. Myostatin and mitochondria

Several studies revealed that myostatin deficiency is associated with a reduction in mitochondrial content in skeletal muscle fibers thus diminishing the mitochondrial oxidative capacity ((Amthor, Macharia et al. 2007), (Ploquin, Chabi et al. 2012)). However, the decrease of mitochondrial mass in *Mstn*<sup>-/-</sup> mice could be the simple consequence of their conversion towards glycolytic fiber phenotype. A reduction of mitochondrial content thus would cause a parallel reduction of mitochondrial respiration, which we (manuscript 2) and others have shown for *Mstn*<sup>-/-</sup> mice. Such decreased mitochondrial respiration is likely responsible for the observed decrease in VO<sub>2max</sub>/kg.

However, the constitutive *Mstn*<sup>-/-</sup> mouse model does not really answer the question whether the decrease of mitochondrial mass might be an indirect effect of the congenital myostatin deficiency or whether in fact myostatin regulates mitochondrial biogenesis throughout life, including the mature adult muscle. Welle *et al.* demonstrated that the post-developmental lack of myostatin does not reduce of the number of mitochondria markers, including expression of mitochondrial enzymes such as citrate synthase (CS) and cytochrome c oxidase (COX) and also the mRNA expression of some mitochondrial proteins (Personius, Jayaram et al. 2010).

In agreement, we demonstrate in manuscript 1 that treatment with sActRIIB-Fc does not influence mitochondrial mass. Indeed, there was no decrease in the copy number of mitochondrial DNA (mtDNA) following treatment with sActRIIB-Fc. **However, does mtDNA content mirrors the mitochondrial mass?** I consider yes: In a previous study on *Mstn*<sup>-/-</sup> mice it has been shown that the decrease of mtDNA correlated with the decrease in mitochondrial number as counted by electron microscopy. However, counting mitochondrial number using electron microscopy is a very unreliable method, as it is now being known that mitochondria are very dynamic organelles that build large networks and constantly fuse and split. In my opinion, other markers such the activity of CS or COX are more reliable references for the determination of mitochondria mass.

We showed that the activity of mitochondrial enzymes such as CS and the mtDNA quantification remained unchanged following treatment with sActRIIB-Fc. Thus myostatin unlikely controls mitochondrial biogenesis in the adult.

***Considering all these results, how can we explain the profound fatigability observed in mice after treatment with sActRIIB-Fc particularly in the mdx context?***

Remarkably,  $^{31}\text{P}$ -NMR spectroscopy on muscles following treatment with sActRIIB-Fc revealed a deficit of phosphocreatine resynthesize (pCr) in *mdx* mice (manuscript 1), indicating a deficit of the oxidative metabolism. **What could be the underlying mechanism?** We hypothesized a problem in the ATP transport from the mitochondria to the cytosol. This transport involves porin channels, which is a protein located in the outer membrane of mitochondria. Our hypothesis was based on a proteomic study that demonstrated a decreased expression of porin in *mdx* heart muscle (Lewis, Jockusch et al. 2010). Indeed, we found that the expression of porin was strongly reduced in wildtype as well as in *mdx* mice following treatment with sActRIIB-Fc (manuscript 1).

As I have already discussed above, the enzyme activity of COX and SDH was not decreased in the mice following the treatment with the sActRIIB-Fc. In fact, COX even was slightly elevated suggesting a the compensatory up-regulation of the OXPHOS complexes. However, measuring single OXPHOS complexes in isolation cannot rule out a deficit in the pathway of mitochondrial respiration for sure. We should repeat the same experiment and analyze the effect of sActRIIB-Fc on mitochondrial respiration and ATP production by polarographic methods. In this context, a recent transcriptome analysis, performed on muscles mice after treatment with sActRIIB-Fc, showed a decrease in the expression of genes related to mitochondrial biosynthesis and oxidative phosphorylation (Rahimov, King et al. 2011). This further supports the view that myostatin regulates muscle metabolism at adult stage.

Taken together, our results show that changes in mitochondrial composition (loss of porin) is likely responsible for the impairment of oxidative metabolism and ATP productin after abrogation of ActRIIB signaling. This could sufficiently explain the observed phenotype of *mdx* mice following sActRIIB-Fc treatment: exercise intolerance and lactic acidosis, both being typical signs of a mitochondrial myopathy.

***Are there additional factors that contribute to the exercise intolerance observed in the mdx mice following treatment with sActRIIB-Fc?***

We easily notice in our study (manuscript 1) that the mitochondrial mass is reduced in the control *mdx* mice as compared to the control *wildtype* mice. Based on this observation and the fact that the oxidative metabolism of muscle is decreased in the *mdx* mice, we can spposet that even mild additional stress can contribute to such exercise intolerance.

## 5. Myostatin and vascularization

Although a mitochondrial dysfunction is the likely cause of exercise intolerance following treatment with sActRIIB-Fc, we cannot exclude a more upstream mechanism such as insufficient oxygen supply of the skeletal muscle. Interestingly, skeletal muscle of myostatin deficient mice (*Mstn*<sup>-/-</sup> and *Cmpt*) demonstrates a decline in capillary density in comparison to normal mice ((Matsakas, Macharia et al. 2012); (Rehfeldt, Ott et al. 2005)). However, this had originally been interpreted as being a secondary event following a switch towards a more glycolytic fiber phenotype.

In manuscript 1, I observed a decrease in the number of capillaries per fiber in sActRIIB-Fc treated mice in parallel to a strong increase of fiber size, which caused an increase of the capillary domain. Further, the decrease in capillary number per fibers was far more severe in sActRIIB-Fc treated *mdx* mice than wildtype mice. I thus assume that ActRIIB signaling is pivotal for the capillary growth during the remodeling of the dystrophic *mdx* muscle. In this respect it is quite interesting that VEGF mRNA-expression was already reduced in *mdx* mice as compared to wildtype mice and did not drop further after sActRIIB-Fc treatment. My data strongly suggest that the reduction in the number of capillaries contributes to the phenotypic alteration of skeletal muscle that further aggravates the secondary metabolic myopathy, especially in *mdx* mice. However, blockade of myostatin by sActRIIB-Fc may not be the only cause of the observed phenotype, since sActRIIB-Fc binds multiple members of the TGFβ family such as GDF11, BMP9, BMP10 and activin ((McPherron 2010); (Lee, Reed et al. 2005); (Lee, Lee et al. 2010); (Souza, Chen et al. 2008)). Notably, BMP9 and BMP10 are important factors that regulate the proliferation and differentiation of endothelial cells (lit). However, the respective role of different ActRIIB receptor ligands following treatment with sActRIIB-Fc on the endothelial cells remains to be determined.

***Does myostatin/ActRIIB signaling directly affects endothelial cells or is this an indirect effect via VEGF regulation.***

Here we showed that endothelial cells strongly express activin type 1 and type 2 receptors, whereas myostatin was only little expressed. This suggests that myostatin acts on endothelial cells in a paracrine or endocrine fashion but not in an autocrine manner. To further approach this question, we treated HUVEC endothelial cells with increasing doses of recombinant myostatin and showed an increase in the cell doubling time *in vitro*. These results strongly suggest that myostatin or homologs may regulate the growth of muscle capillaries in a direct fashion.

It is therefore important to take into consideration the effect of myostatin on muscle vascularization when developing therapeutic strategies based on myostatin blockade.

To have a more global view on the transcriptional changes following treatment with sActRIIB-Fc, we performed a transcriptome analysis. These data have not yet completely been interpreted and are not included in my thesis. Interestingly, *Nos1* expression was the most differentially expressed gene between treated and untreated *mdx* mice and was largely downregulated. I took these results further and performed quantitative real time PCR (RT-qPCR) and found that *Nos1* expression was strongly reduced in control *mdx* mice as compared to control wildtype mice, which confirmed previous studies ((Brenman, Chao et al. 1995); (Chang, Iannaccone et al. 1996)). However, expression levels dropped further after sActRIIB-Fc treatment in wildtype as well as in *mdx* mice. This reduction may contribute to the dysregulation of NO-synthesis, as NO is required for exercise induced vasodilatation as well as for the cellular calcium homeostasis associated with exacerbated post-exercise fatigability. However, protein analysis (Western blot and immunostaining) did not reveal any changes in *Nos1* levels in wildtype mice, while *Nos1* in *mdx* mice was below the detection levels. We therefore failed to validate the transcriptome results at protein level. Thus *Nos1* could be responsible for the observed exercise intolerance following the treatment with sActRIIB-Fc.

In Duchenne muscular dystrophy and its *mdx* mouse model, oxidative metabolism is compromised due to membrane damage ((Jongpiputvanich, Sueblinvong et al. 2005); (Kuznetsov, Winkler et al. 1998)). Therefore, clinical studies are currently ongoing for Duchenne patients in order to improve the oxidative metabolism of their muscles using Idebenone (NCT01027884, ClinicalTrials.gov) or Citrulline (NCT01995032, ClinicalTrials.gov). Another clinical trial in Becker patients is using the Sildenafil to resolve the problem of vascular dysregulation in order to improve muscle perfusion (NCT01350154, ClinicalTrials.gov).

## 6. Myostatin and heart muscle

The likely role of myostatin on heart muscle regulation has also to be taken into account when analyzing the effect of myostatin/ActRIIB blockade. Unfortunately, in our study we did not analyze the heart of the mice (manuscript 1). Indeed, it might be possible that our mice had developed a cardiomyopathy following treatment with sActRIIB-Fc, which could be alternatively responsible for observed fatigability during endurance exercise.

It has already been shown that cardiac cells or cardiomyocytes synthesize myostatin (Rodgers, Interlichia et al. 2009). This cardiac myostatin not only had an autocrine effect on cardiac striated muscle, moreover overexpression of this protein induced a pronounced atrophy of the heart (Heineke, Auger-Messier et al. 2010). Heart myostatin had also an endocrine effect on skeletal muscle and induced skeletal muscle atrophy (Heineke, Auger-Messier et al. 2010). Conversely, overexpression of myostatin in skeletal muscle did not induce any effect on the heart muscle (Artaza, Reisz-Porszasz et al. 2007).

The *Mstn*<sup>-/-</sup> mice showed a cardiac hypertrophy (Rodgers, Interlichia et al. 2009). This was discussed as a physiological adaptive response to the hypermuscular phenotype induced by myostatin deficiency, rather than a pathological response. In a different study, no cardiac phenotype was observed on *Mstn*<sup>-/-</sup> mice (Cohn, Liang et al. 2007). Similarly, a 4-months treatment with sActRIIB-Fc did not affect the cardiac function of young *mdx* mice (Morine, Bish et al. 2010)a. However, another study showed clear signs of increased cardiac dilation in *mdx* mice after long-term treatment over 11 months via AAV-mediated overexpression of a secreted dominant negative myostatin propeptide (Morine, Bish et al. 2010)b.

Taken together, there is a potential risk to aggravate the cardiomyopathy in DMD patients after a long-term treatment. This must also be taken into account when considering myostatin blockade as therapeutic strategy and further investigations are necessary into this direction.

## 7. Myostatin blockade as a therapeutic strategy

In Duchenne muscular dystrophy, skeletal muscle undergoes cycles of degeneration and regeneration, and in consequence, serum creatine kinase is largely increased. Blockade of myostatin has been proposed as a therapeutic approach for Duchenne muscular dystrophy. Importantly, such strategy does not treat the underlying cause of DMD, the absence of dystrophin. The rationale of using myostatin blockade as a therapeutic strategy is based on the idea that myostatin blockade could improve skeletal muscle either by stimulating regeneration or by increasing muscle fiber size and therefore delay or even reverse muscle wasting. Interestingly, some studies have shown that myostatin blockade decreased the level of serum creatine kinase (Bogdanovich, Krag et al. 2002), which was interpreted as an amelioration of the dystrophic phenotype. Partridge *et al.* discussed that the dystrophin-deficient muscle may become more resistant to degeneration if fibers are increased in size, and this may slow down the progression of the disease pathophysiology (Zammit and Partridge 2002). However, other studies did not find a significant decrease in creatine kinase level and there is until now no experi-

mental evidence that larger muscle fiber would be more damage resistant (Wagner, McPherron et al. 2002). One should rather ask whether a strategy, which stimulates the growth of diseased muscle, would convey any therapeutic benefit if used on its own.

Different studies conducted in the *mdx* mouse model have shown the benefit for dystrophic muscle if using myostatin inhibition ((Bogdanovich, Krag et al. 2002); (Morine, Bish et al. 2010); (Pistilli, Bogdanovich et al. 2011); (George Carlson, Bruemmer et al. 2011)). Such promising results formed the rationale to consider clinical phase I/II trials with muscular dystrophy patients. Indeed, Wagner *et al.* showed that the use of anti-myostatin antibodies was tolerated in patients (Wagner, Fleckenstein et al. 2008). However, in most studies conducted in patients, the increase of muscle size was taken as an endpoint. Assuming the fact that big muscles are healthier muscles. None of the studies investigated endurance capacity, which evaluates the effect of a treatment on the physiology of the entire body over a longer time period and would thus be a relevant parameter that could translate into improvement of life quality for patients.

We here treated mice for a period of 4 months, which would be quite a short period for DMD patients, who would require a treatment for many years. In the light of my data, however, this carries a significant risk of developing secondary unwanted effects at the metabolic level. Furthermore, in mice, the large gain in muscle mass due to systemic treatment did not improve the skeletal muscle function. To prevent metabolic adverse effects, I therefore propose a different approach. The first approach would be to determine, which would be the smallest dose of the soluble receptor required to bring benefit on muscle mass without changing muscle metabolism. Another approach would be a pulse therapy for short periods, thus avoiding possible side effects of a continuous application. Such pulse therapy could be considered for many types of muscle atrophy, such as post surgery, cancer induced, cachexia or sarcopenia.

One may also consider to prevent metabolic side effects of myostatin blockade by pharmacological treatment that stimulates oxidative metabolism, e.g. by PPAR $\delta$  agonists. These molecules are known to reduce the oxidative stress and to promote fatty acids oxidation in moderately obese men (Riserus, Sprecher et al. 2008). AMPK agonists (AICAR) also stimulate the fatty acid oxidation in type 2 diabetic patients (Boon, Bosselaar et al. 2008). Clinical trials have already been conducted and showed an increase of fatty acids oxidation. Indeed, Narkar *et al.* have shown that 4-weeks treatment of mice with AICAR (5-aminoimidazole-4-carboxamide-1- $\beta$ -D-ribose) improved endurance and activated genes of the oxidative metabolism (Narkar, Downes et al. 2008). Another study by Bernardo *et al.* showed that the

use of PPAR $\delta$  agonists improved the oxidative properties of muscle with and without the inhibition of myostatin (Bernardo, Wachtmann et al. 2010). Until now, there is still no specific molecule to selectively activate the PGC1 $\alpha$  signaling pathway. It has already been shown that an increase of PGC1 $\alpha$  in aging mice prevented atrophy and preserved the mitochondrial function (Wenz, Rossi et al. 2009). It would also be interesting to cross PGC1 $\alpha$  overexpressing mice with *Mstn*<sup>-/-</sup> mice to see whether this would improve their oxidative metabolism. Interestingly, Hollinger *et al.* overexpressed PGC1 $\alpha$  in *mdx* mice and observed an improvement of muscle function that was accompanied by an increase of markers for oxidative capacity (Hollinger, Gardan-Salmon et al. 2013). Taken together these different observations, I believe that using such therapies in combination could potentiate the benefits on muscle metabolism and prevent the downsides of isolated myostatin inhibition.

Furthermore, the use of sActRIIB-Fc alone, which is a systemic treatment, interferes with the TGF- $\beta$  signaling pathway in muscle and in other cell types and tissues. A phase II clinical trial in DMD patients using the soluble ActRIIB (ACE-031) was stopped prematurely because of the occurrence of side effects (minor nosebleeds and small dilated blood vessels) (NCT01099761, ClinicalTrials.gov). This did not come as surprise to us as we have shown in manuscript 1, that ActRIIB signaling has an influence on capillary density. So far no compound is known that would only abrogate ActRIIB signaling in the muscle and not in neighboring tissues, which could be used as a potentially safer therapeutic strategy. Interfering with the ligands at the extracellular level will always result in off-target effects. It would thus be better to interfere with the intracellular signalling cascade. For this, the molecular mechanism of the muscle growth signaling pathway has to be determined in more detail.

### ***What are the molecular targets of myostatin signaling?***

We do not know yet the immediate molecular targets of myostatin signaling that have an influence on muscle metabolism. Interestingly, a recent study identified a critical role for the bone morphogenetic protein (BMP) pathway in muscle mass regulation (Sartori, Schirwis et al. 2013). The authors showed that BMP signaling is the fundamental hypertrophic signal in mice. Inhibition of BMP signaling caused muscle atrophy and abolished the hypertrophic phenotype of myostatin deficient mice ((Sartori, Schirwis et al. 2013; Winbanks, Chen et al. 2013)). Following these results I hypothesize that the regulation of muscle mass and metabolism of the skeletal muscle may use specific PhosphoSmads: Smad 1/5/8 (BMP signaling) regulating muscle mass and Smad 2/3 (myostatin pathway) regulating muscle metabolism.

It would be very interesting to consider, (i) a combined approach of restoration of dystrophin expression by RNA splicing modulation and (ii) myostatin blockade, as a treatment for DMD patients. In manuscript 3, we have successfully demonstrated the benefits of the restoration of dystrophin in muscle function coupled to the advantage of myostatin inhibition on muscle growth. Unfortunately, the synergistic effect of the two therapies was not very obvious as muscles did not become stronger. It would be very interesting to study metabolic properties in mice that had been treated with a combination of both approaches.

In the light of my results, I cannot recommend the use of myostatin/ActRIIB interference as a therapeutic strategy for Duchenne muscular dystrophy, at least in isolation, because side effects of the treatment may even aggravate the disease.



# **BIBLIOGRAPHY**

- Aartsma-Rus, A., I. Fokkema, et al. (2009). "Theoretic applicability of antisense-mediated exon skipping for Duchenne muscular dystrophy mutations." *Hum Mutat* **30**(3): 293-299.
- Abbs, S. and M. Bobrow (1992). "Analysis of quantitative PCR for the diagnosis of deletion and duplication carriers in the dystrophin gene." *J Med Genet* **29**(3): 191-196.
- Agbulut, O., P. Noirez, et al. (2003). "Myosin heavy chain isoforms in postnatal muscle development of mice." *Biol Cell* **95**(6): 399-406.
- Agbulut, O., A. Vignaud, et al. (2009). "Slow myosin heavy chain expression in the absence of muscle activity." *Am J Physiol Cell Physiol* **296**(1): C205-214.
- Akpan, I., M. D. Goncalves, et al. (2009). "The effects of a soluble activin type IIB receptor on obesity and insulin sensitivity." *Int J Obes (Lond)* **33**(11): 1265-1273.
- Allen, D. L., R. R. Roy, et al. (1999). "Myonuclear domains in muscle adaptation and disease." *Muscle Nerve* **22**(10): 1350-1360.
- Alter, J., F. Lou, et al. (2006). "Systemic delivery of morpholino oligonucleotide restores dystrophin expression bodywide and improves dystrophic pathology." *Nat Med* **12**(2): 175-177.
- Alzghoul, M. B., D. Gerrard, et al. (2004). "Ectopic expression of IGF-I and Shh by skeletal muscle inhibits disuse-mediated skeletal muscle atrophy and bone osteopenia in vivo." *FASEB J* **18**(1): 221-223.
- Amthor, H., R. Huang, et al. (2002). "The regulation and action of myostatin as a negative regulator of muscle development during avian embryogenesis." *Dev Biol* **251**(2): 241-257.
- Amthor, H., R. Macharia, et al. (2007). "Lack of myostatin results in excessive muscle growth but impaired force generation." *Proc Natl Acad Sci U S A* **104**(6): 1835-1840.
- Amthor, H., G. Nicholas, et al. (2004). "Follistatin complexes Myostatin and antagonises Myostatin-mediated inhibition of myogenesis." *Dev Biol* **270**(1): 19-30.
- Amthor, H., A. Otto, et al. (2009). "Muscle hypertrophy driven by myostatin blockade does not require stem/precursor-cell activity." *Proc Natl Acad Sci U S A* **106**(18): 7479-7484.
- Anderson, J. E. (1998). "Murray L. Barr Award Lecture. Studies of the dynamics of skeletal muscle regeneration: the mouse came back!" *Biochem Cell Biol* **76**(1): 13-26.
- Anderson, J. E. (2006). "The satellite cell as a companion in skeletal muscle plasticity: currency, conveyance, clue, connector and colander." *J Exp Biol* **209**(Pt 12): 2276-2292.
- Artaza, J. N., S. Reisz-Porszasz, et al. (2007). "Alterations in myostatin expression are associated with changes in cardiac left ventricular mass but not ejection fraction in the mouse." *J Endocrinol* **194**(1): 63-76.
- Athea, Y., B. Viollet, et al. (2007). "AMP-activated protein kinase alpha2 deficiency affects cardiac cardiolipin homeostasis and mitochondrial function." *Diabetes* **56**(3): 786-794.
- Bahi, L., N. Koulmann, et al. (2004). "Does ACE inhibition enhance endurance performance and muscle energy metabolism in rats?" *J Appl Physiol (1985)* **96**(1): 59-64.
- Baligand, C., H. Gilson, et al. (2010). "Functional assessment of skeletal muscle in intact mice lacking myostatin by concurrent NMR imaging and spectroscopy." *Gene Ther* **17**(3): 328-337.
- Bartholin, L., V. Maguer-Satta, et al. (2002). "Transcription activation of FLRG and follistatin by activin A, through Smad proteins, participates in a negative feedback loop to modulate activin A function." *Oncogene* **21**(14): 2227-2235.
- Barton, E. R., L. Morris, et al. (2002). "Muscle-specific expression of insulin-like growth factor I counters muscle decline in mdx mice." *J Cell Biol* **157**(1): 137-148.
- Bernardo, B. L., T. S. Wachtmann, et al. (2010). "Postnatal PPARdelta activation and myostatin inhibition exert distinct yet complimentary effects on the metabolic profile of obese insulin-resistant mice." *PLoS One* **5**(6): e11307.

- Bhat, H. F., M. E. Adams, et al. (2013). "Syntrophin proteins as Santa Claus: role(s) in cell signal transduction." Cell Mol Life Sci **70**(14): 2533-2554.
- Billat, V. L., E. Mouisel, et al. (2005). "Inter- and intrastrain variation in mouse critical running speed." J Appl Physiol **98**(4): 1258-1263.
- Bish, L. T., M. M. Sleeper, et al. (2011). "Long-term systemic myostatin inhibition via liver-targeted gene transfer in golden retriever muscular dystrophy." Hum Gene Ther **22**(12): 1499-1509.
- Blake, D. J., D. R. Love, et al. (1992). "Characterization of a 4.8kb transcript from the Duchenne muscular dystrophy locus expressed in Schwannoma cells." Hum Mol Genet **1**(2): 103-109.
- Blake, D. J., A. Weir, et al. (2002). "Function and genetics of dystrophin and dystrophin-related proteins in muscle." Physiol Rev **82**(2): 291-329.
- Blau, H. M., J. Dhawan, et al. (1993). "Myoblasts in pattern formation and gene therapy." Trends Genet **9**(8): 269-274.
- Bodine, S. C., E. Latres, et al. (2001). "Identification of ubiquitin ligases required for skeletal muscle atrophy." Science **294**(5547): 1704-1708.
- Bogdanovich, S., T. O. Krag, et al. (2002). "Functional improvement of dystrophic muscle by myostatin blockade." Nature **420**(6914): 418-421.
- Bogdanovich, S., E. M. McNally, et al. (2008). "Myostatin blockade improves function but not histopathology in a murine model of limb-girdle muscular dystrophy 2C." Muscle Nerve **37**(3): 308-316.
- Bogdanovich, S., K. J. Perkins, et al. (2005). "Myostatin propeptide-mediated amelioration of dystrophic pathophysiology." FASEB J **19**(6): 543-549.
- Bonilla, E., C. E. Samitt, et al. (1988). "Duchenne muscular dystrophy: deficiency of dystrophin at the muscle cell surface." Cell **54**(4): 447-452.
- Boon, H., M. Bosselaar, et al. (2008). "Intravenous AICAR administration reduces hepatic glucose output and inhibits whole body lipolysis in type 2 diabetic patients." Diabetologia **51**(10): 1893-1900.
- Boyce, F. M., A. H. Beggs, et al. (1991). "Dystrophin is transcribed in brain from a distant upstream promoter." Proc Natl Acad Sci U S A **88**(4): 1276-1280.
- Brdiczka, D., P. Kaldis, et al. (1994). "In vitro complex formation between the octamer of mitochondrial creatine kinase and porin." J Biol Chem **269**(44): 27640-27644.
- Brenman, J. E., D. S. Chao, et al. (1995). "Nitric oxide synthase complexed with dystrophin and absent from skeletal muscle sarcolemma in Duchenne muscular dystrophy." Cell **82**(5): 743-752.
- Brooke, M. H. and K. K. Kaiser (1970). "Muscle fiber types: how many and what kind?" Arch Neurol **23**(4): 369-379.
- Bulfield, G., W. G. Siller, et al. (1984). "X chromosome-linked muscular dystrophy (mdx) in the mouse." Proc Natl Acad Sci U S A **81**(4): 1189-1192.
- Burrow, K. L., D. D. Covert, et al. (1991). "Dystrophin expression and somatic reversion in prednisone-treated and untreated Duchenne dystrophy. CIDD Study Group." Neurology **41**(5): 661-666.
- Butler-Browne, G. S. and R. G. Whalen (1984). "Myosin isozyme transitions occurring during the postnatal development of the rat soleus muscle." Dev Biol **102**(2): 324-334.
- Byers, T. J., H. G. Lidov, et al. (1993). "An alternative dystrophin transcript specific to peripheral nerve." Nat Genet **4**(1): 77-81.
- Cadena, S. M., K. N. Tomkinson, et al. (2010). "Administration of a soluble activin type IIB receptor promotes skeletal muscle growth independent of fiber type." J Appl Physiol **109**(3): 635-642.

- Cai, D., J. D. Frantz, et al. (2004). "IKKbeta/NF-kappaB activation causes severe muscle wasting in mice." Cell **119**(2): 285-298.
- Campion, D. R. (1984). "The muscle satellite cell: a review." Int Rev Cytol **87**: 225-251.
- Carlson, C. J., F. W. Booth, et al. (1999). "Skeletal muscle myostatin mRNA expression is fiber-type specific and increases during hindlimb unloading." Am J Physiol **277**(2 Pt 2): R601-606.
- Cash, J. N., E. B. Angerman, et al. (2012). "Structure of myostatin.follistatin-like 3: N-terminal domains of follistatin-type molecules exhibit alternate modes of binding." J Biol Chem **287**(2): 1043-1053.
- Cassens, R. G. and C. C. Cooper (1971). "Red and white muscle." Adv Food Res **19**: 1-74.
- Chadt, A., K. Leicht, et al. (2008). "Tbc1d1 mutation in lean mouse strain confers leanness and protects from diet-induced obesity." Nat Genet **40**(11): 1354-1359.
- Chamberlain, J. S., R. A. Gibbs, et al. (1988). "Deletion screening of the Duchenne muscular dystrophy locus via multiplex DNA amplification." Nucleic Acids Res **16**(23): 11141-11156.
- Chang, W. J., S. T. Iannaccone, et al. (1996). "Neuronal nitric oxide synthase and dystrophin-deficient muscular dystrophy." Proc Natl Acad Sci U S A **93**(17): 9142-9147.
- Chelly, J., G. Hamard, et al. (1990). "Dystrophin gene transcribed from different promoters in neuronal and glial cells." Nature **344**(6261): 64-65.
- Childs, T. E., E. E. Spangenburg, et al. (2003). "Temporal alterations in protein signaling cascades during recovery from muscle atrophy." Am J Physiol Cell Physiol **285**(2): C391-398.
- Clerk, A., G. E. Morris, et al. (1993). "Dystrophin-related protein, utrophin, in normal and dystrophic human fetal skeletal muscle." Histochem J **25**(8): 554-561.
- Clop, A., F. Marcq, et al. (2006). "A mutation creating a potential illegitimate microRNA target site in the myostatin gene affects muscularity in sheep." Nat Genet **38**(7): 813-818.
- Cohn, R. D., H. Y. Liang, et al. (2007). "Myostatin does not regulate cardiac hypertrophy or fibrosis." Neuromuscul Disord **17**(4): 290-296.
- Coleman, M. E., F. DeMayo, et al. (1995). "Myogenic vector expression of insulin-like growth factor I stimulates muscle cell differentiation and myofiber hypertrophy in transgenic mice." J Biol Chem **270**(20): 12109-12116.
- Constantin-Teodosiu, D., D. J. Baker, et al. (2009). "PPARdelta agonism inhibits skeletal muscle PDC activity, mitochondrial ATP production and force generation during prolonged contraction." J Physiol **587**(Pt 1): 231-239.
- Cornelison, D. D. and B. J. Wold (1997). "Single-cell analysis of regulatory gene expression in quiescent and activated mouse skeletal muscle satellite cells." Dev Biol **191**(2): 270-283.
- D'Souza, V. N., T. M. Nguyen, et al. (1995). "A novel dystrophin isoform is required for normal retinal electrophysiology." Hum Mol Genet **4**(5): 837-842.
- Darnell, J. E., H. F. Lodish, et al. (1990). Molecular cell biology. New York, Scientific American Books : Distributed by W.H. Freeman.
- David, L., C. Mallet, et al. (2008). "Bone morphogenetic protein-9 is a circulating vascular quiescence factor." Circ Res **102**(8): 914-922.
- David, L., C. Mallet, et al. (2007). "Identification of BMP9 and BMP10 as functional activators of the orphan activin receptor-like kinase 1 (ALK1) in endothelial cells." Blood **109**(5): 1953-1961.
- Davies, K. E. and K. J. Nowak (2006). "Molecular mechanisms of muscular dystrophies: old and new players." Nat Rev Mol Cell Biol **7**(10): 762-773.
- Degenhardt, T., A. Saramaki, et al. (2007). "Three members of the human pyruvate dehydrogenase kinase gene family are direct targets of the peroxisome proliferator-activated receptor beta/delta." J Mol Biol **372**(2): 341-355.

- Deveaux, V., B. Picard, et al. (2003). "Location of myostatin expression during bovine myogenesis in vivo and in vitro." Reprod Nutr Dev **43**(6): 527-542.
- Dressel, U., T. L. Allen, et al. (2003). "The peroxisome proliferator-activated receptor beta/delta agonist, GW501516, regulates the expression of genes involved in lipid catabolism and energy uncoupling in skeletal muscle cells." Mol Endocrinol **17**(12): 2477-2493.
- Dumonceaux, J., S. Marie, et al. (2010). "Combination of myostatin pathway interference and dystrophin rescue enhances tetanic and specific force in dystrophic mdx mice." Mol Ther **18**(5): 881-887.
- Durieux, A. C., A. Amirouche, et al. (2007). "Ectopic expression of myostatin induces atrophy of adult skeletal muscle by decreasing muscle gene expression." Endocrinology **148**(7): 3140-3147.
- Duris, M. P., G. Renand, et al. (1999). "Genetic variability of foetal bovine myoblasts in primary culture." Histochem J **31**(12): 753-760.
- Emery, A. E. (1993). "Duchenne muscular dystrophy--Meryon's disease." Neuromuscul Disord **3**(4): 263-266.
- Emery, A. E. H. (1993). Duchenne muscular dystrophy. Oxford ; New York, Oxford University Press.
- Engel, N. A., J. R. Rodrigue, et al. (1994). "Parent-child agreement on ratings of anxiety in children." Psychol Rep **75**(3 Pt 1): 1251-1260.
- England, S. B., L. V. Nicholson, et al. (1990). "Very mild muscular dystrophy associated with the deletion of 46% of dystrophin." Nature **343**(6254): 180-182.
- Eymard, B., N. B. Romero, et al. (1997). "Primary adhalinopathy (alpha-sarcoglycanopathy): clinical, pathologic, and genetic correlation in 20 patients with autosomal recessive muscular dystrophy." Neurology **48**(5): 1227-1234.
- Fanin, M., G. A. Danieli, et al. (1995). "Dystrophin-positive fibers in Duchenne dystrophy: origin and correlation to clinical course." Muscle Nerve **18**(10): 1115-1120.
- Feener, C. A., M. Koenig, et al. (1989). "Alternative splicing of human dystrophin mRNA generates isoforms at the carboxy terminus." Nature **338**(6215): 509-511.
- Ferreira, R., M. J. Neuparth, et al. (2008). "Evidences of apoptosis during the early phases of soleus muscle atrophy in hindlimb suspended mice." Physiol Res **57**(4): 601-611.
- Fisher, R., J. M. Tinsley, et al. (2001). "Non-toxic ubiquitous over-expression of utrophin in the mdx mouse." Neuromuscul Disord **11**(8): 713-721.
- Forbes, D., M. Jackman, et al. (2006). "Myostatin auto-regulates its expression by feedback loop through Smad7 dependent mechanism." J Cell Physiol **206**(1): 264-272.
- Francke, U., H. D. Ochs, et al. (1985). "Minor Xp21 chromosome deletion in a male associated with expression of Duchenne muscular dystrophy, chronic granulomatous disease, retinitis pigmentosa, and McLeod syndrome." Am J Hum Genet **37**(2): 250-267.
- Furukawa-Hibi, Y., K. Yoshida-Araki, et al. (2002). "FOXO forkhead transcription factors induce G(2)-M checkpoint in response to oxidative stress." J Biol Chem **277**(30): 26729-26732.
- Furuyama, T., K. Kitayama, et al. (2003). "Forkhead transcription factor FOXO1 (FKHR)-dependent induction of PDK4 gene expression in skeletal muscle during energy deprivation." Biochem J **375**(Pt 2): 365-371.
- Gagniere, H., B. Picard, et al. (1999). "Contractile differentiation of foetal cattle muscles: intermuscular variability." Reprod Nutr Dev **39**(5-6): 637-655.
- Gagniere, H., B. Picard, et al. (1999). "Comparison of foetal metabolic differentiation in three cattle muscles." Reprod Nutr Dev **39**(1): 105-112.
- George Carlson, C., K. Bruemmer, et al. (2011). "Soluble activin receptor type IIB increases forward pulling tension in the mdx mouse." Muscle Nerve **43**(5): 694-699.

- Giannesini, B., C. Vilmen, et al. (2013). "Lack of myostatin impairs mechanical performance and ATP cost of contraction in exercising mouse gastrocnemius muscle in vivo." Am J Physiol Endocrinol Metab.
- Giannesini, B., C. Vilmen, et al. (2013). "Lack of myostatin impairs mechanical performance and ATP cost of contraction in exercising mouse gastrocnemius muscle in vivo." Am J Physiol Endocrinol Metab **305**(1): E33-40.
- Girgenrath, S., K. Song, et al. (2005). "Loss of myostatin expression alters fiber-type distribution and expression of myosin heavy chain isoforms in slow- and fast-type skeletal muscle." Muscle Nerve **31**(1): 34-40.
- Gomes, M. D., S. H. Lecker, et al. (2001). "Atrogin-1, a muscle-specific F-box protein highly expressed during muscle atrophy." Proc Natl Acad Sci U S A **98**(25): 14440-14445.
- Goncalves, M. A., G. P. van Nierop, et al. (2005). "Transfer of the full-length dystrophin-coding sequence into muscle cells by a dual high-capacity hybrid viral vector with site-specific integration ability." J Virol **79**(5): 3146-3162.
- Gonin, P., L. Arandel, et al. (2005). "Femoral intra-arterial injection: a tool to deliver and assess recombinant AAV constructs in rodents whole hind limb." J Gene Med **7**(6): 782-791.
- Gonzalez-Cadavid, N. F., W. E. Taylor, et al. (1998). "Organization of the human myostatin gene and expression in healthy men and HIV-infected men with muscle wasting." Proc Natl Acad Sci U S A **95**(25): 14938-14943.
- Gorecki, D. C., A. P. Monaco, et al. (1992). "Expression of four alternative dystrophin transcripts in brain regions regulated by different promoters." Hum Mol Genet **1**(7): 505-510.
- Gorza, L. (1990). "Identification of a novel type 2 fiber population in mammalian skeletal muscle by combined use of histochemical myosin ATPase and anti-myosin monoclonal antibodies." J Histochem Cytochem **38**(2): 257-265.
- Grobet, L., L. J. Martin, et al. (1997). "A deletion in the bovine myostatin gene causes the double-muscling phenotype in cattle." Nat Genet **17**(1): 71-74.
- Grobet, L., D. Pirottin, et al. (2003). "Modulating skeletal muscle mass by postnatal, muscle-specific inactivation of the myostatin gene." Genesis **35**(4): 227-238.
- Grounds, M. D. (1999). "Muscle regeneration: molecular aspects and therapeutic implications." Curr Opin Neurol **12**(5): 535-543.
- Guo, T., W. Jou, et al. (2009). "Myostatin inhibition in muscle, but not adipose tissue, decreases fat mass and improves insulin sensitivity." PLoS One **4**(3): e4937.
- Gussoni, E., G. K. Pavlath, et al. (1992). "Normal dystrophin transcripts detected in Duchenne muscular dystrophy patients after myoblast transplantation." Nature **356**(6368): 435-438.
- Hack, A. A., M. E. Groh, et al. (2000). "Sarcoglycans in muscular dystrophy." Microsc Res Tech **48**(3-4): 167-180.
- Haidet, A. M., L. Rizo, et al. (2008). "Long-term enhancement of skeletal muscle mass and strength by single gene administration of myostatin inhibitors." Proc Natl Acad Sci U S A **105**(11): 4318-4322.
- Hammonds, R. G., Jr. (1987). "Protein sequence of DMD gene is related to actin-binding domain of alpha-actinin." Cell **51**(1): 1.
- Heineke, J., M. Auger-Messier, et al. (2010). "Genetic deletion of myostatin from the heart prevents skeletal muscle atrophy in heart failure." Circulation **121**(3): 419-425.
- Hennebry, A., C. Berry, et al. (2009). "Myostatin regulates fiber-type composition of skeletal muscle by regulating MEF2 and MyoD gene expression." Am J Physiol Cell Physiol **296**(3): C525-534.

- Herzog, R. W., E. Y. Yang, et al. (1999). "Long-term correction of canine hemophilia B by gene transfer of blood coagulation factor IX mediated by adeno-associated viral vector." Nat Med **5**(1): 56-63.
- Hilder, T. L., J. C. Tou, et al. (2003). "Phosphorylation of insulin receptor substrate-1 serine 307 correlates with JNK activity in atrophic skeletal muscle." FEBS Lett **553**(1-2): 63-67.
- Hill, E. W., J. Gu, et al. (2010). "A sequence polymorphism in MSTN predicts sprinting ability and racing stamina in thoroughbred horses." PLoS One **5**(1): e8645.
- Hill, J. J., M. V. Davies, et al. (2002). "The myostatin propeptide and the follistatin-related gene are inhibitory binding proteins of myostatin in normal serum." J Biol Chem **277**(43): 40735-40741.
- Hill, J. J., Y. Qiu, et al. (2003). "Regulation of myostatin in vivo by growth and differentiation factor-associated serum protein-1: a novel protein with protease inhibitor and follistatin domains." Mol Endocrinol **17**(6): 1144-1154.
- Hoffman, E. P., A. P. Monaco, et al. (1987). "Conservation of the Duchenne muscular dystrophy gene in mice and humans." Science **238**(4825): 347-350.
- Hoffman, E. P., J. E. Morgan, et al. (1990). "Somatic reversion/suppression of the mouse mdx phenotype in vivo." J Neurol Sci **99**(1): 9-25.
- Hollinger, K., D. Gardan-Salmon, et al. (2013). "Rescue of dystrophic skeletal muscle by PGC-1alpha involves restored expression of dystrophin-associated protein complex components and satellite cell signaling." Am J Physiol Regul Integr Comp Physiol **305**(1): R13-23.
- Holmes, J. H., C. R. Ashmore, et al. (1973). "Effects of stress on cattle with hereditary muscular hypertrophy." J Anim Sci **36**(4): 684-694.
- Holmes, J. H., D. W. Robinson, et al. (1972). "Blood lactic acid and behaviour in cattle with hereditary muscular hypertrophy." J Anim Sci **35**(5): 1011-1013.
- Holzbaur, E. L., D. S. Howland, et al. (2006). "Myostatin inhibition slows muscle atrophy in rodent models of amyotrophic lateral sclerosis." Neurobiol Dis **23**(3): 697-707.
- Hourde, C., A. Vignaud, et al. (2006). "Sustained peripheral arterial insufficiency durably impairs normal and regenerating skeletal muscle function." J Physiol Sci **56**(5): 361-367.
- Howard, P. L., G. Y. Dally, et al. (1999). "Dystrophin isoforms DP71 and DP427 have distinct roles in myogenic cells." Muscle Nerve **22**(1): 16-27.
- Huang, Z., D. Chen, et al. (2007). "Regulation of myostatin signaling by c-Jun N-terminal kinase in C2C12 cells." Cell Signal **19**(11): 2286-2295.
- Hugnot, J. P., H. Gilgenkrantz, et al. (1992). "Distal transcript of the dystrophin gene initiated from an alternative first exon and encoding a 75-kDa protein widely distributed in nonmuscle tissues." Proc Natl Acad Sci U S A **89**(16): 7506-7510.
- Hunter, R. B. and S. C. Kandarian (2004). "Disruption of either the Nfkb1 or the Bcl3 gene inhibits skeletal muscle atrophy." J Clin Invest **114**(10): 1504-1511.
- Ibraghimov-Beskrovnaya, O., J. M. Ervasti, et al. (1992). "Primary structure of dystrophin-associated glycoproteins linking dystrophin to the extracellular matrix." Nature **355**(6362): 696-702.
- Inouye, S., Y. Guo, et al. (1991). "Recombinant expression of human follistatin with 315 and 288 amino acids: chemical and biological comparison with native porcine follistatin." Endocrinology **129**(2): 815-822.
- Irintchev, A., M. Zwyer, et al. (1997). "Impaired functional and structural recovery after muscle injury in dystrophic mdx mice." Neuromuscul Disord **7**(2): 117-125.
- Ishikawa-Sakurai, M., M. Yoshida, et al. (2004). "ZZ domain is essentially required for the physiological binding of dystrophin and utrophin to beta-dystroglycan." Hum Mol Genet **13**(7): 693-702.

- Izumiya, Y., T. Hopkins, et al. (2008). "Fast/Glycolytic muscle fiber growth reduces fat mass and improves metabolic parameters in obese mice." Cell Metab **7**(2): 159-172.
- Jacobs, P. A., P. A. Hunt, et al. (1981). "Duchenne muscular dystrophy (DMD) in a female with an X/autosome translocation: further evidence that the DMD locus is at Xp21." Am J Hum Genet **33**(4): 513-518.
- Janssen, A. J., M. Schuelke, et al. (2008). "Muscle 3243A-->G mutation load and capacity of the mitochondrial energy-generating system." Ann Neurol **63**(4): 473-481.
- Jearawiriyapaisarn, N., H. M. Moulton, et al. (2008). "Sustained dystrophin expression induced by peptide-conjugated morpholino oligomers in the muscles of mdx mice." Mol Ther **16**(9): 1624-1629.
- Jearawiriyapaisarn, N., H. M. Moulton, et al. (2010). "Long-term improvement in mdx cardiomyopathy after therapy with peptide-conjugated morpholino oligomers." Cardiovasc Res **85**(3): 444-453.
- Jongpiputvanich, S., T. Sueblinvong, et al. (2005). "Mitochondrial respiratory chain dysfunction in various neuromuscular diseases." J Clin Neurosci **12**(4): 426-428.
- Joulia, D., H. Bernardi, et al. (2003). "Mechanisms involved in the inhibition of myoblast proliferation and differentiation by myostatin." Exp Cell Res **286**(2): 263-275.
- Kambadur, R., M. Sharma, et al. (1997). "Mutations in myostatin (GDF8) in double-muscled Belgian Blue and Piedmontese cattle." Genome Res **7**(9): 910-916.
- Kamei, Y., S. Miura, et al. (2004). "Skeletal muscle FOXO1 (FKHR) transgenic mice have less skeletal muscle mass, down-regulated Type I (slow twitch/red muscle) fiber genes, and impaired glycemic control." J Biol Chem **279**(39): 41114-41123.
- Kang, J. K., A. Malerba, et al. (2011). "Antisense-induced myostatin exon skipping leads to muscle hypertrophy in mice following octa-guanidine morpholino oligomer treatment." Mol Ther **19**(1): 159-164.
- Karpati, G., D. Ajdukovic, et al. (1993). "Myoblast transfer in Duchenne muscular dystrophy." Ann Neurol **34**(1): 8-17.
- Kazuki, Y., M. Hiratsuka, et al. (2010). "Complete genetic correction of ips cells from Duchenne muscular dystrophy." Mol Ther **18**(2): 386-393.
- Kemaladewi, D. U., W. M. Hoogaars, et al. (2011). "Dual exon skipping in myostatin and dystrophin for Duchenne muscular dystrophy." BMC Med Genomics **4**: 36.
- Khurana, T. S., S. C. Watkins, et al. (1991). "Immunolocalization and developmental expression of dystrophin related protein in skeletal muscle." Neuromuscul Disord **1**(3): 185-194.
- Kinouchi, N., Y. Ohsawa, et al. (2008). "Atelocollagen-mediated local and systemic applications of myostatin-targeting siRNA increase skeletal muscle mass." Gene Ther **15**(15): 1126-1130.
- Klein, C. J., D. D. Covert, et al. (1992). "Somatic reversion/suppression in Duchenne muscular dystrophy (DMD): evidence supporting a frame-restoring mechanism in rare dystrophin-positive fibers." Am J Hum Genet **50**(5): 950-959.
- Kocamis, H., S. A. Gahr, et al. (2002). "IGF-I, IGF-II, and IGF-receptor-1 transcript and IGF-II protein expression in myostatin knockout mice tissues." Muscle Nerve **26**(1): 55-63.
- Koenig, M., E. P. Hoffman, et al. (1987). "Complete cloning of the Duchenne muscular dystrophy (DMD) cDNA and preliminary genomic organization of the DMD gene in normal and affected individuals." Cell **50**(3): 509-517.
- Koenig, M. and L. M. Kunkel (1990). "Detailed analysis of the repeat domain of dystrophin reveals four potential hinge segments that may confer flexibility." J Biol Chem **265**(8): 4560-4566.
- Koenig, M., A. P. Monaco, et al. (1988). "The complete sequence of dystrophin predicts a rod-shaped cytoskeletal protein." Cell **53**(2): 219-228.

- Koppanati, B. M., J. Li, et al. (2009). "Systemic delivery of AAV8 in utero results in gene expression in diaphragm and limb muscle: treatment implications for muscle disorders." Gene Ther **16**(9): 1130-1137.
- Kuznetsov, A. V., K. Winkler, et al. (1998). "Impaired mitochondrial oxidative phosphorylation in skeletal muscle of the dystrophin-deficient mdx mouse." Mol Cell Biochem **183**(1-2): 87-96.
- Lai, K. M., M. Gonzalez, et al. (2004). "Conditional activation of akt in adult skeletal muscle induces rapid hypertrophy." Mol Cell Biol **24**(21): 9295-9304.
- Lai, Y., G. D. Thomas, et al. (2009). "Dystrophins carrying spectrin-like repeats 16 and 17 anchor nNOS to the sarcolemma and enhance exercise performance in a mouse model of muscular dystrophy." J Clin Invest **119**(3): 624-635.
- Lander, E. S., L. M. Linton, et al. (2001). "Initial sequencing and analysis of the human genome." Nature **409**(6822): 860-921.
- Langley, B., M. Thomas, et al. (2002). "Myostatin inhibits myoblast differentiation by down-regulating MyoD expression." J Biol Chem **277**(51): 49831-49840.
- Langley, B., M. Thomas, et al. (2004). "Myostatin inhibits rhabdomyosarcoma cell proliferation through an Rb-independent pathway." Oncogene **23**(2): 524-534.
- Lapidos, K. A., R. Kakkar, et al. (2004). "The dystrophin glycoprotein complex: signaling strength and integrity for the sarcolemma." Circ Res **94**(8): 1023-1031.
- Lawlor, M. W., B. P. Read, et al. (2011). "Inhibition of activin receptor type IIB increases strength and lifespan in myotubularin-deficient mice." Am J Pathol **178**(2): 784-793.
- Lee, C. H., P. Olson, et al. (2006). "PPARdelta regulates glucose metabolism and insulin sensitivity." Proc Natl Acad Sci U S A **103**(9): 3444-3449.
- Lee, S. J. (2007). "Quadrupling muscle mass in mice by targeting TGF-beta signaling pathways." PLoS One **2**(8): e789.
- Lee, S. J. (2008). "Genetic analysis of the role of proteolysis in the activation of latent myostatin." PLoS One **3**(2): e1628.
- Lee, S. J., Y. S. Lee, et al. (2010). "Regulation of muscle mass by follistatin and activins." Mol Endocrinol **24**(10): 1998-2008.
- Lee, S. J. and A. C. McPherron (2001). "Regulation of myostatin activity and muscle growth." Proc Natl Acad Sci U S A **98**(16): 9306-9311.
- Lee, S. J., L. A. Reed, et al. (2005). "Regulation of muscle growth by multiple ligands signaling through activin type II receptors." Proc Natl Acad Sci U S A **102**(50): 18117-18122.
- Leger, B., W. Derave, et al. (2008). "Human sarcopenia reveals an increase in SOCS-3 and myostatin and a reduced efficiency of Akt phosphorylation." Rejuvenation Res **11**(1): 163-175B.
- Lewis, C., H. Jockusch, et al. (2010). "Proteomic Profiling of the Dystrophin-Deficient MDX Heart Reveals Drastically Altered Levels of Key Metabolic and Contractile Proteins." J Biomed Biotechnol **2010**: 648501.
- Li, S., E. Kimura, et al. (2005). "Stable transduction of myogenic cells with lentiviral vectors expressing a minidystrophin." Gene Ther **12**(14): 1099-1108.
- Li, Y. P., C. M. Atkins, et al. (1999). "Mitochondria mediate tumor necrosis factor-alpha/NF-kappaB signaling in skeletal muscle myotubes." Antioxid Redox Signal **1**(1): 97-104.
- Lidov, H. G., S. Selig, et al. (1995). "Dp140: a novel 140 kDa CNS transcript from the dystrophin locus." Hum Mol Genet **4**(3): 329-335.
- Lin, J., H. B. Arnold, et al. (2002). "Myostatin knockout in mice increases myogenesis and decreases adipogenesis." Biochem Biophys Res Commun **291**(3): 701-706.

- Lipina, C., H. Kendall, et al. (2010). "Mechanisms involved in the enhancement of mammalian target of rapamycin signalling and hypertrophy in skeletal muscle of myostatin-deficient mice." FEBS Lett **584**(11): 2403-2408.
- Lu, Q. L., G. E. Morris, et al. (2000). "Massive idiosyncratic exon skipping corrects the nonsense mutation in dystrophic mouse muscle and produces functional revertant fibers by clonal expansion." J Cell Biol **148**(5): 985-996.
- Lunde, I. G., M. Ekmark, et al. (2007). "PPARdelta expression is influenced by muscle activity and induces slow muscle properties in adult rat muscles after somatic gene transfer." J Physiol **582**(Pt 3): 1277-1287.
- Luquet, S., J. Lopez-Soriano, et al. (2003). "Peroxisome proliferator-activated receptor delta controls muscle development and oxidative capability." FASEB J **17**(15): 2299-2301.
- Luz, M. A., M. J. Marques, et al. (2002). "Impaired regeneration of dystrophin-deficient muscle fibers is caused by exhaustion of myogenic cells." Braz J Med Biol Res **35**(6): 691-695.
- Lynch, G. S., R. T. Hinkle, et al. (2001). "Force and power output of fast and slow skeletal muscles from mdx mice 6-28 months old." J Physiol **535**(Pt 2): 591-600.
- Manno, C. S., A. J. Chew, et al. (2003). "AAV-mediated factor IX gene transfer to skeletal muscle in patients with severe hemophilia B." Blood **101**(8): 2963-2972.
- Matsakas, A., R. Macharia, et al. (2012). "Exercise training attenuates the hypermuscular phenotype and restores skeletal muscle function in the myostatin null mouse." Exp Physiol **97**(1): 125-140.
- Matsakas, A., E. Mouisel, et al. (2010). "Myostatin knockout mice increase oxidative muscle phenotype as an adaptive response to exercise." J Muscle Res Cell Motil **31**(2): 111-125.
- McCroskery, S., M. Thomas, et al. (2003). "Myostatin negatively regulates satellite cell activation and self-renewal." J Cell Biol **162**(6): 1135-1147.
- McFarlane, C., A. Hennebry, et al. (2008). "Myostatin signals through Pax7 to regulate satellite cell self-renewal." Exp Cell Res **314**(2): 317-329.
- McFarlane, C., E. Plummer, et al. (2006). "Myostatin induces cachexia by activating the ubiquitin proteolytic system through an NF-kappaB-independent, FoxO1-dependent mechanism." J Cell Physiol **209**(2): 501-514.
- McPherron, A. C. (2010). "Metabolic Functions of Myostatin and Gdf11." Immunol Endocr Metab Agents Med Chem **10**(4): 217-231.
- McPherron, A. C., A. M. Lawler, et al. (1997). "Regulation of skeletal muscle mass in mice by a new TGF-beta superfamily member." Nature **387**(6628): 83-90.
- McPherron, A. C. and S. J. Lee (1997). "Double muscling in cattle due to mutations in the myostatin gene." Proc Natl Acad Sci U S A **94**(23): 12457-12461.
- McPherron, A. C. and S. J. Lee (2002). "Suppression of body fat accumulation in myostatin-deficient mice." J Clin Invest **109**(5): 595-601.
- Mendell, J. R., K. Campbell, et al. (2010). "Dystrophin immunity in Duchenne's muscular dystrophy." N Engl J Med **363**(15): 1429-1437.
- Mendell, J. R., J. T. Kissel, et al. (1995). "Myoblast transfer in the treatment of Duchenne's muscular dystrophy." N Engl J Med **333**(13): 832-838.
- Mendias, C. L., J. E. Marcin, et al. (2006). "Contractile properties of EDL and soleus muscles of myostatin-deficient mice." J Appl Physiol **101**(3): 898-905.
- Mendler, L., E. Zador, et al. (2000). "Myostatin levels in regenerating rat muscles and in myogenic cell cultures." J Muscle Res Cell Motil **21**(6): 551-563.

- Merkulova, T., M. Dehaupas, et al. (2000). "Differential modulation of alpha, beta and gamma enolase isoforms in regenerating mouse skeletal muscle." Eur J Biochem **267**(12): 3735-3743.
- Michele, D. E. and K. P. Campbell (2003). "Dystrophin-glycoprotein complex: post-translational processing and dystroglycan function." J Biol Chem **278**(18): 15457-15460.
- Mingozzi, F., J. J. Meulenberg, et al. (2009). "AAV-1-mediated gene transfer to skeletal muscle in humans results in dose-dependent activation of capsid-specific T cells." Blood **114**(10): 2077-2086.
- Miura, T., Y. Kishioka, et al. (2006). "Decorin binds myostatin and modulates its activity to muscle cells." Biochem Biophys Res Commun **340**(2): 675-680.
- Mizuno, Y., I. Nonaka, et al. (1993). "Reciprocal expression of dystrophin and utrophin in muscles of Duchenne muscular dystrophy patients, female DMD-carriers and control subjects." J Neurol Sci **119**(1): 43-52.
- Monaco, A. P., C. J. Bertelson, et al. (1985). "Detection of deletions spanning the Duchenne muscular dystrophy locus using a tightly linked DNA segment." Nature **316**(6031): 842-845.
- Monaco, A. P., R. L. Neve, et al. (1986). "Isolation of candidate cDNAs for portions of the Duchenne muscular dystrophy gene." Nature **323**(6089): 646-650.
- Monahan, P. E., R. J. Samulski, et al. (1998). "Direct intramuscular injection with recombinant AAV vectors results in sustained expression in a dog model of hemophilia." Gene Ther **5**(1): 40-49.
- Morine, K. J., L. T. Bish, et al. (2010). "Systemic myostatin inhibition via liver-targeted gene transfer in normal and dystrophic mice." PLoS One **5**(2): e9176.
- Morine, K. J., L. T. Bish, et al. (2010). "Activin IIB receptor blockade attenuates dystrophic pathology in a mouse model of Duchenne muscular dystrophy." Muscle Nerve **42**(5): 722-730.
- Morrison, B. M., J. L. Lachey, et al. (2009). "A soluble activin type IIB receptor improves function in a mouse model of amyotrophic lateral sclerosis." Exp Neurol **217**(2): 258-268.
- Mosher, D. S., P. Quignon, et al. (2007). "A mutation in the myostatin gene increases muscle mass and enhances racing performance in heterozygote dogs." PLoS Genet **3**(5): e79.
- Moss, F. P. and C. P. Leblond (1971). "Satellite cells as the source of nuclei in muscles of growing rats." Anat Rec **170**(4): 421-435.
- Mostacciuolo, M. L., A. Lombardi, et al. (1987). "Population data on benign and severe forms of X-linked muscular dystrophy." Hum Genet **75**(3): 217-220.
- Moulton, H. M. and J. D. Moulton (2010). "Morpholinos and their peptide conjugates: therapeutic promise and challenge for Duchenne muscular dystrophy." Biochim Biophys Acta **1798**(12): 2296-2303.
- Murphy, K. T., A. Chee, et al. (2011). "Antibody-directed myostatin inhibition enhances muscle mass and function in tumor-bearing mice." Am J Physiol Regul Integr Comp Physiol **301**(3): R716-726.
- Murphy, K. T., V. Cobani, et al. (2011). "Acute antibody-directed myostatin inhibition attenuates disuse muscle atrophy and weakness in mice." J Appl Physiol **110**(4): 1065-1072.
- Murphy, K. T., R. Koopman, et al. (2010). "Antibody-directed myostatin inhibition in 21-mo-old mice reveals novel roles for myostatin signaling in skeletal muscle structure and function." FASEB J **24**(11): 4433-4442.
- Murphy, K. T., J. G. Ryall, et al. (2010). "Antibody-directed myostatin inhibition improves diaphragm pathology in young but not adult dystrophic mdx mice." Am J Pathol **176**(5): 2425-2434.
- Musaro, A., K. McCullagh, et al. (2001). "Localized Igf-1 transgene expression sustains hypertrophy and regeneration in senescent skeletal muscle." Nat Genet **27**(2): 195-200.

- Nahle, Z., M. Hsieh, et al. (2008). "CD36-dependent regulation of muscle FoxO1 and PDK4 in the PPAR delta/beta-mediated adaptation to metabolic stress." J Biol Chem **283**(21): 14317-14326.
- Nakatani, M., Y. Takehara, et al. (2008). "Transgenic expression of a myostatin inhibitor derived from follistatin increases skeletal muscle mass and ameliorates dystrophic pathology in mdx mice." FASEB J **22**(2): 477-487.
- Narkar, V. A., M. Downes, et al. (2008). "AMPK and PPARdelta agonists are exercise mimetics." Cell **134**(3): 405-415.
- Nicholas, G., M. Thomas, et al. (2002). "Titin-cap associates with, and regulates secretion of, Myostatin." J Cell Physiol **193**(1): 120-131.
- Nishio, H., Y. Takeshima, et al. (1994). "Identification of a novel first exon in the human dystrophin gene and of a new promoter located more than 500 kb upstream of the nearest known promoter." J Clin Invest **94**(3): 1037-1042.
- Ogata, T. and Y. Yamasaki (1985). "Scanning electron-microscopic studies on the three-dimensional structure of mitochondria in the mammalian red, white and intermediate muscle fibers." Cell Tissue Res **241**(2): 251-256.
- Ohanna, M., A. K. Sobering, et al. (2005). "Atrophy of S6K1(-/-) skeletal muscle cells reveals distinct mTOR effectors for cell cycle and size control." Nat Cell Biol **7**(3): 286-294.
- Pallafacchina, G., E. Calabria, et al. (2002). "A protein kinase B-dependent and rapamycin-sensitive pathway controls skeletal muscle growth but not fiber type specification." Proc Natl Acad Sci U S A **99**(14): 9213-9218.
- Parsons, S. A., D. P. Millay, et al. (2006). "Age-dependent effect of myostatin blockade on disease severity in a murine model of limb-girdle muscular dystrophy." Am J Pathol **168**(6): 1975-1985.
- Partridge, T. A., J. E. Morgan, et al. (1989). "Conversion of mdx myofibres from dystrophin-negative to -positive by injection of normal myoblasts." Nature **337**(6203): 176-179.
- Penn, A. S., R. P. Lisak, et al. (1970). "Muscular dystrophy in young girls." Neurology **20**(2): 147-159.
- Personius, K. E., A. Jayaram, et al. (2010). "Grip force, EDL contractile properties, and voluntary wheel running after postdevelopmental myostatin depletion in mice." J Appl Physiol (1985) **109**(3): 886-894.
- Peters, M. F., H. M. Sadoulet-Puccio, et al. (1998). "Differential membrane localization and intermolecular associations of alpha-dystrobrevin isoforms in skeletal muscle." J Cell Biol **142**(5): 1269-1278.
- Picard, B., H. Gagniere, et al. (1995). "Comparison of the foetal development of muscle in normal and double-musced cattle." J Muscle Res Cell Motil **16**(6): 629-639.
- Pichavant, C., P. Chapdelaine, et al. (2010). "Expression of dog microdystrophin in mouse and dog muscles by gene therapy." Mol Ther **18**(5): 1002-1009.
- Pistilli, E. E., S. Bogdanovich, et al. (2011). "Targeting the activin type IIB receptor to improve muscle mass and function in the mdx mouse model of Duchenne muscular dystrophy." Am J Pathol **178**(3): 1287-1297.
- Ploquin, C., B. Chabi, et al. (2012). "Lack of myostatin alters intermyofibrillar mitochondria activity, unbalances redox status, and impairs tolerance to chronic repetitive contractions in muscle." Am J Physiol Endocrinol Metab **302**(8): E1000-1008.
- Qaisar, R., G. Renaud, et al. (2012). "Is functional hypertrophy and specific force coupled with the addition of myonuclei at the single muscle fiber level?" FASEB J **26**(3): 1077-1085.

- Qiao, C., J. Li, et al. (2008). "Myostatin propeptide gene delivery by adeno-associated virus serotype 8 vectors enhances muscle growth and ameliorates dystrophic phenotypes in mdx mice." Hum Gene Ther **19**(3): 241-254.
- Rabinowitz, J. E. and J. Samulski (1998). "Adeno-associated virus expression systems for gene transfer." Curr Opin Biotechnol **9**(5): 470-475.
- Rahimov, F., O. D. King, et al. (2011). "Gene expression profiling of skeletal muscles treated with a soluble activin type IIB receptor." Physiol Genomics **43**(8): 398-407.
- Rebbapragada, A., H. Benchabane, et al. (2003). "Myostatin signals through a transforming growth factor beta-like signaling pathway to block adipogenesis." Mol Cell Biol **23**(20): 7230-7242.
- Rehfeldt, C., G. Ott, et al. (2005). "Effects of the compact mutant myostatin allele Mstn (Cmpt-dl1Abc) introgressed into a high growth mouse line on skeletal muscle cellularity." J Muscle Res Cell Motil **26**(2-3): 103-112.
- Reisz-Porszasz, S., S. Bhasin, et al. (2003). "Lower skeletal muscle mass in male transgenic mice with muscle-specific overexpression of myostatin." Am J Physiol Endocrinol Metab **285**(4): E876-888.
- Rios, R., I. Carneiro, et al. (2002). "Myostatin is an inhibitor of myogenic differentiation." Am J Physiol Cell Physiol **282**(5): C993-999.
- Riquelme, C., J. Larrain, et al. (2001). "Antisense inhibition of decorin expression in myoblasts decreases cell responsiveness to transforming growth factor beta and accelerates skeletal muscle differentiation." J Biol Chem **276**(5): 3589-3596.
- Riserus, U., D. Sprecher, et al. (2008). "Activation of peroxisome proliferator-activated receptor (PPAR)delta promotes reversal of multiple metabolic abnormalities, reduces oxidative stress, and increases fatty acid oxidation in moderately obese men." Diabetes **57**(2): 332-339.
- Robelin, J., B. Picard, et al. (1993). "Myosin expression in semitendinosus muscle during fetal development of cattle: immunocytochemical and electrophoretic analyses." Reprod Nutr Dev **33**(1): 25-41.
- Rodgers, B. D., J. P. Interlichia, et al. (2009). "Myostatin represses physiological hypertrophy of the heart and excitation-contraction coupling." J Physiol **587**(Pt 20): 4873-4886.
- Rommel, C., S. C. Bodine, et al. (2001). "Mediation of IGF-1-induced skeletal myotube hypertrophy by PI(3)K/Akt/mTOR and PI(3)K/Akt/GSK3 pathways." Nat Cell Biol **3**(11): 1009-1013.
- Rybakova, I. N., J. R. Patel, et al. (2000). "The dystrophin complex forms a mechanically strong link between the sarcolemma and costameric actin." J Cell Biol **150**(5): 1209-1214.
- Sako, D., A. V. Grinberg, et al. (2010). "Characterization of the ligand binding functionality of the extracellular domain of activin receptor type IIB." J Biol Chem **285**(27): 21037-21048.
- Salerno, M. S., M. Thomas, et al. (2004). "Molecular analysis of fiber type-specific expression of murine myostatin promoter." Am J Physiol Cell Physiol **287**(4): C1031-1040.
- Sandri, M., J. Lin, et al. (2006). "PGC-1alpha protects skeletal muscle from atrophy by suppressing FoxO3 action and atrophy-specific gene transcription." Proc Natl Acad Sci U S A **103**(44): 16260-16265.
- Sandri, M., C. Sandri, et al. (2004). "Foxo transcription factors induce the atrophy-related ubiquitin ligase atrogin-1 and cause skeletal muscle atrophy." Cell **117**(3): 399-412.
- Sartori, R., E. Schirwis, et al. (2013). "BMP signaling controls muscle mass." Nat Genet.
- Sartori, R., E. Schirwis, et al. (2013). "BMP signaling controls muscle mass." Nat Genet **45**(11): 1309-1318.
- Savage, K. J. and A. C. McPherron (2010). "Endurance exercise training in myostatin null mice." Muscle Nerve **42**(3): 355-362.

- Schafer, R., U. Knauf, et al. (2006). "Age dependence of the human skeletal muscle stem cell in forming muscle tissue." Artif Organs **30**(3): 130-140.
- Schantl, J. A., M. Roza, et al. (2003). "Small glutamine-rich tetratricopeptide repeat-containing protein (SGT) interacts with the ubiquitin-dependent endocytosis (UbE) motif of the growth hormone receptor." Biochem J **373**(Pt 3): 855-863.
- Schatzberg, S. J., N. J. Olby, et al. (1999). "Molecular analysis of a spontaneous dystrophin 'knockout' dog." Neuromuscul Disord **9**(5): 289-295.
- Schiaffino, S., L. Gorza, et al. (1989). "Three myosin heavy chain isoforms in type 2 skeletal muscle fibres." J Muscle Res Cell Motil **10**(3): 197-205.
- Schirwis, E., O. Agbulut, et al. (2013). "The beneficial effect of myostatin deficiency on maximal muscle force and power is attenuated with age." Exp Gerontol **48**(2): 183-190.
- Schneyer, A. L., D. A. Rzcudlo, et al. (1994). "Characterization of unique binding kinetics of follistatin and activin or inhibin in serum." Endocrinology **135**(2): 667-674.
- Schuelke, M., K. R. Wagner, et al. (2004). "Myostatin mutation associated with gross muscle hypertrophy in a child." N Engl J Med **350**(26): 2682-2688.
- Schuler, M., F. Ali, et al. (2006). "PGC1alpha expression is controlled in skeletal muscles by PPARbeta, whose ablation results in fiber-type switching, obesity, and type 2 diabetes." Cell Metab **4**(5): 407-414.
- Sharma, M., R. Kambadur, et al. (1999). "Myostatin, a transforming growth factor-beta superfamily member, is expressed in heart muscle and is upregulated in cardiomyocytes after infarct." J Cell Physiol **180**(1): 1-9.
- Sharp, N. J., J. N. Kornegay, et al. (1992). "An error in dystrophin mRNA processing in golden retriever muscular dystrophy, an animal homologue of Duchenne muscular dystrophy." Genomics **13**(1): 115-121.
- Shelton, G. D. and E. Engvall (2005). "Canine and feline models of human inherited muscle diseases." Neuromuscul Disord **15**(2): 127-138.
- Sicinski, P., Y. Geng, et al. (1989). "The molecular basis of muscular dystrophy in the mdx mouse: a point mutation." Science **244**(4912): 1578-1580.
- Skuk, D., N. J. Caron, et al. (2003). "Resetting the problem of cell death following muscle-derived cell transplantation: detection, dynamics and mechanisms." J Neuropathol Exp Neurol **62**(9): 951-967.
- Southgate, R. J., B. Neill, et al. (2007). "FOXO1 regulates the expression of 4E-BP1 and inhibits mTOR signaling in mammalian skeletal muscle." J Biol Chem **282**(29): 21176-21186.
- Souza, T. A., X. Chen, et al. (2008). "Proteomic identification and functional validation of activins and bone morphogenetic protein 11 as candidate novel muscle mass regulators." Mol Endocrinol **22**(12): 2689-2702.
- Stavaux, D., T. Art, et al. (1994). "Muscle fibre type and size, and muscle capillary density in young double-muscled blue Belgian cattle." Zentralbl Veterinarmed A **41**(3): 229-236.
- Stitt, T. N., D. Drujan, et al. (2004). "The IGF-1/PI3K/Akt pathway prevents expression of muscle atrophy-induced ubiquitin ligases by inhibiting FOXO transcription factors." Mol Cell **14**(3): 395-403.
- Sugino, K., N. Kurosawa, et al. (1993). "Molecular heterogeneity of follistatin, an activin-binding protein. Higher affinity of the carboxyl-terminal truncated forms for heparan sulfate proteoglycans on the ovarian granulosa cell." J Biol Chem **268**(21): 15579-15587.
- Suzuki, S. T., B. Zhao, et al. (2008). "Enhanced muscle by myostatin propeptide increases adipose tissue adiponectin, PPAR-alpha, and PPAR-gamma expressions." Biochem Biophys Res Commun **369**(2): 767-773.

- Takahashi, S., T. Tanaka, et al. (2006). "Peroxisome proliferator-activated receptor delta (PPARdelta), a novel target site for drug discovery in metabolic syndrome." *Pharmacol Res* **53**(6): 501-507.
- Taylor, W. E., S. Bhasin, et al. (2001). "Myostatin inhibits cell proliferation and protein synthesis in C2C12 muscle cells." *Am J Physiol Endocrinol Metab* **280**(2): E221-228.
- Thies, R. S., T. Chen, et al. (2001). "GDF-8 propeptide binds to GDF-8 and antagonizes biological activity by inhibiting GDF-8 receptor binding." *Growth Factors* **18**(4): 251-259.
- Thomas, M., B. Langley, et al. (2000). "Myostatin, a negative regulator of muscle growth, functions by inhibiting myoblast proliferation." *J Biol Chem* **275**(51): 40235-40243.
- Tinsley, J. M., D. J. Blake, et al. (1993). "Apo-dystrophin-3: a 2.2kb transcript from the DMD locus encoding the dystrophin glycoprotein binding site." *Hum Mol Genet* **2**(5): 521-524.
- Tinsley, J. M., D. J. Blake, et al. (1992). "Primary structure of dystrophin-related protein." *Nature* **360**(6404): 591-593.
- Tinsley, J. M., A. C. Potter, et al. (1996). "Amelioration of the dystrophic phenotype of mdx mice using a truncated utrophin transgene." *Nature* **384**(6607): 349-353.
- Tome, F. M., T. Evangelista, et al. (1994). "Congenital muscular dystrophy with merosin deficiency." *C R Acad Sci III* **317**(4): 351-357.
- Tuffery-Giraud, S., C. Beroud, et al. (2009). "Genotype-phenotype analysis in 2,405 patients with a dystrophinopathy using the UMD-DMD database: a model of nationwide knowledgebase." *Hum Mutat* **30**(6): 934-945.
- Valentine, B. A., B. J. Cooper, et al. (1990). "Canine X-linked muscular dystrophy: morphologic lesions." *J Neurol Sci* **97**(1): 1-23.
- Valentine, B. A., B. J. Cooper, et al. (1988). "Canine X-linked muscular dystrophy. An animal model of Duchenne muscular dystrophy: clinical studies." *J Neurol Sci* **88**(1-3): 69-81.
- Ventura-Clapier, R., A. Kuznetsov, et al. (1998). "Functional coupling of creatine kinases in muscles: species and tissue specificity." *Mol Cell Biochem* **184**(1-2): 231-247.
- Vilquin, J. T., I. Asselin, et al. (1994). "Myoblast allotransplantation in mice: degree of success varies depending on the efficacy of various immunosuppressive treatments." *Transplant Proc* **26**(6): 3372-3373.
- Wagner, K. D. and N. Wagner (2010). "Peroxisome proliferator-activated receptor beta/delta (PPARbeta/delta) acts as regulator of metabolism linked to multiple cellular functions." *Pharmacol Ther* **125**(3): 423-435.
- Wagner, K. R., J. L. Fleckenstein, et al. (2008). "A phase I/II trial of MYO-029 in adult subjects with muscular dystrophy." *Ann Neurol* **63**(5): 561-571.
- Wagner, K. R., X. Liu, et al. (2005). "Muscle regeneration in the prolonged absence of myostatin." *Proc Natl Acad Sci U S A* **102**(7): 2519-2524.
- Wagner, K. R., A. C. McPherron, et al. (2002). "Loss of myostatin attenuates severity of muscular dystrophy in mdx mice." *Ann Neurol* **52**(6): 832-836.
- Wang, H., Q. Zhang, et al. (2003). "hSGT interacts with the N-terminal region of myostatin." *Biochem Biophys Res Commun* **311**(4): 877-883.
- Wang, Q. and A. C. McPherron (2012). "Myostatin inhibition induces muscle fibre hypertrophy prior to satellite cell activation." *J Physiol* **590**(Pt 9): 2151-2165.
- Wang, Y. X., C. H. Lee, et al. (2003). "Peroxisome-proliferator-activated receptor delta activates fat metabolism to prevent obesity." *Cell* **113**(2): 159-170.
- Wang, Y. X., C. L. Zhang, et al. (2004). "Regulation of muscle fiber type and running endurance by PPARdelta." *PLoS Biol* **2**(10): e294.

- Wang, Z., R. Storb, et al. (2010). "Immune responses to AAV in canine muscle monitored by cellular assays and noninvasive imaging." Mol Ther **18**(3): 617-624.
- Wang, Z., T. Zhu, et al. (2005). "Adeno-associated virus serotype 8 efficiently delivers genes to muscle and heart." Nat Biotechnol **23**(3): 321-328.
- Watkins, S. C., E. P. Hoffman, et al. (1988). "Immunoelectron microscopic localization of dystrophin in myofibres." Nature **333**(6176): 863-866.
- Watt, D. J., K. Lambert, et al. (1982). "Incorporation of donor muscle precursor cells into an area of muscle regeneration in the host mouse." J Neurol Sci **57**(2-3): 319-331.
- Weber, J. M. (2011). "Metabolic fuels: regulating fluxes to select mix." J Exp Biol **214**(Pt 2): 286-294.
- Wehling, M., B. Cai, et al. (2000). "Modulation of myostatin expression during modified muscle use." FASEB J **14**(1): 103-110.
- Welle, S. (2002). "Cellular and molecular basis of age-related sarcopenia." Can J Appl Physiol **27**(1): 19-41.
- Wenz, T., S. G. Rossi, et al. (2009). "Increased muscle PGC-1alpha expression protects from sarcopenia and metabolic disease during aging." Proc Natl Acad Sci U S A **106**(48): 20405-20410.
- Weydert, A., P. Barton, et al. (1987). "Developmental pattern of mouse skeletal myosin heavy chain gene transcripts in vivo and in vitro." Cell **49**(1): 121-129.
- Wheater, P. R. and H. G. Burkitt (1987). Functional histology : a text and colour atlas. Edinburgh ; New York, Churchill Livingstone.
- Whittemore, L. A., K. Song, et al. (2003). "Inhibition of myostatin in adult mice increases skeletal muscle mass and strength." Biochem Biophys Res Commun **300**(4): 965-971.
- Wilton, S. D., D. E. Dye, et al. (1997). "Revertant fibres: a possible genetic therapy for Duchenne muscular dystrophy?" Neuromuscul Disord **7**(5): 329-335.
- Winand, N. J., M. Edwards, et al. (1994). "Deletion of the dystrophin muscle promoter in feline muscular dystrophy." Neuromuscul Disord **4**(5-6): 433-445.
- Winbanks, C. E., J. L. Chen, et al. (2013). "The bone morphogenetic protein axis is a positive regulator of skeletal muscle mass." J Cell Biol **203**(2): 345-357.
- Winnard, A. V., J. R. Mendell, et al. (1995). "Frameshift deletions of exons 3-7 and revertant fibers in Duchenne muscular dystrophy: mechanisms of dystrophin production." Am J Hum Genet **56**(1): 158-166.
- Wolfman, N. M., A. C. McPherron, et al. (2003). "Activation of latent myostatin by the BMP-1/tolloid family of metalloproteinases." Proc Natl Acad Sci U S A **100**(26): 15842-15846.
- Wu, B., P. Lu, et al. (2010). "Dose-dependent restoration of dystrophin expression in cardiac muscle of dystrophic mice by systemically delivered morpholino." Gene Ther **17**(1): 132-140.
- Wu, B., H. M. Moulton, et al. (2008). "Effective rescue of dystrophin improves cardiac function in dystrophin-deficient mice by a modified morpholino oligomer." Proc Natl Acad Sci U S A **105**(39): 14814-14819.
- Yang, W., Y. Chen, et al. (2006). "Extracellular signal-regulated kinase 1/2 mitogen-activated protein kinase pathway is involved in myostatin-regulated differentiation repression." Cancer Res **66**(3): 1320-1326.
- Yang, Z. Z., O. Tschopp, et al. (2004). "Physiological functions of protein kinase B/Akt." Biochem Soc Trans **32**(Pt 2): 350-354.
- Yin, H., Q. Lu, et al. (2008). "Effective exon skipping and restoration of dystrophin expression by peptide nucleic acid antisense oligonucleotides in mdx mice." Mol Ther **16**(1): 38-45.

- Yoshida, M. and E. Ozawa (1990). "Glycoprotein complex anchoring dystrophin to sarcolemma." J Biochem **108**(5): 748-752.
- Zammit, P. S. and T. A. Partridge (2002). "Sizing up muscular dystrophy." Nat Med **8**(12): 1355-1356.
- Zhao, B., R. J. Wall, et al. (2005). "Transgenic expression of myostatin propeptide prevents diet-induced obesity and insulin resistance." Biochem Biophys Res Commun **337**(1): 248-255.
- Zhou, X., J. L. Wang, et al. (2010). "Reversal of cancer cachexia and muscle wasting by ActRIIB antagonism leads to prolonged survival." Cell **142**(4): 531-543.
- Zhu, X., M. Hadhazy, et al. (2000). "Dominant negative myostatin produces hypertrophy without hyperplasia in muscle." FEBS Lett **474**(1): 71-75.
- Zhu, X., S. Topouzis, et al. (2004). "Myostatin signaling through Smad2, Smad3 and Smad4 is regulated by the inhibitory Smad7 by a negative feedback mechanism." Cytokine **26**(6): 262-272.
- Zimmers, T. A., M. V. Davies, et al. (2002). "Induction of cachexia in mice by systemically administered myostatin." Science **296**(5572): 1486-1488.
- Zubrzycka-Gaarn, E. E., D. E. Bulman, et al. (1988). "The Duchenne muscular dystrophy gene product is localized in sarcolemma of human skeletal muscle." Nature **333**(6172): 466-469.